Digital Fabrication of Custom Interactive Objects with Rich Materials

A dissertation submitted towards
the degree Doctor of Engineering (Dr.-Ing.)
of the Faculty of Mathematics and Computer Science
of Saarland University

by
Daniel Gröger

Saarbrücken
2019

Day of colloquium:	03.12.2019
Dean of the faculty:	Prof. Dr. Sebastian Hack
Reviewers:	Prof. Dr. Jürgen Steimle Prof. Dr. Jan Borchers Prof. Dr. Antonio Krüger
Chair of the committee:	Prof. Dr. Christian Theobalt
Academic assistant:	Dr. Bruno Fruchard

für Kati

Abstract

As ubiquitous computing is becoming reality, people interact with an increasing number of computer interfaces embedded in physical objects. Today, interaction with those objects largely relies on integrated touchscreens. In contrast, humans are capable of rich interaction with physical objects and their materials through sensory feedback and dexterous manipulation skills. However, developing physical user interfaces that offer versatile interaction and leverage these capabilities is challenging. It requires novel technologies for prototyping interfaces with custom interactivity that support rich materials of everyday objects. Moreover, such technologies need to be accessible to empower a wide audience of researchers, makers, and users.

This thesis investigates digital fabrication as a key technology to address these challenges. It contributes four novel design and fabrication approaches for interactive objects with rich materials. The contributions enable easy, accessible, and versatile design and fabrication of interactive objects with custom stretchability, input and output on complex geometries and diverse materials, tactile output on 3D-object geometries, and capabilities of changing their shape and material properties.

Together, the contributions of this thesis advance the fields of digital fabrication, rapid prototyping, and ubiquitous computing towards the bigger goal of exploring interactive objects with rich materials as a new generation of physical interfaces.

Zusammenfassung

Computer werden zunehmend in Geräten integriert, mit welchen Menschen im Alltag interagieren. Heutzutage basiert diese Interaktion weitgehend auf Touchscreens. Im Kontrast dazu steht die reichhaltige Interaktion mit physischen Objekten und Materialien durch sensorisches Feedback und geschickte Manipulation. Interfaces zu entwerfen, die diese Fähigkeiten nutzen, ist allerdings problematisch. Hierfür sind Technologien zum Prototyping neuer Interfaces mit benutzerdefinierter Interaktivität und Kompatibilität mit vielfältigen Materialien erforderlich. Zudem sollten solche Technologien zugänglich sein, um ein breites Publikum zu erreichen.

Diese Dissertation erforscht die digitale Fabrikation als Schlüsseltechnologie, um diese Probleme zu adressieren. Sie trägt vier neue Design- und Fabrikationsansätze für das Prototyping interaktiver Objekte mit reichhaltigen Materialien bei. Diese ermöglichen einfaches, zugängliches und vielseitiges Design und Fabrikation von interaktiven Objekten mit individueller Dehnbarkeit, Ein- und Ausgabe auf komplexen Geometrien und vielfältigen Materialien, taktiler Ausgabe auf 3D-Objektgeometrien und der Fähigkeit ihre Form und Materialeigenschaften zu ändern.

Insgesamt trägt diese Dissertation zum Fortschritt der Bereiche der digitalen Fabrikation, des Rapid Prototyping und des Ubiquitous Computing in Richtung des größeren Ziels, der Exploration interaktiver Objekte mit reichhaltigen Materialien als eine neue Generation von physischen Interfaces, bei.

We all need people who will give us feedback.
That's how we improve.

— Bill Gates

Acknowledgments

This thesis would not have been possible without the support of many colleagues, friends, and family. I learned a lot, was inspired by thoughts and ideas, and received invaluable support and advice.

First and foremost, I want to thank my advisor Jürgen Steimle. I learned a lot from you and appreciate the continued support throughout this incredible journey. Many thanks to my colleagues for tremendous help and creating an engaging and fun environment to work in. Special thanks to Martin Weigel for being a role model as a researcher and as a PhD student. Thank you for inspiration, support, and your friendship. Sincere thanks to Anusha Withana. I am grateful for your advice, having learned a lot from you, and the enjoyable time we spent together. Thanks to Simon Olberding for leading by example and valuable advice. I also want to thank Aditya Shekhar Nittala and Adwait Sharma for their contagious positive attitude but also crucial help during deadlines. Sincere thanks also to Bruno Fruchard for his advice and always offering help.

Over the past years, I had the pleasure to meet many people, have great discussions, and collaborate with many amazing researchers at Saarland university. This includes former and current colleagues at the HCI Lab but also friends at MMCI, DFKI, MPI, and INM. I want to thank Hans-Peter Seidel and the D4 group at the Max Planck Institute. Thank you for helpful feedback and inspiring me to look beyond the challenges in HCI. Also, thanks to Andreas Karrenbauer for discussing ideas and collaboration. Special thanks to Donald Degraen for many things, including inspiring discussions and crazy ideas. Thanks to Michal Piovarči for his support and help on polishing ideas.

I am also grateful to many students that I had the pleasure to work with. Your hard work was a tremendous help for my research. In alphabetical order: Amr Gomaa, Elena Chong Loo, Jonas Hempel, Julian Haluska, Lena Hegemann, Martin Feick, Muhammad Hamid, Purnendu Mishra, and Sven Ehses.

Finally, I want to thank my friends and family. This thesis would not have been possible without your support and encouragement.

Contents

1 Introduction

Over the past decades, a tremendous change has happened to the form factor of computing, from main frames filling large halls, over personal computers fitting on a desk, to hand-held mobile devices and small wearables that people carry in their pockets or on their bodies. As this trend continues, computing becomes increasingly ubiquitous. As Mark Weiser impressively predicted in his vision of ubiquitous computing [238], computational capability gets embedded deeply in the environment to a point where it vanishes into the background and the digital merges into the physical world.

Core aspects of this vision are on the verge of becoming reality. In everyday life, people deal with an increasing number of objects with embedded computing, for example, smart thermostats, internet-connected refrigerators, or touch-sensitive coffee machines. However, interaction with these objects typically relies on embedded touch-screens as used in current smart phones and tablet computers. Rather than merging the digital and physical worlds, these flat rigid screens act as windows to the digital world. They allow to see digital content but do not allow to grasp and experience it through one's hands and body [83]. In contrast, humans are capable of rich interaction with physical objects through sensory feedback and manipulation capabilities. While exploring an unknown object, for example, one's hands allow for precise control while perceiving rich haptic feedback about shapes and materials. To leverage these skills for interaction with digital media, a stream of research in Human-Computer Interaction (HCI) explores interfaces based on tangible objects. These Tangible User Interfaces (TUIs) [84] have demonstrated how to leverage physical objects and their properties to expand the set of interaction modalities beyond touch on a rigid surfaces. For example, TUIs have used properties including the spatial location and orientation of objects [121, 215, 241, 240], reconfigurable geometry and mechanisms [166, 240], and deformation behavior [141, 161, 193, 198].

This thesis explores a specific form of ubiquitous tangible interfaces: *interactive objects with rich materials*. In contrast to classical TUIs using passive objects, e.g. through optical tracking and projection, interactive objects are largely self-contained objects with embedded interactive capabilities. Just like any real-world object, these interactive objects can be made of various rich materials. In the context of this thesis, rich materials refers to complex geometry, distinct visuo-haptic appearance, or deformability, e.g. softness. In this thesis, we focus on such interactive objects to leverage their rich material for interaction.

Towards realizing interactive objects with rich materials, suitable technologies need to be found that allow creating interactive objects of rich materials with an expressive set of input and output modalities. This is an open research questions since there are many different modalities and a diverse set of rich object properties.

For example, modalities explored by prior work include touch [51, 148, 192, 244], squeeze [69, 198, 220], or bend [7, 198, 219] input and display [148, 242, 244] or tactile [12, 88] output. Examples of object properties include strong doubly-curved geometries, rough surfaces, and soft materials.

As a second point, accessible technologies for prototyping enable a wider audience of researchers and designers to prototype and explore novel interfaces for interactive objects. The key importance of rapid and accessible protoptying techniques has been demonstrated by prior work. For example, the instant inkjet circuit approach by Kawahara *et al.* [104] has enabled and stimulated research in a range of application domains [51, 55, 72, 105, 146, 147, 168]. Thus, an open research question is to make technologies for creating custom interactive objects simple to use, rapid, and accessible to a wide audience. However, this is especially demanding for interactive objects with rich materials as the complexity of creating custom objects increases with their interaction capabilities and diversity of object properties.

This thesis investigates digital fabrication as a key technology towards addressing these research questions.

1.1 Digital Fabrication of Interactive Objects

Digital fabrication approaches, e.g. using 3D printers or laser cutters, enable users to fabricate custom objects with little technical skills or experience. They turn the technically challenging task of fabricating a physical artifact into a partially automated fabrication process based on a digital design. This promises that instead of relying on experience and skill in manual crafting, fabricating a physical artifact becomes more accessible, as even novice users may be enabled to turn digital blueprints into real-world objects.

However, automated fabrication does not entirely solve the problem. It rather transforms the technical fabrication problem into a digital design problem. Thus, the complexity is moved to the digital design. This means that novice users can fabricate an object based on an existing design, but creating a custom design still requires expert skills. We therefore require digital tools that support designers during design and abstract from complexity to make digital fabrication accessible to a wide audience.

The process of digital fabrication is illustrated in Figure 1.1. It involves creating a digital design, commonly through a graphical user interface (GUI), which is then fabricated on a computer-controlled machine to produce a physical object. This general process applies to different technologies. Commonly, however, the digital fabrication process refers to the design and fabrication of 2D or 3D objects through subtractive or additive manufacturing [48]. In this context, fabrication tools produce the physical artifact, e.g. using 3D printers, lasers cutters, or CNC[1] routers. Digital models for these devices are typically created using 3D modeling or computer-aided design (CAD) software, e.g. Autodesk Inventor [6], SketchUp [213], or Rhinoceros 3D [177].

1 computer numerical control

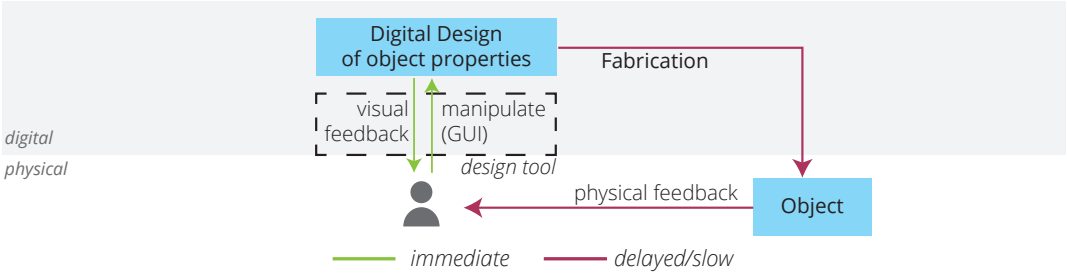

Figure 1.1: Schematic overview of the common digital fabrication process of custom physical objects.

The digital fabrication of custom 3D objects has received increasing research attention in recent years. This is likely due to multiple reasons, including the increasing adoption of 3D printers and the technology's relevance for prototyping in academia, industry, and the maker community. Initial research has focused on designing and fabricating 3D objects with custom geometry. For example, approaches have simplified the design of 3D models [34, 80, 185, 195, 211] and extended fabrication capabilities to produce a larger variety of objects [13, 16, 24, 27, 115, 136, 137, 216].

Towards the digital fabrication of interactive objects with rich materials, the problems and solutions of custom 3D geometries remain relevant. However, the aspects of interactivity and rich materials add new dimensions to the problem space. Interactivity, in contrast to static 3D objects, requires solutions for designing and fabricating integrated input and output capabilities. Rich materials require design and fabrication approaches to customize a diverse set of object properties, e.g. geometry, deformability (softness & stretchability), and visuo-haptic feedback (surface roughness, visual appearance).

In consequence, this thesis focuses on addressing the following three challenges regarding the digital fabrication of interactive objects with rich materials, illustrated in Figure 1.2.

Challenge 1: High-level Digital Design

The first challenge is **reducing the complexity of manually designing interactive objects with rich materials**. The design of 3D objects grows more complex with added functionality and custom material properties. Examples include designing necessary integrated electronics or detailed geometrical structures for desired material behavior. Traditional modeling software, however, offers little support for such tasks. Advanced software to design electronics, for example, is often geared towards expert designers and requires extensive knowledge and experience.

In contrast, computational design tools offer an interface to specify desired high-level properties of a design. Such approaches have facilitated design in a variety of domains, including designing mechanical mechanisms [34, 80, 81], structurally sound furniture [115, 185], or 4D-printed object geometries [4, 227]. High-level digital design of interactive objects with rich materials, however, has been left largely unaddressed.

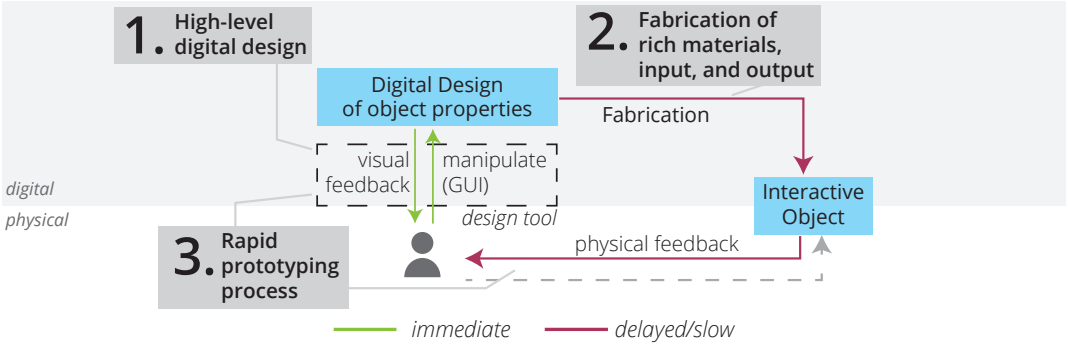

Figure 1.2: Challenges within the digital fabrication process of custom interactive objects with rich materials.

The high-level digital design of interactive objects has been limited to a few examples, e.g. designing objects with embedded deformation sensors [7] or designing objects that are folded from printed electronics [148]. These approaches enable designing interactive objects that are deformable or bendable but not designing custom rich materials. In addition they offer a limited set of supported modalities and materials, e.g. they do not support designing custom tactile output or custom stretchability.

Designing objects with custom material properties has been explored more extensively. Approaches have enabled designers to specify desired properties, including softness [17, 196], deformation behavior [81], or surface texture [211]. The object's geometry or material composition is then generated to match the target specification, e.g. through optimization [17, 81, 196]. These approaches reduce the complexity of designing custom material properties but do not incorporate interactivity.

Addressing the **design of custom interactivity and custom rich materials** is thus a major challenge towards the high-level digital design of interactive objects with rich materials. On the one hand, high-level design approaches need to ensure the compatibility of electronics with the designed material properties. For example, soft and stretchable interactive objects require stretchable electronics while most current approaches are limited to rigid [192] or flexible electronics [7, 148]. On the other hand, the high-level design needs to account for dependencies between interactivity and material properties. For example, increasing stretchability may reduce a material's conductivity and thus affect generated circuits.

Challenge 2: Fabrication Support of Rich Materials and Interactivity

The second challenge is **facilitating the physical fabrication of custom interactive objects with rich materials**. This includes extending designers' capabilities to digitally fabricate objects of custom interactivity and rich materials and increasing accessibility and fabrication speed.

Prior work has presented approaches to fabricate interactive objects with various input and output capabilities. However, these approaches were either limited in terms of supported geometries or materials, too slow for quick iterations during rapid prototyping, or inaccessible due to required equipment, materials, or skills.

Accessible approaches for input and output on 3D objects have been realized through 3D-printing. Touch and deformation input have been enabled through printing conductive and non-conductive materials [193, 192, 194] and output by printing light pipes [244]. 3D-printing supports doubly-curved geometries but is slow and limited to printed plastics. Accessible approaches with faster fabrication have been realized through folding 3D geometries from 2D sheets [148, 249]. They offer touch and deformation input through printed sensors and display output through printed EL displays [148] or attached LEDs [249]. While folding objects is fast and offers versatile input and output capabilities, it is limited to foldable geometries and thin sheet-based materials. Similar modalities as enabled by approaches using folding have been realized while supporting stretchable materials by approaches based on casting silicone [142, 242]. The fabrication process, however, is slow and complex, relies on manual skills, and offers limited support for complex 3D geometries.

Research in material science offers an additional direction towards fabricating custom electronics compatible with object geometries and rich material properties. Examples include stretchable and soft conductors [76, 124] or printing conductors on varied materials and non-developable geometries [2, 87, 257]. While the presented results are promising for creating interactive objects with rich materials, they leverage sophisticated machinery, processes, and inks. Examples include fabrication steps such as spin-coating [76], curing in a nitrogen oven [76], or UV–ozone treatment [124]. In contrast, **accessible fabrication approaches** should be easily replicated by researchers and makers with their commonly available equipment, e.g. in a fabrication lab or maker space.

In addition to supporting geometries and materials, a challenge is extending digital fabrication approaches to **support further input and output modalities**. For example, display output has been limited to slightly-curved geometries [148, 242, 244] and the digital fabrication of tactile output was left unaddressed so far.

Consequently, novel approaches are required for extending designers' capabilities to digitally fabricate objects with custom interactive elements and rich material properties. They shall be accessible, offer additional modalities, and support rich materials.

Challenge 3: Rapid Prototyping Process for Interactive Objects with Rich Materials

The third challenge is **enabling rapid prototyping of interactive objects with rich materials**. While the previous two challenges focused on facilitating high-level digital design and improving fabrication in terms of accessibility and capabilities, this challenge focuses on reducing the required time to reach a satisfying result, e.g. through faster or fewer iterations.

In the classical digital fabrication process, the designer relies on digital design followed by physical fabrication. The designer uses a design tool to create and adapt the digital design. After design, the object is fabricated and inspected by the designer. Additional iterations then repeat the process starting with adapting the digital design. The speed at which the designer can iterate thus largely depends on the time required by the fabrication process to produce a physical object to inspect

and verify the result. The number of iterations, on the other hand, is affected by the digital design capabilities, i.e. whether the designer received feedback to anticipate the fabricated result and has the ability to manipulate the design to implement desired changes.

Research has contributed approaches for the rapid prototyping process in both regards. One stream of research has investigated increasing the fabrication speed to enable faster iterations, for example through rapid fabrication of tangible design representations [16, 137, 136, 139, 234]. Improving feedback and manipulation during digital design, has been addressed through incorporating physical elements in the process. For example, hands-on shaping geometry from malleable material [94, 187, 234] or annotating modification on physical proxy objects [187, 199] aim to provide improved manipulation capabilities. Tangible tools [233] or augmented reality [156, 235] have been used to improve feedback when designing 3D geometries.

While prior work demonstrated promising directions for improving the digital fabrication process of custom geometry, the design and fabrication of interactive objects with rich materials remains largely unaddressed. This leaves important open challenges. One the one hand, fabrication of interactive elements and rich materials complicates the fabrication process. It is thus a challenge to **speed up the fabrication process of interactive objects with rich materials to allow for rapid iterations**. On the other hand, the design of interactivity and rich materials offers additional challenges for manipulation and feedback. For example, visual feedback and 2D manipulation, e.g. via screen, mouse and keyboard, are most likely insufficient for designing custom tactile feedback or specifying the desired stretchability of an object. It is thus a challenge to **improve feedback and manipulation during design of interactive objects with rich materials, to reduce the number of required iterations**.

1.2 Contributions

This thesis contributes a series of four novel design and fabrication approaches for interactive objects with rich materials that advance the fields of digital fabrication, rapid prototyping, and ubiquitous computing. **The contributions enable easy, accessible, and versatile design and fabrication of custom interactive objects**:

- **with extended support for custom geometries and materials.** This thesis contributes accessible approaches for interfaces with custom stretchability, shape, and compliance. It further contributes the first approach for interfaces with multiple seamless areas of custom stretchability.
- **with advanced input and output capabilities.** This thesis contributes a novel digital fabrication approach for tactile output on 3D geometries. It presents an approach for input and output on stretchable interfaces and an approach to embed capabilities for shape and compliance change in objects. It further extends existing technologies for touch input and display output to support rich materials, including support for strong doubly-curved geometries, fine-detailed surface structure, and diverse materials.

- **with high-level digital design through computational models and parametric patterns.** This thesis contributes novel approaches for high-level digital design of stretchable circuits, tactile input and output on 3D geometries, and embedded capabilities for shape and compliance change.
- **with an enhanced rapid prototyping process.** This thesis presents approaches to increase fabrication speed for rapid prototyping and approaches that leverage the interactivity of the fabricated object to ease digital design and reduce the number of required iterations.

The contributions of this thesis are situated in a space at the intersection of interactive objects, rich materials, rapid prototyping, and digital fabrication. This space spans several dimensions, including properties of rich materials, input modalities, and output modalities. As orthogonal dimension to these capabilities, the space spans the three challenges to address high level digital design, fabrication support, and enhancing the rapid prototyping process (illustrated in Figure 1.3).

Rich materials

Everyday objects offer a large range of diverse geometries and material properties, e.g. organic geometries [74], softness, or fine-detailed surface structure. In the context of this thesis, we use the term rich materials when referring to such geometries and materials. In particular, this thesis focuses on three aspects of rich materials that go beyond simple geometries, rigid objects, and plain materials:

First, it focuses on interfaces on *complex geometries*. Complex geometries are strong doubly-curved (non-developable) or offer filigree details. Examples of such geometries include round and spherical objects or geometries with holes or fine details, e.g. as present in jewelry. Second, this thesis focuses on *deformable materials* that are soft or stretchable. These materials offer new dimensions for interaction beyond common touch interaction on rigid surfaces. Third, this thesis focuses on materials with distinct *surface structure* that offers visuo-haptic feedback, e.g. commonly found in natural materials such as wood or stone.

Input modalities

Related work has demonstrated numerous input modalities in the context of rapid prototyping interactive objects, including touch input [51, 147, 190, 192], pressure input [51, 77], and deformation input [7, 193, 198]. The contributions in this thesis focus on touch and deformation-based input. *Touch input* is a key modality as it is commonly used in prototyping and current interaction devices, e.g. smart phones or tablet computers. *Deformation-based input* on the other hand is of key relevance to leverage rich material properties for interaction, e.g. softness and stretchability through bend or stretch sensing.

Output modalities

Output modalities presented in related work range from visual output via displays [148, 242], over auditory [82, 146] and haptic feedback [90, 109, 155], to shape change as a means for actuation [71, 148] and visual feedback [31]. The contributions

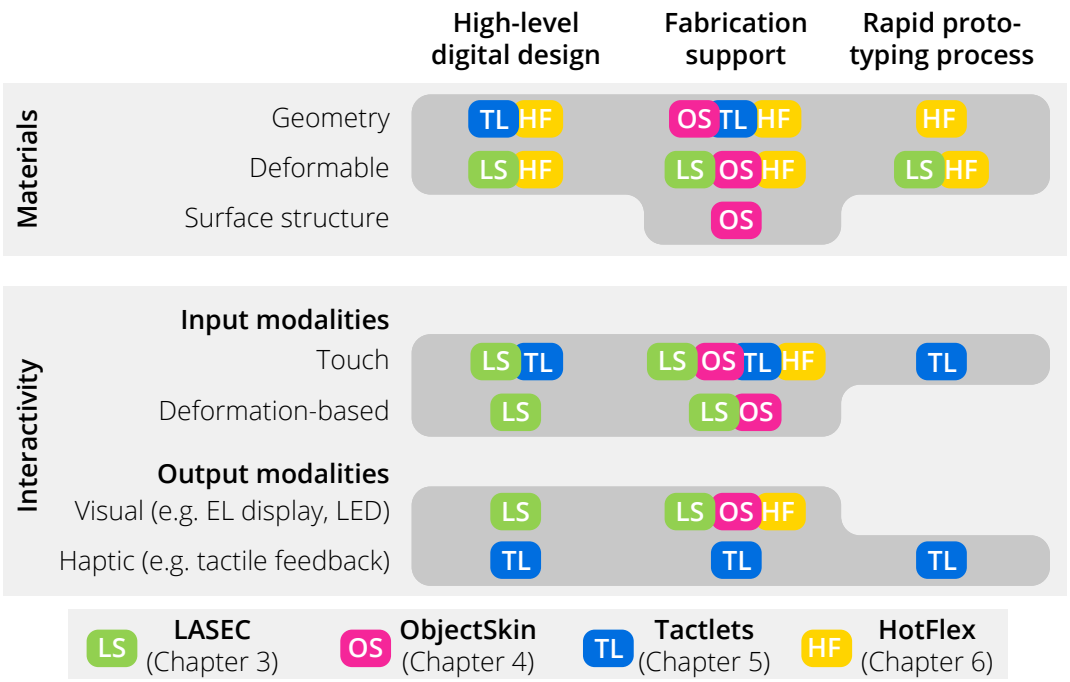

Figure 1.3: Each chapter of this thesis addresses key points in a design space at the intersection of rich materials, interactive objects, and rapid prototyping through digital design and fabrication.

of this thesis focus on visual and haptic output. *Visual feedback* is a common modality available in many interfaces and devices. This includes high-resolution displays in smart phones, segmented number displays, or simple visual feedback in the form of notification LEDs. Computer-controlled *haptic output*, on the other hand, is less common. Haptic output has been demonstrated using various means, including mechanical actuation [88], compliance change [134], or tactile stimulation [12, 18, 109]. This thesis explores tactile feedback which has been shown to enhance touch interfaces [64, 111, 143] and compliance change as a haptic output means based on rich material, i.e. a material's softness.

Together, the contributed approaches of this thesis cover key points of this space. Each approach focuses on certain object properties and interaction modalities while addressing the challenges introduced earlier, as illustrated in Figure 1.3.

As we present the four contributions in this thesis, we will refer to this design space to illustrate the key points that are covered. At the same time, we will step-by-step explore how to enhance the design and fabrication process for interactive objects (Figure 1.2) compared to the process for static objects of custom geometry (Figure 1.1). We will further discuss how each solution addresses the three challenges above, as illustrated in Figures 1.4 through 1.7.

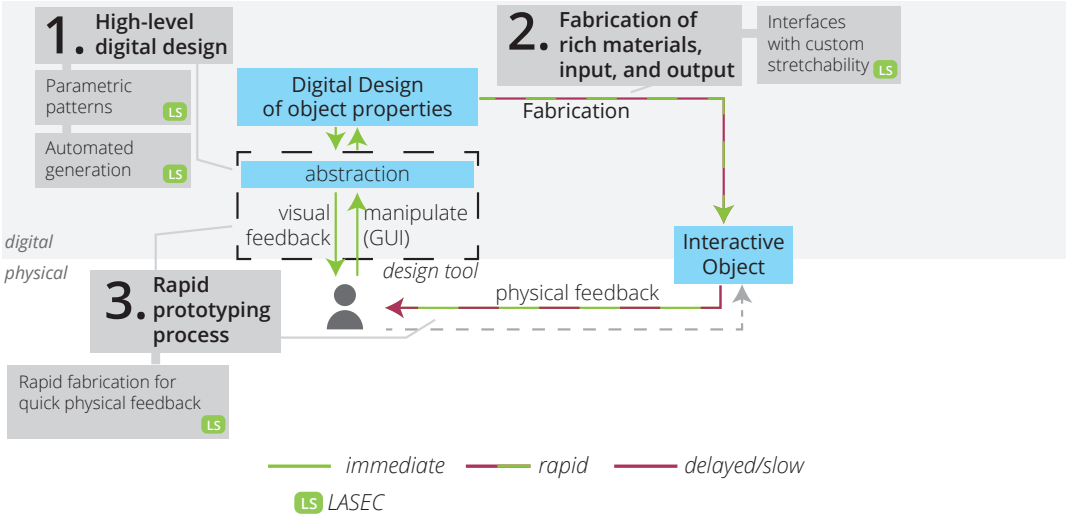

Figure 1.4: Illustration of the design and fabrication process and the contributions of *LASEC* (Chapter 3).

1. LASEC: Rapid Design and Fabrication of Stretchable Interfaces

The first contribution of this thesis, *LASEC*, focuses on interactive objects with rich materials of custom *stretchability*. Stretchability is a promising property for interaction with objects beyond touch on rigid surfaces, as it has proven to enable a wide range of novel interactions, e.g., with smart textiles [154, 224], with skin-overlays on the body [236], or with deformable physical devices [214]. However, the design and fabrication of interfaces with custom stretchability remain difficult. With *LASEC*, this thesis contributes a novel approach enabling high-level design and rapid fabrication of interfaces with custom circuitry and custom stretchability.

LASEC is the first technique for instant do-it-yourself fabrication of circuits with custom stretchability on a conventional laser cutter and in a single pass. The approach is based on integrated cutting and ablation of a two-layer material using parametric design patterns. These patterns enable the designer to customize the desired stretchability of the circuit, to combine stretchable with non-stretchable areas, or to integrate areas of different stretchability. For adding circuits on such stretchable cut patterns, this thesis contributes routing strategies and a real-time routing algorithm. An interactive design tool assists designers by automatically generating patterns and circuits from a high-level specification of the desired interface. The approach is compatible with off-the-shelf materials and can realize transparent interfaces. It is also versatile and can be used for applications in various domains, including wearable computing, interactive textiles, and stretchable input devices.

This contributions of this thesis regarding *LASEC* enhance the design and fabrication process of interactive objects with rich materials. Figure 1.4 illustrates the contributions regarding the three challenges introduced earlier. It also illustrates the high-level contribution of the *LASEC* approach: facilitating and speeding-up the

design and fabrication of interfaces with custom circuitry and custom stretchability (fabrication speed is indicated by color in Figure 1.4).

High-level digital design (Challenge 1) The design tool enables high-level digital design of stretchable circuits by abstracting from low-level fabrication parameters. It uses parametric patterns for stretchability and implements a novel approach for real-time routing on stretchable circuits to automatically generate low-level design files for fabrication. In addition to stretchability, the tool supports versatile input and output modalities through integrating conventional electrical components (illustrated as key points in Figure 1.3).

Fabrication support (Challenge 2) The novel approach for instant fabrication of stretchable circuits using a standard laser cutter facilitates the fabrication of stretchable circuits and makes it more accessible. In addition, the novel approach enables interfaces with multiple areas of custom stretchability extending the set of digitally fabricated material properties for interactive objects.

Rapid Prototyping Process (Challenge 3) Instant fabrication enables designers to get hands-on feedback on the designed stretchability throughout the iterative design process by rapidly designing and fabricating prototypes. This improves the rapid prototyping process towards rapid prototyping of custom shape and stretchability, as key points in the design space (Figure 1.3).

2. ObjectSkin: Augmenting 3D Objects of Rich Materials with Custom Interfaces

Moving from 2D to 3D, the second contribution of this thesis, *ObjectSkin*, explores the digital fabrication of interactive objects of complex 3D geometries and diverse materials. Pioneering work has explored the design and fabrication of interactive 3D objects of simple shape (e.g. developable [148]) and plain materials (e.g. 3D-printed plastic [21, 192, 244]). Everyday objects, however, commonly exhibit strongly-curved geometries and diverse materials. To enable interfaces on this richer variety of objects, this thesis explores the boundaries of adding input and output capabilities to everyday objects. To this end, *ObjectSkin* contributes a versatile approach to augment existing objects through fabricating conformal thin-film overlays.

ObjectSkin is a fabrication technique for adding conformal interactive surfaces to rigid and flexible everyday objects. It enables multi-touch sensing and display output that seamlessly integrate with highly curved complex geometries. The approach is based on a novel water-transfer process for interactive surfaces. It leverages off-the-shelf hobbyist equipment to fabricate thin, conformal, and translucent electronic circuits that largely preserve the surface characteristics of everyday objects. It offers two methods, for rapid low-fidelity and versatile high-fidelity prototyping, and is applicable to a wide variety of materials. This thesis presents results from a series of technical experiments that provide insights into the supported object geometries, compatible object materials, and robustness. This thesis further presents seven example cases that demonstrate how *ObjectSkin* makes it possible to leverage

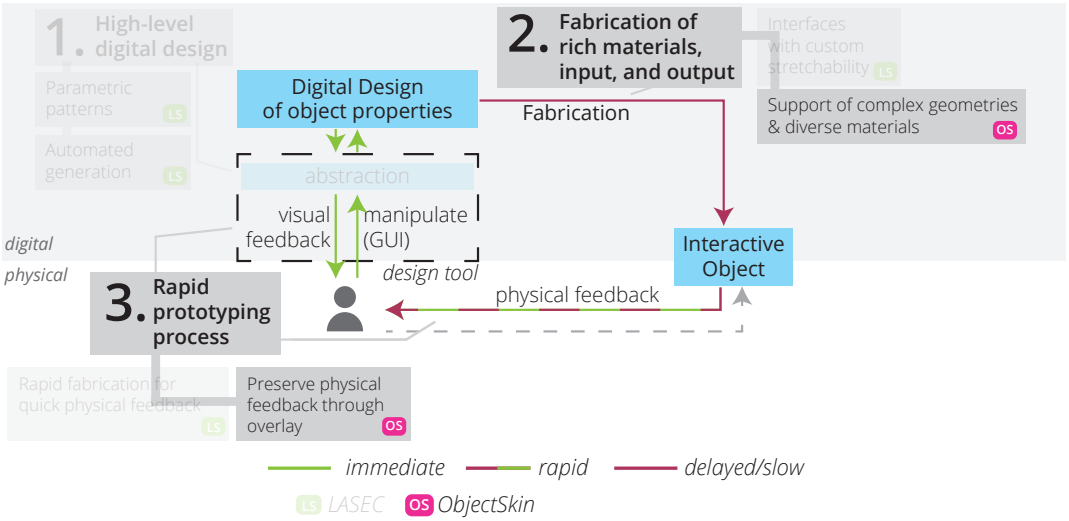

Figure 1.5: Illustration of the design and fabrication process and the contributions of *ObjectSkin* (Chapter 4).

geometries, surface properties, and unconventional objects for prototyping novel interactions for ubiquitous computing.

ObjectSkin explores augmenting existing objects with interactivity through fabrication of conformal thin-film overlays. It addresses two of the challenges introduced above, as illustrated in Figure 1.5.

Fabrication support (Challenge 2) The novel fabrication approach enables printing custom-shaped touch sensors and electroluminescent (EL) displays onto objects of strong double curvature and a wide range of materials, including flexible material (key points in Figure 1.3). This expands the object geometries and materials supported for fabricating custom interactive objects and allows for novel interaction. For example, surface structure, object holes, and unconventional objects may be leveraged for interaction. It also allows for a tighter integration of sensing and output compared to *LASEC*, by using thin, conformal overlays instead of rigid components.

Rapid Prototyping Process (Challenge 3) In contrast to fabricating objects from scratch, as in *LASEC*, *ObjectSkin* explores augmenting existing objects with interactivity. It enables the designer to explore the rich material of an already existing object before deciding where to place interactive elements. The thin and conformal overlays then add interactivity after fabrication while largely preserving the object's surface characteristics. The approach thus enhances the rapid prototyping process through physical exploration of the resulting object during design.

3. Tactlets: Design and Fabrication of Tactile Interfaces on 3D Objects

Moving beyond visual feedback as an interactive output modality, the third contribution of this thesis, *Tactlets*, explores designing and fabricating computer-controlled

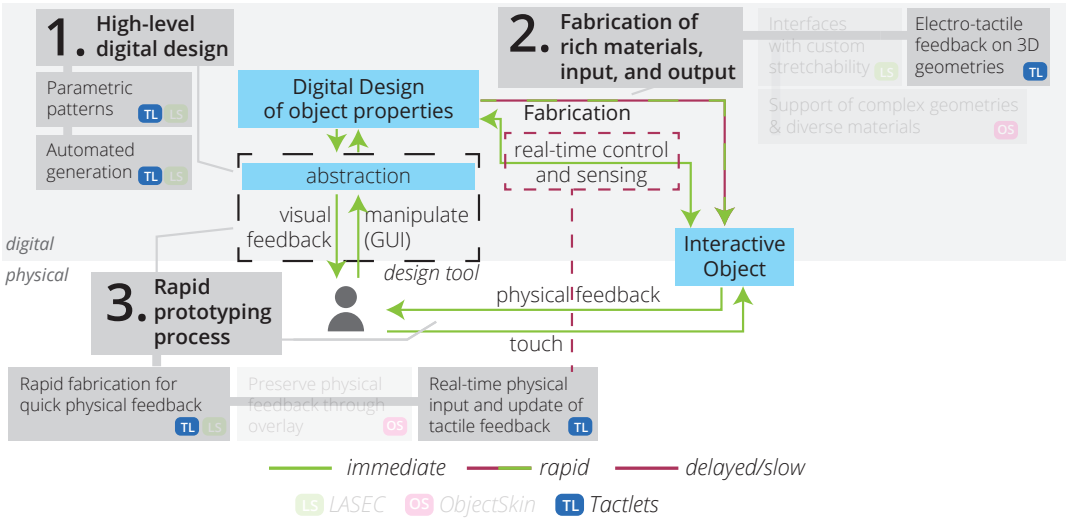

Figure 1.6: Illustration of the design and fabrication process and the contributions of *Tactlets* (Chapter 5).

haptic feedback on 3D objects. Embedding haptic or tactile feedback in objects has been widely used to increase the user experience and interaction capabilities of mobile and physical computing devices [131]. For example, haptic feedback is utilized to offer physical feedback for visual controls [64, 143, 160, 252, 253, 263] and icons [18, 132] or for rendering virtual textures and geometric features [12, 111, 173]. However, fabricating custom interactive objects that include computer-controlled tactile output still relies on manually assembling conventional components [88, 155]. Moreover, the rather large form factors of typical motors and mechanical actuators tend to be incompatible with demanding object geometries. To address these challenges, this thesis contributes a novel digital design and fabrication approach for conformal haptic interfaces on 3D objects.

With *Tactlets*, this thesis presents a novel digital fabrication approach for printing custom, high-resolution controls for electro-tactile output with integrated touch sensing on interactive objects. It supports curved geometries of everyday objects. One contribution is a design tool for modeling, testing, and refining tactile input and output at a high level of abstraction, based on parameterized electro-tactile controls. A second contribution is an inventory of 10 parametric Tactlet controls that integrate sensing of user input with real-time electro-tactile feedback. This thesis presents two approaches for printing Tactlets on 3D objects, using conductive inkjet printing or FDM[2] 3D printing. It further presents empirical results from a psychophysical study and findings from two practical application cases confirming the functionality and practical feasibility of the Tactlets approach.

The contributions regarding *Tactlets* address the three challenges introduced earlier, illustrated in Figure 1.6.

High-level digital design (Challenge 1) The Tactlets design tool enables high-level design of desired tactile input and output capabilities on a 3D object model

2 Fused Deposition Modeling

(illustrated as key points in Figure 1.3). The abstract design is enabled by the inventory of parametric Tactlet controls and through automatic generation of low-level printable designs.

Fabrication support (Challenge 2) The novel fabrication approach expands the possible capabilities of digitally fabricated interactive objects. It enables printing conformal, high-resolution controls for tactile input and output that are compatible with demanding object geometries. This enables interaction to leverage object geometries, for example, input controls on a distinct edge of an object as tactile guidance.

Rapid Prototyping Process (Challenge 3) Last, *Tactlets* offers a new approach for tangible feedback and manipulation during design. Instead of iteratively fabricating prototypes and subsequently testing the design, as in *LASEC*, *ObjectSkin*, and classical iterative prototyping, *Tactlets* leverages the interactivity of the fabricated object to enhance the design process. To this end, the *Tactlets* design tool offers live control of the object's tactile feedback capabilities and real-time touch sensing on the fabricated object (illustrated in Figure 1.6). This enables real-time exploration and hands-on refinement of the design instead of fabricating a new prototype to implement design changes.

4. HotFlex: Fabricating Objects with Customizability of Shape and Compliance

Beyond computer-controlled visual and haptic output elements, e.g. as in *ObjectSkin* and *Tactlets*, the fourth contribution of this thesis, *HotFlex*, focuses on computer-controlled change of physical shape and material properties. *HotFlex* explores a novel class of interactive objects with embedded capabilities for on-demand customization of their shape and compliance. While prior work has focused on digitally designing and then fabricating interactive objects of custom shape, this novel class of objects can be physically adapted *after* fabrication. It thus enables customization decoupled from the initial design and fabrication without requiring special skills or prior knowledge. To this end, this thesis contributes a novel fabrication approach for on-demand shape and compliance change for 3D objects.

HotFlex is a new approach allowing precisely located parts of a 3D object to transition on demand from a solid into a deformable state and back. This approach enables intuitive hands-on remodeling, personalization, and customization of a 3D object after it is printed. This thesis introduces the approach and presents an implementation based on computer-controlled printed heating elements that are embedded within the 3D object. It further presents a set of functional patterns that act as building blocks and enable various forms of hands-on customization. This thesis also demonstrates how to integrate sensing of user input and visual output in *HotFlex* objects. To demonstrate the practical feasibility of the approach, this thesis presents a series of technical experiments and various application examples.

HotFlex explores computer-controlled hands-on customization of an object's shape and compliance. The contribution regarding *HotFlex* address the challenges introduced above, as illustrated in Figure 1.7.

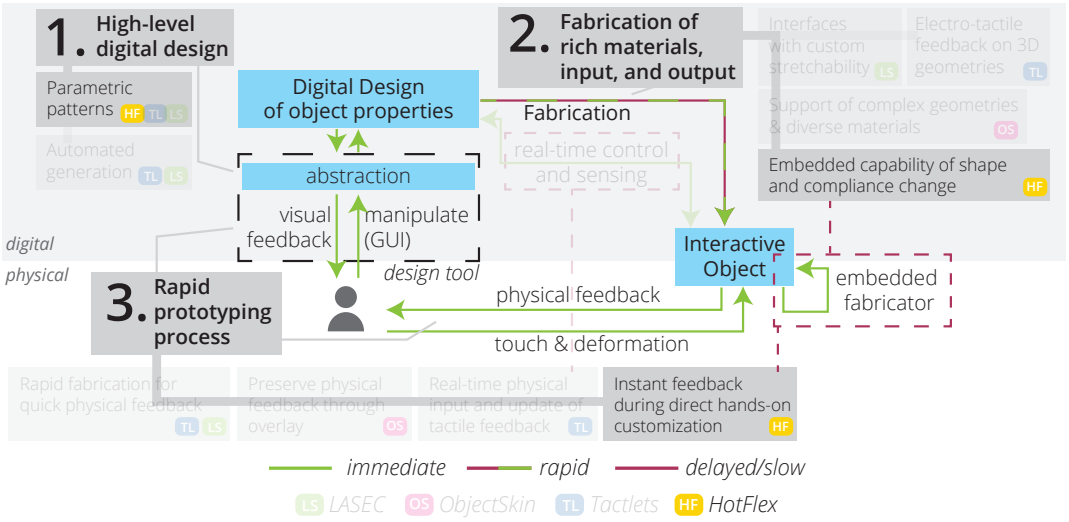

Figure 1.7: Illustration of the design and fabrication process and the contributions of *HotFlex* (Chapter 6).

High-level digital design (Challenge 1) The set of structural primitives and functional patterns facilitate the digital design of HotFlex objects. Four structural primitives give guidance on what form of customizability can be embedded. Functional patterns abstract from low-level complexity by realizing one specific type of object customization, in terms of shape or compliance (Figure 1.3), as reusable parameterized components.

Fabrication support (Challenge 2) *HotFlex* extends the fabrication possibilities of interactive 3D objects using an accessible approach. Embedding the computer-controlled composite structure enables custom objects capable of on-demand shape-change and compliance change using conventional printers and off-the-shelf hardware components. It further allows to finalize the fabrication by customizing the object without access to a fabrication device. In addition to custom shape and compliance, the *HotFlex* fabrication approach enables integration of touch sensing and display output (key points in Figure 1.3).

Rapid Prototyping Process (Challenge 3) *HotFlex* enables hands-on customization of an object's shape and compliance to provide tangible feedback and direct manipulation. To this end, the approach offers a different perspective on the design and fabrication process of interactive objects. Instead of designing the final object in an iterative cycle of design and fabrication, e.g. as in *LASEC*, the design incorporates a certain degree of customizability. The object is then finalized after fabrication, e.g. by adapting it's shape to fit the user's body.

1.3 Publications

The work of this thesis has been published at international peer-reviewed conferences and journals in the field of fabrication technologies and rapid interface

prototyping as subfields of Human–Computer Interaction (HCI). The research has been published as two full papers the ACM Conference on Human Factors in Computing Systems (CHI) [P1, P3], one full paper at the ACM Symposium on User Interface Software and Technology (UIST) [P4], and one journal article in the Proceedings of the ACM on Interactive, Mobile, Wearable and Ubiquitous Technologies (IMWUT) [P2].

P1. **Daniel Groeger**, Elena Chong Loo, and Jürgen Steimle. 2016. *HotFlex: Post-print Customization of 3D Prints Using Embedded State Change.* In Proceedings of the 2016 CHI Conference on Human Factors in Computing Systems (ACM CHI '16). **ACM CHI 2016 Honorable Mention Award**

P2. **Daniel Groeger** and Jürgen Steimle. 2018. *ObjectSkin: Augmenting Everyday Objects with Hydroprinted Touch Sensors and Displays.* In Proceedings of the ACM on Interactive, Mobile, Wearable and Ubiquitous Technologies, Vol. 1, No. 4 (Jan. 2018)

P3. **Daniel Groeger** and Jürgen Steimle. 2019. *LASEC: Instant Fabrication of Stretchable Circuits Using a Laser Cutter.* In Proceedings of the 2019 CHI Conference on Human Factors in Computing Systems (ACM CHI '19).

P4. **Daniel Groeger**, Martin Feick, Anusha Withana, and Jürgen Steimle. 2019. *Tactlets: Adding Tactile Feedback to 3D Objects Using Custom Printed Controls.* In Proceedings of the 32nd Annual ACM Symposium on User Interface Software and Technology (ACM UIST '19).

In addition to the main publications, the author has contributed to the following relevant publication which developed the technical solution that underlies the work on *Tactlets*:

P5. Anusha Withana, **Daniel Groeger**, and Jürgen Steimle. 2018. *Tacttoo: A Thin and Feel-Through Tattoo for On-Skin Tactile Output.* In Proceedings of the 31st Annual ACM Symposium on User Interface Software and Technology (ACM UIST '18).

1.4 Structure of this thesis

This thesis is structured into seven Chapters, as follows:

- **Chapter 2** provides an overview of the state-of-the-art in the fields of digital fabrication technologies, rapid prototyping of interactive objects, and computational design.
- **Chapter 3** presents *LASEC*, a novel digital design and fabrication approach for interfaces with custom circuitry and custom stretchability.
- **Chapter 4** presents *ObjectSkin*, a novel approach to augment existing objects of strongly curved geometries and diverse materials with conformal touch sensors and displays.

- **Chapter 5** presents *Tactlets*, a novel approach for the digital design and fabrication of tactile input and output controls on 3D objects.
- **Chapter 6** presents *HotFlex*, a novel approach to create custom interactive objects with embedded capabilities for hands-on customization of geometry and compliance.
- **Chapter 7** concludes this thesis with a summary and discussion of the presented contributions and an outlook at future work.

2 State of the art

This thesis is related to research in three main fields: digital fabrication technologies, rapid prototyping of physical user interfaces, and digital design for fabrication. This chapter provides an overview of relevant related work in these fields.

We start by presenting the background of digital fabrication technologies as well as related work on approaches to realize custom rich materials and custom electronics. Next, this chapter will discuss related work on rapid prototyping of physical user interfaces. The goal of this section is to provide an overview of the possible input and output modalities of custom physical interfaces and how they have been realized in prior work. The third section then presents related work on approaches to enhance the digital design. It discusses approaches for computational high-level design and related work on improving manipulation and feedback during digital design. Last, we will discuss conclusions of this chapter.

2.1 Digital fabrication of geometries, materials, and electronics

Digital fabrication involves a computer-controlled machine fabricating a physical object based on a digital design. This process originates from the early development of computer numerical control (CNC) in the 1950s, when researchers at the Massachusetts Institute of Technology (MIT) started using digital computers to control fabrication machines [178].

Digital fabrication initially involved subtractive fabrication processes. These processes produce custom geometry by selectively removing material from a workpiece, e.g. a solid block of material. Examples of subtractive fabrication devices include milling machines, lathes, and laser cutters.

The development of additive manufacturing, or commonly referred to as *3D printing*, added new digital fabrication capabilities in the 1980s [79]. Additive processes build an object layer by layer which can produce internal structures. This is an advantage over subtractive processes. For example, joints or hinges can be 3D-printed as a finished assembly in one process, while subtractive fabrication requires fabricating and assembling multiple parts.

Gershenfeld describes this development as part of a new "Digital Fabrication Revolution", which is centered around the "ability to turn data into things and things into data" [48, p. 44]. In contrast to mass manufacturing, digital fabrication offers the ability to produce physical items from a digital model in low volume.

This enables custom one-off production using precise machines instead of manual crafting.

This revolution seems to become reality, as fabrication devices become affordable and their adoption increases. Today, a large selection of digital fabrication machines are readily available. Examples include desktop milling machines, laser cutters and 3D-printers, all available below $500 [14, 254, 114, 127]. An increase in adoption is indicated by the sales of desktop 3D printers that have steadily increased for the past years, although the initial growth (doubled every year until 2015 [246]) has slowed down in recent years [247].

A full survey of research on digital fabrication at a large is beyond the scope of this thesis. This thesis focuses on rapid prototyping of interactive objects with rich materials. Thus, this section will discuss digital fabrication technologies in the context of rapid prototyping and will focus on related work on fabricating objects of custom rich materials and fabricating custom electronics. Regarding materials, this section will particularly focus on the aspects covered in this thesis: custom geometries and deformation properties. As a basis for this discussion, this section will first provide background information on digital fabrication of custom 3D objects.

2.1.1 Background on digital fabrication of custom 3D objects

The early development of digital fabrication technologies, e.g. CNC milling machines, focused on automating the fabrication of custom parts, i.e. objects of custom shape, using subtractive fabrication [178].

Subtractive fabrication selectively removes material from a *workpiece*, commonly a block or sheet of material. For a CNC mill, the workpiece is attached to a table underneath the machine tool. The machine tool, usually a rotary cutting tool, removes material while the machine changes the relative position between the workpiece and the tool in three dimensions (X, Y, and Z). CNC mills typically use a moving table in the X and Y dimensions and a machine tool moving linearly on the Z axis.

This principle is similar across many different subtractive techniques and machines, although details vary. 5-axis mills, for example, add two additional rotational dimensions allowing for more complex geometries to be fabricated. CNC routers have the workpiece mounted on a fixed table, while the cutting spindle in mounted on a gantry system allowing movement in X, Y, and Z direction. This allows to work on larger workpieces but is commonly designed for flat materials offering less movement in the Z dimension than CNC mills. Laser cutters use a focused laser beam to remove material e.g. by melting, burning, or vaporizing, instead of a rotating cutting tool. Cutting plotters, on the other hand, use a cutting blade that is moved across the workpiece, usually a material in a flat form factor like paper.

Additive manufacturing approaches, e.g. 3D printing, were first developed in the 1980s, with stereolithography (SLA) being the first technique being patented in 1986 [79]. Since then, a range of additive technologies have been developed that use

the same principle of building an object layer by layer. One accessible technology commonly used for rapid prototyping and also used in this thesis is fused deposition modeling (FDM).

Fused deposition modeling (FDM), also called Fused Filament Fabrication (FFF), was developed in 1988 [30]. The technology creates object geometries by heating plastic material beyond its melting point and selectively extruding it. The hot material is extruded onto a flat print bed, where it cools down and solidifies to form a solid layer of material. The material is extruded by a print head that moves in X and Y direction to form a desired pattern. Once a layer is finished, the print bed moves in Z dimension and the next layer is added. FDM is a versatile technology. It supports a large selection of materials [1] including conductive materials [164], and offers the ability to print multiple materials, e.g. through dual-extrusion setups.

In industry *formative processes* are commonly used in addition to subtractive and additive technologies. Formative processes form a material into a desired shape, e.g. by injection molding, stamping, or pressing. However, these processes are typically used for classical fabrication rather than digital fabrication. Creating a custom geometry from a digital design via injection molding, e.g., commonly depends on fabricating a mold first using either additive of subtractive fabrication. Yet, processes proposed by research may incorporate formative elements, as discussed below.

2.1.2 Fabricating custom geometry

3D-printing offers a powerful means to create custom 3D geometries. Examples are myriad and on-line platforms such as thingiverse[1] offer a large selection[2] of 3D models. These models feature diverse geometries and are designed for various purposes, including functional objects like phone cases and artistic objects, e.g. a bust, but commonly are designed to be 3D-printed within the limits of commodity FDM printers. Research has explored extending the fabrication of geometries beyond these limits and toward new scales.

One stream of research has investigated rapid fabrication of large scale structures. For example, Luo *et al.* [129] presented an approach to realize objects the size of furniture (Figure 2.1b). They partition a given 3D model into 3D-printable parts and generate necessary connectors. The parts can then be printed individually and assembled. Fabricating even larger structures using a commodity 3D printer has been presented by Kovacs *et al.* [115] (Figure 2.11). Their approach uses custom-printed connectors and common plastic bottles to rapidly fabricate structures on an architectural scale, e.g. a 2.5m bridge or a 5m high pavilion. The resulting structures can be strong enough to carry a person and can be assembled quickly.

A second stream of research has investigated how to extend fabrication capabilities of custom geometries towards supporting fine-detailed structures. In contrast to common 3D-printed objects of larger sizes, e.g. the handle of a coffee mug or a small button on a watch, such structures may affect the tactile feedback of a surface,

1 `https://www.thingiverse.com`

2 more than 1.5 million 3D models on thingiverse.com as of September 9, 2019 [133]

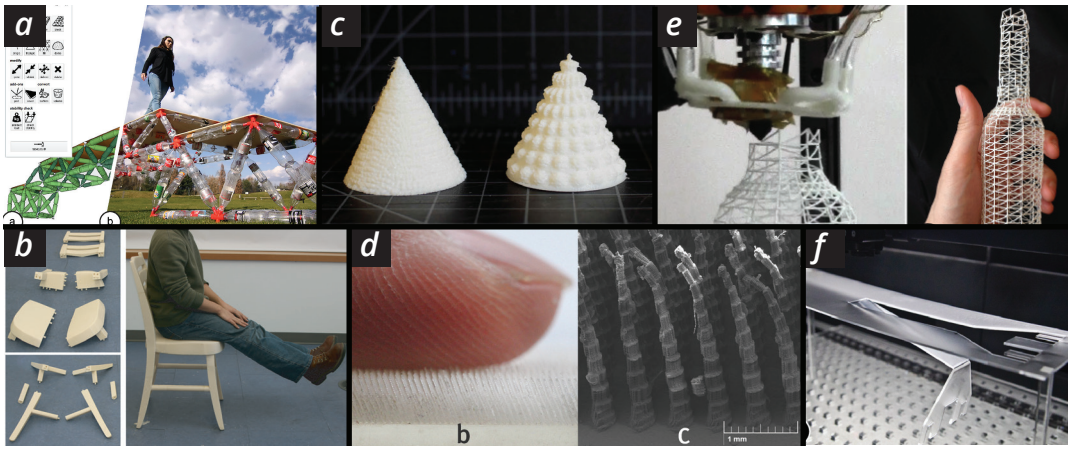

Figure 2.1: Related work on fabricating custom geometry has explored approaches to enable fabrication at new scales and to speed up the fabrication process. Large-scale structure have been fabricated from (a) existing objects and fabricated connectors [115] or (b) by partitioning the object into 3D-printable parts [129]. Small-scale structures have been realized by (c) FDM-printing 2.5D textures [211] or (d) SLA-printing hair-like structures [151]. 3D geometries can be fabricated at faster speeds compared to regular 3D printing by (e) printing wire frame structures [136] or (f) using rapid subtractive approaches that cut and bend a 2D sheet into a 3D geometry in an "origami"-like fashion [137].

e.g. comparable to the grain of wood or roughness of a stone surface. Approaches that fabricated such surface structure have been explored based on 3D printing [120, 151, 209, 211]. *HapticPrint* [211], for example, explores the use of patterns based on height maps to FDM print 2.5D tactile surface structure (Figure 2.1c). They study how identifiable different structures are by comparing detailed surface structure with coarser textures (e.g. iconic bumps or symbolic arrows). They show that a detailed surface structure is printable but provide little insights into parameters or possible feature scale. Also based on FDM printing, Takahashi *et al.* [209] investigate the effect of different printing parameters on expressiveness of FDM printing. Their technique is able to produce a set of surface structures, including detailed features that are described as "weaver-nest-like" or "hamper-like" by printing zig-zag or coil-like patterns [209]. Finer, hair-like structures are produced by an approach of Laput *et al.* [120]. Their approach leverages the stringing behavior of extruded plastic during FDM printing to produce thin hair-like structures or thicker bristles. An approach offering more precise control and higher resolution of such structure was presented by Ou *et al.* [151] (Figure 2.1d). Their approach is based on DLP[3] printing and a novel pixel-based generation of small-scale hair-like features. It offers control down to the individual DLP pixel (50 by 50 μm on the used Autodesk Ember device) and can produce fine-detailed structures on flat and curved surfaces.

3 digital light projector (DLP) printing is a variant of stereolithography (SLA). Stereolithography creates solid layers of material based on selectively curing a liquid photopolymer resin [79].

Rapid fabrication of custom geometry

One major drawback of 3D printing, e.g. compared to subtractive methods, is that it is typically slow, requiring multiple hours to create a physical object. Quickly iterating multiple times to achieve the desired geometry is thus not feasible. Research has presented different approaches for rapid fabrication, addressing this limitation.

One approach is to print low-fidelity wire frame structures [136, 159]. *WirePrint* [136], for example, proposed to generate 3D models that can be printed by extruding wires of material instead of layer by layer fabrication (Figure 2.1e). They demonstrated a speed-up factor up to 10 compared to typical layer by layer printing. Similarly, Peng *et al.* [159] propose to print wire frame structure. They present a novel 5-axis 3D printer allowing for coarser wire frames compared to *WirePrint* and thus an additional speed up.

A different stream of research explores 3D printing flat structures that morph into 3D geometries [4, 59, 228, 227], often referred to as *4D printing*. *Thermorph* [4], for example, 3D-prints a layered structure from thermoplastic polyurethane (TPU) and polylactide (PLA) material that leverages the shape memory effect of PLA. Once the flat printed structure is exposed to heat after printing, e.g. in hot water, it bends depending on the printed structure. *Thermorph* simulates the bending behavior and thus allows to print sheets that bend into desired 3D shapes. *4DMesh* [228] leverages a similar approach but focuses on mesh-like structures, while Wang *et al.* [227] present a similar approach based on morphing one-dimensional line structures. An alternative approach has been presented by Guseinov *et al.* [62]. They 3D-print rigid material onto pre-stretched fabrics. Once released, the fabric contracts and creates a desired 3D shape depending the printed pattern. They use simulation to determine the printed pattern based on a desired target geometry.

These approaches leverage the fact that additive fabrication processes are typically faster in the XY plane than in the Z dimension. This principle also applies for other additive and subtractive processes, as have been explored by related work. *Printflatables* [183], for example, presents a novel additive device that layers sheets of material and selectively welds them together. Based on the welding pattern, these multi-layer sheets form 3D structures when inflated. In contrast, *LaserOrigami* [137] uses subtractive laser cutting. The approach allows to cut and bend a sheet of acrylic at desired position by focusing or defocussing the laser respectively. Combining cutting and bending, allows to create 3D objects at a fast speed in an "Origami-like" fashion but is limted in terms of supported geometries (Figure 2.1f). *Kyub* [13] allows to create 3D objects based on assembling laser-cut plates. The approach allows models to be created from cube or tetrahedron based voxels. The approach then generates plates for laser cutting with fitting connectors and hinges based on the model. As an alternative, recent work by Mueller *et al.*[140] explores a formative fabrication process to increase fabrication speed. They use a robot arm for selectively heating and forming acrylic sheets into 3D geometries.

These approaches allow to increase fabrication speed as a trade-off for less supported geometries. This makes them suitable especially in early prototyping phases to design the coarse geometry of the object. For later prototyping of details, novel approaches are required that allow rapid fabrication and support complex and

detailed geometries. As an alternative, this thesis contributes a novel approach that allows to fabricate objects with embedded capabilities to modify their detailed shape (Chapter 6). This complements the approach of rapid prototyping though iterative fabrication by allowing hands-on customization of the detailed design after the object has been printed.

2.1.3 Fabricating objects of custom deformation properties

Deformation generally describes the difference between two geometric configurations of an object or material, e.g. induced by a load applied to it. In the context of this thesis, we thus refer to deformation properties as those properties that affect how an object or material can be deformed. This is mostly expressed by *compliance*, or also called *softness*, which includes the resistance to deformation (i.e. stiffness) and resistance to indentation (e.g. hardness) given an applied force. We may however, also refer to *flexibility* when describing a similar property of a sheet-like or rod-like material or object. Last, we may discuss *stretchability* as a special case related to compliance that is concerned with a material's ability to stretch. Making a distinction between compliance and stretchability may be relevant in cases where achieving stretchability is more complicated that achieving compliance or compression, e.g. in the case of custom electronics.

Flexible and soft objects can be made using different techniques. 3D printing, for example, supports elastic materials, e.g. Ninjaflex filament [44] for FDM printers. As an alternative, silicone allows to choose a desired softness depending on the used silicone mixture. Laser cutting silicone has been used by different approaches [128, 236, 142] while recently silicone has become available as a material for industrial 3D-printing [25]. Other approaches fabricate objects using soft material like yarns and textiles, e.g. by printing [78, 175], embedding in 3D prints [176], or stacking cut layers [158].

These techniques enable creating deformable objects, however, typically with uniform deformation properties. In contrast, creating custom deformation properties allows the designer to specify the desired properties for individual parts of the object. This, however, is more challenging.

Customizing softness of parts of the object is possible with advanced 3D printers that can mix materials to produce custom properties. Stratasys polyjet technology [204] for example, can mix multiple liquid polymers to achieve a spectrum of elastic properties. Such printers have been used to fabricate objects of custom softness [17]. However, they are expensive and not easily accessible. Other approaches have used specialized machines to create objects of custom softness [232, 258]. Zehnder *et al.* [258], e.g., inject a dopant material using a modified FDM printer into silicone objects to vary softness (Figure 2.2d).

Accessible fabrication equipment and materials have been used by approaches that rely on internal structures to create custom softness. HapticPrint [211], for example, modifies the infill pattern of an object printed with soft material on an FDM printer. In contrast, Schumacher *et al.* [196] rely on a single stiff material and achieve custom softness using solely microstructures (Figure 2.2a). Instead of material softness,

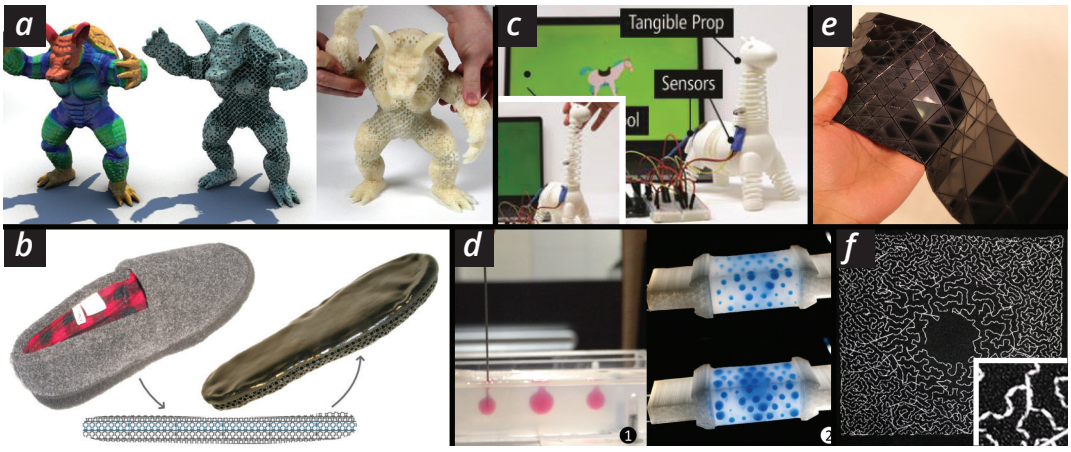

Figure 2.2: Custom deformation properties have been fabricated using additive and subtractive approaches. Approaches based on 3D-printing have realized custom softness through (a) printing mircostructures from a single stiff material [196] or (b) microstructures in combination with multiple materials of varying stiffness [17]. (c) 3D-printing springs allows to incorporate parts of custom stretchability inside objects [70]. (d) Using a modified 3D-printer, dopant material can be inserted into objects made from PDMS to achieve a desired softness [258]. For flat sheet-like materials (e) custom bending behavior can be achieved based on laser cutting a special compound material [24]. (f) Local control of stretchability can be achieved by sewing a yarn pattern into stretchable fabric [135].

fabricating custom stretchable elements have been demonstrated in very recent work by He *et al.* [70]. Their approach prints custom springs on an FDM printer to realize desired stretchability for selected parts of the object (Figure 2.2c).

For two-dimensional sheet-like objects approaches have been presented that allow for custom bend and stretch behavior. For instance, *FoldEm* [24] allows to control the bending behavior of a special layered compound material (Figure 2.2e). The material comprises layers of materials with different stiffness. Selectively laser-cutting the material at a specific depth allows to control the bending and folding behavior of the material. A general approach for making flexible 2D materials stretchable through cutting special patterns, often referred to as *Kirigami*, has been explored in material science and product design [60, 61, 53, 117, 118, 22, 231, 218]. The main principle is to cut a sheet so that the material deforms, e.g. buckles out-of-plane, at the cut locations when the sheet undergoes tensile strain. Depending on the cut, the achieved stretchability can be estimated, e.g. based on beam theory [22], or determined based on simulation, e.g. using finite element analysis [218]. Approaches using this technique have largely focused on uniform stretchability. In contrast, localized customization of stretchability has been explored in textiles by Moore *et al.* [135] using a computational approach (Figure 2.2f). They control the local stretchability of a stretchable fabric by sewing a special pattern of yarn, which results in less stretchable regions depending on the pattern.

This thesis contributes beyond prior work towards fabricating custom deformation properties in two aspects. First, it enables rapid fabrication of materials with multiple seamless areas of custom stretchability from different flexible base mate-

rials. Chapter 3 presents a novel approach that leverages cut patterns inspired by work in material science [60, 22, 218] to support user-defined areas with defined stretchability in one or multiple directions, seamless transitions between areas, and gradients of stretchability. Second, this thesis contributes towards creating objects with customized softness. Chapter 6 presents a novel approach to fabricate objects with embedded capabilities for hands-on customization of compliance. This approach allows the designer to incorporate areas with a varying degree of softness in the object model that the user can customize after initial fabrication.

2.1.4 Fabricating custom electronics

Digital fabrication of custom interactive objects is about adding input and output capabilities to objects as an interface to a computing system, e.g. an embedded microcontroller. These capabilities commonly rely on electrical circuits that use components, e.g. a sensor or actuator, or process electrical signals, e.g. a change in voltage. This section provides a brief overview of digital fabrication technologies to create custom circuits and relevant related work.

Digital fabrication of custom circuits using additive technologies has its origins in the invention of printed circuit boards (PCBs) in the early 20th century. At the time, several technologies were developed that allowed to partially automate the prior manual process of making custom circuit boards [112]. One fabrication technique that is commonly used today and closely related to the approaches of this thesis is printed electronics.

Printed electronics

Printed electronics commonly refers to processes that produce electronic circuits or components based on printing technology as used in graphic printing. Suganuma [205] defines printed electronics as "a technology that merges electronics manufacturing and text/graphic printing. By this combination, one can manufacture high-quality electronic products that are thin, flexible, wearable, lightweight, of varying sizes, ultra-cost-effective, and environmentally friendly." [205, p. 1]

Printing electronics has been demonstrated using a range of printing technologies, including ink-jet printing, screen-printing, gravure printing, offset printing, and flexography printing [205]. These technologies share the common principle of printing a functional ink, e.g. conductive ink, onto a substrate material, e.g. paper, to create a desired pattern, e.g. circuit traces to connect mounted components. This section focuses on ink-jet printing and screen-printing as two techniques that are commonly accessible to researchers and hobbyists.

The key difference between printed electronics and common graphic printing is the use of functional ink instead of color ink. As a basic functional material conductors are printed, e.g. to create electronic circuits. Conductors are typically printed from ink based on metals, conductive polymers, or carbon. For metals, inks based on silver, copper, or gold nano-particles are commonly used. PEDOT:PSS[4] is a commonly used conductive polymer. Carbon-based inks are commonly made

4 Poly(3,4-ethylenedioxythiophene)-poly(styrenesulfonate)

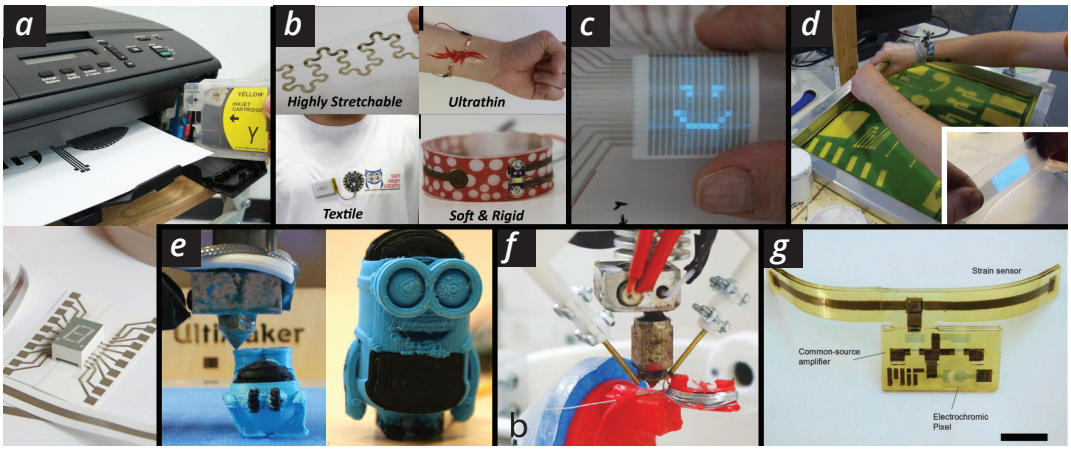

Figure 2.3: Printed electronics have enabled rapid fabrication of custom electronics. Rapid and fully-digital fabrication is enabled through ink-jet printing. (a) Initial work allowed for ink-jet printing conductors onto specially coated substrates [104]. (b) This approach has been extended to print a variety of functional inks onto diverse substrates [108]. Screen-printing multiple layers including translucent conductors and electroluminescent ink allows to print (c) custom-shaped flexible displays onto diverse materials [149] and (d) stretchable displays [242]. (e) FDM 3D-printing supports printing custom carbon-based conductors alongside regular plastic material [192]. Digitally fabricating electronics on 3D objects that rely on conductors of lower resistance, e.g. electromagnetic devices, or different material properties, e.g. translucent conductors, have been demonstrated using a specialized equipment. (f) A 5-axis 3D printer allows to add highly conductive metal wire while FDM 3D-printing parts [157]. (g) A sophisticated 3D printer with multiple ink-jet heads and curing devices allows to 3D-print multi-material objects with stretchable and translucent conductors [207].

of carbon or graphene particles or contain carbon nanotubes (CNTs). In addition, other materials are used, including dielectric ink, e.g. PVP[5], to create multi-layer electronics and electroluminescent (EL) inks, e.g. containing phosphor particles, to create light-emitting displays. For an in-depth review of printing techniques and materials the interested reader is referred to [205].

In the context of research on rapid prototyping of custom sheet-based circuits, ink-jet printing and screen-printing have been used.

Accessible and rapid fabrication of custom circuits based on ink-jet printing was pioneered by Kawahara *et al.* [104] (Figure 2.3a). They presented an approach of printing conductive ink using a commodity ink-jet printer. Ink-jet printing allows for rapid fabrication of custom circuits within seconds. It is a fully-digital approach that produces a digitally designed circuit with high precision and without manual printing effort. The approach by Kawahara *et al.* uses conductive ink based on silver nanoparticles and is limited to specially coated sheets of paper and plastic as substrate materials. *PrintEm* [23] later contributed an alternative approach that requires a special layered material but uses regular ink instead of special conductive ink. Their approach prints a mask in regular black ink on the

5 PolyVinylPyrrolidone

layered material that includes layers of copper foil and UV-activated adhesive and a backing layer. Printing the mask and then activating the unmasked glue via UV-light allows to peel off the desired copper pattern from the material stack. This approach is compatible with consumer printers filled with regular ink but requires a special fabricated compound material. In a very recent approach, Khan *et al.* [108] extended the supported inks and substrates for rapid prototyping on commodity ink-jet printers (Figure 2.3b). They presented conductive metal-based inks, conductive stretchable polymer-based ink, and dielectric ink that can be printed on various substrates, including stretchable thermoplastic polyurethane (TPU), ultra-thin temporary tattoo transfer paper, textile iron-on transfer material, and thermoplastic shrinking material [108]. Their approach is an important step towards enabling versatile printed circuits using rapid and accessible ink-jet printing technology.

Screen-printing has been used as an alternative method for printing electronics that offers additional functional materials and supports more substrate materials. However, it is typically time-consuming compared to ink-jet printing and requires manual effort. The versatility of the process has been demonstrated in early work by Olberding *et al.* [149] (Figure 2.3c). They presented an accessible approach to create custom multi-layer electronics, enabling fabrication of custom-shaped EL displays with integrated touch sensing. To this end, they screen-printed a conductor based on silver-nanoparticles, a translucent conductor based on PEDOT/PSS, dielectric material, and EL ink based on phosphor particles. They further demonstrated the approach's versatility by printing on various materials, including leather, stone, and wood and its accessibility by using hobbyist equipment and off-the-shelf materials. Wessely *et al.* [242] later extended this approach by screen-printing on silicone layers to produce custom stretchable displays (Figure 2.3d).

Towards rapid prototyping of interactive 3D objects, 2D-printed electronics have been used for simple curved geometries, e.g. a watch strap [149], a folded lamp shade [148], or a coffee mug [51]. 2D-printing has been leveraged for 3D objects by attaching the printed sheet [51, 149], folding the object from 2D [148], and by embedding the 2D sheets in 3D objects fabricated by paper lamination [146]. They support rapid prototyping, e.g. through folding, and a variety of materials by attaching circuits, but are limited to developable 3D surfaces. This means that they are restricted to surface geometries that can be made from a flat sheet by folding, bending, cutting, and/or gluing, without use of stretching.

In contrast, 3D-printing generally supports non-developable object geometries, overcoming this limitation. It allows to create conformal electronics on non-developable surfaces by printing parts of an object using conductive or non-conductive materials. Conductive wires can be routed inside the volumetric object. However, 3D-printing is limited in terms of functional materials. Commercially available is mostly conductive filament for FDM printers which is typically based on carbon particles, as used in [21, 192, 193, 194]. This has enabled the fabrication of capacitive touch, proximity, and deformation sensors embedded inside 3D objects [21, 192, 193, 194]. Schmitz *et al.* [192], for example, have demonstrated 3D-printing custom-shaped electrodes embedded inside an object to enable capacitive touch sensing (Figure 2.3e).

Currently, however, the available material is a major limiting factor of the technique. The high resistivity of carbon-based filament[6] compared to metal-based inks, e.g. silver nanoparticle screen-printing paste[7], limits the supported electronic circuit capabilities, e.g. high-frequency signals via I²C. It also requires conductors with a larger cross section to achieve lower resistance. This complicates routing internal printed wires and hinders support for more demanding geometries, which for instance may include holes or many small or thin parts. In addition, the conductor is printed as rigid plastic with limited flexibility which complicates the fabrication of soft deformable objects.

Alternative approaches have been presented in the context of rapid prototyping. Savage *et al.* [189], for example, have printed tubes inside the object and filled those with conductive paint. This provides higher conductivity than carbon-based filament but complicates the fabrication process by requiring manual steps. Peng *et al.* [157] have demonstrated a special 5-axis printer that integrates metal wires in 3D-prints, to enable printing electromagnetic devices (Figure 2.3f). This requires a special printer and introduces geometrical limitations as the wire cannot be printed using the common layer by layer approach.

Promising approaches to fabricate 3D objects with integrated electronics have been presented in material science. Sundaram *et al.* [207], for example, presented a specialized 3D-printer capable of printing multiple materials, including conductors (Figure 2.3g). They build a special printer with multiple ink-jet heads, allowing to print functional materials and to cure them via UV light or heat. This enables the printer to create objects from UV-curable rigid or soft material (e.g. similar to the Stratasys Polyjet technology [204]) and functional materials including PEDOT:PSS and a stretchable silver-based conductor [207]. While this approach is promising, it relies on a sophisticated experimental printer operating on a similar principle as Polyjet printers. Machines using this technology are commonly expensive and not accessible for users outside of well-equipped research labs.

In the context of this related work, this thesis advances fabrication of interactive objects via printed electronics on 3D geometries. Chapter 4 presents a novel approach based on water-transfer of functional inks that allows highly-conductive inks, dielectric inks, EL inks, and translucent conductors to be transferred onto complex 3D geometries using accessible hobbyist equipment. It thus expands the capabilities of printed electronics towards fabrication of interactive 3D objects.

Soft and stretchable electronics

Digital fabrication of soft and stretchable electronics is an important challenge in respect to supporting rich materials for interactive objects, e.g to realize stretchable sensors [154, 224, 236, 242, 256] or displays [242]. Related work has presented digital fabrication approaches for stretchable electronics, although primarily focused on sheet-like materials.

6 ProtoPasta Conductive PLA: 15 Ω-cm [164]
7 Gwent C2180423D2: 2×10^{-4} Ω-cm [63]

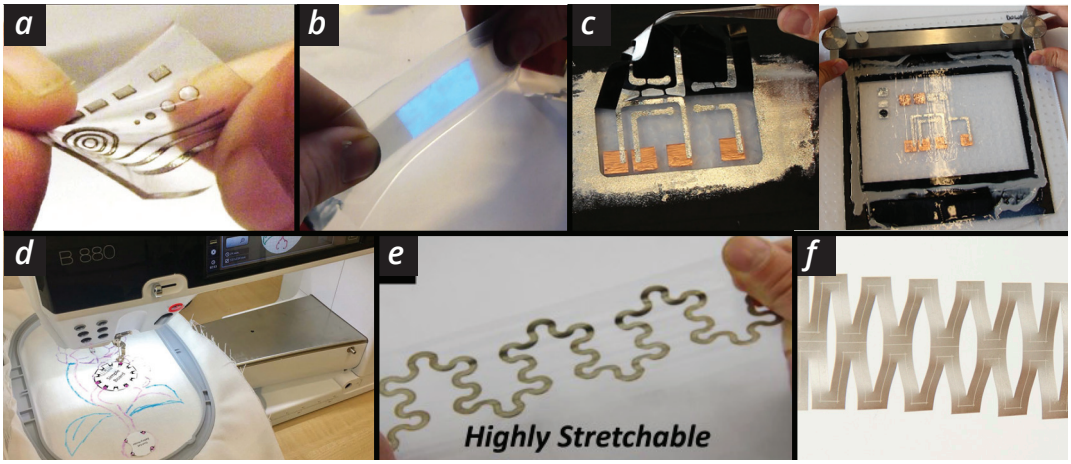

Figure 2.4: Stretchable electronics have been digitally fabricated using additive and subtractive techniques. Based on PDMS, approaches have used (a) laser patterning of cPDMS and EGaIn [128], (b) printing translucent conductors [242], and (c) laser cutting of stencils for liquid Galinstan [142] to create custom stretchable electronics. Additive approaches have used (d) automated embroidery to create soft textile circuits [65] or (e) rapid ink-jet printing to create circuits on soft and stretchable material [108]. (f) This thesis contributes a novel approach based on combined laser cutting and ablation to create circuits of custom stretchability (Chapter 3).

One stream of research has presented approaches based on PDMS[8], often referred to as silicone, as a stretchable material. To create electronics, approaches have used conductive materials in addition to PDMS. Approaches have used laser patterning to incorporate conductive materials, including PDMS filled with carbon particles (cPDMS), EGaIn[9], and Galinstan[10] [128, 142, 236]. Lu *et al.* [128] presented a first approach in the material science community to pattern silicone and sheets of cPDMS or EGaIn (Figure 2.4a). Their approach enables multiple layers of stretchable conductive or non-condutive material by patterning and stacking individual layers. Weigel *et al.* [236] extended this approach by introducing novel layer configurations and electrode designs to enable stretchable touch and pressure sensors. Wessely *et al.* [242] create stretchable electronics from PDMS using screen printing. They apply a special binding layer onto the PDMS and print transparent electrodes using PEDOT:PSS via screen-printing (Figure 2.4b). Nagels *et al.* [142] demonstrated an advanced fabrication technique in recent work that enables multi-layer stretchable devices including off-the-shelf components [142]. The approach combines silicone casting with laser patterning to embed Galinstan as a liquid conductor inside patterned channels (Figure 2.4c).

In addition to silicone, textiles have been used as a soft material that offers potential for stretchable circuits. Digital fabrication of multi-layer soft circuits on textiles has been realized by Hamdan *et al.* [65]. They use automated embroidery to fabricate user designed circuits and enable attaching standard components as well as fabri-

8 Polydimethylsiloxane
9 eutectic gallium–indium
10 gallium–indium–tin

cating various textile touch sensors (Figure 2.4d). Towards stretchable electronics on textiles, manual fabrication approaches have demonstrated stretchable sensors using sewing conductive yarns [224] and using a multi-layer composite structures of off-the-shelf fabric [154]. Parzer *et al.* [154] use off-the-shelf sheets of conductive "zebra" fabric, i.e. alternating rows of conductive and non-conductive fabric, to create a matrix-style pressure sensors. In contrast, Vogl *et al.* [224] explore sewing conductive yarn, similar to the one used for circuits by Hamdan *et al.* [65], in special patterns to allow for stretchable sensors.

These approaches enable digital fabrication of stretchable circuits and demonstrate advanced capabilities, e.g. to produce fully integrated devices. However, fabricating a stretchable prototype with these techniques typically takes multiple hours and requires expertise in silicone casting, manual sandwiching, or sewing. In contrast, this thesis focuses on rapid and accessible fabrication. In very recent work, Khan *et al.* [108] have presented a promising approach for rapid and accessible fabrication of stretchable circuits (Figure 2.4e). Their approach based on a commodity ink-jet printer allows to print conductive traces onto a TPU substrate of uniform stretchability and allows to selectively cover the traces with isolating PVP.

This thesis advances the rapid and accessible fabrication of stretchable electronics beyond prior work. In contrast to prior work that largely focused on custom stretchable circuits of uniform stretchability, this thesis contributes an novel technique for fabricating custom circuits with custom areas of stretchability (Chapter 3, Figure 2.4f). In addition, the technique enables prototyping circuits of custom stretchability within minutes and without expertise in manual fabrication. The approach is inspired by prior work in material science that investigated the use of cut patterns for electronic components, typically at a micro-scale, for applications including supercapacitors for energy storage [61], stretchable graphene and metallic electrodes [9, 218], or stretchable nanocomposites as plasma electrodes [22]. Zhao *et al.* [262] have further proposed to 3D print silver wires on top of Kirigami-patterned PDMS. In contrast, the approach presented in this thesis is the first to demonstrate patterns designed for integrated circuits, i.e. routing paths through the stretch pattern using selective ablation.

2.2 Rapid prototyping of interactive objects

As the digital merges with the physical world, an increasing number of physical objects become interactive through embedded computer interfaces. There are countless examples ranging from smart home appliances to interactive wearables. In this context, a growing stream of research has focused on exploring new designs of interfaces that offer custom geometry and custom interactive functionality. As a result, rapid prototyping of custom interactive objects has become an essential means for quick exploration and iterative design.

Two approaches to create interactive 3D objects were proposed by pioneering research in the late 1990s and early 2000s. One approach was introduced by Raskar *et al.* based on their work in computer graphics [169, 11, 170]. It uses external

projectors and optical tracking to augment a 3D geometry with a visual projection and to allow input via a tracked pointing device [170].

While this initial approach of *Spatial Augmented Reality* [169] by Raskar *et al.* was concerned with visualizing virtual objects in a real environment, later work focused on visual output on 3D objects [11, 170]. More recent work in HCI has used similar projection-based approaches but extended the interaction capabilities [67, 202, 248]. OmniTouch [67], for example, turns object surfaces into touch areas, while Steimle *et al.* [202] use projection and optical tracking to turn sheets of different materials into deformable displays, e.g. to spatially explore 3D content. Optical tracking by itself has further been demonstrated to add input capabilities to 3D objects. Corsten *et al.* [35], for example, proposed the use of everyday objects as "Instant User Interfaces", using a marker-less tracking approach. In this case, feedback for the user's action was provided using an alternative device, e.g. a computer screen or mechanical control.

Adding interactivity through external augmentation has the advantage of not requiring modification of the object. This allows for rapid and flexible prototyping, e.g. by being able to use different objects. However, this form of augmentation requires external equipment, commonly part of a stationary setup, and is often constrained by line-of sight, i.e. through occlusion of projection or optical tracking. This makes these techniques less suitable for self-contained interactive objects or objects used in mobile scenarios. In addition, the approach is most suitable for visual output. Other modalities, e.g. tactile feedback, are difficult or impossible to realize.

In contrast to external augmentation, other approaches are based on building custom prototypes from scratch, which allows for self-contained interactive objects. One pioneering approach to realize such physical interfaces was introduced by Greenberg and Fitchett [52]. They proposed a novel concept of physical widgets, or *Phidgets*, to enable the easy development of physical interfaces. Interactive 3D objects could be assembled based on a set of Phidgets that encapsulate a physical interactive element, e.g. a servo motor, in an accessible form factor. Phidgets are commercially available and offer a diverse set of components.

The Phidgets approach but also more recent work based on classical engineering, rely on manually designing prototypes and physically assembling them from a selection of components. Phidgets are designed to make this process easier. They abstract from low-level electronics to enable quick an easy use, making them suitable for rapid prototyping. Villar *et al.* [223] later presented *.NET Gadgeteer* as an alternative platform aiming to reduce the size of components and offering a simple solder-less connection of components. However, components were still rigid and of rather large form factor due to necessary solder-less connectors. Conventional electronic components, on the other hand, offer a myriad of available options including specialized components and a greater flexibility regarding their form factor. Approaches using classical engineering have been demonstrated sophisticated devices based on conventional components in a broad range of domains from haptic devices [46, 88], over shape input devices [38], to social robots [20]. However, the required complex engineering and assembly is less suitable for rapid prototyping.

As an alternative to manual engineering approaches, a range of digital fabrication technologies have been presented that aim to enable designers, researchers, and makers to rapidly prototype interfaces. These offer to create custom objects with a range of input and output modalities, including touch and deformation-based input, displays, and tactile feedback.

The remainder of this section will provide an overview of relevant related work to realize input and output modalities using digital fabrication approaches. Within this broader topic, the discussion will focus on work closer related to the approaches in this thesis. As such, it focuses on modalities included in the design space and on digital fabrication approaches using custom electronics. Other modalities and approaches will be discussed briefly where appropriate. A comprehensive overview of additional modalities and approaches in the context of 3D-printed interactive objects was presented by Ballagas *et al.* [10].

2.2.1 Input sensing

Touch input

Touch is the most common input modality of current mobile devices, e.g. smart phones, tablet computers, or smart watches. Touch input has been studied extensively HCI. Various approaches and sensing techniques have been proposed to sense touch for interactive objects. These enable different forms of touch input on 3D objects: touch contact at a fixed physical location on an object, touch contact at multiple locations, and input of a discrete or continuous touch position on the object. Common approaches to detect touch are based on electrical, optical, or acoustic sensing. This discussion focuses on electrical sensing enabled by fabricating custom electronics.

Single touch contact
In its simplest form, touch is detected as finger contact at a fixed location or within a fixed region on the object. The location or region is determined during design, typically by placing a sensor element on the object.

One common approach is to place one or multiple sensor electrodes at the desired touch location to use *electrical touch sensing*, i.e. detecting a change in an electrical property upon touch.

One common sensing technique is capacitive touch sensing, where the touch contact changes electrical capacitance. Touch at a single location can be detected by a single electrode using loading-mode self-capacitive sensing. A capacitor is formed between the sensor electrode and a finger in close proximity. As the distance between finger and electrode decreases, the capacitance increases until the finger touches the electrode. The change in capacitance is measured by a micro-controller and touch is commonly detected using a thresholding approach. This approach allows to detect touch within a custom-shaped region by using a single custom shaped electrode. It is compatible with various fabrication approaches for custom conductors. As such, it can be realized on developable 3D geometries, e.g. through cutting copper tape [190], inkjet-printing [146, 148], or screen-printing [148], and on

non-developable geometries, e.g. by 3D-printing [21, 192] (Figure 2.5a) or casting conductive material [189] (Figure 2.5b).

Electrical touch sensing at a single location has further been realized using resistive touch sensing [73, 226, 236]. One approach using resistive sensing infers when a finger causes electrical contact between two electrodes. This is commonly used in resistive touch screens [226] but also in fabricated prototypes [73, 236]. iSkin [236], for example, fabricated two conductive layers separated by a perforated spacing layer using laser patterning. When touched with sufficient force, the two conductive layers make electrical contact (Figure 2.5c). This approach has been demonstrated as fabricated overlays overlay on developable curved objects [73] and slightly double-curved body geometries [236].

Other approaches are less common. *Optical sensing* integrated into objects, for example, was demonstrated by 3D-printing light pipes inside an object [244]. The light pipes are routed from a light source and light sensor to the desired touch position on the object's surface. Upon touching the end of the pipe, the amount of reflected light changes, which is detected by the light sensor (Figure 2.5d). *Acoustic sensing* leverages a similar principle of emit and receive but using acoustic waves. Touch locations are defined by creating holes in a hollow object [101] (Figure 2.5e) or channel under the object's surface [119]. The acoustic waves are emitted inside the hollow structure. They reflect from the inside walls but can escape through the holes. If a hole is covered by a finger, the reflected sound pattern changes, which is detected by a microphone [119, 101].

Multiple touch contacts
The approaches above have in common that the touch location is defined by the physical placement of the sensor. This can be extended to multiple locations by placing multiple sensors. A different stream of research uses a single sensor on the object and infers one or multiple touch locations through machine learning. These approaches are potentially compatible with custom fabricated objects, but have so far been demonstrated only on existing objects. One Example is *Touché* [184] which is based on capacitance. It infers different touch locations on a conductive object by analyzing the response to a swept AC signal. This method is also capable of detecting different grasp gestures. A second example is *Touch & Activate* [150] which is based on acoustic sensing. It uses a sweep signal emitted from a vibration speaker and captures the response via a piezoelectric microphone. Touching different locations changes the received response, which is recognized using a machine learning approach.

Touch position
Beyond individual touch locations, approaches enable to sense a touch position within an area on the object.

In a simple form this can be realized using a single conductive layer which contains a grid of single touch contact sensors, e.g. via loading mode capacitive sensing [51, 147]. These grids typically offer a limited resolution of position, since the individual electrodes are large and require sufficient spacing to route wires to each electrode (Figure 2.5f). Alternatively, resistive sensing allows to create a grid of connected touch points [73]. The touch points are connected by a graph of resistors. Current is

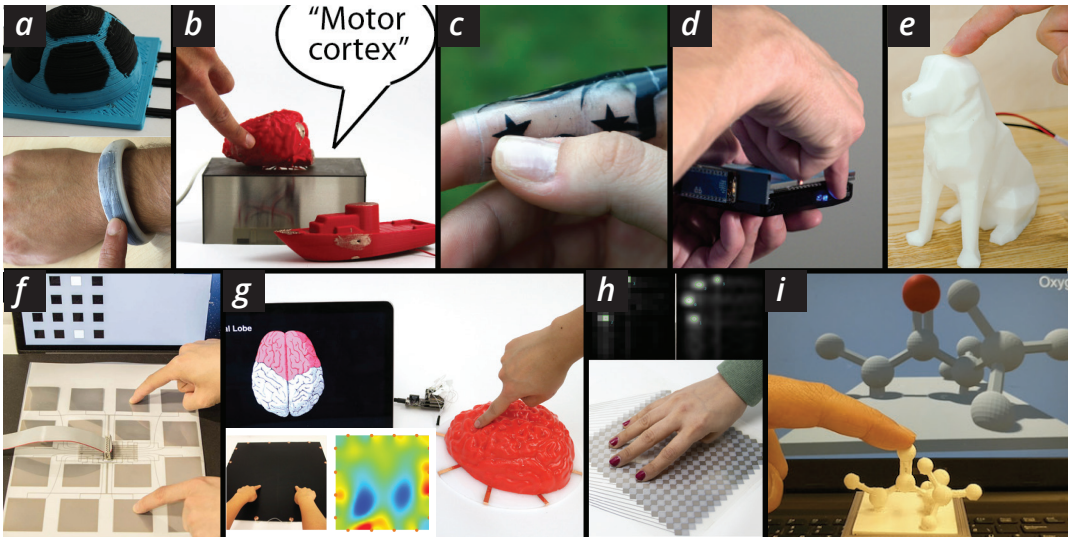

Figure 2.5: Examples of approaches realizing touch input. Detecting touch at a single location via self-capacitive sensing on 3D-printed objects using (a) conductive filament [192] or (b) channels filled with conductive ink [189], (c) resistive sensing [236], (d) optical sensing [244], (e) or acoustic sensing [101]. (f) Detecting multiple touch contacts and inferring the discrete touch position within a grid of inkjet-printed electrodes based on self-capacitance [147]. Detecting continuous touch location using (g) electric field tomography on a brain model cast from Jell-O [260], (h) high-resolution mutual-capacitance sensing [162], or (i) triangulation of capacitive sensor readings [194].

applied to the graph and the current flow is measured. When a grounded object touches the graph at a location it disturbs the current flow, which is mapped to the touch position. The grounded object can be a second layer on top of the resistor graph layer or a finger connected to ground. Both techniques have been demonstrated as sheet-like overlays on developable geometries, through conductive ink-jet printing [51, 147] or by cutting conductive vinyl [73]. A grid of 3D-printed electrodes for loading-mode capacitive sensing has been demonstrated on non-developable 3D geometries [21, 192] (Figure 2.5a).

Other less common approaches have been demonstrated to infer touch position on 3D objects. Electric field tomography [260] uses an array of electrodes distributed around the conductive touch sensitive area. Current is injected into the conductive area using one pair of electrodes at a time. Voltage is measured at all other pairs. From these measurements a 2D map of the current density is reconstructed and touch inferred where a touching finger causes a low density (Figure 2.5g). This approach allows to easily add touch input to an object's entire surface, as Zhang *et al.* [260] have demonstrated by coating the entire object with conductive material. In contrast, approaches based on printed electrodes may be more suitable for single or small touch locations and for multi-touch sensing. Zhang *et al.* report limited capabilities for multi-touch sensing for their approach. As the reconstruction via electric field tomography is rather coarse, their exploration revealed a minimum distance between two touches of 10cm to be recognized [260].

In contrast, approaches based on printed electrodes promise to enable high resolution multi-touch touch sensing. One common technology for this purpose is mutual-capacitive sensing, which is used for high-resolution multi-touch sensing on flat surfaces, e.g. touch screens of current smart phones [226]. Recent work has demonstrated the feasibility of this approach on curved surfaces down to a radius of 15 mm [162] and slightly curved non-developable surfaces, such as different body locations [144]. Mutual capacitance touch sensing leverages pairs of electrodes, typically arranged in two layers forming a row-column style matrix. A capacitor is formed at each intersection of a row and column, as a voltage is applied to either the rows or columns. A touching finger changes the mutual capacitance between the electrodes at the touch location. This approach enables high-resolution multi-touch input (Figure 2.5h), e.g. for expressive multi-touch gestures, but requires multi-layer circuits with high conductivity. Realizing such circuits on complex geometries is an open challenge. This thesis contributes a novel approach towards addressing this challenge, which enables multi-layer circuits with high conductivity on complex highly curved 3D geometries. Based on this approach, we demonstrate fabrication of a multi-layer row-column style multi-touch sensor using loading mode capacitive sensing.

As an alternative to touch electrodes on or close to the surface of an object, very recent work by Schmitz *et al.* [194] has contributed a novel approach based on capacitive trilateration. Their approach uses multiple capacitive sensor electrodes inside the object. Each electrode acts as a proximity sensor, since its measured capacitance changes with proximity of a finger. Combining reading from multiple sensors allows to triangulate the position of the finger in 3D space and to infer touch on the object's surface (Figure 2.5i).

Pressure-based input

Pressure sensing adds force as an additional dimension to touch contact. On rigid surfaces a common approach is to use force-sensing resistors (FSRs) [229] or similar approaches based on resistance change on printed conductors [51]. Both make use of the principle of percolation, i.e. with increasing pressure the resistive contact area between two inter-digitated electrodes is increased and thus the resistance between them reduced. While printed approaches use the finger to make contact between the electrodes [51], commercial FSRs often use a piezo-resistive polymer as an overlay on top of the electrodes. This allows to further use the piezo-resistive effect, i.e. the change of the material's resistance with pressure, for sensing. Presented approaches have made use of attaching individual off-the-shelf sensors [229] or thin-film ink-jet printed overlays [51] on developable geometries. Pressure-based input on doubly-curve geometries has been limited to objects placed on an external sensor, as demonstrated by Hudin *et al.* [77]. In contrast to digitally fabricated pressure sensors, e.g. presented in [51], their approach does not support customization of the sensors and requires the sensor and object to be placed on a flat surface, e.g. a table. By placing the external force sensor between the object and the flat solid surface, force applied to the object can be measured by the sensors. This allows to infer touch contact and touch force [77]. On soft surfaces, applying pressure causes deformation, which can be sensed using different approaches, as discussed below.

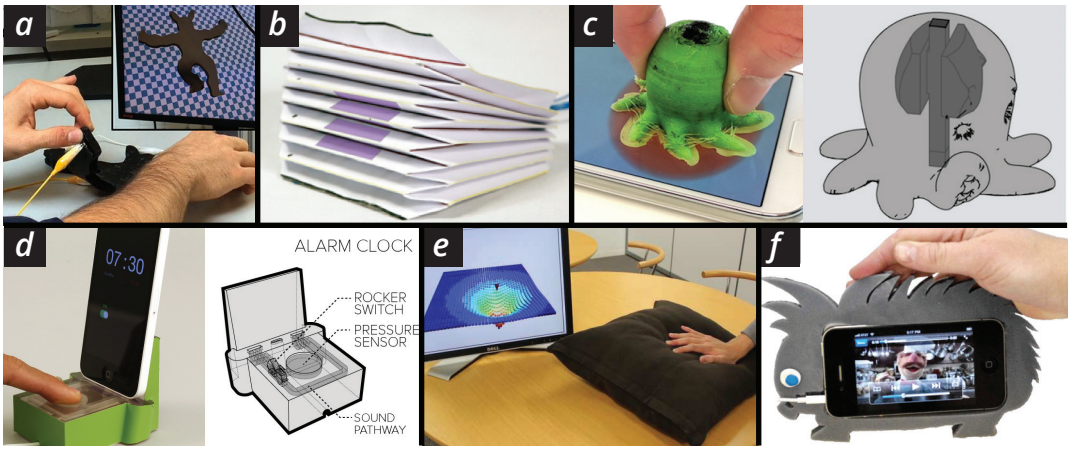

Figure 2.6: Examples of deformation-based input. Digital fabrication via printing has been used in (a) 3D-printed deformable objects with embedded piezo-resistive wires [7], (b) deformable objects folded from sheets of 2D printed electronics using capacitive emit-and-receive sensing [148], (c) 3D-printed objects printed from deformable material and conductive filament that leverage capacitive sensing [193], or (d) 3D-printed air chambers that sense pressure via acoustic sensing [119]. Alternative sensing methods have been demonstrated on manually fabricated objects, including (e) sensor modules that estimate an objects infull density based on photoreflectivity [206] and (f) special geometries with attached sesnsor electrodes that make electrical contact when the object is deformed [198].

Deformation-based input

Deformation-based input is receiving growing attention in HCI research. It leverages interfaces and objects that are deformable, e.g. bendable, stretchable, or squeezable and offers expressive interaction beyond touching an object. Several approaches have been presented that enable sensing of an object's deformation.

Approaches based on digital fabrication of custom electronics have used different sensing approaches to infer the deformation of an object. A common principle for sensing bending, also called flexion, is using resistive flex sensors (RFSs) [181]. These sensors typically rely on a thin-film conductor that changes its resistance upon bending. This principle is employed in commercial bend sensors [200] and also in custom-shaped sensors, e.g. through ink-jet printing [146, 219]. Bächer *et al.* [7] have presented an approach extending this principle to 3D objects by embedding conductive wire inside the object (Figure 2.6a). Their approach optimizes the placement of one or multiple wires inside the object so that pre-defined deformations of the object can be inferred by measuring the wires' resistances. They have demonstrated sensing of versatile deformation, including bending, twisting, stretching, and compression, however, primarily focused on rather flat 3D structures.

Other approaches for bend sensing on sheet-like objects have used printed bend sensors based on piezo-resistive material [174] or printed electrode pairs to use a capacitive emit-receive sensing schemes [51, 148]. Rendl *et al.* [174] use a sparse set of piezo-resistive sensors printed on a flexible sheet to infer the deformation of the sheet. They contribute a novel algorithm that integrates the different sensor readings

to reconstruct the sheet's deformed shape, e.g. through bending or twisting. A capacitive emit-and-receive sensing scheme has been demonstrated using pairs of printed electrodes. Gong *et al.* [51] presented the approach based on an array of electrodes printed onto a sheet of material. For each pair of electrodes, one electrode emits an AC signal while the other electrode receives the signal. Bringing the two electrodes closer, e.g. by bending the sheet, changes the received signal accordingly. Olberding *et al.* [148] used the same principle for bending and folding detection but also for compression and stretch sensing on folded 3D geometries. For compression and stretch sensing they leverage a bellow structure folded from a 2D sheet with printed electrodes (Figure 2.6b). Emit-and-receive sensing between pairs of electrodes on the structure's folds allows to infer the angle between electrodes and thus compression or stretch of the overall folded structure.

Alternative forms of capacitive sensing have been used for deformation sensing on 3D-printed objects. *Flexibles* [193] proposes structures of conductive, very flexible, and less flexible 3D-printed material for deformation sensing. The 3D-printed object makes contact with a common capacitive multi-touch surface for sensing, e.g. by placing it on a tablet's touchscreen. Deformation is sensed by measuring changes in distance between embedded electrodes or change in the intensity of a capacitive reading caused by the deformation (Figure 2.6c). They demonstrate various forms of press, squeeze, and bend detection, however, limited to objects on or including a device with touch screen. In recent work, Schmitz *et al.* [194] have proposed an alternative approach for stand-alone objects based on capacitive triangulation. The approach sensed the finger's 3D location and thus can infer when a finger deforms the object by pressing on it.

Other approaches have used digital fabrication of custom geometry instead of custom electronics to sense an object's deformation. 3D-printing special air chambers of soft material, for example, has been used to sense deformation based on change in air pressure [197, 222] or specific acoustic patterns [69, 119]. For instance, Slyper and Hodgins [197] presented a set of soft 3D-printed structures that cause a detectable change in air pressure when deformed. They are able to sense bend, twist, stretch, or compression using a simple off-the-shelf air pressure sensor. Laput *et al.* [119] presented an approach based on fabricated soft chambers and an acoustic emit-and-receive scheme. They emit an acoustic sweep pattern through the printed chambers and connecting channels using a standard speaker and receive the response using a microphone. For deformation sensing, they presented a soft pressure sensor which detects a change in signal when it is pressed (Figure 2.6d).

Additional sensing principles have been presented in related work based on manual rather than digital fabrication. They commonly rely on embedding sensors in the object and leverage special infill material or special geometries, which may be automated by future digital fabrication approaches to use similar sensing principles. The *Skweezee System* [220], e.g., uses conductive infill material to measure the change in resistance between multiple embedded electrodes upon deformation. The electrodes consist of conductive yarn that is sewed into the object's soft textile shell. Automating the sewing process, e.g. through automated embroidery as in [65], could enable digital fabrication of such sensors. Sugiura *et al.* [206], on the other hand, use non-conductive "fluffy" stuffing material, such as wool, feathers, and cotton,

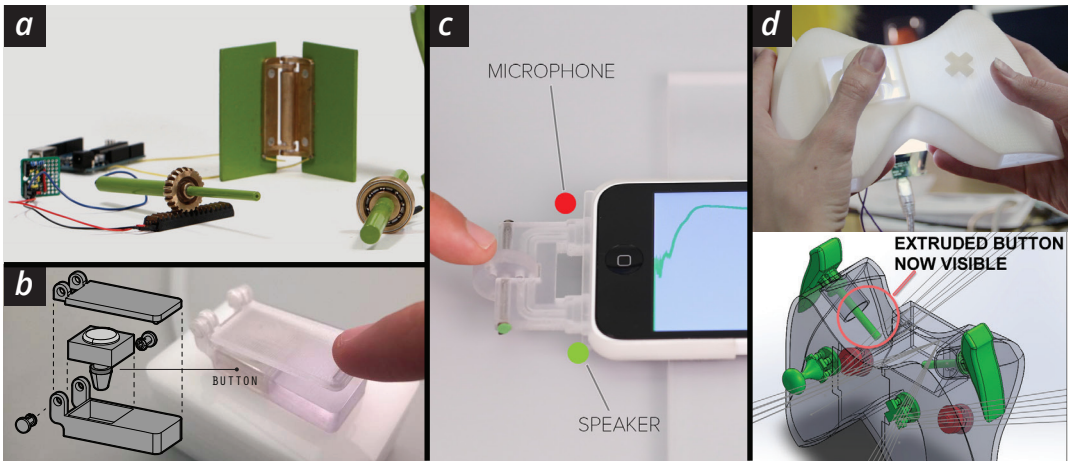

Figure 2.7: Examples of fabricated mechanical input controls: (a) 3D-printing metal allows to integrate analog electrical sensing to interaction with a mechanisms [221]. 3D-printing hollow chambers and tubes has been used to realize custom controls based on (b) sensing air pressure [222] or (c) emit-and-receive sensing based on sweeped acoustic signals [119]. (d) 3D-printing has further been used to fabricate custom controls with dedicated geometry to be tracked by an embedded camera for sensing [186].

to sense a change in material density through photoreflectivity when deformed (Figure 2.6e). They embed sensor modules consisting of multiple photoreflectors inside the object. The modules measure the change of infill density based on reflected infrared light. Instead of special infill material, Slyper *et al.* [198] presented an approach based on embedding off-the-shelf magnetic distance sensors inside soft objects. Their approach relies on measuring the distance between sensors that were manually embedded in holes at different locations inside the object. Based on these measurements, they infer deformation of the objects, e.g. stretch or compression. They further present a different principle which relies on attaching electrodes to comb-like structures of an object. Bending the structure causes electrical contact between the electrodes and allows to infer deformation (Figure 2.6f).

The approach for deformation sensing presented in this thesis relies on a resistive approach to sense stretch (Chapter 3). In contrast to prior work, the approach is based on rapid fabrication of custom circuits with custom stretchability. The approach allows to customize the stretchability of the sensor and to seamlessly embed it into interfaces with multiple areas of custom stretchability.

Mechanical input controls

Mechanical input controls, e.g. buttons, rotary dials, or sliders, have been used to make objects interactive. They offer unique haptic qualities that can be beneficial for interaction, e.g. in an eyes-free context. Related work has presented digital fabrication approaches that focus on embedding existing off-the-shelf components in objects [40, 94, 93, 167, 187] and approaches that allow to fabricate custom mechanical input controls [75, 119, 188, 186, 221].

For approaches that rely on embedding standard components, digital fabrication in typically used to create a custom enclosure with geometry to attach the desired components [93, 167, 187]. Savage et al [187], for example, propose a system to sculpt the geometry of an object and annotate placement of components that shall be integrated. After scanning the sculpted geometry with markers, the system generates the necessary mounts for components. The resulting geometry is 3D-printed and assembled manually. Similarly, RetroFab [167] relies on scanning a geometry as input. Their approach allows to scan an existing device, to digitally annotate the device's existing interface, and to add a new interface to retro-fit the existing device. Their approach then generates the necessary structures to mount off-the-shelf components implementing the retro-fit interface. Jones *et al.* [93] presented an approach that relies on digital modeling of the geometry and allows to place desired components via drag and drop. Their approach also generates the necessary geometry to manually attach the components.

Digital fabrication of custom mechanical controls, on the other hand, allows to create controls that can be adapted to the designer's needs, e.g. to fit an object's geometry. Several approaches have been presented in related work based on fabricating specific geometric assemblies to enable customized input. An approach for fabricating custom input controls based on electrical sensing has been presented by Vasilevitsky and Zoran [221]. Their approach uses 3D-printed assemblies from metal and plastic to enable sensing of the configuration of four different types of mechanical elements (Figure 2.7a). They integrate a voltage divider inside a mechanical linear gear system, a variable capacitor into a hinge, a pressure sensor using piezo-resistive material into a screw, and an electrical switch inside a ball bearing. Each assembly allows to measure its state using analog electrical sensing.

Other approaches have used digital fabrication of custom geometry for acoustic, pneumatic, and optical sensing of custom input controls. *Acoustruments* [119], e.g., presents a set of controls based on air pipes, including push buttons, sliders, turning knobs and rotary encoders. Each control contains and arrangement of pipes and elements that modify the acoustic signal passing through the pipes in a unique way depending on the interaction. This allows to create custom controls using only a speaker and a microphone (Figure 2.7c). Similarly, *Lamello* [188] uses a microphone to capture the unique acoustic signals emitted when using custom fabricated dials, buttons, and sliders. The signals are produced by elements striking individual parts of a generated comb-like structure and allow to infer the interaction with a control. Based on pneumatics, Vazquez *et al.* [222] presented an approach for 3D printing custom controls (Figure 2.7b). Their approach relies on fabricated controls that contain pressurized air chambers. They measure the change of air pressure caused by interaction or embed standard linear or rotary potentiometers for sensing.

Optical approaches have made use of 3D-printed geometry and optoelectronic sensors or cameras. Willis *et al.* [244] presented an approach based on 3D-printed light pipes and optoelectronic sensors. They print controls with embedded optical elements, e.g. light fibers or masks. Interaction affects how these elements pass IR light to a sensor This enables controls that sense various interactions, including pushing, rotation, linear movement, and acceleration. Savage *et al.* [186] present an alternative optical approach based on an embedded camera. Their approach

3D-prints custom mechanical controls with dedicated geometric features that extend into the camera's field of view (Figure 2.7d). Interaction with the controls is sensed by tracking movement of these geometries using the embedded camera.

In the context of mechanical input controls, this thesis contributes a novel digital fabrication approach enabling to selectively lock and unlock the movement of mechanical assemblies (Chapter 6). This could be leveraged to lock or unlock mechanical input controls. In contrast to prior work, e.g. using pneumatics [222], the approach enables permanently stable states without requiring energy or constant pressure.

2.2.2 Output modalities

Visual displays

Visual displays are the predominant output modality for today's computer interfaces. Research has investigated a wide range of approaches to enable visual display output based on different technologies, including EL[11] [149, 148, 242], E ink[12] [41], and thermochromic [98, 212] displays. We will shortly discuss digital fabrication approaches for displays, focusing on approaches that enable custom-shaped displays.

Printed electronics has been used as an approach to realize different types of displays. Olberding *et al.* [149], for example, introduced the custom fabrication of EL displays using hobbyist equipment. They print displays that consist of four layers: one bottom electrode, one dielectric layer, one layer of EL ink, and a final electrode layer. When an AC voltage is applied between the electrodes, the EL layer emits light. Thus, at least one electrode layer needs to be translucent. Olberding *et al.* demonstrate fabricating custom-shaped light-emitting regions or pixel-addressable matrix configuration based on this principle. Olberding *et al.* [148] later extended this approach to 3D objects by folding 2D printed sheets which allows displays on developable geometries (Figure 2.8a). Non-developable geometries are supported by stretchable printed EL display overlays, as presented by Wessely *et al.* [242]. However, these overlays are quite thick, which limits their use to slightly double-curved geometries (Figure 2.8b). In contrast, this thesis contributes a novel approach to realize printed El displays on complex strongly-curved 3D-object geometries (Chapter 4). The approach is based on a novel water-transfer approach that allows thin and conformal overlays to augment objects (Figure 2.8c).

Other approaches have fabricated thermochromic displays, primarily on flat 2D surfaces or on slightly curved body geometries [98, 99, 212, 230]. These thermochromic displays are commonly fabricated using a custom-shaped heater and a layer of thermochromic material, e.g. ink. Applying heat changes the color of the material. This typically requires longer transition times between on and off states than other display technology, e.g. fabricated EL displays. Torres *et al.* [212] present an approach to fabricate such displays based on printed electronics. They print custom-shaped heating elements using conductive ink-jet printing onto 2D sheets or

11 electro-luminescence
12 electrophoretic ink [32]

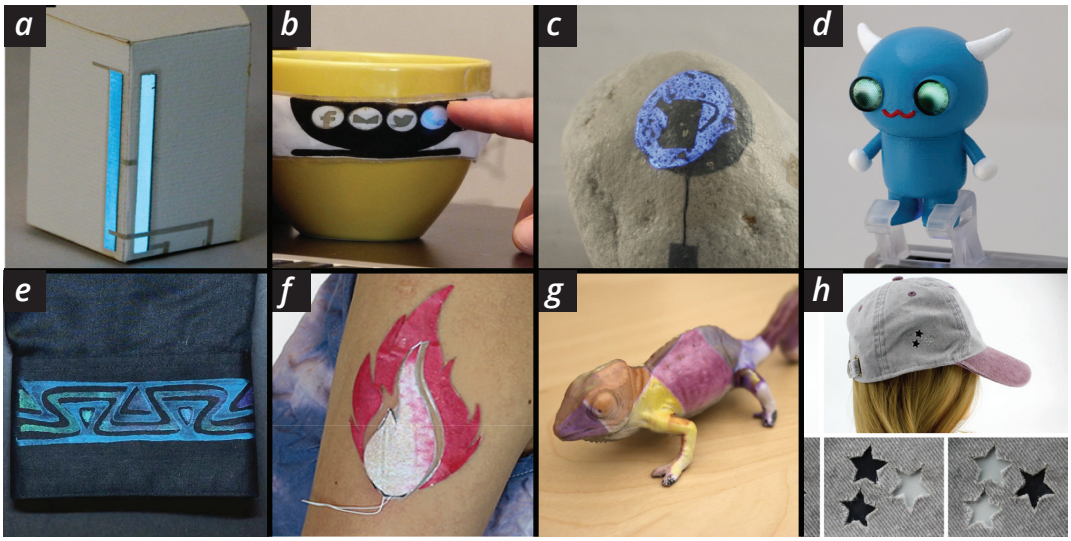

Figure 2.8: Examples of fabricated display output. Printed electronics have enabled custom-shaped light-emitting displays on (a) objects folded from 2D sheets [148] or (b) as thick silicone-based overlays [242]. (c) Chapter 4 enables conformal printed displays on non-developable geometries. (d) 3D-printed light pipes route output from an external display to an object's surface [244]. Thermochromic displays have been realized using custom-shaped heating elements, e.g. (e) inkjet-printed and integrated in textile [212] or (f) on-body via a cutting plotter [98]. Other approaches use (g) special photochromic ink activated via projection [91] or (g) embedded e-ink displays [41].

paint directly onto fabric over an embedded heater (Figure 2.8d). Other approaches that have realized thermochromic displays on slightly curved body geometries have used digital fabrication using vinyl cutters [98] (Figure 2.8e) or manual fabrication using conductive thread [99, 230]. Kao *et al.* [98] fabricate a stencil using a vinyl cutter and manually apply gold leaf using the stencil to create custom heating elements.

Other approaches have realized custom-shaped displays by fabricating objects with embedded optical guides [19, 122, 244]. These guides are designed to selectively route the light from a conventional display component, e.g. an LCD screen or projector, to the surface of the object. Willis *et al.* [244] presented an approach based on 3D-printed light fibers. Single light fibers are routed from an object's surface to source display to realize point-like visual output. Bundles of fibers are routed to realize pixel-based output (Figure 2.8f). They presented 3D-printed objects placed on a pico projector or a projected tabletop surface as source displays. Ledo *et al.* [122] presented an approach based on 3D printing and manually embedding light pipes. They embed an entire device that features a screen,e.g. a smart watch or phone, inside the object as a source display. These approaches enable display output on non-developable geometries. However, objects rely on embedding or attaching a conventional display components and routing internal light pipes. This makes these approaches less suitable for small objects and objects with small features, e.g. jewelry.

As an alternative to embedding display output, recent approaches based on digital fabrication and photochromic inks have demonstrated how to fabricate textures on 3D objects that can be changed permanently through external activation [91, 165]. Punpongsanon *et al.* [165] presented an approach based on 3D printing special photochromic ink on a custom Polyjet 3D inkjet printer. After printing, the appearance of the material can be changed by shining light patterns, e.g. of different wavelengths, on the object. Jin *et al.* [91] extended this approach in very recent work. Instead of 3D printing voxels of different photochromic properties, they mix a photochromic ink that can change its color within a multi-color spectrum (Figure 2.8g). This allows to fabricate an object from a single material and change its texture based on special projected light patterns. While these approaches rely on external activation, they present an potentially promising technology for visual output on interactive objects.

Other technologies have been demonstrated for visual output on objects, however based on manual fabrication. For example, Umetani and Schmidt [217] have used conventional LEDs and EL wire as output on a 3D object's surface. These can be applied to non-developable surfaces and offer simple visual output as single points or lines. In contrast, embedding commercial e-ink displays allows for high-resolution output on flat or developable surfaces, as proposed by Dierk *et al.* [41]. They integrate the off-the-shelf display component into apparel and achieve an apparent custom display shape by adding a masking layer on top of the rectangular display (Figure 2.8g).

Haptic feedback

Haptic feedback has been explored extensively as a general means to deliver information. Examples are myriad and include tactile icons [18] and patterns [245, 255] stimulating the finger tip, information encoded by rotating a knob held between fingers [132], and haptic actuators mounted to a persons back [86] or wrist [155].

However, digital fabrication of haptic feedback capabilities on 3D objects has received little attention. Initial work in this area has explored fabrication of haptic feedback based on pneumatic actuation [189, 222]. Savage *et al.* [189], for example, presented an approach to create tubes inside an object. Creating a tube which is sealed with a soft membrane on the object's surface allows to create haptic feedback via pneumatic actuation (Figure 2.9a). Vázquez *et al.* [222] present an alternative approach to create haptic feedback for mechanical controls based on embedded air chambers (Figure 2.9b). They demonstrate fabrication of soft buttons, rotary knobs, and linear slider controls with haptic feedback based on controlled activation force using air pressure. These approaches enable haptic feedback at one specific location or for one mechanical control.

Fabrication of more localized or fine-grained haptic feedback capabilities has been demonstrated using 2D printed electro-tactile interfaces [102, 245]. These interfaces rely on electrodes in contact with the skin. They provide tactile sensations comparable to mechanical vibrations by directly stimulating nerve stems in the skin using controlled electric current impulses [97]. Kato *et al.* [102] presented an approach for fabricating thin-film interfaces that provide electrostatic force and electro-tactile

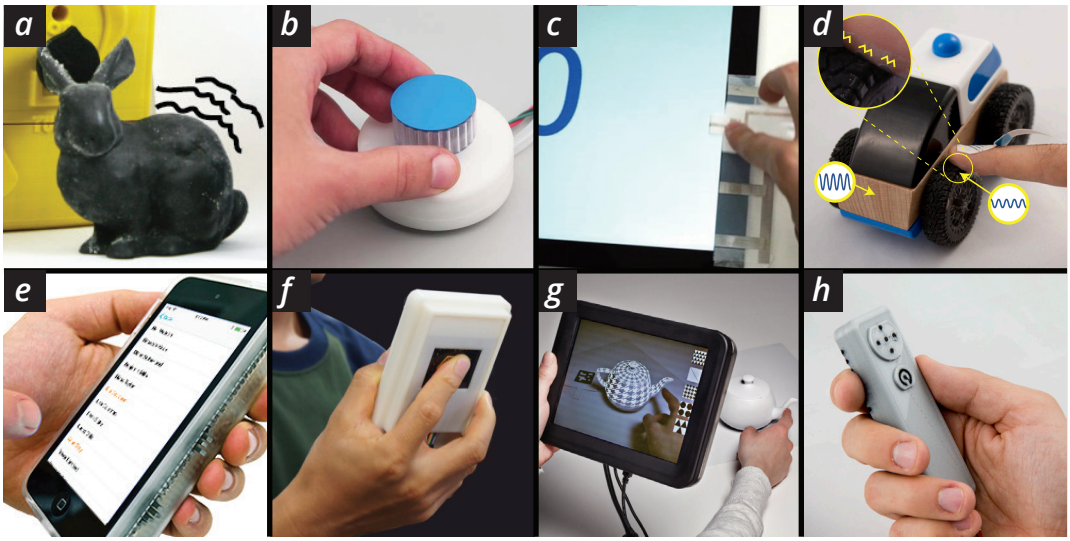

Figure 2.9: Examples of haptic feedback: 3d-printing has enabled haptic feedback through pneumatic actuation via (a) embedded tubes and soft membranes [189] or (b) air chambers in mechanical controls [222]. Printed electronics have realized higher spatial resolution using electro-tactile interfaces (c) on flat geometries [102] and (b) attached to the user's finger [245]. Manually built devices have provided feedback via (e) arrays of moving pins [88] or (f) attached electro-tactile displays [109]. (g) Augmenting the user allows for feedback via electro-vibrations while sliding the finger on an object [12]. (h) Chapter 5 enables digital fabrication of high-resultion tactile interfaces on 3D geometries.

feedback using ink-jet printed electrodes. They demonstrate haptic feedback on a 3D object by attaching a printed sheet to the flat bezel of a tablet computer (Figure 2.9c). Their printed design implements a slider control for scrolling content on the screen that allows to selectively control the friction at four locations of the slider. In contrast to this simple flat geometry, this thesis focuses on complex 3D geometries. Withana *et al.* [245] presented a different approach based on printed electrodes for electro-tactile. They focus on haptic feedback as a body-worn interface by attaching a thin electro-tactile interface to the user's finger. They realize an array of individual taxels (tactile pixels) by screen-printing an arrangement of electrodes. The electrodes are printed onto a temporary tattoo transfer paper that is then applied to the user's finger. The approach allows to deliver high-resolution tactile feedback when touching an object by tracking the finger and the object (Figure 2.9d). In contrast, this thesis focuses on interactivity embedded in self-contained objects rather than augmenting the user.

Instead of digital fabrication, other approaches for haptic feedback have relied on consumer devices that offer haptic actuators, custom-engineered devices, or augmenting the user.

A large body of work has used vibrotactile feedback on flat touch surfaces, e.g. using the touch screen and vibration motor of a tablet computer. Examples include providing physical feedback for visual controls [64, 143, 160, 252, 263] or rendering virtual textures and geometric features [111, 173]. Other approaches have used

custom-built devices that enable haptic feedback by locally changing a physical structure overlaid on a flat touch screen. Examples include selectively solidifying a gel layer [134] or selectively changing the viscosity of magnetorheological fluid using a magnetic field [90].

Towards haptic feedback on 3D objects, related work has presented engineered devices with an embedded array of moving pins [88, 155], attached electro-tactile displays [109], or capabilities of texture and compliance change [45, 250]. For example, Jang *et al.* [88] present a smart phone with a "haptic edge display" using a linear array of moving pins (Figure 2.9e). They demonstrate how this haptic feedback enhances interaction with content on the smartphone's screen and in an eyes-free context, e.g. when the phone is inside a pocket. An alternative approach by Khurelbaatar *et al.* [109] attaches an electro-tactile display component to the back of a smart phone (Figure 2.9f). This offers tactile stimuli to a finger on the back of the phone while holding the device without requiring moving parts. Yao *et al.* [250] present a different approach based on pneumatic actuation and particle jamming. Their structures cast from silicone enable computer-controlled change of stiffness and texture.

Other approaches have relied on augmenting the user to provide haptic feedback. Attaching a magnet to a user's finger, for example, allows to provide haptic feedback on and above a 2D touch screen using a computer-controlled magnetic field, as presented by Weiss *et al.* [239]. Augmenting the user's finger for haptic feedback on 3D objects has further been demonstrated by Bau *et al.* [12]. They inject an AC signal into the finger, which allows to create electro-friction on grounded objects in the environment. By tracking the object and the finger, the friction can be varied according to the touched location on the object (Figure 2.9g).

This thesis advances the field of digital fabrication towards haptic feedback capabilities on 3D objects in two ways. First, it contributes a novel digital design and fabrication approach for high-resolution taxel-based output controls on 3D geometries (Chapter 5). To this end, this thesis investigates the design space, fabrication methods, and stimulation approaches to augment physical objects with electro-tactile stimulation. Furthermore, it proposes to combine tactile stimulation and touch sensing to create interactive tactile controls and demonstrates how to 3D print electro-tactile interfaces (Figure 2.9h). Second, this thesis contributes a novel approach for fabricating objects capable of computer-controlled on-demand compliance change as a form of haptic feedback (Chapter 6).

Shape change & mechanical actuation

Shape-change and mechanical actuation have been explored as a versatile means to change the configuration of an object or to provide movement as a form of visual or haptic feedback. A comprehensive review of shape-changing interfaces has been presented by Rasmussen *et al.* [171]. We will briefly discuss digital fabrication approaches that have enabled creating custom actuated or shape-changing objects.

Several approaches have made use of printing technology to digitally fabricate actuated or shape-changing objects. Printing conductors has enabled fabrication of custom-shaped shape-memory polymer composites [148]. Olberding *et al.* [148]

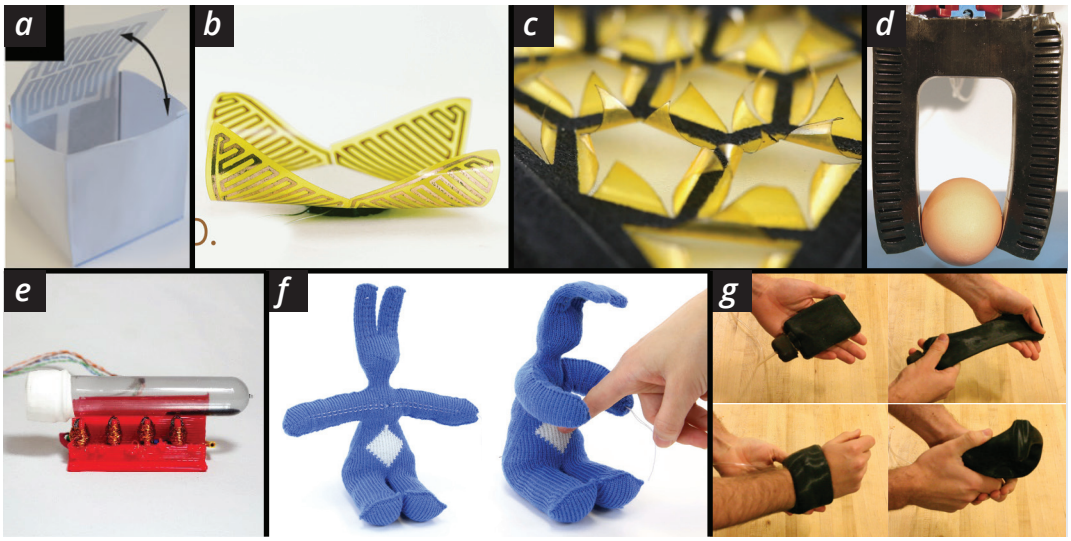

Figure 2.10: Examples of fabricated shape-change capabilities. SMP-based actuators have been realized by fabricating custom-shape heating elements via (a) screen-printing of conductive ink [148] or (b) printing solid ink and etching [71]. (c) Printed biological actuators change their shape based on humidity [251]. 3D-printing enables shape-change based on (d) printing hydraulic mechanisms [130] or (e) embedding wire for custom electro-magnetic devices [157]. (f) String have been embedded in machine knitted objects for actuation [3]. Manual fabrication of particle jamming structures allows on-demand deformability [45].

screen-print conductive ink to create custom-shaped heating elements on thin paper. They then attach a layer of polyethylene tape. Polyethylene expands faster than paper when heated, which causes the composite structure to bend (Figure 2.10a). Heibeck *et al.* [71] proposed a similar approach based on printing a mask of solid ink onto copper followed by an etching process to create custom heating elements. In addition to bending, they demonstrate other shape-change based on this principle, including twisting, folding, and curling (Figure 2.10b). Yao *et al.* [251] use a similar principle to achieve shape-change of flat sheet-like structures. Instead of custom heating-elements, they manually deposit or ink-jet print Bacillus Subtilis natto cells that expand or contract based on humidity (Figure 2.10c). They demonstrate the use of such interfaces based on a change in humidity caused by sweating for a wearable interface and computer-controlled through a humidifier or printed heating elements.

Towards actuated 3D objects, 3D printing has been used to create mechanical assemblies, e.g. joints, and means to actuate those assemblies. For example, Peng *et al.* [157] have proposed a novel 5-axis 3D-printer capable of embedding metal wire inside FDM printed parts to realize electromagnetic devices. They demonstrate fabrication of different devices, including solenoids, electro motors, and electro magnets moving fluid magnetic material (Figure 2.10e). MacCurdy *et al.* [130] presented an alternative approach of printing custom 3D geometries with embedded fluid. Their approach allows to digitally fabricate custom hydraulic mechanisms to create actuated objects. They demonstrate complex mechanical assemblies printed

in a single pass, e.g. a hexapod robot driven by a single DC motor or a soft hydraulic gripper [130] (Figure 2.10e).

In addition to printing, soft actuated objects have been fabricated using fabric and embedded strings that act as "tendons"[3, 15]. For example, Albaugh *et al.* [3] presented an approach based on automated machine knitting that produces a soft shell with integrated strings for actuation. After manually filling the objects with material, pulling the strings allows to move parts of the object (Figure 2.10f).

In addition to actuation, other approaches have enabled objects with computer-controlled deformability based on manual fabrication [45, 153]. Particle or layer jamming has been used to create objects that transition between a deformable and rigid state. This effect is achieved by enclosing loose particles or sheets of material inside an air-tight soft shell. The overall structure is deformable unless negative air pressure is applied. Negative air pressure causes the shell to deflate and to compress the particles or layers, resulting in a non-deformable structure. For example, Follmer *et al.* [45] use particle jamming for a phone prototype that can be deformed into the shape of a remote control, watch, or game controller (Figure 2.10g). Out *et al.* [153] focused on thin re-shapable structures via layer jamming, for example, to create a stiffness-changing display or deformable furniture.

In contrast, this thesis contributes a novel approach for computer-controlled deformability based on digital fabrication (Chapter 6). Chapter 6 presents an approach based on 3D printing and 2D-printed heating elements that enables computer-controlled on-demand capabilities to change an object's 3D shape or compliance.

2.3 Digital design of interactive objects

The first fabrication machines controlled by digital computers were developed in the 1950s. At the time, digital design was done by writing computer programs in an "assembler"-style language to control the machine [178]. Abstraction was introduced soon after to facilitate the digital design. Ivan Sutherland pioneered the concept of graphical design instead of writing code with his *SketchPad* system in 1963 [208]. This pioneering work was followed by further development towards graphical user interfaces (GUIs) with major contributions by Douglas Engelbart and researchers at Xerox Palo Alto Research Center in the 1960s and 1970s [43, 89]. They developed the fundamental of GUIs, for example, introducing the concept of windows, icons, menus, and pointers (WIMP) [36].

For modern GUIs a second layer of abstraction facilitates creating custom interfaces. Modern GUI frameworks, e.g. *JavaFX* [50], *GTK* [210], or *SwiftUI* [5], provide abstract control elements (also called widgets or controls), e.g. buttons, sliders, or menus. These controls are software components that encapsulate an element of interaction allowing high-level design of custom GUIs. Low-level details, e.g. how the control is rendered, are handled by the system or framework.

Modern design for digital fabrication makes use of GUIs as part of computer-aided design (CAD) applications, e.g. *Rhino3D* [177] or *Autodesk inventor* [6]. This software allows for graphical design of custom geometries, abstracting from the concrete

code required to fabricate the part. However, little support is offered at a higher level of abstraction, e.g. encapsulating functionality as demonstrated by GUI frameworks.

This section provides an overview of research on high-level design that uses abstraction to ease the design of complex objects. We will discusses related work on high-level design of custom objects and towards design for interactive objects with rich materials. As a second important aspect regarding design, this section discusses improving feedback and manipulation during digital design to enhance the digital fabrication process.

2.3.1 High-level digital design

High-level design tools allow the designer to specify desired design properties, abstracting from low-level parameters. Based on this specification, the computational tool then generates the necessary low-level details. Such high-level approaches have been demonstrated in a variety of domains. Examples include abstracting from design details of complex mechanisms [34, 81], optimized geometry [28, 185], or creating meta-materials [17, 196, 81].

For designing mechanical mechanisms, computational tools allow the designer to specify a desired motion path of the mechanism. This has facilitate digital fabrication of mechanisms. For example, Coros *et al.* [34] have presented an approach that generates an assembly of mechanical moving parts to achieve a desired motion. Ion *et al.* [81] have presented an alternative approach that generates cells of a meta-material structure to closely match the specified movement. The resulting structure can be 3D-printed as one piece.

Other approaches support the designer by automatically generating load-bearing structures to be digitally fabricated from a high-level specification [28, 185]. For example, Saul *et al.* [185] propose a system to design stable chairs to be fabricated on a laser cutter by sketching a coarse shape. Their tool allows to tailor the chair in respect to ergonomics and supports designing stable chairs using physical simulation. As an alternative approach, *Forte* [28] allows the user to sketch an approximate shape of a geometry and define desired loads. The system then generates a geometry based on 2D topology optimization that can be 3D-printed.

Towards fabrication of rich materials, the design of custom material properties has been supported by high-level design approaches that generate geometric structures or material composition for 3D-printing [17, 196]. Schumacher *et al.* [196] presented an approach that takes a 3D model with specified elastic parameters as input. Their approach then generates a low-level design based on geometric microstructures. The result is optimized to be 3D-printable from a single material and to closely match the desired elastic behavior. Bickel *et al.* [17] presented an alternative approach where the user specifies the desired material by providing example deformations and corresponding forces. Their data-driven approach then generates a layered composite material comprising microstructures and layers created from a mixture of two different materials.

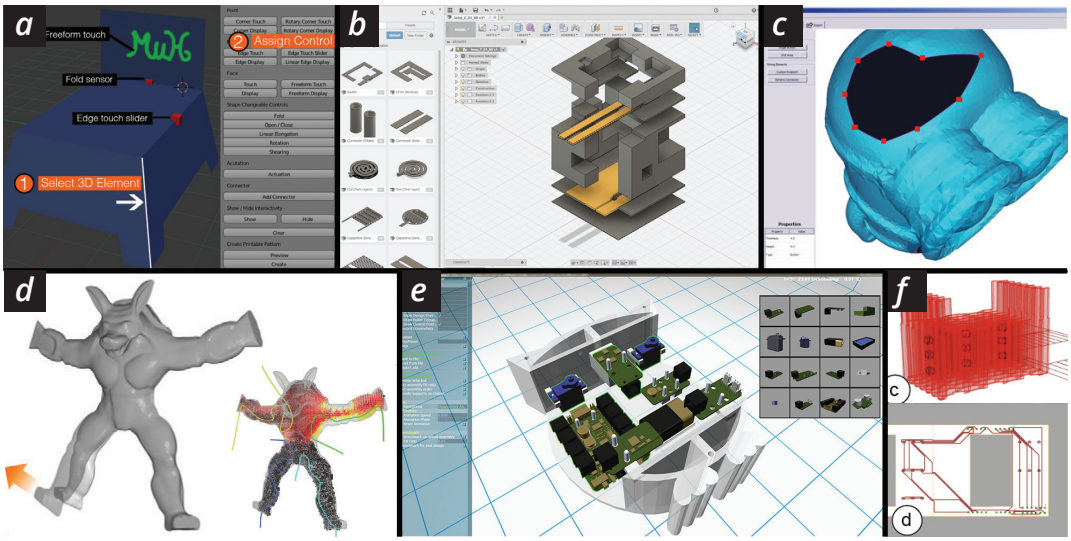

Figure 2.11: Examples of design tools for interactive objects. Parametric components enable high-level design of (a) objects folded from 2D-printed electronics [148] or (b) objects made of stacked layers with embedded 2D-printed electronics [146]. Other tools allow to define (c) desired touch sensitive areas [192] or (d) desired sensed deformation [7] on 3D-printed objects. Using standard components is supported by (e) optimizing placement in a 3D enclosure for electro-mechanical devices [40] or (f) fabricating objects with embedded components from 2D sheets that are folded into structures made of honeycomb cells [249].

While a large body of research has simplified design of complex 3D objects including custom material properties, high-level design of interactive objects with digitally fabricated electronics has been addressed by a limited amount of prior work.

Olberding *et al.* [148] presented a first approach for high-level design of interactive 3D objects using printed electronics. Their approach allows high-level specification of desired input and output capabilities on a 3D model using parametric design of printable components. They presented a set of input components, including touch, fold, proximity, elongation, shear, and rotation sensing, and output components, including light-emitting displays and printed actuators. Based on the high-level design using a graphical design tool (Figure 2.11a), their approach generates low-level files for conductive inkjet printing or functional screen-printing. To this end, they contribute an algorithm that transforms the 3D model into a flat foldable structure. The printed sheets can then be cut out and assembled to developable 3D geometries via folding. Oh *et al.* [146] presented an alternative approach based on fabricated senors and actuators. Their design tool allows to place parametric components on a 3D model and produces low-level files for a fabrication process based on "3D sculpting" with embedded 2D printed electronics (Figure 2.11b). The sculpting process builds the object layer by layer by stacking selectively cut sheets of paper. This allows to insert sheets of 2D printed electronics. These approach extend beyond prior work that enabled high-level design of printed 2D interfaces [168]. However, they are limit custom-printed electronics to developable surfaces.

Initial work towards supporting high-level design of custom electronics on non-developable geometries has been presented by Schmitz *et al.* [192]. Their approach enables the design and fabrication of custom-shaped touch electrodes for 3D-printed objects. They contribute a design tool allowing the designer to specify a region for touch sensing on the object (Figure 2.11c). The tool then generates an electrode pattern within the target region, routes the necessary wires through the object, and generates files for 3D printing.

A first approach for high-level design of deformation sensors for 3D objects was presented by Bächer *et al.* [7]. Their approach optimizes the placement of one or multiple parametric piezo-resistive wires inside a deformable object to match a target deformation defined by the user (Figure 2.11d). Based on their optimization they also generate a mapping from low-level sensors readings to user defined input actions.

In contrast to fabricated electronics, other approaches facilitate the design of interactive objects using standard electrical components. For example, *Makers' Marks* [187] and *RetroFab* [167] generate mounting structures for conventional components based on a digital design of their placement in the object. Desai *et al.* [40] present an approach that optimizes the layout of standard components inside an object with respect to a desired configuration and assembly constraints (Figure 2.11e). Yamaoka *et al.* [249] present an approach that generates a foldable honeycomb structure for embedding standard components. Their tool converts the 3D model into a foldable honeycomb structure and allows to place components within that structure (Figure 2.11f). It then routes connecting wires between the components and produces files for fabricating a flat multi-layer structure on a cutting plotter. The resulting sheet can be folded into the desired 3D geometry. In contrast to using individual components, Ledo *et al.* [122] present a design approach based on embedding an entire electronic device, e.g. a smart watch, inside the object. The components their tool offers allow to expose functionality of the embedded device on the object's surface. Visual output, for example, is routed from the device's screen to the surface using light pipes while touch is rerouted using conductive material. The design tool generates these routing structures and produces the necessary files for fabrication via 3D printing.

In the context of this prior work, this thesis advances the high-level design of interactive objects with digitally fabricated electronics in two aspects. First, it enables high-level digital design of tactile input and output controls on non-developable geometries, which was prior unsupported (Chapter 5). Second, it advances the field towards high-level digital design that simultaneously addresses the design of custom fabricated electronics and custom material properties (Chapter 3).

2.3.2 Digital design using physical elements

High-level abstraction eases the digital design of complex objects and thus facilitates the digital fabrication process. A second major aspect to enhance the digital fabrication process is to improve feedback and manipulation during design. This section discusses related work that addresses the shortcomings of traditional visual

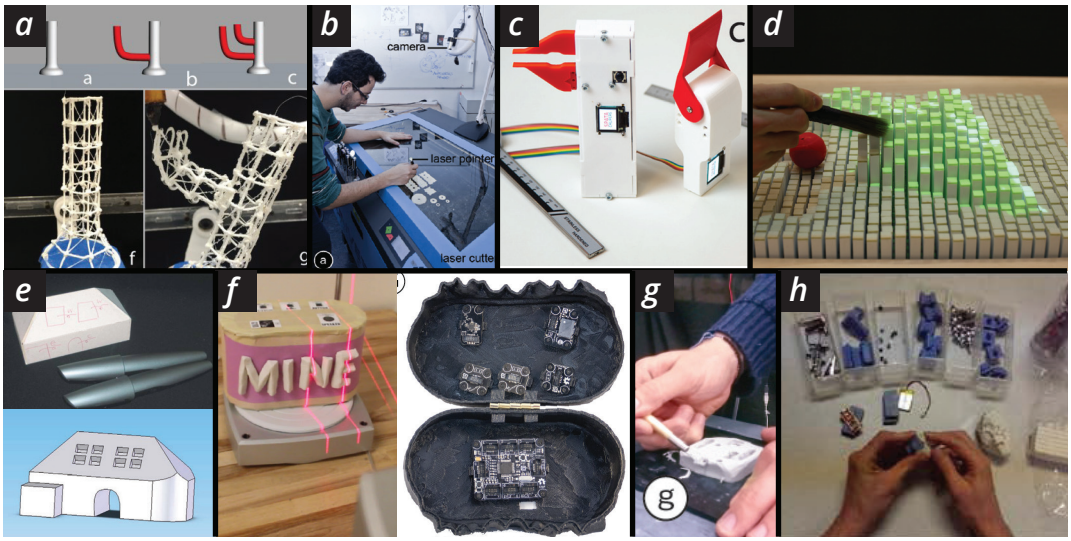

Figure 2.12: Examples of incorporating physical elements in the digital design process: providing physical feedback through (a) 3D-printing and cutting for updating a physical wireframe model [159] or (b) cutting and engraving the workpiece as immediate response to design actions [138]. Shape-changing (c) tools [233] or displays [46] offer physical feedback and manipulation during design. Physical hands-on design is enabled by annotating (e) desired geometry modification on a paper model with a digital pen [199] or (f) desired placement of electrical components on a sculpted model [187]. (g) Sculpting allows to physically form a custom geometry that is later scanned [234]. (h) Placement of custom electronic components can also be done during the sculpting process by using 3D-printed proxy objects [94].

feedback and 2D manipulation during design, e.g. via screen, mouse and keyboard. In particular, it focuses on incorporating physical elements in the digital design process as one promising direction to improve feedback and manipulation.

Several approaches have explored physical feedback to enhance digital design. Examples include rapid fabrication of tangible representations [16, 136, 139], physical feedback using the fabrication device [140, 138, 159], and shape-changing interfaces and tools [46, 233]. Similarly interaction in a physical, tangible form has been explored to improve manipulation during design. Approaches have proposed forming custom geometry from malleable material, annotating modifications of physical props, and incorporating real-world objects or measurements into the digital design. These approaches demonstrate the benefit of providing physical feedback or means for physical manipulation in the context of designing custom geometry. A major open challenge, however, is whether similar principles can be applied to support the design of interactive objects with rich materials. This has been left largely unaddressed, with a few exceptions that focused on physical design of custom rigid geometry that incorporates standard electric components [94, 187].

In this context, this thesis enhances the digital fabrication process towards design of interactive objects with rich materials. It contributes two approaches that incorporate physical elements in the process by leveraging the fabricated interactive object as a

feedback and manipulation tool (Chapter 5 & 6). These approaches are inspired by the following aspects of prior work.

Chapter 5 introduces an approach that provides immediate physical feedback for designed tactile output on the fabricated object. This draws inspiration from approaches that provide immediate physical feedback for design changes by updating the shape of a fabricated representation or dedicated device. For example, Peng *et al.* [159], propose a system that updates a physical wireframe model through 5-axis 3D-printing and cutting as the digital design is modified (Figure 2.12a). Mueller *et al.* [138] presented an approach to specify a 2D design directly on the flat workpiece inside a laser cutter. The laser cutter then provides immediate physical feedback for every design step, e.g. by engraving or cutting the workpiece (Figure 2.12b). In contrast, Weichel *et al.* [233] proposed a set of shape-changing spatio-tangible tools (Figure 2.12c). Their physical tools resemble calipers providing feedback on length and bevel protractors communicating an angle measurement. Measuring size or angle in the digital model is reflected by adapting either tool's respective physical length and angle. Follmer *et al.* [46] presented a 2.5D shape display that provides more detailed feedback on the digital model's geometry (Figure 2.12d). The display renders an object's shape by moving an array of pins. This allows to dynamically update the displayed physical representation as the digital design changes. This thesis expands the concept of providing immediate physical feedback during design to interactive objects and shows the novel possibilities that fabricating interactive objects offers in this regard (Chapter 5). It further demonstrates that physical feedback is highly relevant for designing interactive capabilities, using the example of designing tactile interfaces.

In addition to physical feedback, the approach presented in Chapter 5 enables hands-on physical refinement of the digital design on the fabricated object. This is inspired by prior work that enabled design manipulation on physical props [187, 199]. For example, *ModelCraft* [199] allows sketching geometric modifications, e.g. holes, with a pen on architectural paper models (Figure 2.12e). Savage *et al.* [187] enables designers to attach stickers onto an object geometry to define the placement of electrical standard components (Figure 2.12f). The object with stickers is then scanned and the design tool creates a 3D-printable hollow object with dedicated geometry to mount the standard components. Chapter 5 uses a similar physical interaction by leveraging the fabricated tactile input controls, allowing the designer to refine the design, e.g. the lengths of a placed control.

Chapter 6 presents an alternative approach that incorporates physical elements in the design process. It allows to incorporate capabilities for physical hand-on customization in the fabricated object. This approach draws inspiration from approaches that have explored hands-on modeling using physical material, e.g. by sculpting and scanning an object [94, 187, 234]. For instance, *ReForm* [234], allows to sculpt and refine a malleable physical model that was 3D-printed from clay (Figure 2.12g). The model is then 3D scanned to update the digital model. Other approaches have similarly relied on sculpting and scanning an object but incorporate standard electrical components [94, 187]. Savage *et al.* [187] use stickers that can be attached to the object (Figure 2.12f). Jones *et al.* [94] embed physical 3D-printed representations in the sculpted model (Figure 2.12h). This thesis expands the concept

of hands-on modeling of malleable material to customizing an object rather than initially designing custom geometry. The approach embed computer-controlled elements that enable the object to be customized in shape and compliance. As a result, the approach allows the initial digital design to be less precise and instead offers physical customization after initial fabrication.

2.4 Discussion and conclusions

This chapter has provided an overview of related work on digital fabrication technologies, rapid prototyping of physical user interfaces, and digital design for fabrication. The presented work has contributed approaches towards digital design and fabrication of custom 3D geometries, custom material properties, and custom capabilities for input and output. One key insight from this overview is that open challenges remain particularly at the intersection of these properties, where the goals is to enable digital design and fabrication of custom interactivity and custom rich materials simultaneously.

2.4.1 Digital fabrication of geometries, materials, and electronics

For fabrication technologies this chapter has discussed a range of promising work that addressed challenges regarding the fabrication of either custom geometry, custom deformable objects, or custom electronics. One major open challenge is the accessible and rapid fabrication of custom electronics for deformable objects and for objects of complex geometries. This thesis contributes towards addressing this challenge.

In particular, two major contributions address the fabrication of custom stretchable electronics and electronics on complex geometries. Chapter 3 presents a novel approach enabling rapid and accessible fabrication of custom circuits with custom stretchability. It enables rapid prototyping where prior work relied on slower fabrication approaches to create stretchable circuits. It also advances fabrication to support multiple seamless areas of custom stretchability, whereas other approaches offered primarily uniform stretchability.

At the intersection of custom electronics and custom geometry, Chapter 4 contributes a novel fabrication approach for thin and conformal printed electronics on complex geometries and diverse materials. The approach enables digital fabrication of metal-based conductors with high conductivity, translucent conductors, and multi-layer circuits on complex geometries. It thus extends the capabilities of fabrication beyond prior work that was limited to carbon-based conductors or developable geometries.

Last, Chapter 6 contributes an approach for digital fabrication of custom geometry and custom deformation properties. This complements prior work that has demonstrated approaches to increase fabrication speed at the cost of less-detailed geometry. While these approaches implement large changes by fabrication objects from scratch, Chapter 6 presents an approach that allows for rapid adaptation of detailed geometry after initial slow fabrication.

2.4.2 Rapid prototyping of interactive objects

For rapid prototyping of interactive objects one major challenge is to advance the digital fabrication of custom input and output capabilities that promises to ease rapid prototyping compared to manual fabrication and use of less customizable standard components. This chapter presented related work on multiple modalities and discussed printed electronics as one promising approach to digitally fabricate interactive objects with rich materials. Two remaining challenges are to advance approaches towards supporting complex geometries and rich materials, and to extend the supported input and output capabilities.

This thesis addresses the former challenge by contributing an approach enabling custom-shaped touch input and display output on complex geometries by fabrication thin and conformal overlays (Chapter 4). This improves over prior work that was limited to developable geometries, to touch input, or to thicker less conformal overlays.

Furthermore, this thesis contributes two approaches to extend input and output capabilities. Chapter 5 contributes towards extending the capabilities of haptic feedback on 3D objects through digital fabrication. It presents a novel approach for digital fabrication of high-resolution taxel-based tactile input and output on 3D geometries. This approach extends beyond initial exploration of digitally fabricated haptic output of low spatial resolution [189, 222] or on few geometries [102, 245]. Chapter 6 contributes a novel approach for digital fabrication of haptic feedback and shape change capabilities. It extends beyond prior work that relied on manual fabrication to achieve computer-controlled on-demand deformability.

2.4.3 Digital design of interactive objects

Towards improving digital design of interactive objects with rich materials this chapter discussed related work regarding high-level digital design and improving feedback and manipulation during design. For high-level design, this demonstrated that design of custom fabricated electronics for 3D objects has been limited to a few initial approaches. This limits high-level design support to a few modalities or in terms of geometries. This thesis expands the supported modalities by contribution a novel approach for the high-level design of tactile input and output controls on 3D geometries (Chapter 5). As a second challenge for high-level design the discussion highlighted the lack of approaches that address the fabrication of custom electronics and custom material properties in one holistic solution. In this regard, this thesis contributes a first approach that enables high-level digital design of custom circuits for interactivity and custom stretchability as a material property.

In respect to improving feedback and manipulation during design, this chapter discussed a range of approaches that demonstrate the benefit of incorporating physical elements in the design process. This discussion pointed towards one major challenge of exploring approaches to improve feedback and manipulation during design of interactive objects with rich materials. In contrast to custom geometry, this remains largely unaddressed. Towards addressing this challenge, this thesis contributes two approaches incorporating physical elements in the design of custom

interactive objects (Chapter 5 & 6). With these approaches, this thesis demonstrates a promising direction of leveraging the capabilities of fabricated interactive objects for feedback and manipulation during digital design.

3 Rapid Design and Fabrication of Stretchable Interfaces

As pointed out in the introduction, stretchability is a promising property for interaction with objects beyond touch on rigid surfaces. Stretchable interfaces are receiving growing attention, as they allow designers to integrate interfaces in materials with elastic properties, such as textiles [154, 224] or human skin [236], and enable novel physical interactions [214].

However, creating functional prototypes to explore interaction with stretchable interfaces remains difficult. Prior work has relied on fabrication processes such as casting and sandwiching silicone layers with embedded conductors [142, 236, 242] or stitching conductive yarn in textiles [154, 224]. While these processes enable versatile circuit capabilities, they are time-consuming and rather complex. Moreover, existing techniques do not support the designer in easily defining the desired stretchability of a circuit, or including areas of different stretchability. These aspects are essential for many interactive applications in HCI, which may require stretchable regions for buttons to push, rigid islands for mounting conventional electronic objects such as LEDs, or areas on wearable interfaces customized for the stretchability required on specific body locations.

This thesis addresses these challenges by contributing *LASEC*[1]: Laser-fabricated Stretch-able Circuits, the first instant technique for fabricating stretchable interfaces with custom circuitry and custom stretchability. Inspired by work in material science [22, 61, 218], it builds on parametric patterns of thin slits laser cut into a flexible compound material made of a non-conductive and a conductive layer. The pattern allows the surface to stretch at defined areas, in defined directions and up to a desired extent. In the same step, a custom electrical circuit is fabricated by using the laser at a lower intensity to ablate the conductive layer at specific locations.

As a main contribution, this chapter demonstrates the feasibility of rapid iterative design and fabrication of interactive objects with rich materials.

For rapid design, this thesis contributes a computational design tool to assist designers in creating custom stretchable circuits. With a simple modeling application, it allows defining custom stretchable areas and the desired placement of electronic components at a high level of abstraction (Challenge 1). The tool then automatically generates the cut-and-ablation patterns required to fabricate the custom design on

1 This chapter is based on [58]. As the first author, I led the conceptual design, development of the design and fabrication process, implementation of the design tool, evaluation of the fabrication technique, and implementation of application prototypes. The bachelor student Sven Ehses helped with implementing the calibration tool, running the evaluation, and implementing the design tool. The student assistant Muhammad Hamid helped with creating the illustration in Figure 3.2. My supervisor Jürgen Steimle advised me on the conceptual design, evaluation, and applications. He further contributed to the structure and writing of the publication.

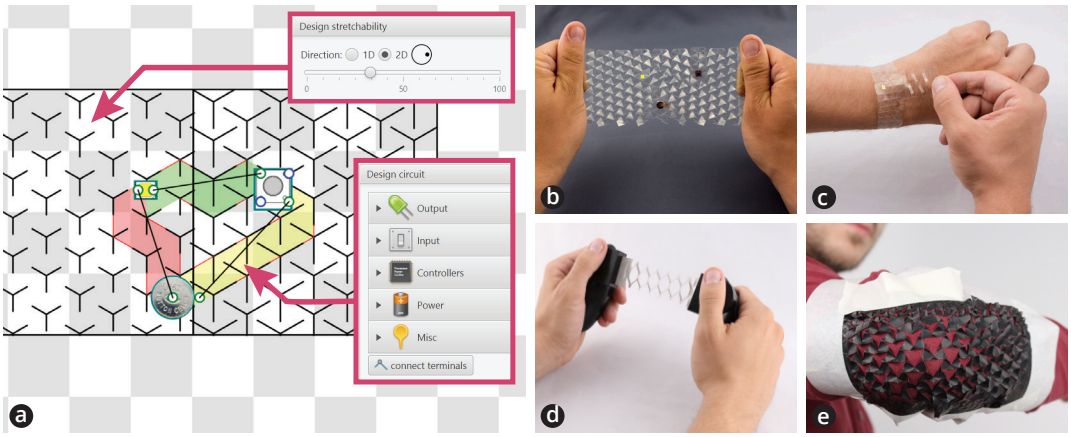

Figure 3.1: The LASEC technique uses a commodity laser cutter to fabricate stretchable circuits of custom stretchability, custom shape and with desired circuitry within minutes. (a) A design tool auto-generates cut-and-ablation patterns from a high-level specification of the circuit. (b) The resulting stretchable circuits can include electronic components, (c) can be transparent, and (c-d) support multiple areas of linear or omnidirectional stretchability.

the laser cutter. To realize this tool, this chapter further presents the first approach to realize circuits on such stretchable structures produced by cut patterns. The major challenge this addresses is routing on these structures despite the bottlenecks created by the large number of cuts. This chapter proposes routing strategies for these structures and contributes a graph-based approach to enable real-time routing, which is crucial for instant feedback during the design step.

For fabrication, LASEC delivers *instant* results, as it implements a one-step laser ablation and cutting process to create both single-layer circuitry and desired stretchable behavior of the interface in a single pass. This process overcomes the inherent limitations of multi-step approaches, which not only consume more time, but also partially rely on manual fabrication requiring expertise to achieve high-quality results. Fig. 3.1 illustrates several examples with stretchable circuits fabricated automatically in less than 5 minutes, a considerable improvement over fabrication times of state-of-the-art related work that reported one hour or multiple hours [142]. Furthermore, the approach is *accessible* to a broad audience, as it relies on a conventional laser cutter available in many labs, schools, and maker spaces (Challenge 2).

In addition to rapid design and fabrication, this chapter presents an approach for fabricating interfaces with one or multiple areas of customized stretchability, based on parametric cut patterns. The approach is the first to support user-defined areas with defined stretchability in one or multiple directions, seamless transitions between areas, and gradients of stretchability. It thus extends the possible capabilities of custom interactive objects with rich materials (Challenge 2).

Together, these contributions enhance the design and fabrication process for rapid prototyping. They speed-up design and fabrication, enabling designers to get hands-on feedback on the designed rich material properties throughout the iterative design process (Challenge 3).

Furthermore, this chapter illustrates the *versatility* of the LASEC technique. It is compatible with many materials of different properties. This chapter presents four compatible materials, including low-cost DIY and off-the-shelf materials and materials for transparent stretchable circuits. It further provides material recommendations for different use cases and a tool for automatic calibration of laser settings to enable easy replication of the approach.

The remainder of this chapter is structured as follows. Section 3.1 introduces the LASEC fabrication technique, its main principle, and the design and fabrication process. Section 3.2 presents the approach for custom stretchability through parametric cut patterns. Section 3.3 describes the contributions towards creating stretchable circuits through routing on cut patterns. Section 3.4 presents results from a controlled technical evaluation. Section 3.5 discusses limitations of the LASEC approach. Last, Section 3.6 provides conclusions based on this chapter's contributions.

3.1 Design and fabrication process

We present a novel fabrication technique that allows designers, makers, and HCI researchers to fabricate stretchable circuits rapidly and with common lab tooling. Both stretchable behavior and electrical circuitry can be custom-designed. Figure 3.1 depicts several circuits that were fabricated using this technique. This section presents the basic principle and gives an overview of the design tool and fabrication process.

3.1.1 Main Principle: Integrated Cutting and Ablation

The LASEC fabrication process works with a deformable two-layer compound material: a non-conductive base material is covered with a continuous conductive layer. This material by itself does not have to be stretchable. The key idea underlying the fabrication process is to combine two steps of subtractive fabrication that are both executed with a standard laser cutter in very little time (see Fig. 3.2): The deformable material is made stretchable by *cutting* slits into both layers using specific parametric patterns (Fig. 3.2b). These slits allow the surface to stretch when tensile force is applied (Fig. 3.2d). By adapting parameters of the pattern, the degree and direction of stretchability can be controlled. At the same time, traces of a custom stretchable circuit are created by selective *ablation* of the upper layer (Fig. 3.2a). During ablation, the laser operates at a lower power level to selectively vaporize patterns on the conductive top layer, while keeping the underlying base layer intact. By combining cutting and ablation (Fig. 3.2c) a stretchable circuit is created (Fig. 3.2d).

The principle is compatible with all common laser cutters. In fact, the approach could also work with other subtractive devices, e.g. milling machines. We use an Epilog Zing CO_2 laser cutter, a common model available in many labs and maker spaces.

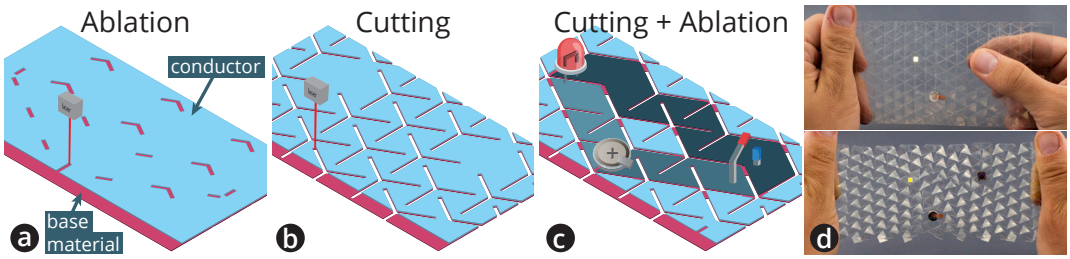

Figure 3.2: The LASEC principle combines ablation of the conductive top layer (a) with cutting of both material layers for stretchability (b) to create stretchable circuits (c). This example shows 3 created traces (c, highlighted) to connect an LED with a button and battery on a stretchable circuit (d).

Any material compound can be used that is deformable, offers sufficient conductivity, and is compatible with laser cutting. Examples include commercially available ITO-coated (Indium Tin Oxide) sheets or standard plastic films coated with conductive ink or paint.

3.1.2 Overview of the Design and Fabrication Process

1. Digital design with design tool

The process starts with the digital design, which is the most crucial step. Creating a manual design for cutting and ablation that defines a desired stretchable behavior and electrical circuitry would be complex and time-consuming. It would also require the designer to have extensive knowledge of the mechanical and electrical properties of the material.

We contribute a design tool to make the technique accessible to a wide audience. It is depicted in Fig. 3.3. The tool allows the designer to easily specify the functional behavior at a high level. Using direct manipulation, the user specifies:

- the location, size, and shape of one or multiple stretchable areas, by drawing circles, rectangles, or 2D polygons
- the degree of stretchability of each area, by dragging a linear slider
- the direction of stretchability of each area: angle of linear stretchability or stretchable in both dimensions
- the electrical circuit, by placing components from a library[2] via drag-and-drop and specifying which terminals shall be connected by traces.

Based on this input specification, the tool automatically generates a custom-designed cut and ablation pattern, which is used as input for the laser cutter. Internally, the tool automatically maps the stretchability settings to the multiple low-level parameters of the cut pattern that together define the stretchable properties of the respective area. The tool then uses our novel routing approach, presented below, to compute the routing paths and to generate the required ablation pattern in real-time.

2 The tool uses the Fritzing part format, with an open source library of more than 1500 components.

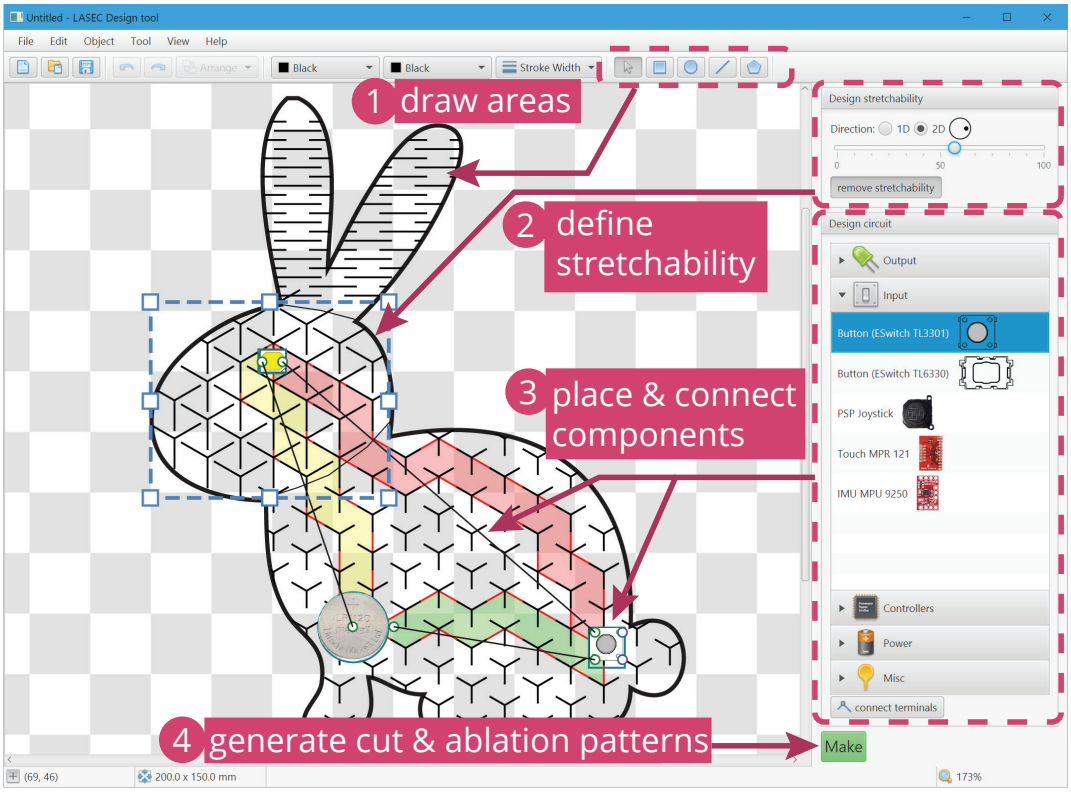

Figure 3.3: The LASEC design tool allows drawing areas and individually defining the stretchability and stretch direction of each area. Circuits can be defined by placing components from a library and connecting the required terminals. The tool immediately generates and visualizes the pattern parameterization and routing. To fabricate a design, it automatically generates the cut & ablation pattern.

The design tool employs the designer-in-the-loop approach: The generated design is instantly visualized. Also while the user is dragging the stretchability slider, the generated cut pattern and circuitry is continuously updated. This allows the user to directly inspect the generated result.

2. Material selection

Next, the user chooses a compatible material compound to fabricate the stretchable circuit. We provide four material choices and recommendations on what materials to choose. A summary is provided in Table 3.1.

The most accessible and easiest to use material option is *ITO-coated PET sheets*. ITO forms a fully transparent conductive layer of relatively high conductivity (60Ω/□). The compound material is available off-the-shelf (Sigma Aldrich 639303) and widely used in industry and DIY projects. However, the material has a comparably high cost (~$15/A4 sheet) and is less mechanically robust than our other options.

A cheaper and more versatile approach is to DIY coat a base material with a conductive layer, using a spray, brush or squeegee. A wide choice of conductive paint and inks is available. If high conductivity is a key requirement, we recommend commercially available *silver-nanoparticle (Ag) ink* (Gwent C2131014D3). With a low

Compound material	*Ease of use*	*Conductivity*	*Robustness*
ITO	●●●	●●○	●○○
Ag	●○○	●●●	●●○
PEDOT:PSS	●○○	●○○	●●●
Carbon	●●○	●○○	●●○

Table 3.1: Overview of compatible materials.

sheet resistance of $0.1\Omega/\square$ it is suitable for high-fidelity circuits, e.g. including I2C, serial communication, or PWM. The most robust circuits can be fabricated using *PEDOT:PSS*, a conductive polymer that is intrinsically stretchable (Gwent C2100629D1), which however has a higher sheet resistance of $500 - 700\Omega/\square$. Silver and PEDOT:PSS can be coated with a simple squeegee, a mayer rod, or a blade coater and cured at $80°C$ for 5 and 3 minutes respectively. *Carbon paint* (MG Chemicals 838AR, $1k\Omega/\square$) can be easily applied by brushing, rolling, or spraying and does not need any post-processing. Despite higher sheet resistances, ITO, PEDOT:PSS, and carbon are still suitable for prototyping circuits, as has been demonstrated, e.g., for touch sensing [237, 242, 260] and EL-displays [149, 148, 242]. Carbon and PEDOT:PSS are the cheapest options (∼$3/A4), with silver being slightly more expensive (∼$4/A4).

These coatings can be applied to a large variety of readily available prototyping materials. We recommend using laminating pouches and inkjet PET film, which are inexpensive ($0.05 and $1/A4) and result in elastic behavior with stretchability over 100% in one and up to 30% in two dimensions (see Evaluation section below).

For precise ablation of a given material on a laser cutter, the laser settings (i.e., power and speed) have to be calibrated once per material. This can be done manually by cutting traces on a material sample with increasing power until conductivity is lost. To ease this task for novice users and enable quicker exploration of additional various materials, we provide an automated calibration tool. It uses a simple breadboard-based resistance measuring device (microcontroller, Bluetooth module, and clips to connect to the material sample) that can be connected to a material sample and placed inside the laser cutter. A PC software rapidly determines cutting and ablation parameters for a given compound material.

3. Laser cutting and ablation

The user places the material in the laser cutter and clicks on "Make" in the design tool. The tool generates a vector graphics file (SVG) color coded to represent laser settings, i.e. power and speed. The file is sent to the laser cutter, which fabricates the stretchable circuit fully automatically within a few minutes. The wristband and elbow patch in Fig. 3.4 were fabricated in 2 and 6 minutes respectively.

4. Connecting components

To finalize the device, the user connects wires and electronic components to the circuit, e.g., using conductive adhesives[3]. Placing components on "islands" in between cuts that undergo minimal deformation, as opposed to connections, improves adhesion.

To attach larger components, e.g. a microcontroller or a battery, the circuit can include "rigid" islands, a common practice in stretchable circuits, that can be easily designed and fabricated with LASEC as non-stretchable areas.

3.2 Parametric Cut Patterns for Custom Stretchability

This section presents parametric cut patterns that turn a deformable sheet into a stretchable surface. The key novelty is to allow designers to freely define custom areas of different stretchability and to support seamless transitions across areas. The patterns are chosen to be compatible with routing of circuits and auto-generated by the LASEC design tool.

3.2.1 Cut Patterns for Custom 1D and 2D Elastic Behavior

As an initial step, we identified parametric patterns suitable to be used for circuits. Two key requirements need to be met: First, to support routing and placement of components, the pattern should leave as much material connected as possible. This requires narrow cuts, while cutting holes or empty spaces should be avoided. This requirement excludes patterns based on auxetic beam-like or linkage-based structures, which have considerable empty space between beams [54, 80, 152, 191]. Second, the pattern must ensure that there is sufficient connected space in-between cuts for routing conductive traces. This contrasts with the common modeling of parametric cut patterns that treats connections between elements of the pattern as point connections without surface area [113].

1D Pattern:

We base our parametric design on a pattern of parallel cuts, used in [60, 61, 22, 231], for its property allowing stretch in only one defined direction. Using this 1D pattern enables the designer to specify in which direction stretchability is desired. The pattern is shown in Fig. 3.4a. It offers considerable connected space for routing of circuitry, does not contain holes, and has been shown to support stretch up to 2000% in [60]. Two parameters influence the stretchability: L and S. Decreasing S or increasing L increases the stretchability, which scales with $\frac{(2L-S)^3}{S}$, as derived in [22] based on beam theory. A third parameter (α) is kept constant for alignment.

3 We used 3M™ Z-Axis Conductive Tape 9703 and copper tape

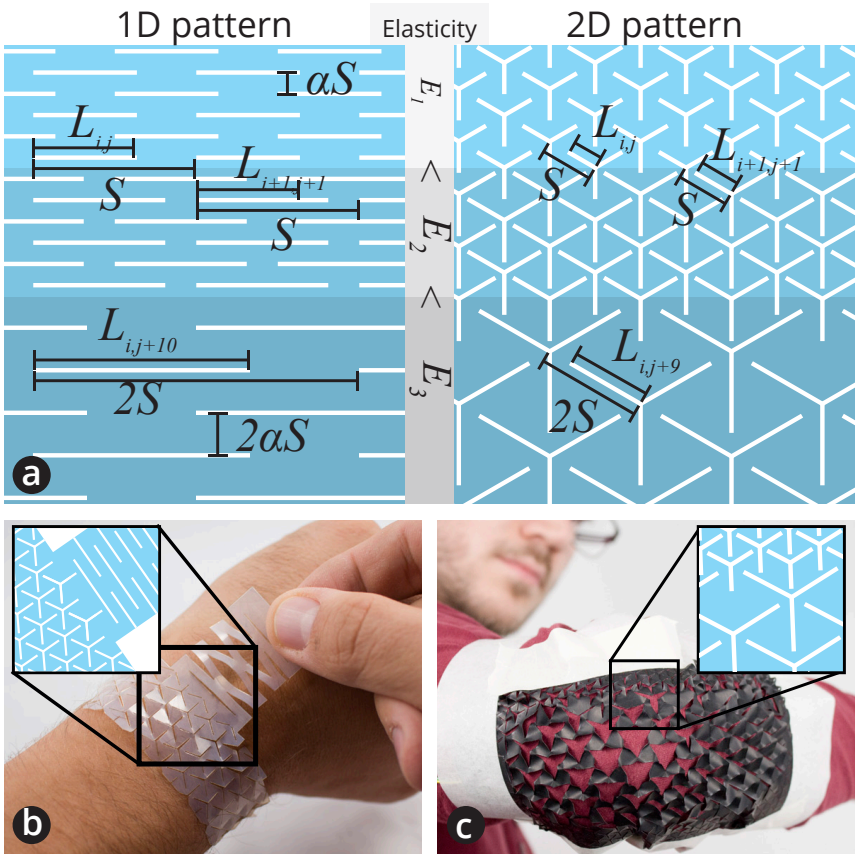

Figure 3.4: Interfaces can have multiple regions of different 1D stretch and 2D stretch behavior (a). To increase stretchability the cut ratio (L/S) is increased (from E_1 to E_2). To keep a minimal gap size ($S - L_{E_2}$), the cut ratio at E_2 cannot be increased further. To increase the stretchability beyond this limit, a scale transition is used (S is doubled). The bottom region E_3 is more stretchable than E_2, while its cut ratio is lower ($L_{E_3}/2S < L_{E_2}/S$) and the gap size wider ($2S - L_{E_3} > S - L_{E_2}$). These patterns allow interaction designers to define the direction of stretch (b) and to adapt the stretchability of different regions, e.g. to match stretch across joints (c).

2D Pattern:

To add the option of stretching in two dimensions, we use a second pattern. This pattern is based on Y-shaped cuts (as used in [218]). In contrast to the parallel alignment of the 1D pattern, cuts in the 2D pattern are oriented at 120 degree angles. Therefore, stress in multiple directions can be distributed across cuts, enabling adjacent regions with stretch in perpendicular directions. Hence, circuits can stretch over doubly-curved geometries.

The pattern has two parameters that affect the stretchability: L and S, see Fig. 3.4a. Increasing L or decreasing S increases the stretchability. Increasing both L and S while keeping L/S constant, i.e. scaling the entire pattern, also increases the stretchability. For a similar pattern, prior work has reported a logarithmic reduction in spring constant with a linear increase in L/S ratio [218]. In contrast to [218], we do not vary a third parameter w, the width of each cut, as this would introduce holes. Instead we keep the width of cuts at the minimum of the laser cutter (<0.3mm).

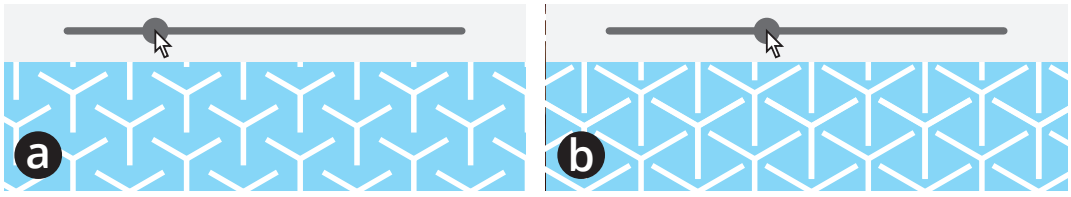

Figure 3.5: The tool allows adaptation of the stretchability of a region using a linear slider: e.g. from lower (a) to higher (b) stretchability.

To support designers in directly and more intuitively defining the desired behavior, our design tool abstracts from these multiple low-level parameters. When the designer sets a desired stretchability using the linear slider, the tool automatically parameterizes the pattern accordingly (Fig. 3.5). We map the slider's value to a relative change in stretchability by adapting the L/S ratio of the pattern.

3.2.2 Multiple Areas of Different Elasticity

If the design contains two adjacent areas of different stretchability, alignment issues arise, as both cut patterns locally interact at the boundary in unforeseen ways. This results in inconsistent stretchable behavior and may create intersecting cuts that lead to holes in the material. We contribute a solution to create seamless transitions between adjacent areas. This also allows us to support stretchability gradients, where the stretchability continuously changes across an area.

Our approach keeps the grid for aligning the individual cut elements constant across areas of different stretchability. We call this the global *scale* of the pattern, i.e. the parameter S in the 1D and 2D patterns. As default we found $15mm$ and $5mm$ for 1D and 2D respectively to be a good compromise between little out-of-plane buckling and large stretchability. The stretchability of each area is then controlled by varying the size of the individual cut element. We call this the local *cut ratio*, i.e. L/S.

However, keeping the global scale fixed has its limitations. On the one hand, it may become necessary to use a larger scale, as it allows for a larger stretchability. This is easy to see: using a constant global scale, the stretchability of the pattern is increased by increasing the size of the cut elements. At one point, the element is as large as the grid size, preventing any further increase in size. On the other hand, it is also not desirable to always use a very large global scale, as this would result in larger out-of-plane buckling.

Our approach is to keep the scale of the pattern constant and as small as possible. Only if the desired stretchability exceeds the maximum stretchability supported by this scale is the scale increased by a factor of two. By only using multiples of the initial scale, the elements stay in a grid of even spacing for alignment (see Fig. 3.4a). The parameters of the local cut ratio (L/S) are adapted such that the desired stretchability is met. This results in overall larger cut elements but more space in-between cuts. This approach works with both cut patterns. Fig. 3.4c shows examples generated by our design tool that contain two directly adjacent areas of

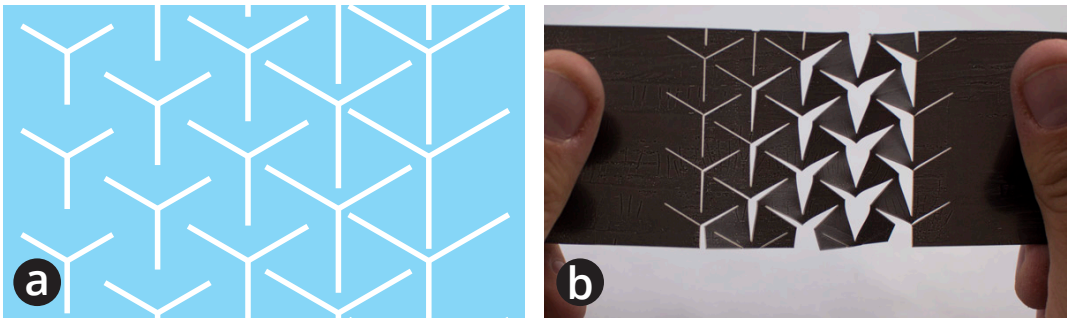

Figure 3.6: Using a gradient pattern from low to high stretchability (a) results in interfaces that stretch progressively from high to low with increasing force (b).

low and high stretchability and Fig. 3.6 a surface with a continuous stretchability gradient.

Adjacent areas of stretchability in different directions are enabled by the 2D pattern, as illustrated in Fig. 3.4b. In the example, the 2D pattern along the wrist enables stretching perpendicular to the 1D pattern, even in the top region where the patterns are connected. A 1D pattern would be constrained by the non-stretchable edge at the connection. Similarly, a 2D pattern enables stretchable regions enclosed within a non-stretchable region, e.g. for a stretchable push button. To combine a 1D and 2D pattern, a minimal space with no cuts is required to avoid alignment issues. In our implementation, this space is a strip as wide as the minimum trace width used for routing.

3.3 Circuit routing on cut patterns

After generating the custom cut pattern for an interface of desired stretchability, the circuit is added by realizing conductive traces. Contrary to common conductive surfaces and printed circuit boards, the stretchable pattern contains a large number of cuts. These create serious bottlenecks for routing, which poses new challenges that were not addressed in prior work. We address them by proposing three general strategies for routing circuits on cut patterns and by contributing a novel routing algorithm that enables instant feedback while the designer is exploring design options (designer-in-the-loop approach).

3.3.1 Routing Strategies for Cut Patterns

We propose three general strategies for routing circuits on a stretchable cut pattern. These ensure that conductive traces of acceptable resistance can be routed between desired terminal points despite the bottlenecks created by the cut pattern. The strategies are implemented in our design tool:

Prioritize less stretchable areas

The first and simplest strategy is to prioritize areas with less stretchability. Those have wider bottlenecks than areas of higher stretchability (see Fig. 3.7a). Wider

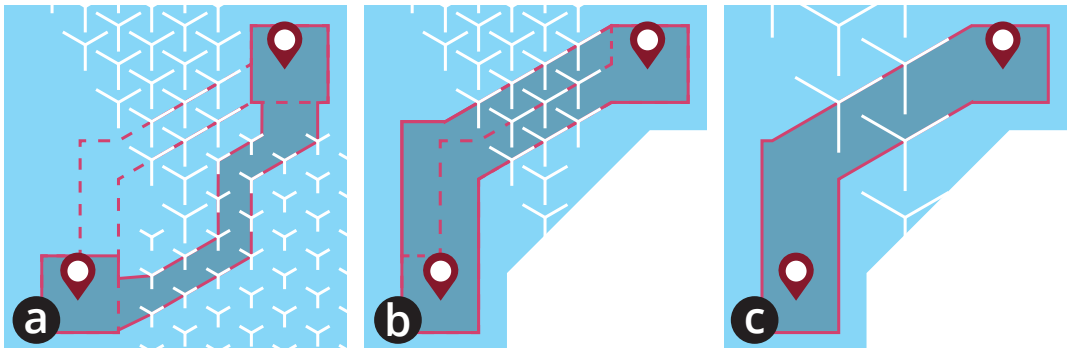

Figure 3.7: Three routing strategies allow coping with narrow bottlenecks to reduce a trace's resistance and increase its robustness by: (a) prioritizing areas of lower stretchability with wider bottlenecks (solid outline) over areas of higher stretchability (dashed outline), (b) routing via multiple adjacent paths through the pattern, or (c) adapting the cut pattern to increase the bottlenecks' width (compared to dashed outline in (a).

bottlenecks allow for wider traces, hence reducing the resistance. For example, Fig. 3.7aillustrates the shortest path through a region of lower stretchability has 82% wider bottlenecks than the 14% longer path through a region of higher stretchability (dashed outline); this reduces the resistance by 37%. It further enhances the mechanical robustness by virtue of less strain expected along the path. Areas with higher stretchability allow for larger stretch and thus may experience higher strain.

Our tool applies this strategy first, during initial routing of all traces. For each trace, the stretchability along its path in addition to its length is considered to find an optimal path. To this end, our tool uses the width of the bottlenecks of each area as weights in our graph representation for routing discussed below. This allows the tool to route traces along paths with less stretchability and wider bottlenecks for higher durability and lower resistance than shorter alternative paths.

Multipath routing

This strategy increases the conductivity of a connection across the cut pattern by using multiple parallel paths (see Fig. 3.7b). Fig. 3.7b illustrates the resistance between the two indicated points is approximately divided by two by using two parallel paths.

Our tool applies this strategy iteratively for all routed traces. For every trace, the tool checks for each bottleneck along the path to determine whether the trace can be widened by adding a parallel path through adjacent bottlenecks. For a single trace through a stretchable area, the tool widens the trace to the maximum extent. For multiple traces, the tool iteratively grows each trace in turn to find a common boundary between two adjacent traces.

Adapting the cut pattern

This strategy leverages the customizability of the cut pattern and adapts it to reduce or remove bottlenecks. The main limiting factor for routing of conductors at a bottleneck is the width of the remaining sheet's surface between two or more cuts

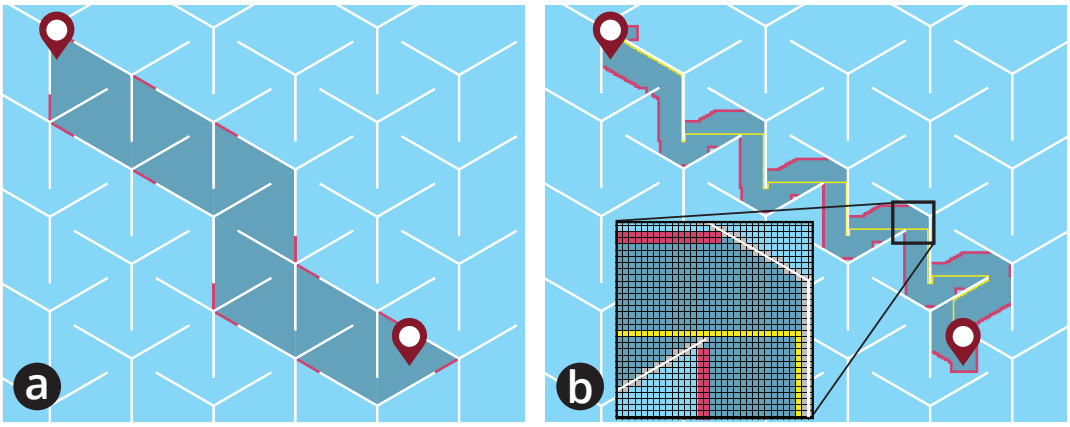

Figure 3.8: Comparison of routing result: our graph-based approach (a) requires a few nodes while maze routing requires a high resolution grid with many cells to model cuts as obstacles in sufficient detail (b).

(compare gap width $S - L$ in Fig. 3.4a). This width defines the effectively available area for routing.

This width can be enlarged without an effect on stretchability by increasing the overall scale of the pattern, as we have discussed in the previous section. Our tool applies this strategy if traces have a too high resistance despite applying the two previous strategies. Fig. 3.7c shows the bottlenecks to be 93% wider, reducing the resistance by 48%.

In some cases, the tool may not find a solution for routing all traces, e.g., in a case with many conductive traces, small bottlenecks, and little available space. The design tool then automatically determines if reducing the stretchability (and in turn reducing bottlenecks) would allow for solving this task. Internally, it incrementally reduces the stretchability of all areas and each time calculates possible routes until a solution is found or the stretchability cannot be further reduced. It then communicates to the designer that not all traces could be routed using the desired stretchability settings. The tool also indicates the reduced stretchability level for which it was able to generate a solution. The designer can then accept the less stretchable version or adapt the terminal placement for routing along a different path.

3.3.2 Real-time Routing on a Cut Pattern

To implement these routing strategies and to provide a fast approach to finding routes despite the many obstacles created by cuts, we propose a novel routing approach that runs in real time. This enables a designer-in-the-loop approach, where the designer can instantly see the effect of changes in stretchability on the generated routing.

In contrast, standard routing techniques, for instance Maze routing [123] as commonly used in prior work [190, 148], are not efficient for routing on cut patterns. For modeling the cut surface in sufficient detail, a very small grid size and hence a very

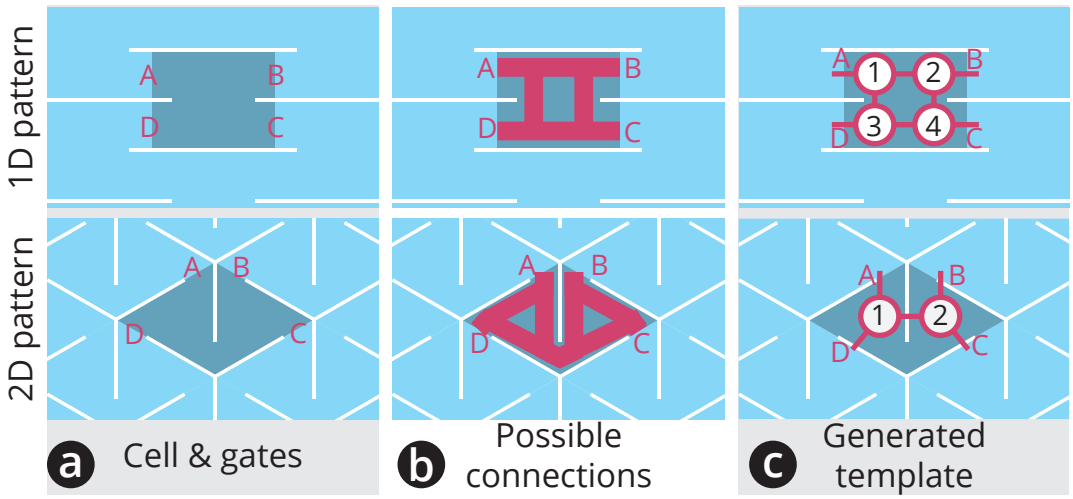

Figure 3.9: Pattern cells with gates labeled A-D (a), possible connections betweeen gates at given trace width (b), and the generated template with nodes and edges (c).

large number of cells would be required. Even a small example[4] would require > 1 mio. grid cells and 126*ms* (on a 2.2GHz i7 CPU). Achieving a real-time update rate of at least 10Hz for circuits with ∼10 traces would require a significantly shorter routing time of $< 10ms$ per trace.

The key idea of our novel real-time approach is to leverage the repetitive structure of the pattern and model its geometry in a simplified graph structure, using pre-computed templates. Routes can then be calculated more efficiently on this graph using an existing graph-based routing algorithm.

Step 1: Offline generation of cell templates

The graph is constructed using offline pre-computed templates that model the routing-relevant properties of the pattern's basic elements, which we call cells. For a given parametric pattern, the cuts form the boundary of a repeating structure of tiled cells. The cell structures for our patterns are illustrated in Fig. 3.9a. A cell consists of a *body* (its inner area) and several *gates* (openings where it connects to adjacent cells).

To automatically model the cell's routing-relevant properties with a minimum number of nodes during (offline) template creation, our algorithm computes how many connections can be routed across the gates and between gates inside the cell at a given minimal trace width (Fig. 3.9b). Note that this depends on the geometry of the gates and the space available in its body, which defines the cell's "bottlenecks". The algorithm creates a template that stores the number of nodes to be generated for the cell, the edges to be created between these nodes, and the "gate" edges to be created between these nodes and nodes of adjacent cells (Fig. 3.9c).

The template is created only once. Our tool stores templates in a database and performs a simple look-up for the correct template in the next step.

4 10x10cm sheet of 2D pattern ($L = 4.36mm$, $S = 5.45mm$) with three conductive traces; modeling this pattern requires a grid size of 0.1x0.1mm, as in Fig. 3.8b.

Step 2: Generating the routing graph

The entire graph is generated by adding one template for each cell of the pattern and then adding edges between nodes of adjacent cells connected through a gate.

For the example from above, the routing graph has 522 nodes and 737 edges (in contrast to >1 Mio. grid cells for Maze routing). Generating the graph takes $0.5ms$.

Step 3: Calculating routes

This compact graph representation then allows for efficient calculation of conductive routes using a graph-based routing algorithm. Our tool uses the A* algorithm [68] to route all traces of the circuit.

For the example from above, routing the three traces on the 10x10cm sheet takes $0.9ms$. This is about 140 times faster than the standard maze router and enables real-time feedback in the design tool.

Step 4: Generating ablation paths

When the user is satisfied with the routing and clicks "Make", our tool generates the ablation path. Since the entire sheet is one conductive layer, every routed trace needs to be isolated from the remaining surface through ablation. Since the entire surface is represented by our graph and conductive connections by edges, all locations are ablated that correspond to an edge connecting a routed path to the remaining graph. The final ablation pattern is stored color-coded in the SVG file sent to the cutter for fabrication.

3.4 Validation

To validate the LASEC technique, we have empirically evaluated the main technical properties and furthermore demonstrated the practical feasibility by fabricating interfaces for 3 application cases.

3.4.1 Technical evaluation

In three technical experiments, we investigated material compatibility and electrical behavior and durability of stretchable circuits.

To this end, we subjected material samples to controlled stretch tests. We used a custom-built automatic extensometer that uses a linear actuator (Drive-Systems Europe DSZY1-Poti) controlled by a Teensy 3.5 microcontroller for stretching the sample by a defined displacement, once or repeatedly. The setup contains a precision multimeter (Fluke 8846) for four-point probe resistance measurement during stretching.

	[kΩ]						[Ω]	
	Carbon		ITO		PEDOT		Ag	
Cycle	1D	2D	1D	2D	1D	2D	1D	2D
0	148.5	11.2	17.9	2.6	46.5	9.4	11.4	6.5
10	148.6	11.5	18.4	3.3	46.3	9.4	11.5	6.9
100	148.5	12.3	19.3	5.0	46.1	9.3	11.9	9.0
1000	148.7	14.6	20.6	11.7	46.2	9.5	12.7	17.6

Table 3.2: Baseline resistance after 0, 10, 100, and 1000 stretches.

Material compatibility

For our initial pilot exploration of compatible materials, we collected and tested a broad selection of laser-compatible prototyping materials readily available online or in a hardware or office supply store. These include various types of plastic foils (plastic stretch wrap, vapor barrier foil, laminating pouches, overhead foil, inkjet PET film), acrylic sheets (Plexiglas) and acrylic films, paper, cardboard, wood veneer, leather, and cotton fabric.

While many materials could be coated, cut, and ablated, we identified two plastics (Fellowes laminating pouches and Mitsubishi inkjet PET film) to yield the most stretchable elastic deformation.

Next, we investigated the bounds of stretchability of the 1D and 2D patterns with different pattern parameters. We stretched four samples (5x10cm) of inkjet PET film in 5% increments to the point of rupture. The samples were cut with the 1D patterns of low stretchability (S=44, L=10, αS=3 mm) and high stretchability (S=44, L=40, αS=3 mm) as well as the 2D patterns of low (S=10.9, L=7.5 mm) and high (S=10.9, L=9.5 mm) stretchability.

Our results show a maximum stretch of 40% for the 1D low stretchability sample, while the 1D high stretchability pattern remained intact at 100% stretch, the limit of our stretch setup (20cm extension). In the 2D case, we found the low stretchability sample to rupture after 20% stretch and the high stretchability sample after 40% stretch.

Durability of stretchable circuits

In a dynamic durability test, we validated the endurance of the electrical functionality and mechanical integrity of LASEC circuits. We add to findings from prior work in material science that has used different materials and parameters [61, 218]. We subjected samples (5x10cm) made of four conductive materials (ITO, sprayed carbon, and silver and PEDOT:PSS applied with squeegee on PET film) and cut with both patterns (1D and 2D) to 1000 repeated stretching cycles. Based on the previous results, we selected the pattern parameters for high stretchability, which represent an upper bound and thus the most challenging conditions. We stretched the samples by 100% in the 1D and 30% in the 2D case (10% safety margin to point before rupture). We continuously measured the resistance.

Absolute measurements of baseline resistance after 0, 10, 100 and 1000 stretching cycles are given in Table 3.2. The results show that all materials with both patterns remain functional after 1000 stretching cycles.

PEDOT shows a very small change in baseline resistance for both patterns ($\sim$1%), indicating high durability. This compares favorably with the behavior of recent state-of-the-art DIY solutions for stretchable devices in HCI that use liquid metals in silicone casts.[5]

The other materials also achieve suitable durability, especially for prototyping purposes, where the range of < 100 stretches is most relevant. Compared to related work, even the largest baseline drift after 1000 cycles (ITO with 2D pattern: $\sim$350% increase) is an order of magnitude lower than results reported on DIY stretchable displays using conductive polymer printed on silicone.[6] While PEDOT:PSS also compares favorably with results of deposited metal films [218], the other materials may benefit from the approach of [218]. It shows improved robustness for a horseshoe-style variant of the pattern, while offering, however, only minimal surface area to attach components.

This high endurance, despite brittle silver and ITO conductors, can be explained by the fact that common approaches physically elongate the material while stretched, while our cut patterns allow elastic deformation by bending material out-of-plane at the connection points between cells. This significantly reduces stress [218] on the conductive traces.

Behavior during stretching

Fig. 3.10 depicts the effect of stretch on resistance during a stretching cycle, for the 1D and 2D pattern and all four conductive materials. For 1D stretch of 100%, the relative change of resistance remains below 2% for all materials. This is in line with results for other materials, which show a low change for stretch up to 300% [231] or even 2000% [60]. This change is below tolerances of common resistors (5%) and thus has no significant effect on the circuit. For 2D stretch of 30%, the relative resistance change remains within a typical range for stretchable circuits ($1 - 30\%$).[7]

This relatively small effect of stretch on resistance also holds true after the sample underwent repeated stretching and releasing cycles. After 1000 cycles, PEDOT:PSS and carbon show the same resistance increase of 1% and 10% respectively. Silver exhibits a change below 30% for the first 100 cycles and settles around 35% after $\sim$200 cycles. ITO shows a larger (60%) increase during initial stretching, likely due to micro cracks forming, which decreases to $\sim$30% after 10 cycles (as shown in Fig. 3.10) and settles at $\sim$10% after 50 cycles. Based on these results, we recommend initializing ITO by stretching 10 times before using it with a 2D pattern. We further recommend PEDOT:PSS as the most robust material, as it is least affected by stretch, with a relative change of $< 1\%$ in all cases.

5 [142] reported a resistance increase of 5.7% after 1000 cycles at 200% strain.

6 6450% after 10 stretching cycles at 50% strain [242]

7 For comparison, [236] reported a 32.4% increase at 30% stretch; [142] reported a $\sim 60 - 250\%$ increase at $30 - 100\%$ stretch.

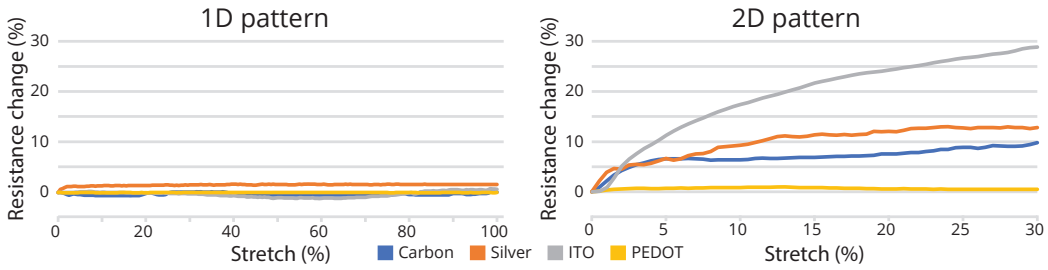

Figure 3.10: Relative change in resistance during stretch of 1D pattern (left) and 2D pattern (right).

3.4.2 Example applications and use cases

We validated the suitability of LASEC for prototyping stretchable interfaces by implementing three applications for interactive accessories, physical input devices, and interactive clothing. The applications demonstrate LASEC's rapid fabrication speed, support of circuits with high frequency signals, and simple stretch sensing, alongside its capability of realizing circuits of custom stretchability.

Interactive transparent wristband

To demonstrate the fabrication of transparent stretchable interfaces and integrating areas of very differing stretch properties, we implemented an interactive stretchable wristband using ITO, shown in Fig. 3.11b. It features an LED for output and allows the user to interact using two gestures: pulling on the band itself, which is enabled by a 2D stretchable area along the band, and pulling an additional orthogonal strap, which is inspired by a watch crown and realized with a 1D stretchable area (Fig. 3.1c). In our example application, the wristband is used as a countdown timer for running. Pulling the strap is mapped to the frequent action of starting/stopping the timer. Resetting the timer is performed by pulling the band.

The stretchable circuit on the wristband contains four traces: two for controlling the LED, one for sensing pulling on the band, and one for sensing pulling on the orthogonal strap (Fig. 3.11a).

The six endpoints are tethered to a Teensy 3.5 microcontroller, a voltage divider, and a battery. By measuring the resistance across both sensing traces, we can detect both gestures using a simple thresholding approach.

To explore the desired stretchability for both pulling interactions and to ensure a comfortable fit of the wristband, we quickly iterated over the design. Using LASEC, adapting the stretchability and fabricating the design for one iteration takes less than 2 minutes. We reached the final design after 4 iterations (Fig. 3.11a) and within 10 minutes.

3D-printed stretchable game controller

LASEC circuits allow rapid prototyping in many scenarios where custom stretchability is key. In this example, we are prototyping a custom 3D-printed stretchable game controller, shown in Fig. 3.11c and d. It features two 3D-printed handles,

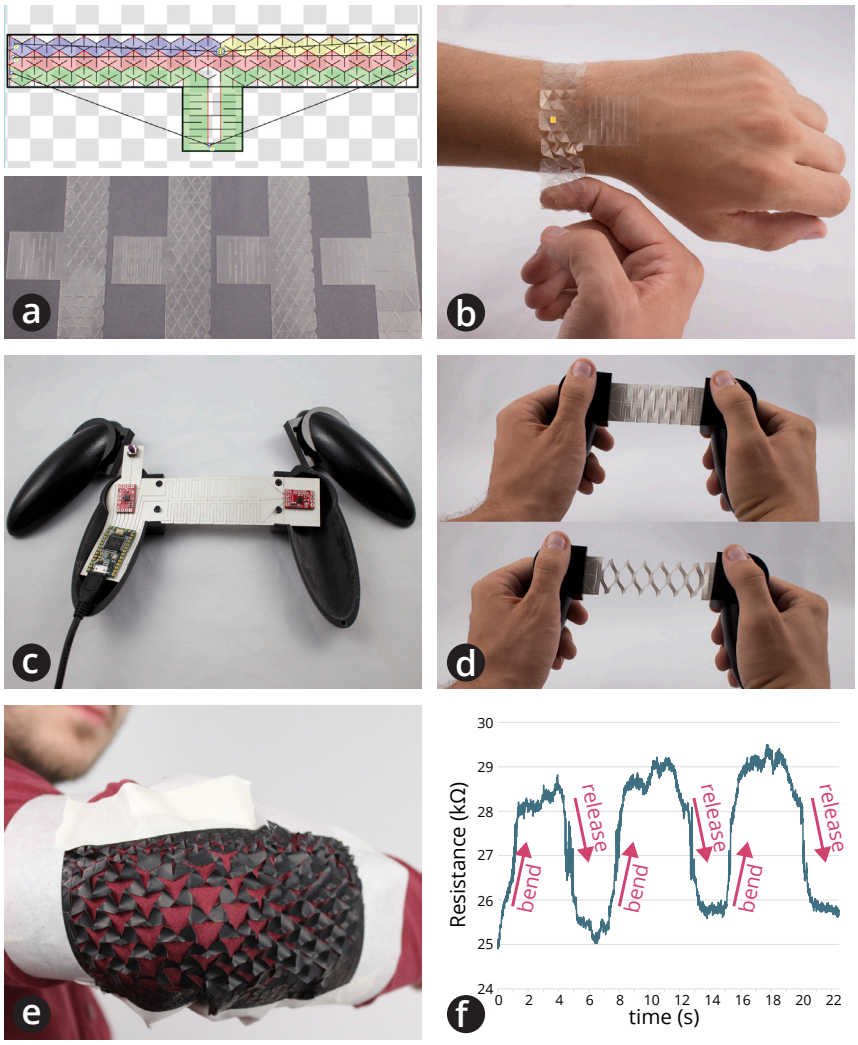

Figure 3.11: Example applications: wristband design with four fabricated prototypes (a) and a pull gesture being performed (b), game controller circuit (c) and prototype being stretched state (d), and textile sensor patch on bent elbow (e) and resistance reading for 3 bending cycles (f).

which are connected with a custom stretchable circuit on silver-coated PET. One inertial measurement unit (IMU) in each handle allows inferring their relative position, while one button allows triggering actions. The circuit also contains a commodity Teensy 3.2 microcontroller.

The 3D-printed handles themselves are passive and printed on a conventional 3D printer (Objet260 Connex3). All interactive functionality is added through a single stretchable circuit that was fabricated using LASEC. The circuit features two non-stretchable areas for holding the components inside each handle, and a stretchable center area that contains four traces for connecting the IMU in the left handle with the microcontroller in the right handle using I²C.

Textile sensor patch for joint angle estimation

We implemented a smart textile patch, worn on the elbow, that contains an integrated stretch sensor for capturing the angle of the elbow joint (see Fig. 3.11e). This application demonstrates LASEC's support for custom-shaped designs, multiple seamlessly connected stretchable areas, and simple integrated stretch sensing. The stretchable interface features two concentric, elliptical areas that are stretchable in 2D: a less stretchable outer area, where the patch is attached, and a more stretchable inner area that stretches when the joint is bent. A conductive trace was laid out on the stretchable surface such that it undergoes a large physical deformation when the inner area is stretched.

We chose carbon as a conductive material due to its suitable properties (robustness and consistent change in resistance) for stretch sensing. The stretchable circuit was laser-fabricated within 6 minutes. A small Teensy 3.5 microcontroller, voltage divider, and a battery were connected to the circuit. Using a conservative mapping, the continuous signal of resistance change, e.g. plotted in Fig. 3.11f, is mapped to one of four discrete bending states. We attached the finished patch onto the elbow region of a long-sleeve shirt. A user wearing the shirt can thus interact through arm gestures that are captured using the stretchable circuit.

3.5 Limitations

The benefits of the LASEC approach – a considerable speed-up of stretchable circuit fabrication and a customizable stretch behavior of the circuit – come with several limitations:

First, our approach is currently restricted to single-layer circuits to enable rapid and simple fabrication. In contrast, multi-layer approaches would require a manual multi-step process. This may introduce misalignment issues because a sheet needs to be removed from the laser cutter for a subsequent coating or a double-sided sheet needs to be manually flipped over. From our experiments, we can report anecdotally that VIAs for two-layer circuits can be realized using multiple subsequent coatings. After ablating the first conductive layer, a dielectric layer (GWENT D2180423D3) is coated on top. VIA locations are then ablated in the dielectic layer and finally a second conductive layer is coated and ablated to form the second circuit layer. In future work, we plan to investigate this extension to multi-layer circuits and address the resulting alignment problem, e.g., through visual markers or a detachable alignment frame on the cutting bed.

The supported complexity of single-layer circuits with LASEC depends on the width of ablation paths and material conductivity. With our laser we can ablate paths of $\sim 0.3mm$ width. Silver traces down to $\sim 0.3mm$ width yield a reasonable resistance ($3.3\frac{\Omega}{cm}$). This results in a minimum width of $\sim 0.4mm$ per trace and makes it possible to pass multiple traces through one connecting point of the 1D pattern (as illustrated in Fig. 3.4) or 2D pattern. As an example, we were able to route 20 wires through the pattern of the controller (Fig 3.11c), with a bottleneck width of

$8mm$. A cell between two of such connectors could thus hold a 40-pin component with a minimum pitch of $\sim 0.4mm$.

The minimum size of a stretchable circuit is defined by the minimum width of the connecting elements required for mechanically stable connections. In our case, this is 1.6mm, resulting in a minimum pattern spacing of $S = 2.88$mm at a mimimum stretchability ($\frac{L}{S} = 0.6$). For our selected materials, we fabricated circuits as small as 7x7mm (3x3 cells). The maximum size of a stretchable interface is limited by the size of the laser cutter's bed. Various approaches have been investigated to extend beyond this general restriction of laser fabrication, such as side-ways sliding of the sample. These approaches are compatible with LASEC, provided they keep the sample at a constant distance from the laser.

Our design tool is based on parametric models that describe the stretchable behavior of the material. We opted against including a module for physical simulation because finite element modeling (FEM), which is required to simulate our 2D pattern, is too computationally intense to comply with the hard real-time constraint of our designer-in-the-loop modeling approach (>10Hz updates). Future work may investigate how to incorporate such a simulation, as it could provide helpful insights into stress concentration and material-dependent behavior.

During stretch, the fabricated circuits exhibit a unique deformation behavior due to the out-of-plane buckling for stress relief. In some cases, this may be undesirable. In these cases, LASEC can be a very helpful tool for rapid iterations in early prototyping, while a more time-consuming approach (e.g., based on silicon) may be used for the final high-fidelity product. Future work may be able to reduce the buckling by minimizing the patterns' scales, possibly down to the micro- or even nano-scale [218].

Laser ablation is used on flat materials, as the laser is focused on a specific distance. This excludes materials with a coarse surface structure as well as 3D-shaped objects. Future work could investigate automatic focusing of the laser or automatic positioning of 3D objects [137] to support fabrication of stretchable 3D objects with LASEC.

3.6 Conclusion

This chapter contributed a novel approach for the rapid design and fabrication of stretchable interfaces with custom circuitry and custom stretchability. Inspired by work in material science, LASEC combines laser cutting of parametric patterns for stretchability with ablation for custom circuits. We have introduced the technique and presented novel approaches that address the technical challenges to realize LASEC. These include generating cut patterns for multiple areas of customized stretchability and a novel approach to realize circuits on such cut patterns. In addition, this chapter contributes a design tool allowing designers to specify the stretchable and electrical properties of a circuit and auto-generating the files for fabrication. Finally, this chapter demonstrated the practical feasibility and versatility of the approach.

This chapter advances the field of rapid prototyping of interactive objects with rich materials by addressing the three challenges introduced in the introduction.

This chapter addressed the challenge of design abstraction for combining custom interactivity and custom rich materials. As a solution, the contributed design tool abstracts from two aspects: the generation of low-level patterns for stretchability and the creation of ablation patterns by automated routing. Abstracting from both aspects during real-time design is enabled by the contributions of this chapter, e.g. the novel routing approach.

The proposed approach extends the capabilities of custom fabricated interfaces to feature multiple seamless areas of custom stretchability. This enables interfaces that leverage multiple areas of stretchability, for example, to fit body parts, to incorporate non-stretchable areas for component, or to support different deformation-based interaction in one interface.

The LASEC approach explores rapid design and fabrication as a viable feedback mechanism for the design of interactive objects with rich materials. To this end, the contributions in this chapter enable speeding up the design and fabrication process towards completing multiple iterations of a design within the time frame of a few minutes. This demonstrates the potential of rapid fabrication to provide hands-on feedback on the designed material properties throughout the iterative design process.

Together, the contributions of this chapter advance the field of rapid prototyping of interactive objects with rich materials towards quicker iterations and additional capabilities. However, the approach focuses on two-dimensional interfaces. Towards supporting three-dimensional interactive objects, the next chapter investigates custom interfaces on complex highly-curved geometries.

4 Augmenting 3D Objects of Rich Materials with Custom Interfaces

The previous chapter introduced LASEC, a novel approach for the rapid design and fabrication of stretchable interfaces. LASEC focused on stretchability and versatile circuits based on standard components. It addresses challenges regarding design and fabrication, however, limited to 2D interfaces.

This chapter[1] moves beyond 2D interfaces towards 3D objects and focuses on integrating custom electronics into objects and surfaces in our environment. This focus is motivated by the vision of ubiquitous computing. Blending interfaces with existing objects and surfaces in our environment promises computing to ultimately become one of the technologies that "weave themselves into the fabric of everyday life until they are indistinguishable from it." [238]

While existing technologies allow to augment everyday objects with sensors and output, they are limited in important aspects to leverage the full potential of existing objects for interaction. One is the wide variety of complex geometries of everyday objects that are designed for ergonomic use and have been perfected over many centuries. Recent work supports only a limited subset of geometries to be augmented. While simple developable geometries can be covered by a flexible sensor or display sheet [51, 149, 148, 190], more complex geometries remain out of reach. A second aspect is the diversity of object materials with distinct visual and tactile features, which not only contribute to the aesthetics of everyday objects, but also serve as cues for interaction. Existing technologies are limited in their supported materials, e.g. a few 3D-printable polymers [21, 192, 244], or do not preserve the visuo-tactile properties of an object's surface [125, 242, 260].

These constraints have so far limited the possibilities for prototyping interaction on ubiquitous everyday objects. They especially limited the exploration of objects that are made of natural materials, such as leveraging the tactile cues of wood grain on carved objects, the natural patterns in plants and flowers, or the variety of different surfaces made from stone. Regarding geometries, they have also hindered research to go beyond the outer, easy-to-augment, surfaces, such as a watch strap [149], the outside of a coffee mug [51], or the head of a toy figure [21, 192, 244]. In contrast, everyday objects offer many more facets, including the inside of holes in rings or lattice structures, many small or thin parts in filigree jewelry, or highly-curved surfaces in tools, toys, and accessories. Thus far, these remain unsupported.

1 This chapter is based on [57]. I led the conceptual design, development of the fabrication technique, investigation of materials and geometries, evaluation, and implementation of application examples. The master student Jonas Hempel helped with fabricating samples, conducting the technical experiments, and fabricating the application prototypes. The student assistant Lena Hegemann helped with the illustration in Figure 4.1. My supervisor Jürgen Steimle advised me on the conceptual design and evaluation and contributed to writing the article.

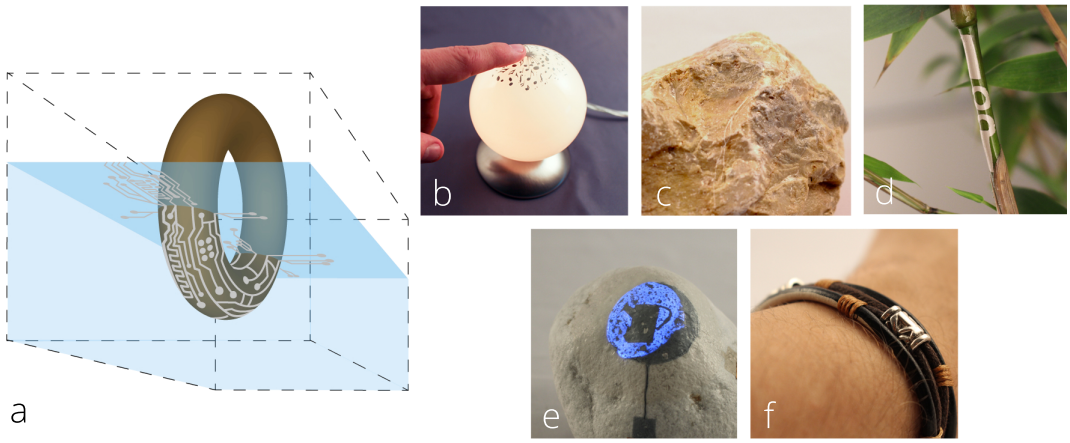

Figure 4.1: ObjectSkin is a fabrication technology for adding interactive surfaces to everyday objects (a). It is used to realize custom sensors and displays that seamlessly conform to highly curved geometries (b) and the detailed surface structure (c) of a wide variety of everyday objects, including live plants (d), garden stones (e), and aesthetic wearables (f).

This chapter addresses these limitations by contributing ObjectSkin: a fabrication technique for adding very slim interactive surfaces to rigid and flexible everyday objects. ObjectSkin is the first technique to add conformal touch sensors and displays to highly curved and irregular geometries of everyday objects, e.g. a spherical lamp shade, a plant's stem, or fine-detailed jewelry (cf. Figure4.1). It uses hobbyist equipment available in HCI labs or maker spaces and enables thin, conformal, and translucent electronics on a wide range of materials, largely preserving the object's visual and tactile surface structure. This allows sensors and displays to seamlessly blend with the object's surface.

As a main contribution, this chapter explores the use of existing everyday objects for rapid prototyping of interactive objects with rich materials.

To realize the ObjectSkin approach, this chapter addresses two fabrication challenges expanding the possibilities of fabricating custom interactive objects with rich materials (Challenge 2). First, it enables creating interfaces that are compatible with strongly-curved geometries and diverse materials of everyday objects. Second, it enables blending these interfaces with existing objects while largely preserving the objects' surface characteristics.

To this end, this chapter contributes a novel fabrication technique, which is based on a water-transfer process of printed stretchable functional inks. It presents the fabrication process in detail, including approaches for rapid low-fidelity and versatile high-fidelity prototyping.

In addition, this chapter investigates what materials and geometries are supported by this technique, compares them with related work, and validates the results through a series of technical experiments. Their results confirm the method's ability to conform to highly curved geometries, to support a wide variety of materials, and to be long-lasting and robust against deformation on flexible geometries. We

further illustrate the method's capabilities for prototyping interactive surfaces by showing how to realize non-invasive multi-touch sensing and display output on highly curved and rough surfaces.

This novel fabrication approach enables using existing objects to prototype interactive objects. It enables designers to leverage an object's existing rich material, including geometries and material properties, for interaction. This approach stands in contrast to digitally designing and fabricating an object from scratch, as in the previous chapter, and offers the opportunity for hands-on exploration of important properties early in the design process (Challenge 3).

Finally, this chapter demonstrates how the ObjectSkin fabrication method can enable new interactions on real-world objects, by leveraging newly supported complex geometries and the object's surface structure. To this end, it presents seven diverse everyday objects that were augmented using the approach. A wooden ring and honeycomb pendant illustrate the use of the object's geometry, including holes, for geometry-guided touch gestures. A rough rock's surface structure serves as tactile feedback for eyes-free touch interaction. A collection of unconventional objects is enhanced with interaction capabilities, e.g., a live plant featuring a growing touch sensor.

The remainder of this chapter is structured as follows. Section 4.1 will first introduce the ObjectSkin approach and present the steps of the fabrication technique. Next, Section 4.2 will investigate a variety of object materials and object geometries, which are commonly used in physical prototyping, and empirically assess their compatibility with the fabrication technique. Section 4.4 will then introduce how to use ObjectSkin to augment real-world objects with conformal sensors for touch and multi-touch input as well as with light-emitting displays. This enables novel interactions for HCI that will be presented in Section 4.5. Section 4.6 will provide a discussion of limitations and directions for future work. Finally, Section 4.7 draws conclusions based on this chapter's contributions.

4.1 Design and fabrication process

We contribute ObjectSkin, a fabrication technique to add surface-conformal input and output capabilities to 3D objects. It is the first technique to transfer printed electronic circuits for sensing and conformal displays onto 3D objects using a water-transfer approach. This allows for enhancing a wide range of geometries and materials that previously could not be augmented with conformal electronics, using simple off-the-shelf equipment and supplies.

4.1.1 Challenges

The development of ObjectSkin was driven by four main fabrication challenges, which are key to augmenting existing 3D objects with interactive surfaces:

1. Very **thin**, **conformal**, ideally **transparent** electronics, to only minimally alter the visuo-tactile properties of the object surface

2. Support of **non-developable** object surfaces
3. Compatible with a **variety of functional inks** for sensors and displays
4. **Non-invasive** approach, to be applicable to many materials and existing objects

To account for the varying demands of early and later phases of the design process, we present two approaches: one approach is tailored for the rapid fabrication of interactive low-fidelity prototypes, while a second approach is more versatile and yields higher quality results for fabricating high-fidelity prototypes. We start by introducing the main principle and will then detail the individual steps of the fabrication method.

4.1.2 Background

Our fabrication technique takes inspiration from hydrographic printing [106]. Hydrographic printing is a specialized process used to cover three-dimensional surfaces with visual patterns. It is commonly used for car parts, such as wheels, interior panels, or side mirror casings, but also for other complex geometries, including rifles, helmets, or game controllers. Its main benefit over other printing techniques, such as tampon printing, is that it is compatible with strongly curved and irregular geometries.

In hydrographic printing, a pattern is printed onto a water-soluble film (typically PVA) with color pigment-based ink. The film is then placed into a water basin, where it starts to dissolve into a viscous liquid, letting the ink pigments of the printed pattern float on the water surface. When an object is dipped through the ink and the film into the water, the printed pattern wraps around and closely conforms to the object. During this process, the film and ink stretch along the object's surface, allowing the ink pattern to cover the inside of holes and other difficult-to-reach areas.

In contrast to printing color images, printed electronics leverage the capabilities of a variety of functional inks, including conductors, dielectric materials, and electroluminescent inks. These functional inks differ from color pigment inks in multiple aspects, including their material composition, viscosity, and particle size. Moreover, they typically require bonding into a continuous functional layer, to ensure end-to-end conductivity or insulation. Patterns that are discontinuous cause a loss of functionality. In contrast, printed visual patterns do not need to be continuous; half-toning, for instance, makes use of this very property by printing small unconnected dots to vary the perceived color intensity.

Since hydrographic printing relies on stretching the ink on the water surface, a large amount of stretch (as resulting from conforming to curved surfaces) will simply result in low color intensity. For functional inks, however, this potentially results in loss of functionality, a major challenge which has not been addressed by related work [180]. To addresses this challenge, we propose a novel fabrication approach based on transferring liquid functional ink and provide an evaluation of the supported geometries, as we discuss in Section 4.3.

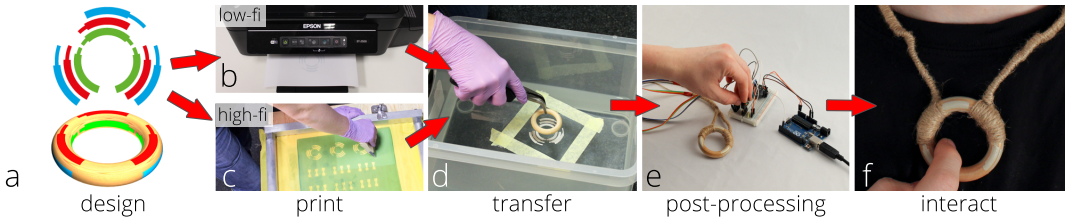

Figure 4.2: ObjectSkin fabrication process. The digital design (a, color indicates mapping) is printed using the low-fidelity inkjet-based (b) or high-fidelity screen printing (c) approach onto a PVA transfer film. The object is dipped through the printed ink and dissolved transfer film, allowing the ink to conform to the object (d). After post-processing and connecting to a microcontroller (e), the prototype is ready for interaction (f).

4.1.3 The ObjectSkin Fabrication Method

Fabricating an interactive object with ObjectSkin consists of four steps: digital design, print, water transfer, and post-processing. We will now describe each step and illustrate the process using an example: how to augment a wooden ring with a set of conformal touch sensors, to create a new wearable input device.

Digital design

The designer first creates a digital design, which defines the sizing, placement, and interconnect of the desired sensor or display components. Figure 4.2a shows an example circuit layout, created in a vector graphics application, and the corresponding 3D rendering. Both have been color-coded to illustrate the mapping. The layout features 9 electrodes: 3 on the front (red), 3 wrapping to the outside (blue), and 3 wrapping to the inside (green) of the ring. We have manually created all designs for this paper in Adobe Illustrator.

The design is now ready to be printed onto a water-soluble transfer film (PVA[2]), either using the more rapid low-fidelity printing method or the more versatile high-fidelity method.

Low-fidelity printing

For rapid low-fidelity prototyping, fabrication speed is the key factor. The quickest way to achieve custom printed electronics is typically using inkjet technology [104, 180]. However, available approaches are limited to specially coated paper [104], which is not compatible with water transfer, or require specialized printers [180], not commonly available in HCI labs.

We thus investigated the possibility to rapidly inkjet-print conductors on PVA film using standard desktop inkjet printers. Based on the available off-the-shelf inks, we selected a conductive polymer (heat-curable PEDOT:PSS ink, Heraeus CLEVIOS P JET 700 N). PEDOT:PSS has the advantage of being translucent, which allows the object's visual appearance to be preserved. While PEDOT:PSS in a similar

2 We used "DP PrintXer" film purchased from http://hydrographics-shop.com

formulation has been used to print conductors onto PET film using a desktop inkjet printer [201], we had to examine its suitability for hydroprinted interactive surfaces. To this end, we tested the ink's compatibility with the PVA film and water-transfer process using a consumer-grade inkjet printer (Epson ET-2500).

Our results show that in addition to the fast printing speed (less than a minute in our example) and high printing resolution (5.760 x 1.440 dpi), the approach produces very thin ($\sim 2\mu m$) and translucent conductive layers. These are well-suited for low-fidelity prototyping of touch sensing, despite the quite low conductivity of printed traces. By printing two layers of ink, we achieved an approximate sheet resistance of $900k\Omega/\square$. This is not unexpected, however, since inkjet printing of conductors on many materials using consumer-grade hardware is still an ongoing research topic in material science. For robust touch sensing, designers should ensure that the size of electrodes exceeds $15x15mm^2$.

High-fidelity printing

In contrast to low-fidelity prototyping, high-fidelity prototyping focuses on quality over fabrication speed. For prototyping interactive surfaces with printed electronics, this translates to higher spatial sensor resolution, enabled by smaller minimum feature sizes thanks to conductors with a higher conductivity, and additional interface elements, e.g. multi-layered touch sensors and displays enabled by a larger variety of functional inks supported by this approach.

Our high-fidelity printing method is based on screen printing of functional inks, which offers a wide variety of compatible inks and requires simple hobbyist screen printing equipment [149]. In contrast to classical screen printing of circuits, however, our fabrication method exhibits different demands, as the printed pattern must be water-transferrable. We therefore investigated the following functional inks, to realize multi-layer electronics, displays, and transparent conductors.

- A highly conductive silver ink that can be used for printing conductive structures of small feature size: Gwent, C2131014D3, $0.1\Omega/\square$, $25\mu m$ layer height
- A translucent polymeric PEDOT-based conductor with lower conductivity: Gwent, C2100629D1, $500 - 700k\Omega/\square$, typically 0.5-1.5μm layer height [172]
- A dielectric ink that can be used for printing insulating or dielectric layers: Gwent, D2070209P6, $10\mu m$ layer height
- An electroluminescent ink that can be used for printing light-emitting displays: Gwent, C2061027P15, $30\mu m$ layer height

The results of our experiments show that these inks, printed on hobbyist screen printing equipment, are compatible with the water-transfer step. They further show that this approach is capable of printing conductors with much lower resistance compared to the low-fidelity approach (approx. $0.25\Omega/\square$, see Section 4.2.1). These capabilities enable printing of small feature sizes, e.g. traces of 1mm width, multi-layer touch sensors, and EL displays, as we discuss in detail in Section 4.4 (Sensors & Displays) below.

For our example, a negative mask containing the design is created; then one layer of conductive silver ink is screen-printed onto the PVA film (see Figure 4.2c).

Water transfer

To transfer the ink onto the object, the approach employs a water-transfer process. The PVA film is placed (ink side up) onto a basin filled with warm water (27-30°C). Within 60-80 sec. the film dissolves into a viscous liquid. To further dissolve the film and facilitate ink adhesion to the object, an activator[3] is sprayed onto the film. The object, in our example the wooden ring, is then dipped through the film into the water (see Figure 4.2d). This allows the film to wrap around the object.

During dipping, the object needs to be aligned with the pattern on the water surface. To ease replication of the technique and to support rapid prototyping, our approach employs a manual alignment and dipping process. We tested the practical feasibility using a range of different patterns and everyday objects. Our results show that manual alignment is precise enough for many prototyping applications. We could achieve an alignment error below $1mm$ for smaller objects and objects with holes, such as the honeycomb pendant (see Figure 4.9c). Larger and bulkier objects make it more difficult to precisely align the design, as they tend to offer less fine-grained visual cues that help with the alignment. Our results show that this level of precision is still sufficient for many applications. For instance, the multi-touch stone has a misalignment of $< 5mm$ and is fully functional (see Figure 4.8b). However, for more precise alignment and increased quality, additional measures can be taken, e.g. by improving visibility through a mirror of the basin's floor, by simple rods for mechanical guidance, or by fully automated approaches, as proposed in [261].

Next, to attain its functional properties, the ink needs to be heat-cured. We could successfully cure all inks with a heat gun after they had been water-transferred. We cured silver, dielectric, and phosphor inks for 3 minutes, screen-printed PEDOT for 5 minutes and inkjet-printed PEDOT for 3 minutes. Our results also show that drying the film before curing for about 5 minutes with a fan improves surface conformity. While these experiments show that the water transfer is possible, the effect of the water-transfer step on the conductivity of transferred patterns remains unclear. We investigated this question in a technical experiment:

Method: We applied two traces of silver ink (5 x 10 mm) onto polished marble. One trace was directly screen printed onto the marble object, while the other was realized using our high-fidelity water-transfer approach. Both traces were cured under the same conditions. We took 10 resistance measurements for each trace (over its diagonal) using a multimeter (Fluke 8846A).

Results: Both traces achieved comparable resistance, with measurements ranging between between 0.7Ω and 1Ω (screen-printed: mean 0.88 Ω, SD=0.09; water-transferred: mean 0.75 Ω, SD=0.18). This suggests that the water-transfer process does not have a negative effect on the ink's conductivity.

3 We used MST-Design Dippdivator (4-Methyl-2-pentanone) from `https://www.amazon.de/dp/B004HU87JA`

Post-processing & connecting

In hydrographic printing, the remaining PVA layer on top of the color ink is washed off and an additional clear coat is applied. For our fabrication technique, washing and leaving the PVA film on the object each have their respective advantages.

For rapid prototyping, the PVA film can remain on the object. This speeds up the fabrication process and protects the functional layer. As the PVA is very thin ($\sim 4\mu m$), conformal, and transparent, it has little effect on the resulting interactive surface.

For high-fidelity prototyping, the PVA layer is washed off. We found $\sim$3 min washing to be sufficient, as we illustrate for various materials in Section 4.2.2. This allows layers that are transferred on top to connect to the underlying layer, e.g. for multi-layer electronics with VIAs. It also produces thinner and more conformal results.

In the last step, the printed circuit is connected to the controller hardware, e.g. a microcontroller and a battery. When keeping the PVA film, connectors are attached to the object before transferring the circuit. The printed circuit is then water-transferred directly onto these connectors. In our experience, this works well with connectors made of adhesive copper tape. For washed prototypes, a connector is connected directly on top of the printed layer.

In our example, we wash off the PVA film and connect wires using z-axis conductive adhesive tape[4]. The wires are then connected to an MPR121 chip and Arduino Uno for touch sensing (see Figure 4.2e). The ring is now ready to sense the user's interaction (see Figure 4.2f). In a final optional step, one can perform additional post-processing, for instance applying a clear coating to further protect the printed layers.

4.2 Object materials

Everyday objects are made of many different materials with diverse visual and tactile properties. These are important cues for an object's look and feel. Despite its apparent relevance for prototyping, adding conformal input and output to a wide range of object materials is largely unexplored. While printed electronics on flat surfaces have been shown to support a variety of substrates [149], conformal electronics for 3D geometries have only been demonstrated on skin for on-body interaction [98, 110, 126, 237] and conductive traces transferred onto 3D-printed plastic and glass [180].

In this section, we show how ObjectSkin contributes towards filling this gap. To this end, we evaluate the approach regarding three main questions relevant for prototyping ubiquitous interactive surfaces:

- Which materials, typically used for prototyping, can be augmented?

4 We used 3M™ Z-Axis Conductive Tape 9703

Figure 4.3: Materials. Top left: sample covered with transparent PVA transfer film, bottom right: after washing the PVA transfer film off.

- How do these materials affect the achievable functional quality, i.e. conductivity?
- How robust and durable are the results, especially against typical deformation of flexible materials, e.g. bending and stretching?

To answer these questions, we carefully selected a set of sample materials and tested two important criteria: conductivity and ink adhesion. For flexible materials, we further evaluated mechanical robustness. Since an exhaustive evaluation of all material properties is beyond the scope of this work, we selected materials that are frequently used for prototyping, but also included edge cases with potentially challenging material properties. We further ensured that the selected materials would vary regarding the following properties: class (e.g. ceramics, polymers, naturals, and composites [26]), water-absorbing vs. water-repelling (since our technique relies on water transfer), surface roughness (for conformity), and flexibility. According to these characteristics, we selected rigid plastic (PLA), flexible plastic (Stratasys TangoBlack+), polished marble, rough marble, pine wood, leather, and organic sponge, as illustrated in Figure 4.3.

4.2.1 Conductivity

The conductivity of hydroprinted conductors is the primary indicator of material compatibility. It also indicates the achievable quality, as higher conductivity allows for smaller electrode sizes and more precise sensing.

Method: We tested the conductivity in terms of approximated sheet resistance, similar to [104]. We screen-printed and transferred 6 silver samples of 20mm length and varying width (0.8, 0.9, 1.0, 1.2, 1.6, 2.6 mm) onto a sample of each material and cured them under the same conditions. We then measured the resistance R of each sample, calculated the sheet resistance R_s according to the formula $R_s = R\frac{width}{length}$, and averaged the results for each material. We use this approximation since special sheet resistance probes for smooth sheets of material cannot be applied to the rough surfaces we tested.

Results: The results are illustrated in Figure 4.4. The resistances range between $0.15\Omega/\square$ and $0.64\Omega/\square$, excluding the sponge which exhibits higher resistance ($0.36\Omega/\square$ to $1.45\Omega/\square$). These results show that the approach achieves good results

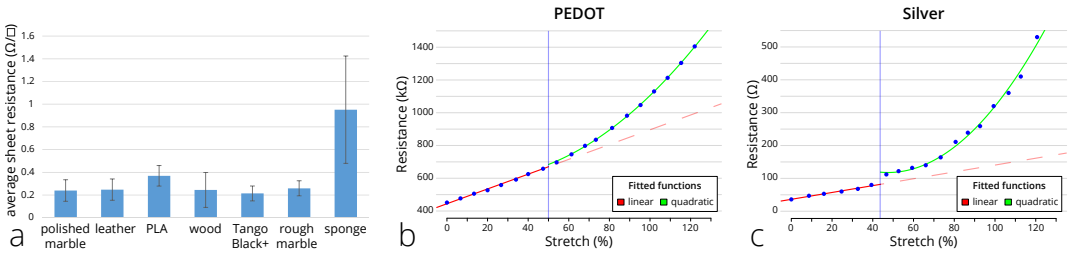

Figure 4.4: Evaluation results: a) Sheet resistance on different materials using the high-fidelity approach. b) and c) Change in resistance by stretching for PEDOT and silver ink respectively. Trends are indicated by a fitted linear model (red) for data points below the blue line and quadratic fit (green) for points above. The dashed red line illustrates the continuation of the linear model.

on a wide range of materials, comparable to conductive inkjet (0.2Ω/□ [104]) and traditional screen-printing (ink's reference sheet resistance: 0.1Ω/□ at 25μm). This even holds true for rough, soft, and flexible materials. Not surprisingly, our challenging edge case, the sponge, showed a higher resistance and high variability. Nevertheless, these are still in an acceptable range for prototyping many types of ubiquitous interactive surfaces.

4.2.2 Ink adhesion

We further tested for ink adhesion, as an additional indicator of material compatibility. Ink adhesion is important for the printed sensors and displays to retain their designed shape on the object.

Method: We tested ink adhesion using a pattern of silver ink (10x10mm) that was screen-printed and transferred onto a sample of each material. We cured all samples under the same conditions. The samples were then washed thoroughly under flowing water while rubbing (∼3 minutes) to remove the PVA film. This serves as a conservative estimate for ink adhesion, because rubbing is not necessarily required for removing the PVA film if the film is washed for a longer duration (∼8 minutes). We visually inspected all samples before and after washing and documented the results in photographs. We further verified that all samples remained conductive after washing.

Results: Figure 4.3 shows the resulting images. Our results show good adhesion for all materials before washing. After washing and rubbing, the results are still surprisingly good, with the exception of our edge case (sponge). Our results indicate no visible difference in adhesion in relation to the material's flexibility (e.g. marble vs. leather) or roughness (e.g. rough vs. polished marble).

4.2.3 Robustness

We evaluated the mechanical robustness of our approach regarding stretch and repeated bending of flexible geometries. This test provides further insight into

material compatibility, since flexible materials are bent and occasionally stretched during use. We further evaluated the long-term conductivity of the printed traces.

Stretching

Method: We printed and transferred traces of screen-printed silver and PEDOT on two samples of elastic thermoplastic elastomer (NinjaFlex filament printed on FDM printer). The conductive traces were designed using a horseshoe pattern (15 x 10 mm, 3 windings), which initial testing revealed to be necessary for robustness against stretch. We stretched the samples up to 120% and measured their resistance in $1mm$ ($\sim 7\%$) intervals.

Results: We found the resistance to increase approximately linearly until 39% stretch for silver (resistance increased 2.2x, 36 Ω to 80 Ω) and 54% for PEDOT (resistance increased 1.5x, 451 kΩ to 697 kΩ). Both samples remained conductive beyond these points, but their resistance increased non-linearly. We fit linear and quadratic models to the respective ranges of the data, as illustrated in Figure 4.4b and c, to visualize these trends. Adjusted R-squared for the linear models for silver and PEDOT is 99.45% and 97.97% respectively. The Residual Standard Error for the quadratic fit is 12.32Ω and $2.755k\Omega$ respectively.

These results suggest that sensors printed on flexible materials are robust to occasional moderate stretching ($< 10\%$). Even for greater stretching the functionality can be retained; however, the corresponding increase in resistance may reduce the sensing quality.

Bending

Method: We evaluated the robustness to repeated bending using a narrow (2 x 20 mm) and a wide (5 x 10 mm) silver trace transferred to two pieces of the same leather using our approach. As a conservative estimate for robustness, we bent each piece 10, 30, and 50 times around a cylinder smaller than a finger (4 mm radius). We measured the resistance in the initial condition, directly after each trial, and after 1, 5, and 60 minutes.

Results: The narrow trace remained conductive after being bent 10 times, but broke during the second trial with 30 repetitions. The wide trace remained conductive through all 80 repetitions. Its initial resistance (1.4Ω) increased up to 30Ω during the last trial. We observed a slow recovery down to 10Ω after 60 minutes, similar to the behavior of nanoparticle-based strain gauges[182].

These results indicate that the printed sensors are sufficiently robust to be used in interactive prototypes based on flexible materials. Since such an interaction is typically less demanding than our conservative estimate, even narrow traces can be used. For demanding cases, wider traces increase the robustness.

Long-term conductivity

Method: We transferred and cured 5 samples (5 x 40 *mm*) each of screen-printed silver and PEDOT onto a 3D-printed material (Stratasys VeroWhite+). We then measured the resistance of the samples over the course of 6 months.

Results: For both samples, we measured a change in resistance of less than 1% (silver: 0.45Ω, PEDOT: 43.3kΩ). These results indicate that there is no temporal degradation of the conductors printed with our approach within a reasonable time-span for use of a prototype.

4.2.4 Discussion

Our evaluation regarding material compatibility and robustness shows that ObjectSkin supports diverse materials for prototyping. On our selection of materials, the approach achieves conductivity similar to approaches used for prototyping interactive surfaces on flat sheets [104, 149, 148]. Similarly, the ink adheres well to the materials, with or without washing. For flexible materials, our results indicate sufficient robustness against common deformation. Thus, the tested materials provide a basic inventory for many prototyping applications. The results further indicate that the approach is likely to be compatible with a larger variety of materials that exhibit similar properties. However, edge cases with different properties, as demonstrated with the sponge, can also produce results that are still acceptable for prototyping. This is in line with anecdotal evidence we gained when we successfully used the approach on additional materials, including glass, a live plant, different types of wood, and other 3D-printed materials, including elastic TPU (NinjaTek NinjaFlex), rigid ABS (FormFutura EasyFIll ABS), and clear PolyJet material (Stratasys VeroClear). However, we also identified a few samples of less compatible materials. These include silicone and latex, due to insufficient ink adhesion, and textiles, where coarse woven structures and a high demand of stretchability remain difficult challenges.

4.3 Object geometries

In this section, we discuss object geometries, a second crucial aspect for prototyping interactive surfaces on diverse everyday objects. We present ObjectSkin's capabilities to support highly curved and irregular geometries and discuss its contributions towards prototyping on *developable* and *non-developable* (also called *doubly-curved*) geometries.

4.3.1 Non-developable surfaces

Adding conformal sensors and displays to non-developable surfaces offers many geometric challenges. These include surface structures of different roughness, holes and cavities, and varying degrees of curvature in two dimensions. To augment such

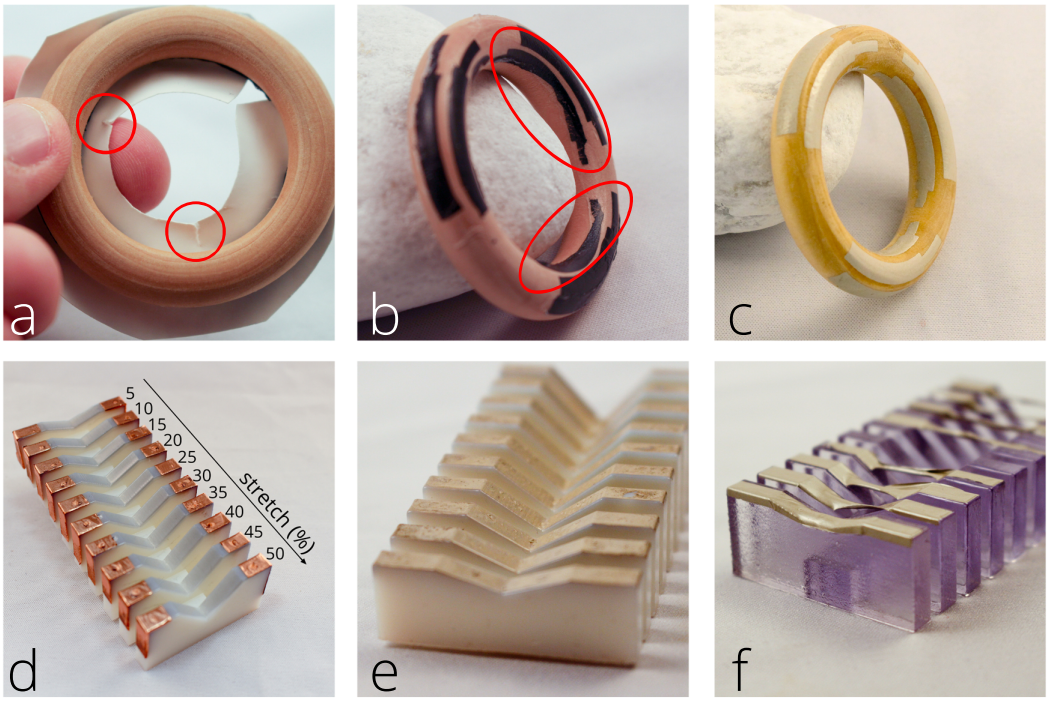

Figure 4.5: Evaluation of supported geometries. a) A non-elastic transfer layer cannot wrap around a non-developable geometry. The layer tears where an elastic layer would expand (red circles). b) As a result, the pattern is distorted and cannot fully cover the torus' inside surface (red ellipses). c) Our approach produces the expected conformal result covering the inside surface to the full extent. d) 3D-printed geometry to evaluate different percentages of stretch during dipping. e) Silver ink stretches and conforms to the geometry using our approach. f) Traces sintered before transfer form bridges instead of stretching and conforming.

geometries with a thin overlay requires the overlay to be elastic, i.e. to conform to non-developable curvature by stretching.

While this fundamental requirement excludes approaches that use conventional printed electronics [51, 149, 148] or other sheet material [23], related work on skin-worn electronics has presented solutions for conformal electronics on different body locations [98, 110, 126, 237]. They transfer an elastic electronics layer, which is able to conform to the skin's wrinkles. However, since they use a non-elastic transfer layer, i.e. tattoo paper backing [98, 126, 237] or a PVA sheet[110], to directly apply the electronics to the target surface, their method is limited to slightly doubly-curved geometries, e.g. the forearm. This problem becomes apparent when trying to apply a tattoo film or PVA film to strongly-curved non-developable geometries, e.g. a sphere or a torus. The non-elastic transfer layer cannot conform closely enough (see Figure 4.5a) and hence inevitably causes wrinkles and distortions (see Figure 4.5b).

ObjectSkin, in contrast, uses an *elastic* transfer layer. By dissolving the PVA layer on the water bed, it can stretch during the transfer process and therefore makes it possible to add sensors and displays to strongly-curved non-developable geometries (see Figure 4.5c). However, in addition to the elastic transfer layer, the electronics must also be elastic during transfer to conform to non-developable geometries.

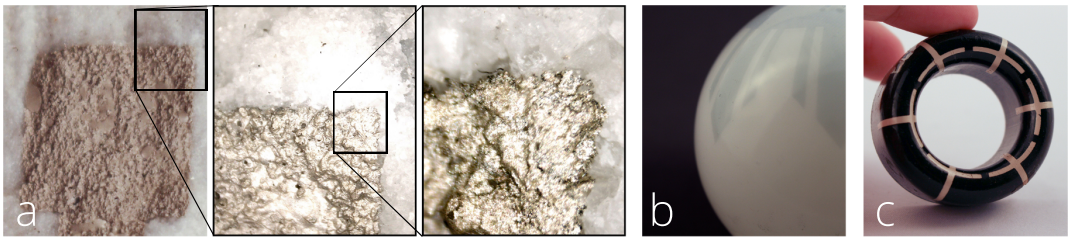

Figure 4.6: Printed electronics transferred with the proposed approach conform closely to highly curved non-developable geometries. a) Silver conductor conforming to a rough stone surface (image of $1cm^2$ patch and magnification of selected area). b) Translucent PEDOT conductor conforms to white glass sphere without distortion. c) Silver traces wrapping into hollow cylinder geometry.

To this end, our approach sinters the inks *after* the water transfer, since sintering drastically reduces the elasticity of the material. To illustrate the importance of this step, we created a prototype with conductive traces that we had already sintered before water-transferring them, as proposed in [180]. The results are depicted in Figure 4.5f. It can be clearly observed that instead of stretching and conforming, the sintered traces form bridges over the concave area. In contrast, our method is able to closely conform to the geometry (Figure 4.5e).

In consequence, the supported non-developable geometries essentially depend on the ink's ability to stretch on the water surface during the water-transfer process. We therefore conducted an experiment to determine the maximum amount of stretch after which the conductive and dielectric layers can still gain their respective functionality (after sintering).

Method: We transferred 10 samples (5 x 40 *mm*) of each ink (screen-printed: silver, PEDOT, and dielectric ink; inkjet: PEDOT) onto a 3D-printed test geometry. The geometry was designed to stretch the midsections (10 *mm* long) of the 10 parallel strips from 5% to 50% in 5% increments (see Figure 4.5d). For the dielectric material, we covered the test geometry with conductive copper tape before and after printing and tested for conductivity between both copper layers. For the conductors, we measured the resistance of each sample.

Results: We found silver could be successfully stretched up to 30% (resistance increase 3.8x, 0.45Ω to 1.71Ω), screen-printed PEDOT up to 15% (resistance increase 1.6x, 43.3 kΩ to 77.8 kΩ), and inkjet-printed PEDOT up to 10% (resistance increase 3.2x, 230 *M*Ω to 741 *M*Ω). The dielectric ink insulated both copper layers up to 30% stretch. These confirm the potential of functional patterns to conform to non-developable geometries. They also reveal that the high-fidelity approach is better suited for strongly-curved geometries.

This makes it now possible to augment unusual and novel geometric features with interactive surfaces, as we illustrate with three examples:

- The approach enables thin sensors that closely conform to rough surface structures and retain their tactile properties. Figure 4.6a illustrates how closely the transferred traces conform to the surface structure.
- It allows covering strongly curved surfaces without creating bumps or wrinkles. We demonstrate this with the smooth conformal results of a translucent conductor transferred onto a sphere, depicted in Figure 4.6b.
- Sensors and displays can be smoothly wrapped into and through holes, while closely conforming to the surface. Figure 4.6c shows an example of a hollow cylinder with a doubly-curved top surface. The electrodes conform along both curvatures and wrap onto the inside surfaces of the hole.

4.3.2 Developable surfaces

ObjectSkin also supports developable geometries, which can be augmented by existing fabrication approaches [51, 148]. The approach improves upon prior work by adding support for developable geometries that so far had required cutting and gluing. We present three examples that illustrate the advantages of our fabrication method:

- A closed cylinder made from a sheet of paper requires cutting and gluing. Thus, a sensor or display across its curved edge would have to be cut as well, which is not possible in many cases. ObjectSkin allows printed electronics to be wrapped across the edge without cutting or gluing (Figure 4.7a).
- A sensor applied over the corner of a cube illustrates the same advantage: One edge would require cutting and gluing when folded from a sheet-based sensor. In contrast, our approach forms a smooth continuous layer by wrapping and stretching (Figure 4.7b).
- Our approach enables traces across sharp edges. We successfully transferred traces to angles as sharp as the edge of a $\sim 0.1mm$ thin piece of paper (Figure 4.7c). The traces remain conductive while an angle this sharp would break a trace folded from a sheet sensor.

4.4 Sensors and displays

In this section, we present how input sensing and display output can be realized, leveraging the fabrication capabilities of ObjectSkin.

4.4.1 Touch sensing

Touch is a common modality for interaction, which has been used extensively in related work [51, 149, 148, 190, 260]. Capacitive loading mode sensing, which is supported by prototyping platforms such as the Arduino[5], makes it possible to

5 https://www.arduino.cc/

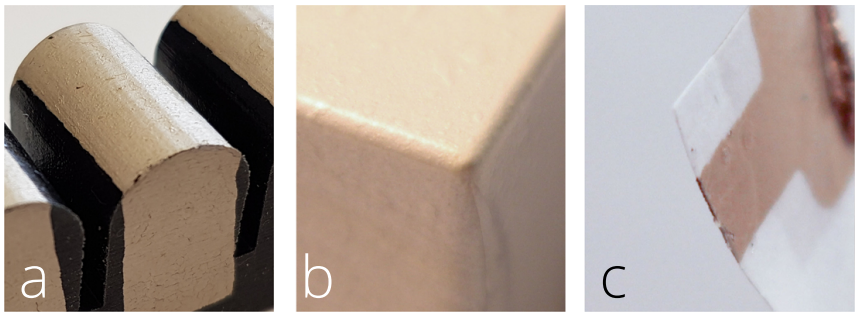

Figure 4.7: ObjectSkin facilitates augmentation of developable geometries. a) A touch sensor conforms to the round edge of a half-cylinder shape. A sheet-based sensor would have to be cut along the edge to conform without wrinkles. b) Transferring a sensor onto a cube's corner results in a smooth continuous layer. A sheet-based sensor would have to be cut along one edge and thus be discontinuous. c) A conductive trace conforms to a very thin edge ($\sim 0.1mm$) by wrapping onto both sides of a piece of paper (one side and the edge is pictured).

rapidly and easily create touch sensors that require only one simple electrode [8]. With ObjectSkin, we enable such electrodes on highly curved geometries.

Both the low-fidelity and the high-fidelity approach can be used. The low-fidelity approach offers a thin translucent conductor, which enables electrodes to be placed over distinct visual features of everyday objects. We have successfully implemented touch sensors ($10mm$ radius, see Figure 4.1b) based on loading mode capacitive touch sensing, using the CapSense library [8] for Arduino or a dedicated touch sensor chip (Freescale Semiconductor MPR121).

The high-fidelity approach supports a more conductive translucent conductor (PEDOT) and a highly conductive opaque conductor (silver). This supports smaller electrodes and longer conductive traces. Our results show that the MPR121 chip could detect touch reliably for conductive traces as thin as 3 mm (PEDOT) and 1 mm (silver).

In addition to dedicated sensing hardware, ObjectSkin makes it possible to leverage existing touch sensors in everyday objects, such as those found in lamps or smart phones. To this end, a conductive trace connects to and extends an existing touch surface. This principle has been presented for sticker sheets [103]. Our approach extends beyond prior work in enabling such traces to closely conform to the object's geometry, allowing for a seamless integration even on highly curved and irregular object geometries (Figure 4.8a).

4.4.2 Multi-touch sensing

While a single conductive layer with individual electrodes is sufficient to sense touch at a few locations, this technology does not scale to higher-resolution multi-touch sensing. Thus, commercial multi-touch sensors use multi-layer matrix electrode

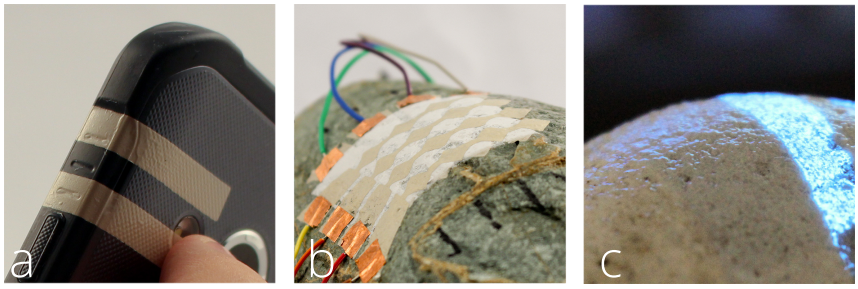

Figure 4.8: Conformal sensors & displays: touch extension on smart phone (a), multi-touch matrix on rock (b), and electroluminescent display on stone (c).

layouts. However, these have not been supported on highly curved geometries so far.

To enable multi-layer electronics on highly curved object geometries, we had to address three challenges:

- Transferring multiple layers of different functional inks, which retain their functionality
- A means to insulate adjacent conductive layers (also on highly curved geometries)
- An approach to connect the controller to the printed multi-layer circuit

We address the first challenge by transferring and curing each layer one after another, aligning them on top of each other on the object. Transferring all layers at once would require curing them in advance, thus removing their ability to stretch during dipping. In consequence, the overlay would conform less to the surface, as we discuss in Section 4.3.1. For quick prototyping, the PVA film can be left on each layer. To achieve thinner and more conformal multi-layer structures, the PVA film is washed off after curing.

To insulate adjacent conductive layers, a layer of dielectric ink is added between them. As this layer is digitally designed and printed, the designer can flexibly define locations that should be insulating. VIAs (conductive connections between two adjacent layers) can be created by modifying the design of the dielectic layer to feature holes at location where conductivity between layers is desired. At those locations, the PVA film must be washed off because otherwise it would act as an insulator.

The main concern for highly curved geometries is that the insulation could break down and cause a short circuit, because of the inherent stretch those geometries generate. Therefore we investigated whether the dielectric layer remains functional when stretched up to 30%, which is the maximum stretch factor we identified in Section 4.3.1 above.

For connecting the controller to multiple layers, we present three possible approaches. The fastest approach is to modify the design such that it features exposed conductive pads for each individual layer. It must be ensured that those pads are

not covered by subsequently transferred layers. Wires can then be attached to those pads after all layers have been water-transferred. As a second approach, each layer can be connected before the next layer is water-transferred on top of it. The most elegant approach consists of using VIAs to route all connecting traces to one layer for connection to the controller.

To verify the feasibility of this approach, we realized a capacitive row-column scanning multi-touch sensor on a particularly demanding object: the non-developable and rough surface of a stone (Figure 4.8b). It consists of a 4 x 4 diamond pattern matrix [42] (4 x 4cm). The sensor comprises three functional layers overall: two layers of conductive electrodes (silver) that are separated by one dielectric layer. The printed sensor was controlled using an MPR121 chip. The sensor is fully functional and highly conformal to the fine details of the stone's surface (see Figure 4.8b).

4.4.3 Display output

In addition to sensing, ObjectSkin also supports the fabrication of active light-emitting displays. Our approach is based on screen-printing of thin-film electroluminescent (TFEL) displays [149].

Our approach consists of transferring and curing four functional layers: a layer for the bottom electrode (silver), a dielectric layer, a layer of electroluminescent ink (blue phosphor, Gwent C2061027P15), and a translucent top electrode (PEDOT). As each of the slim layers is transferred and cured one after another, each conforms closely to doubly-curved and rough surfaces before curing. We thereby improve on prior work that applied TFEL displays to developable geometries [149], wrapped thicker silicone overlays [242], or applied a complete cured stack [237].

To demonstrate the technical feasibility, we have realized a TFEL display segment that conforms to a rough stone's surface, as illustrated in Figure 4.8c.

4.5 Novel interactions for HCI

ObjectSkin is an enabling technology for input and output on a wide variety of everyday objects. In this section, we present an exploration of novel interaction possibilities that our method enables. They are based on new geometries, the object's surface structure, and use of unconventional objects.

4.5.1 Geometry-guided touch gestures

Everyday objects offer a vast variety of complex geometries, e.g. in toys, tools, or filigree jewelry. Prior HCI research has mostly focused on a subset of geometries, consisting of easier-to-augment object surfaces, e.g. the head or belly of a toy figure [21, 192, 244], the outside of a mug [51], or the top of a folded lamp shade [148].

ObjectSkin allows us to approach everyday objects from a new perspective: imagining interaction on all their surfaces, including those that are more difficult to augment, e.g. with holes or many small or thin parts. We demonstrate how this

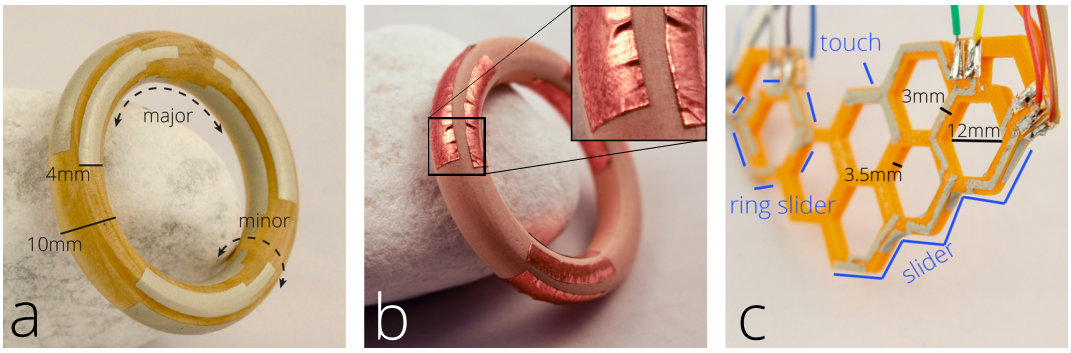

Figure 4.9: Prototyping geometry-guided touch gestures. A wooden ring (a) is augmented with 9 conformal electrodes to support circular gestures following its major and minor radii. In contrast, adhesive copper tape causes wrinkles due to the non-developable geometry and edges due to its thickness (b). A honeycomb pendant (c) illustrates three geometry-guided touch interactions.

enables novel interaction possibilities, by exploring touch gestures on two example objects: a wooden torus ring and a filigree honeycomb-style pendant.

4.5.1.1 *Torus ring*

From many available objects with holes, we selected a wooden ring, which we imagine could be worn on a necklace, for its aesthetics and appealing shape (see Figure 4.9a).

In an initial expert group brainstorming session, we explored the geometry's affordances. Our results show that the continuous curved surface allows users to perform a set of different touch gestures and fluently combine them:

- sliding with one or multiple fingers along the ring's major radius (on its inside, outer side, front, or back)
- sliding inwards or outwards in the perpendicular direction (along the ring's minor radius), at various locations on the ring, either by touching with one finger or by pinching with two fingers

We transferred these findings into the design of a novel interaction device: a music player control embedded in the ring, which is worn on a necklace. The device supports 3 circular sliding gestures in both directions along its major radius. These are mapped to continuous seeking inside a song, changing tracks, and changing the album. In addition, the device features 6 inward- or outward-rotating gestures to adjust the volume, turn the device on or off, and switch between equalizer presets.

Based on this design, we created a prototype using our high-fidelity approach. We completed the prototype using the MPR121 chip, which reliably detects touch input on all electrodes. Gestures are classified with a simple rule-based classifier, based on the sequence of touch locations.

To investigate the benefits of ObjectSkin, we compared our prototype to two baseline alternatives: manual application of adhesive copper tape (similar to [190]) and a temporary tattoo-based approach (as presented in [237]). Aligning the different

electrodes with adhesive copper tape was challenging and we quickly noticed that the copper tape did not conform well enough. The resulting surface was not smooth, which disturbed the gestures' execution and made them feel less fluid. This was mainly due to edges that result from the tape's thickness and due to small wrinkles that result from wrapping non-stretchable copper tape onto the non-developable geometry (Figure 4.9b). The tattoo paper resulted in a much thinner layer that did not produce noticeable edges. However, due to the paper backing of the tattoo paper, it was not possible to wrap the electrodes onto the torus' geometry without distortion, especially onto the inside of the hole (Figure 4.5a and b). In contrast, our approach results in a smooth surface and successfully conforms to the non-developable geometry (Figure 4.9a).

4.5.1.2 *Honeycomb pendant*

As a second example for advanced geometry, we selected a honeycomb-style pendant. It features a filigree geometry with thin structures and many small faces on all sides (See Figure 4.9c). Expert group brainstorming revealed four main types of touch gestures:

- Discrete circular motion along the six sides inside a honeycomb cell
- Touching either side of a cell similar to a six-way joystick
- Sliding along the top or bottom edge of the pendant, spanning multiple honeycomb cells
- Using the connection point between three adjacent honeycomb cells as a discrete touch point

Considering the wearable form factor of the pendant, we envision it being used for quick gesture-based interaction in various mobile scenarios, including interpersonal communication, navigation, and smart home applications. We designed an example device that implements the four touch gestures and illustrate their use in different use cases.

In a smart home environment, we leverage the honeycomb cell structure to conveniently control the ambient light. To this end, the six inside faces of a cell are mapped to six positions on a color wheel, allowing the user to fluently browse through the color spectrum in an eyes-free manner. We found the leftmost, rightmost, and bottom cell most convenient to access. Accordingly, we augmented the leftmost cell with six electrodes, one on each inside face (see Figure 4.9c), to capture the circular movement. In addition, we designed a slider to allow changing the light's brightness. It is located on the structure's bottom edge for convenient access. It features four touch electrodes to increase or decrease the brightness with a sliding gesture. To illustrate the use of honeycomb intersections for touch, we added a discrete touch button at an intersection point in the top center to quickly turn the light on or off.

As the pendant would be worn throughout the day, its controls support different application scenarios. For mobile navigation, for instance, the touch button could quickly open a map showing the user's current position for orientation. Once the

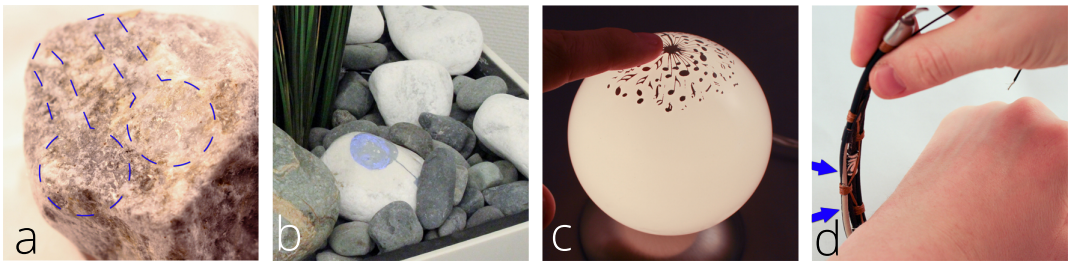

Figure 4.10: Augmented everyday objects for novel interactions. A rock is augmented with two translucent electrodes (marked with dashed lines), leveraging two areas of distinct roughness for eyes-free interaction (a). Prototyping interaction on unconventional everyday objects: a garden stone (b), a glass lampshade (c), and a leather bracelet (d, electrodes at arrows).

map is displayed, e.g. in a head-mounted display, it could be zoomed in or out using the slider control. However, the sensor designs themselves are versatile to support different interaction for versatile scenarios. The electrodes of the circular slider, for example, also detect discrete touch contact on each of the six sides of a honeycomb cell. One might leverage this, for instance, for interpersonal communication, allowing six distinct actions to be performed for each contact assigned to an individual cell.

In total, our design uses 11 very small (6 x 2 *mm*) electrodes to implement the described controls (see Figure 4.9c). Adding this large number of electrodes to the filigree structure makes it very demanding to route conductive traces on the object that connect electrodes with the controller. In order to route connecting traces for all 11 electrodes to two endpoints (top left, top right), the traces need to be applied across edges, e.g. to use the front, outer, and inner sides of the hexagon pattern for routing.

It would be very time-consuming and prone to misalignment if one had to manually add those traces to the filigree geometry, as required in established approaches using copper tape or temporary tattoo paper. For such geometries, ObjectSkin offers the advantage of wrapping all traces automatically during dipping. This allowed us to use more complex routing. We fabricated the final prototype using our high-fidelity approach with silver ink, as illustrated in Figure 4.9c. For sensing, we connected an MPR121 chip, which reliably detected touch input on all electrodes.

4.5.2 Surface structure for eyes-free touch interaction

Besides their individual geometries, everyday objects vary in the tactile cues their surfaces provide. This tactile feedback is central to how a user perceives a surface.

ObjectSkin enables sensors that closely conform to an object's surface structure, as illustrated in Figure 4.6a, allowing its tactile feedback to be preserved. We demonstrate the benefits of this capability by adding touch sensors onto surface structures with distinct tactile cues, allowing for eyes-free touch interaction.

We implemented a prototype based on a rock that features areas of different roughness (see Figure 4.10a). We identified two adjacent areas that exhibit different roughness and distinct tactile feedback. We then designed and transferred two electrodes (15*mm* diameter, spaced 5*mm* apart) onto the rock using our low-fidelity approach. We used the MPR121 chip for capacitive touch sensing. The prototype demonstrates that the sensor electrodes conform closely to the surface structure and preserve the tactile feedback, providing sufficient tactile cues for the user to distinguish the two touch elements without visual feedback.

4.5.3 Interaction on unconventional objects

ObjectSkin is capable of augmenting a wide variety of everyday objects. We present four application examples of how unconventional objects can be augmented and used for interaction.

Growing touch sensor on live plant.
We augmented a live bamboo plant with a touch sensor. As bamboo grows fast, the sensor is designed to stretch and grow with it. Therefore the touch electrode (9 x 15 *mm*) is laid out in a stretchable horseshoe pattern (Figure 4.1d). Touch contact is captured using the MPR121 chip.

Interactive glass lampshade.
We turned a conventional lamp into a customized interactive piece of furniture. We applied artwork, depicting a "music flower", in silver ink onto the lamp's spherical glass shade. The artwork acts as a touch sensor to turn on and change the brightness (4 levels) of the lamp, but also blocks part of the light for a unique artistic effect (Figure 4.10c).

Leather bracelet for activity tracking.
A sensor measuring the electro-dermal activity (EDA) was applied to the inside of a leather bracelet. It allows the wearer to measure the EDA in a subtle manner, for example to gather data on the stress level. Two electrodes are applied to one thin band of leather, making use of our approach's ability to conform to delicate details (Figure 4.10d).

Garden stone as peripheral display.
We augmented a garden stone with an electroluminescent display to act as a subtle reminder for watering the plants. The stone fits into a natural stone arrangement surrounding a plant. Based on readings from a connected moisture sensor, it displays an unobtrusive visual notification for the user when the soil gets too dry (Figure 4.10b).

4.6 Discussion

We have demonstrated that ObjectSkin supports input and output modalities on a wide variety of materials and non-developable geometries. It offers novel capabilities for prototyping interaction on everyday objects, making it an enabling technology for makers and HCI researchers.

Scalability

We have printed on transfer film up to A3 size and used a water basin with a slightly larger opening and 30 cm depth. Since multiple layers can be connected, ObjectSkin can exceed these dimensions as long as the part to augment can be submerged in the basin. We have demonstrated this by printing on a large bamboo plant for which we only submerged individual stems into a small basin.

The maximum number of sensor and output components is defined by the capabilities of the controlling hardware. The MPR121 touch sensing chip is limited to 12 electrodes but multiple chips can be used in parallel via an I2C connection. As electronics are getting smaller, thinner, more flexible, and increasingly powerful, we believe that in the future interactive objects can be realized in a fully self-contained way by including microcontrollers and batteries on the surface.

The resolution of sensors and displays is limited depending on the printing method. For low fidelity, fingertip-sized ($\sim 15x15mm^2$) touch sensors can be realized. However, since the inkjet printer provides a much higher spatial resolution (5.760 x 1.440 dpi), ink with better conductivity could allow for smaller sizes. For high-fidelity prototyping, we were able to print traces as thin as $300\mu m$ and realize touch electrodes as small $2mmx6mm$.

Quality

Our results regarding geometries show that the conductivity of a transferred pattern depends on the amount of stretch it underwent during the water transfer. This implies that the uneven structure of highly textured surfaces, e.g. rough wood or stone, can result in a locally inhomogeneous conductivity. For touch sensors, we could not observe an effect of this inhomogeneity on a variety of highly textured surfaces. For display output, however, it affects the luminance, which can be observed as darker spots (see Figure 4.8c). While the resulting displays are still well-suited for prototyping purposes, this effect needs to be considered when prototyping on highly textured surfaces.

Ease of fabrication

We could verify that two days of experience are sufficient for non-experts to learn the screen-printing process, as reported in [149]. The water transfer does not add significantly to the overall difficulty. We found that about 10 trials were enough to achieve less than 5 mm misalignment and avoid artifacts, such as air bubbles. A steady hand improves both printing and the transfer. The transfer does not require any special equipment, except for the materials used and a water container. Printing, transferring, and post-treatment of a single functional layer takes between 20 and 40 minutes.

Advanced fabrication options

To make our fabrication technique reproducible, we relied on standard inks and equipment. It remains to be investigated how the process can be further improved with optimized ink formulations. UV curing could allow for curing on more materials. In hydrographic printing, pre-processing, e.g. priming or smoothing, is used to facilitate ink adhesion. Post-print finishing, e.g. sprayed clear coating, helps to better protect the ink but also offers artistic options. While these steps are potentially beneficial to further enhance the quality and robustness of ObjectSkins, we purposefully omitted them in favor of preserving the materials' visuo-tactile properties.

Advanced sensing

ObjectSkin brings printed electronics to highly-curved non-developable surfaces of 3D objects. Our results show that this enables them to sense interaction on the surface. Given related work that employs sensors on the outside of an object to infer what is happening inside, e.g. by electrical impedance tomography [259] or pressure sensors [39], we believe our fabrication technique bears the potential to also sense phenomena inside the object.

Design

We have demonstrated that manual design is feasible for complex components, e.g. multi-layer displays, and doubly-curved geometries. To further ease the design, we envision the user being supported by a 3D design environment with abstraction algorithms, which allow the user to design the sensors and output directly on the 3D model. In particular, calculation of the distortion caused by stretching of the ink, as proposed by [261], can be helpful for complex geometries and non-expert or novice users. However, our results show that for many rapid prototyping applications slight distortion can be accounted for or even neglected in manual design. Nevertheless, our quantitative findings, including maximum stretch, conductivity based on materials, and limits on electrode dimensions, form the basis for a formal model required in a computational design tool for ObjectSkin.

Safety

For our fabrication process, we recommend using standard protection measures, e.g. rubber gloves and goggles, and following the guidelines on health and safety that are supplied with the materials' safety data sheets.

4.7 Conclusion

This chapter contributed ObjectSkin, a fabrication technique for adding slim, conformal, and translucent interactive surfaces to rigid and flexible everyday objects. It

comprises two variants, for low-fidelity and for high-fidelity prototyping, based on water transfer of printed electronics. We described in detail how the technique can be replicated with hobbyist equipment available in HCI labs or maker spaces.

ObjectSkin supports a wide variety of materials and enables augmenting highly curved and rough non-developable surfaces. This chapter presented experimental evidence on material compatibility, highlighting the approach's applicability in many prototyping applications. It further illustrated the novel geometric possibilities ObjectSkin enables compared to related work and substantiated the results with experiments on the geometric limitations.

To show the approach's capabilities for interactive surfaces, this chapter presented the fabrication of conformal touch sensors and multi-layer electronics for multi-touch sensing and electroluminescent display output. Together with ObjectSkin's newly supported geometries, these capabilities enable prototyping of novel interactions on everyday objects.

This chapter advances the field of rapid prototyping of interactive objects with rich materials in two ways: First, it extends touch input and display output capabilities to strongly-curved and fine-detailed 3D geometries and a large variety of object materials. Second, the approach enables conformal object overlays to add interactivity to everyday objects while largely preserving their visuo-tactile feedback. This enriches the possibilities of investigating interaction on novel geometries and materials. This chapter demonstrated interactions that leverage the object's surface structure and geometry, in a series of prototyping examples. These include geometry-guided touch interaction, surface roughness for eyes-free interaction, and augmentation of unconventional objects.

The examples in this chapter demonstrate that leveraging the geometries and material properties of everyday objects bears potential to investigate novel interactions for interactive objects with rich material. Yet, the input and output modalities were limited to touch input and visual output. In contrast, many of the used features of everyday objects are of haptic nature, e.g. geometries to grasp and surface structures to touch. The next chapter thus explores rapid prototyping of haptic interfaces for interactive 3D objects.

5 Design and Fabrication of Tactile Interfaces on 3D Objects

The previous chapter on ObjectSkin contributed a novel fabrication approach for augmenting 3D objects with touch input and visual output capabilities. ObjectSkin focused on objects of complex strongly-curved geometries and diverse materials. The previous chapter demonstrated how to leverage an object's existing tactile features for touch interaction. Output, however, was limited to visual displays.

This chapter[1] moves beyond visual feedback as an interactive output modality by exploring the digital design and fabrication of computer-controlled haptic feedback on 3D objects. Like the previous chapter, this chapter uses digital fabrication via printed electronics to extend the capabilities of custom interactive objects with rich materials. By printing the custom device, rather than manually assembling it from conventional electronic components, the fabrication process can be considerably simplified and sped up. At the same time, as printable electronics commonly are very thin and deformable, more demanding geometries and advanced input and output capabilities can be realized.

Prior work has demonstrated approaches based on printed electronics to equip custom-shaped 3D objects with various types of printed sensors for capturing user input [148, 189, 192, 244] and printable output components, including light-emitting displays [149, 244] and actuators for shape-change [46, 251]. While the previous chapter focused on extending such capabilities to more complex geometries and diverse materials, this chapter focuses on tactile output which was so far left unaddressed. Fabricating custom interactive objects that include computer-controlled tactile output still relies on manually assembling conventional components [88, 155]. Moreover, the rather large form factors of typical motors and mechanical actuators tend to be incompatible with demanding object geometries.

To address these challenges, this chapter introduces a novel digital fabrication approach for printing custom, high-resolution controls for tactile input and output on 3D objects. We call these controls *Tactlets*.

1 This chapter is based on [56]. As the first author, I led the conceptual design, development of the design tool, design of the parametric Tactlet controls, development of the fabrication approaches, design and execution of the user study, and implementtion of application cases. The research intern Martin Feick contributed to ideas for the design tool, the parametric templates, and application cases. He helped with the implementation of the design tool, fabrication approach, and application cases. Anusha Withana developed the hardware controller and helped implementing the touch sensing component. He further contributed to ideas for application cases, the analysis of the study results, presentation of the study results (Figure 5.12), and writing of the publication. The student assistant Amr Gomaa helped with implementing the hardware controller and conducting the user study. My supervisor Jürgen Steimle advised me on the conceptual design, design tool, paramteric controls, evaluation, and applications. He further contributed to the structure and writing of the publication.

Figure 5.1: Tactlets is a novel approach enabling digital design and rapid printing of custom, high-resolution controls for tactile output with integrated touch sensing on interactive objects. (a) A design tool allows a designer to add Tactlet controls from a library and customize them for 3D object geometries. The designer can then fabricate a functional prototype using conductive inkjet printing (b) or 3D printing (c), and explore the interactive behavior of the Tactlet control. (d) This approach allows for rapid design iterations to prototype tactile input and output on a variety of objects.

A Tactlet comprises a custom-printed arrangement of taxels (tactile pixels) that each sense touch input and deliver electro-tactile output. This makes Tactlets highly customizable and allows them to integrate with a wide variety of object geometries while augmenting them with virtual tactile feedback. One example is a touch slider that allows the user to set a continuous value via touch input and tactually renders virtual tick marks as well as the slider's current position.

This chapter presents three main contributions, enabling rapid prototyping of tactile interfaces on 3D objects using digital design and fabrication.

First, this chapter contributes a high-level digital design approach for tactile interfaces on 3D objects (Challenge 1). The design tool, a plug-in for the widely used 3D-modeling software Rhino3D [177], enables the user to easily augment a 3D-object model with desired tactile input and output capabilities at a high level of abstraction. The user can place and scale Tactlets on the 3D object and adjust high-level parameters. The design tool then automatically parameterizes the Tactlet accordingly and generates the low-level printable design.

In addition, this chapter contributes an inventory of 10 parametric Tactlet controls. The inventory comprises several types of buttons and contributes several types of sliders, for tactile input, tactile output, tick marks, dynamic ranges, etc. Each template encapsulates a model of a Tactlet's interactive behavior, i.e. mapping between sensed user input and real-time tactile feedback, and a parametric model

to generate its print design. In addition, it exposes high-level properties to the designer (e.g. enabled/disabled state, selected value, or output resolution).

Second, this chapter presents two accessible approaches for fabricating Tactlets on 3D objects through printing (Challenge 2). One approach enables rapid prototyping of thin (270μm) electro-tactile overlays using conductive inkjet printing. The other approach comprises 3D printing of objects with embedded electro-tactile taxels using a standard multi-material 3D printer and conductive filament. For both approaches individual taxels are realized as two or more printed electrodes that generate localized electro-tactile output and capture user input with a resistive touch-sensing scheme.

Third, this chapter contributes an approach that leverages the fabricated object's interactivity for physical feedback and manipulation of the design (Challenge 3). As is common for digital fabrication approaches, Tactlets are digitally designed and then printed. However, after printing the design tool offers a novel *real-time design mode*. In this mode, the tool offers live control of the object's tactile sensing and feedback. This allows for real-time exploration and refinement of design choices, such as dynamically adjusting parameters of Tactlets during hands-on interaction with the interactive object. In contrast, common iterative approaches for interactive objects rely solely on digital manipulation and require repeated fabrication to implement changes to the design [146, 148, 192, 244, 249].

Last, this chapter validates the functionality and practical feasibility of the Tactlets approach. It presents results from a psychophysical experiment, the iterative design process using two application cases, and a discussion of lessons learned.

The remainder of this chapter is structured as follows. Section 5.1 first introduces the design and fabrication process of Tactlets. Section 5.2 then presents the inventory of Tactlet templates. How Tactlets are realized through printing, will be presented in Section 5.3. Next, Section 5.4 provides details on the evaluation. Last, Section 5.5 concludes this chapter with a discussion of this chapter's contributions.

5.1 Design and fabrication process

An overview of the digital design and fabrication process of Tactlets is illustrated in Figure 5.2. We contribute a novel *high-level digital design* approach, based on standard 3D modeling and new parametric controls, that enables easy placement and customization of Tactlets on a 3D object. Once designed, a physical prototype can be quickly *realized through printing*. To further ease and speed up iterative prototyping, we contribute a *real-time design mode*. It enables hands-on testing and design refinement on the fabricated prototype, while instantly propagating design updates of the interative behavior, e.g. parameters of the electro-tactile stimulation, between the design tool and the fabricated prototype.

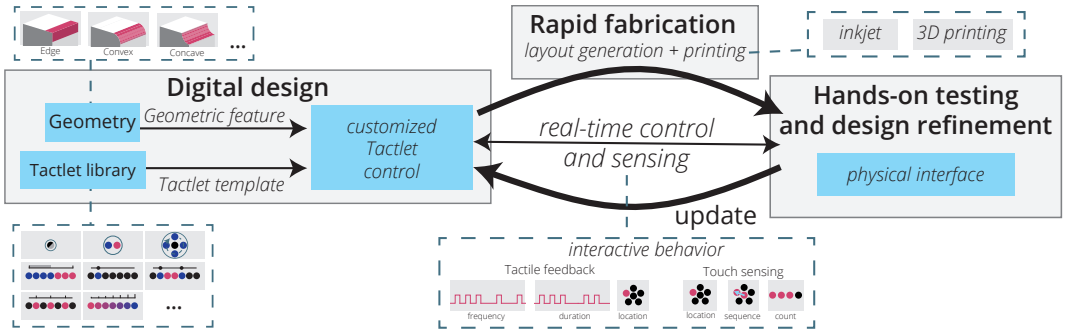

Figure 5.2: Conceptual overview of the design and fabrication process.

5.1.1 Digital design

The process starts with the digital design. The goal is to enable the designer to easily and rapidly define the tactile input and output capabilities for a desired 3D object. Inspired by the success of toolkits for Graphical User Interfaces (which abstract from pixel-level I/O to high-level user interface controls), our approach allows for designing at a high level of abstraction.

To this end, we contribute the Tactlets design tool (see Fig. 5.3), which allows the designer to select Tactlet templates from a library, place them on a 3D model, and customize them. The design tool is implemented in C# as a plugin for Rhino3D, a popular computer-aided design (CAD) application, using the RhinoCommon .NET SDK[2]. This enables the designer to use all of Rhino's standard 3D-modeling features and to import models. The design tool offers a library of Tactlet templates, including buttons and sliders (see section Tactlet Templates).

The designer first selects a desired Tactlet template. Then she places it at the desired location on the mesh of the 3D-object model. This is done either by selecting the Tactlet's center point and size, or by selecting its start and end point, or by defining a free-form curve on the mesh that the Tactlet shall be mapped to (see Fig. 5.3).

The tool then passes the selected geometry to the template, which based on its model automatically parameterizes the concrete taxel layout (i.e., size and placement of taxels). For instance, to create a slider Tactlet on an edge of the object, the slider template generates taxels along the edge's path in the 3D model. It sets the radius of taxels to the default value stored in its model and spaces taxels with the maximum possible density to yield the highest possible resolution of sensing and output. The design tool immediately visualizes the Tactlet design by rendering the individual taxels on the 3D model (see Fig. 5.3). The designer can then further customize the Tactlet by adapting its parameters (e.g. resolution of the slider) or by changing the shape or placement of the Tactlet (e.g. adapting the curve of a slider). The tool visualizes changes in real-time.

2 https://developer.rhino3d.com/guides/rhinocommon/

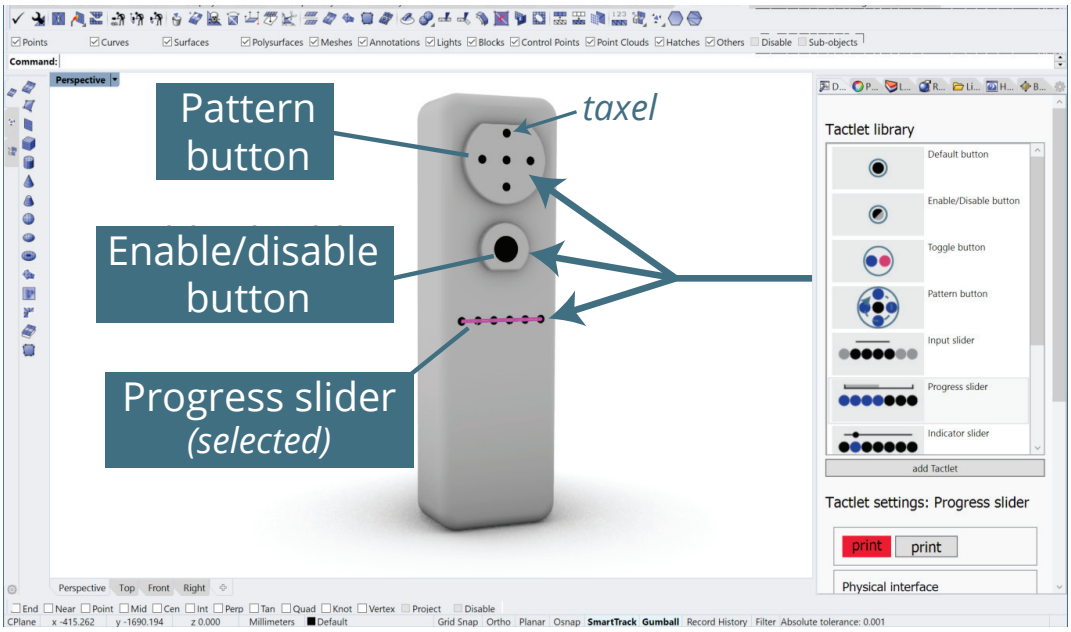

Figure 5.3: Digital design example: A prototype of a new tangible presenter device with tactile feedback is designed in the Tactlets design tool. It should let the user monitor the progress of a slide presentation and slide timing. The 3D model features two button-shaped protrusions. From the library of Tactlet templates, two Tactlet buttons, "next" and "previous", are placed on the two protrusions of the model. A slider is placed on the front of the device that will give tactile output about the slide progress.

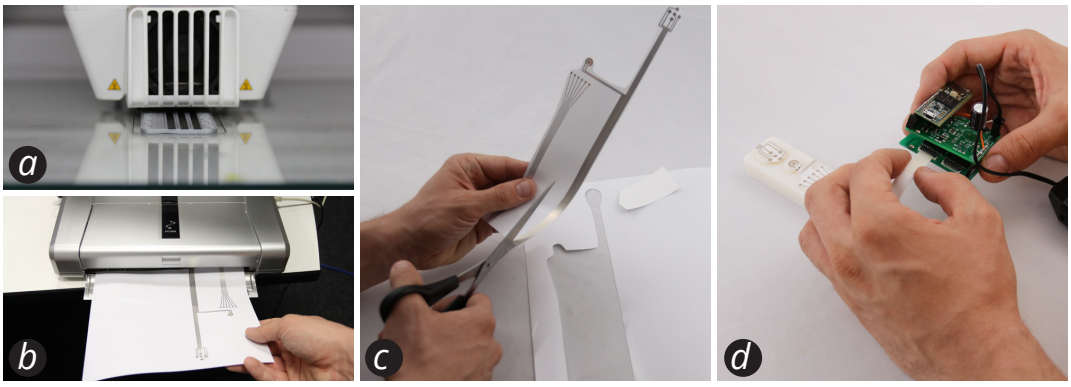

Figure 5.4: Rapid fabrication example: The designer prints the physical prototype on a 3D printer (a). Alternatively, she prints the interface on a conductive inkjet printer (b), cuts it out (c), and attaches it. Finally, the prototype is connected to the Tactlets controller (d). The entire fabrication (b-d) of the presenter prototype takes less than 5 minutes.

5.1.2 Rapid fabrication

To fabricate the interactive object, the design tool generates a printable low-level electrode layout of the electro-tactile interface. The generated design is then printed using one of two alternatives: For rapid fabrication within minutes, conductive inkjet printing [102, 104] can be used to print a thin, flexible electro-tactile overlay to be attached to the object. Alternatively, the interactive object can be 3D printed using a commodity FDM 3D printer and conductive filament, realizing the object with the embedded electro-tactile interface in a single pass. Both techniques enable a taxel density of 2mm diameter at 4mm center-to-center spacing.

After printing, the interface is connected to the Tactlets controller, a custom hardware unit that interfaces with the printed electrodes to control the electro-tactile stimulation and to sense touch input. The controller allows selection of the intensity/amplitude (0–3 mA, in 15μA steps), the frequency (1–200 Hz), and duration (1ms steps) of the electro-tactile stimulus. The hardware supports stimulating one single taxel or multiple taxels at the same time through temporal multiplexing. It is extensible to support multiples of 8 taxels. Our configuration supports 16. For integrated sensing of user input, we employ a resistive sensing scheme using the same electrodes used for stimulation. Sensing is time-multiplexed with stimulation and runs at 25Hz. Details on the implementation of the hardware controller are given below.

5.1.3 Real-time design mode: Hands-on testing and refinement

The design tool contributes a *real-time design mode* to support rapid hands-on testing and design refinements using the printed prototype. We consider this a critical feature, as tactile feedback cannot be adequately conveyed through a rendering in the design tool and instead needs to be physically experienced. In this mode, the design tool and the fabricated prototype are connected and synchronized in real-

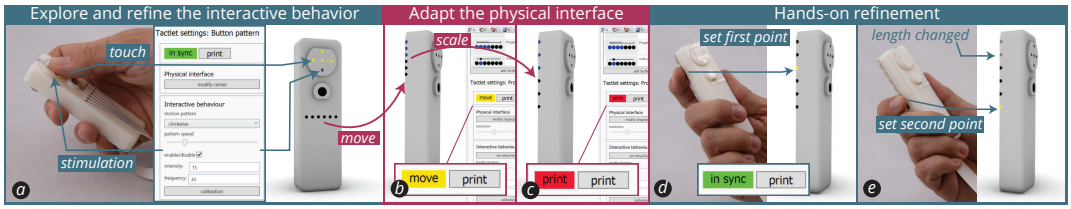

Figure 5.5: Real-time design mode example: (a) the designer explores the tactile output of the designed Tactlets. She can adjust and test different high-level parameters, e.g. the slider's progress value. Touch input is visualized on the 3D model in real-time. The designer moves the slider from the front (a) to an edge on the model's backside (b), as tactile guidance. (b) The tool indicates that the printed physical interface can be moved to the new location on the object and does not need to be re-printed. (c) The designer then increases the slider's length, a refinement which requires to re-print the interface. (d & e) After printing, the designer quickly adapts the length of the progress slider to be within comfortable reach of her finger. She first selects the start point directly on the object (d), followed by the end point (e). The length is updated immediately and visualized in the design tool (e).

time. To physically explore design options, the design tool offers live control of the prototype's interactive behavior. Conversely, by leveraging the sensing capabilities of Tactlets, the properties of a Tactlet can also be changed directly on the prototype itself and the digital design instantly updated.

To support rapid testing and refinement of a design, the design tool offers various options. It allows customizing the interactive behavior, moving a Tactlet on the object or modifying its size or shape, and adding or removing a Tactlet.

Explore and refine the interactive behavior

In the real-time design mode, Tactlets are interactive. The design tool processes captured input and renders tactile output according to the Tactlet's defined interactive behavior. A dedicated thread handles real-time processing of incoming touch data, sending actuation commands to the controller. The touch data are thresholded and touch-up and touch-down events distributed in an event-driven architecture. Tap events (i.e., lifting the finger within $< 30ms$ [145]) are detected based on timing of touch events and made available for listeners.

When the designer modifies properties of a Tactlet in the graphical design tool (e.g., enabled/disabled, selected position of a slider, etc.), the behavior of the physical prototype is updated accordingly in real-time. This allows the designer to physically experience the interactive behavior of a Tactlet and, if desired, refine the design. To ease debugging of a design, the design tool visualizes any user input sensed as well as all tactile stimuli provided on the physical object (see Fig. 5.5a). For rapid testing, the tool further offers a procedure to calibrate the user-dependent intensity of electro-tactile stimulation to a comfortable level.

Hands-on refinement

Modifying the behavior of the physical prototype through adjusting properties in the graphical user interface creates an indirection, requiring the designer to switch back and forth between the object and the graphical user interface. Since Tactlets feature input-sensing capabilities, the tool offers an alternative option: *hands-on refinement* to change properties of Tactlets directly on the physical object. To do so, the user selects a property to modify in the user interface and then physically sets it to the desired value.

Hands-on refinement can be used to change properties that define the tactile stimulus (e.g. frequency, temporal patterns, enabled/disabled state). While the designer is touching the taxel, the tool continuously sweeps through the valid range of values and renders the tactile stimuli accordingly. When the desired value is reached, the designer releases the touch, which sets the new value. In addition, it is possible to change properties defined by selecting a taxel location. For instance, the length of a tactile slider control can be dynamically shortened by defining a start and end taxel within the overall length of the slider (this results in outer taxels being disabled), as illustrated in Fig. 5.5d & e.

Adapting the physical design

Moving, scaling, or deleting a Tactlet is enabled through direct manipulation in the design tool's 3D view. The Tactlet directly adapts its taxel layout to the new 3D-object geometry. The tool then automatically determines whether the change can be realized by keeping the current printed prototype. A Tactlet can be deleted or downscaled by disabling all or some of its taxels, respectively, while keeping the prototype. Some cases of moving can be dealt with by simply physically moving the printed overlay to a different location on the object (in case conductive inkjet printing was used for fabrication). If so, the tool provides visual indications that guide the designer to perform this step. In all other cases, the tool indicates that printing a new version of the physical interface is required.

5.2 Library of Tactlet templates

In this section, we present an inventory of 10 Tactlet templates. They allow the designer to realize interactive objects with a variety of tactile behavior, including various types of buttons and slider elements.

Each template is implemented as a C# class that encapsulates the taxel layout generation and the interactive behavior. A template defines high-level properties that can be set in the design tool or at run-time (e.g., enabled/disabled). In addition, it defines events (e.g., button clicked) with corresponding listeners. The interactive behavior is implemented by taking touch and tap events as input and then correspondingly stimulating individual taxels.

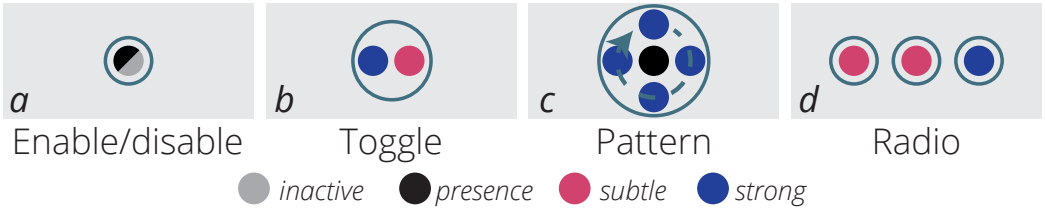

Figure 5.6: Templates for button Tactlets

5.2.1 Basic Building Block: Electro-tactile Taxel

A taxel is the basic building block of Tactlet templates. A taxel senses touch contact via resistive sensing. In addition, each taxel allows for electro-tactile output of varying duration (ms) and frequency (Hz). For most Tactlets two levels of distinguishable frequency are sufficient. We use default frequencies of 10Hz for *subtle* and 150 Hz for *strong* output (reflected as color of taxels in Fig. 5.6 and 5.8). We opted against using stimuli of different amplitude, as the perception of amplitude is very user-dependent, and instead calibrate the intensity to a level that the user perceives as comfortable. By default, upon touch contact, a taxel provides a *presence feedback*: a subtle pulsating output (150/50*ms* on/off). This feedback allows the user to discover the presence of a taxel, and therefore the Tactlet, during eyes-free interaction.

Taxels are circular to ensure a uniform current distribution [95]. Their size is scalable, ranging from 1-3mm radius. Several taxels can be arranged to enable spatial elements (such as a linear slider) and high-resolution tactile output, i.e. a density comparable with the highest tactile acuity for electro-tactile stimulation at 4mm center-to-center spacing [96].

5.2.2 Tactile Buttons

The most basic control is a **tactile button**. It consists of a single taxel, parameterized by its *location* (X,Y, Z) and *radius* (mm). By default, a button provides presence feedback while it is being touched. Tapping a button triggers a selection event (sent to all registered listeners). The designer can change this to a double-tap, if desired.

Disabling presence feedback allows creation of an **enable/disable button** that when disabled can no longer be discovered using taction (Fig. 5.6a & 5.7a). It offers the additional boolean parameter *enabled*. This feature can be used to temporarily hide functions that are currently unavailable.

Graphical user interfaces offer several types of buttons that provide additional states, e.g., a toggle button or checkbox. We realize a **tactile toggle button** that when tapped toggles between two states and triggers an event. It is composed of two taxels (Fig. 5.6b). For either *toggle state*, one of the taxels provides continuous strong output, while the other provides continuous subtle output. Both taxels are spaced with a 5 mm distance, to ensure that both taxels can be simultaneously felt when the finger pad touches the button.

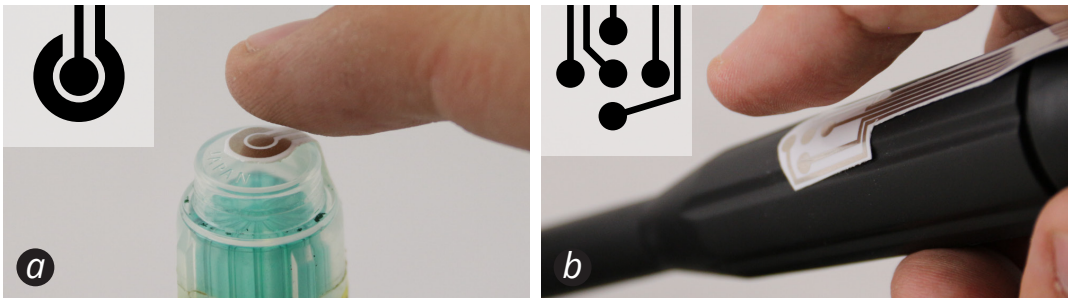

Figure 5.7: Two printed button Tactlets placed on curved geometries: (a) enable/disable button and (b) pattern button.

Tactile radio buttons allow selection of one from a set of choices. They are realized by grouping multiple buttons, of which only one can be *selected*. Selection is reflected as continuous strong output (Fig. 5.6d). The designer is free to define a custom arrangement of buttons belonging to one radio group. For instance, she may place each button on a distinct geometric feature to allow for eyes-free exploration.

Adding more taxels allows for buttons that offer more versatile patterns of tactile feedback. We illustrate this with a **tactile pattern button** (Fig. 5.6c & 5.7b). It comprises one center taxel and 4 additional taxels arranged in a concentric circle of 3 mm radius. It offers circular tactile output by stimulating taxels in one circular *direction* (clockwise or counter-clockwise) as a sequence of strong pulses at *pattern speed* (Hz). This pattern can be used to convey additional states, e.g., indicating direction (forward or backward) in a video or slide presentation.

5.2.3 Tactile Sliders

Extending the size of a Tactlet beyond the size of a finger pad enables Tactlets that can be actively explored using finger movement. A basic example consists of a series of taxels arranged along a path (e.g. line, curve, circle) on the object's surface. We refer to them as a *tactile slider*. The placement of a slider is parameterized by setting the property *path* (NURBS). Of note, a slider can be placed on a distinct geometric feature, such as following an edge, ridge, groove, or going across a curved surface. This enhances eyes-free discoverability and offers tactile guidance of the user's finger when sliding. An additional property is output *resolution* defining the number of taxels along the path. Taxels are spaced at least 4mm apart to be distinguishable.

By default, all taxels of a slider provide presence feedback upon touch for discoverability. Disabling selected taxels, however, allows dynamically adapting a slider's length. For this purpose, the properties *start taxel* and *end taxel* can be set to define the bounds of the active area of the slider (Fig. 5.8a). For instance, this can be a useful property to adapt the length of a slider on a handheld object such that it is within finger reach for a given user's hand size (see Fig. 5.5d & e).

In a basic case, such a series of taxels allows for tactile rendering of a *one-dimensional* variable: A **tactile progress slider** provides continuous strong output on a percentage of taxels that corresponds to the current *value* ([0..1]), whereas the remaining

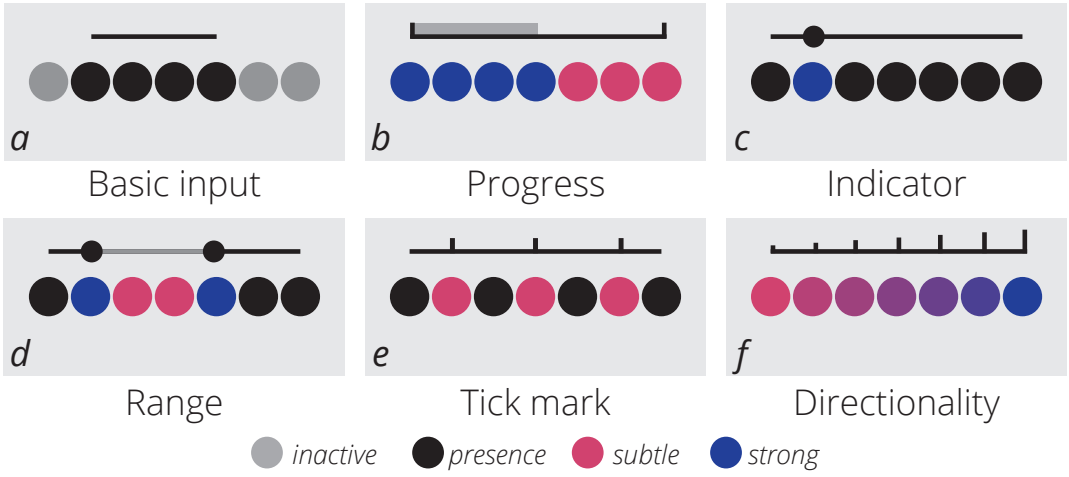

Figure 5.8: Templates for Slider Tactlets.

taxels provide continuous subtle output (Fig. 5.8b). Thus the current state can be explored with one finger.

For input, a **tactile input slider** lets the user set a *value* by tapping on a location on the slider (Fig. 5.8a). Tactile exploration (remaining $> 30ms$ at a taxel) provides presence feedback.

Inspired by traditional mechanical sliders or sliders in GUIs, we realized an advanced control that combines selection with tactile feedback of the selected value. A **tactile indicator slider** renders a tactile indicator, like a "knob", at the position on the slider representing the currently selected *value* ([0..1]), illustrated in Fig. 5.8c). The tactile indicator is rendered as strong pulsating output (150/50 ms on/off). It can be selected by tapping, which changes the pulsation to a continuous output while the user is dragging the indicator to the desired position. Once the finger is lifted, the new value is set and the indicator again rendered as pulsation. A **range slider** extends this Tactlet by adding a second virtual indicator, allowing selection of a *range* ([0..X,X..1]) of values (Fig. 5.8d). The selected range between indicators is rendered as continuous subtle output.

In addition to active virtual elements, e.g. indicators that can be dragged, sliders can also incorporate passive virtual elements. Adding a subtle continuous output at selected taxels allows adding **virtual tick marks** (Fig. 5.8e). These support rapid tactile discovery of key positions on the slider. Tick marks are defined as *positions* ($\{x \in [0..1]\}$).

For tactile discovery and guidance, it may be desirable to provide feedback on the directionality of a slider, i.e. in which direction the input *value* is increasing or decreasing. A **directionality slider** provides such tactile feedback using continuous output on all taxels, with varied frequencies (Fig. 5.8f). The taxel corresponding to the lowest value is set to subtle (10 Hz), while the taxel corresponding to the highest value is set to strong (150 Hz) output. The remaining taxels are assigned a linearly increasing frequency from subtle to strong. For instance, a linear input slider has taxels with increasing frequency from one end to the other, while a

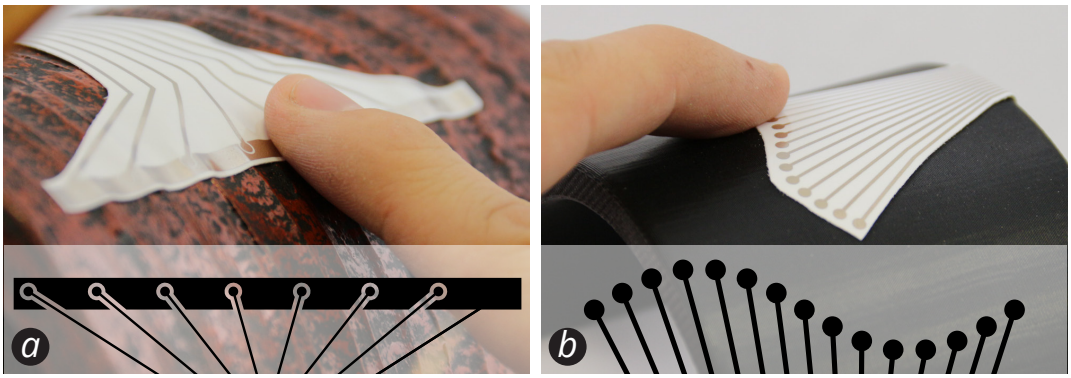

Figure 5.9: Two printed slider Tactlets with (a) lower and (b) higher taxel resolution placed on curved geometries.

slider for audio balance could feature a low frequency in the center and increasing frequency towards both ends of the slider.

5.3 Printing of Tactlets

To physically realize Tactlets, we contribute an approach for printing electro-tactile feedback alongside touch sensing on 3D objects. It comprises a method for automatically generating a low-level printable layout from the high-level design specified in the design tool. Furthermore, we present two fabrication approaches for printing the physical interface: using conductive inkjet printing or 3D printing.

5.3.1 Generating the Printable Layout

Our algorithm for generating a printable layout leverages the fact that a Tactlet is modular and parametric, consisting of a specific arrangement of taxels. Therefore, the basic approach is to map each taxel to one printed electrode (of equal radius). This electrode acts as an anode for electro-tactile stimulation and as one of the electrodes for resistive sensing of touch input. Stimulation and sensing require the user to simultaneously touch another electrode for ground. The algorithm first checks whether there is an electrode of another taxel in close proximity (distance $\leq 4mm$). In this case, this electrode can temporarily act as the ground while the present taxel is stimulated or sensed. We call this principle *mutual ground* (Fig. 5.10a). If no other electrode is neighboring, the tool adds a *dedicated* grounding electrode. This electrode is extended as a ground for multiple isolated taxels (Fig. 5.10b).

For conductive inkjet printing, a 2D-vector layout is generated. Each electrode is generated as a circle of the taxel's radius. The electrode locations are mapped such that they preserve the surface distance between taxels across the 3D mesh. To help the user attaching the printed overlay on the correct location on the 3D object, markers for visual alignment are generated. The resulting layout is exported as a vector graphic for printing.

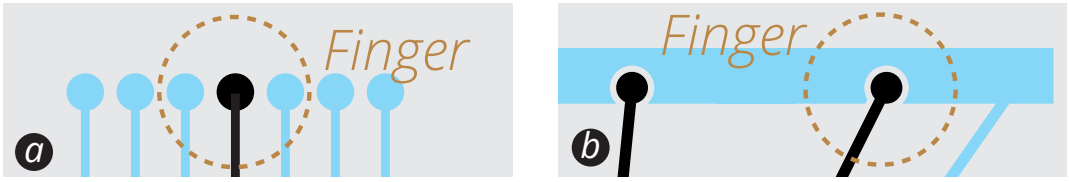

Figure 5.10: Approaches for realizing the low-level electrode layout for a taxel: (a) temporarily using a neighboring electrode as a taxel's ground electrode or (b) generating a dedicated, additional ground electrode.

To generate a printable layout for 3D printing, a 3D model is generated that is partitioned into conductive parts (electrodes, traces) and non-conductive parts (the actual 3D object). Each electrode is generated by calculating the intersection between a sphere at the taxel's center and the taxel's radius with the 3D model. Two 3D-printable STL files are created by subtracting the conductive parts from the model (boolean difference).

In our current implementation, traces to connect the electrodes are routed manually. Future versions could integrate established auto-routing approaches, e.g. as used in [148, 192].

5.3.2 Conductive inkjet printing

The tactile interface can be printed using a commodity inkjet printer (Canon Pixma IP 100) filled with silver-nanoparticle ink (Mitsubishi NBSIJ-MU01) [104]. We use coated paper (Mitsubishi NB-RC-3GR120). Once printed, one or multiple interfaces can be easily attached as an overlay onto a 3D-printed or real-world object using double-sided tape (Tesa universal). This is the preferred method for rapid low-fidelity prototyping, as the interface can be printed, attached, moved or re-printed within minutes. We found the interfaces to be robust to repeated use during prototyping over multiple days.

5.3.3 Conductive 3D printing

For high-fidelity prototyping, interactive objects can be 3D printed with the tactile interface integrated in a single pass. We use a commodity dual-material FDM 3D printer (Ultimaker S5) with off-the-shelf PLA (Ultimaker) for the model and conductive PLA (cPLA, Protopasta conductive filament [164]) for the embedded electrodes (see Fig. 5.4a). We 3D printed multiple prototypes (including those shown in Fig. 5.1c and 5.13c) that were fully functional and successfully tested by the authors. 3D printing allows for a wider range of supported geometries and interfaces that better integrate with real tactile cues. Although cPLA printed structures have low electrical conductivity, the highest resistance we observed in our 3D-printed models (cross section $6mm^2$, length $90mm$), ranges in the 10s of $k\Omega$. This is an order of magnitude less than average skin resistance (100s of $k\Omega$ [245]) and below the maximum supported resistance of our hardware ($320k\Omega$ for 1.25mA/400V). Therefore, cPLA conductivity does not affect the performance of the tactile stimulation. 3D printing is, however, slower than inkjet printing and

requires printing the entire object. To our knowledge, this is the first 3D-printed electro-tactile interface presented in the literature.

5.3.4 Hardware Controller

The implementation of the hardware controller for electro-tactile output is based on the schematic presented in [245]. It comprises a voltage-to-current converter (0-3mA), two output multiplexers (Supertex HV513) with 16 parallel output channels, and a Teensy 3.2 microcontroller, which connects to the design tool via serial port (Bluetooth or USB). Stimulation uses a controlled current with a variable voltage up to 400V. It requires calibration per user. Dynamic changes in contact resistance (e.g. through moisture) are automatically compensated.

We added resistive touch sensing by leveraging the fact that to receive electro-tactile stimuli at a taxel a user must touch at least two electrodes. The controller sends a low probing current to each electrode (82.5μA, 200μs), at an intensity well below the absolute threshold of electro-tactile perception [245]. We measure the voltage between the active electrode and ground (all other electrodes) using the ADC input of Teensy and a voltage divider circuit. Since the pulses are current controlled, touched electrodes result in a lower voltage than non-touched electrodes (i.e. open circuit). A threshold to detect touch is set in the design tool (default: 7.4$V \approx 90k\Omega$). Sensing one electrode takes 2.5 ms, during which actuation for 2ms is interleaved with sensing for 0.5ms. Electrodes are scanned sequentially, resulting in a sensing frame rate of 25Hz for 16 electrodes.

The hardware features two standard FPC connectors (pitch 1mm, 8pins) to connect the printed interfaces. For 3D-printed objects, the 3D-printed wires are connected to copper wires soldered to a FPC breakout board (Adafruit 1325), which is connected to the controller using a standard FPC cable. Inkjet-printed sheets are directly clipped into the FPC connector.

5.4 Validation

To validate the functionality and practical end-to-end feasibility of our proposed method, we conducted a psyhcophysical evaluation and realized two application cases using the Tactlets approach. Each application case comprised the design and implementation of an interactive object and involved several design iterations. We present the results and discuss insights and lessons learned.

5.4.1 Empirical Evaluation of Sensing and Tactile Feedback

While prior work has demonstrated the functionality of printed electrodes for electro-tactile stimulation [102, 245], these were limited to planar geometries or interfaces that wrap around the finger. In pilot experiments, we found that other geometries, e.g. including convex curvature, can pose problems to deliver stimulation and to sense touch. While the soft finger conforms to a certain extent to

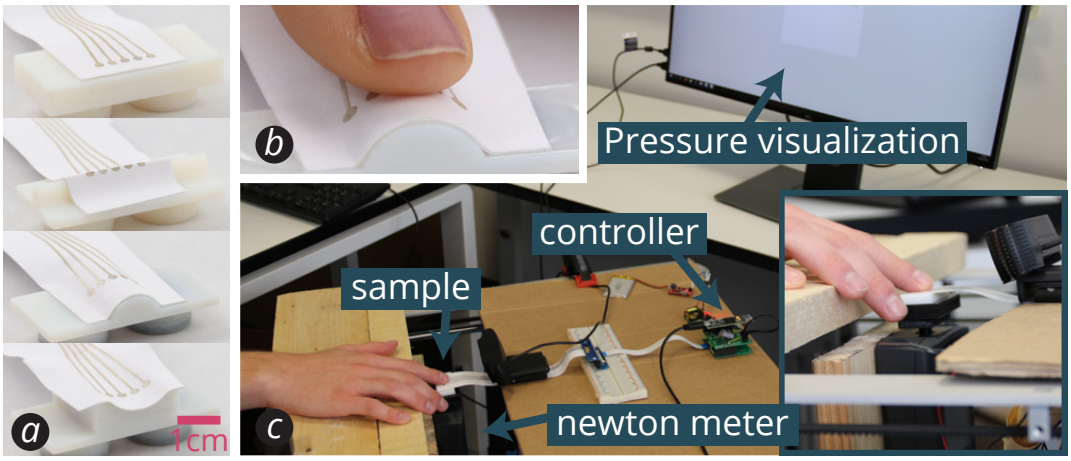

Figure 5.11: Study overview: (a) planar, convex and concave geometries used; (b) finger on convex curved geometry, and (c) study setup.

the geometry, depending on the curvature and inter-electrode spacing, the finger may fail to make contact with two neighboring electrodes, the requirement for electro-tactile stimulation (cf. Fig. 5.11b). To confirm the functionality of our printed interfaces, we thus conducted a psychophysical study with users, which tested the absolute threshold of sensation at taxels on geometries of various curvature and at various finger positions.

Pilot study

In a pilot we identified suitable geometries and a suitable taxel spacing for the experiment. As a baseline reference, we used a *planar* geometry. We then identified challenging yet realistic cases of curved surfaces: a *convex curvature* of 13mm diameter (used as smallest curvature in [179]) and a *concave curvature* of 19mm diameter (index finger width of adult western males [85]). For electrodes aligned orthogonally to an edge, we noticed that it is not possible to touch multiple electrodes simultaneously, even at a small taxel spacing (2mm), unless the angle of the edge is quite large ($> 120°$). Sharp edges with smaller angles are supported, however, if the electrodes are oriented along the edge, e.g. for a slider (Fig. 5.5d). We thus included this condition ($60°$ *edge*) as a realistic sharpest feature to augment with tactile output (see Fig. 5.11a).

We further explored a suitable taxel spacing. We found 3mm center-to-center spacing to be the maximum distance so that people with small fingers could still make contact with two adjacent taxels on convex curved surfaces (see Fig.5.11b).

Method

Our hypothesis was that participants could consistently perceive electro-tactile stimulation on all four geometries (planar, concave, convex, edge) at two points on the finger (centered under finger pad and offset by 3mm), at a light contact force ($0.1–0.7N \approx$ force during tactile exploration).

We recruited 15 participants (5 female, age 22 to 41) from our university campus. We 3D printed the four geometries and attached printed overlays, each with 5 electrodes in a straight line (3mm center-to-center, 2mm radius), shown in Fig. 5.11a. To enable direct comparison to related work, we screen printed the overlays. Our method is based on the classical method of limits [49, 92]. We used a random double-staircase method (to minimize errors of habituation and expectation [33]), with 20 steps per staircase. Staircase steps were presented with frequency 30Hz, carrier pulse 200μs, and intensity steps of 0.1mA, as in prior work [245]. The starting intensity for the descending staircase was calibrated for each taxel by increasing the intensity to a comfortable level. Each step was presented for a maximum of 3 seconds followed by one second of rest. Participants pressed the space bar on a keyboard when they felt a stimulus. Contact force was measured using a digital force gauge and visualized on a computer screen. Participants were asked to keep the force in the target interval ($0.1 - 0.7N$) to avoid an effect of contact force.

We collected data on 4,800 trials (20 points per staircase x 2 staircases x 2 taxels x 4 geometries x 15 subjects). We further recorded voltage values reported by our sensing component for all electrodes and captured a close-up video of the finger placement on the sample to enable later in-depth inspection. Participants were asked to describe their perception and comfort of the stimulation after the experiment.

The data analysis revealed that the 20 staircase steps, which we had identified in a pilot study to be sufficient for convergence of staircases, were not sufficient to reach convergence in a total of 6 cases (5 participants). While in all those cases the participants did perceive the stimulation on both taxels, we could not determine a reliable estimate for the sensation threshold. Therefore, we excluded the data of these 5 participants.

Results

Figure 5.12 plots the absolute thresholds for all four geometries and all participants, averaged for both taxel locations. Thresholds range from $0.15mA$ to $0.73mA$ mA. The highest absolute threshold recorded (P08, convex geometry) is 4.32 standard deviations ($\sigma = 0.52$) below the maximum stimulation intensity of our controller ($3mA$). 14 participants reported pulsating or vibration-like sensations. If stimuli were strong, 8 participants described that they felt needle-like sensations.

To evaluate touch sensing, we calculated the average signal-to-noise ratio (SNR) for all users (across all taxels and all geometry conditions). It amounts to 51.4 ($SD = 22.1$). This indicates our sensing system works well above the expected SNR for a robust touch sensor (e.g. in capacitive sensors robust SNR is 15) [37].

These results confirm the technical feasibility of electro-tactile stimulation on planar, convex, concave and edge geometries and verify the maximum distance between electrodes (3mm) that works robustly for users.

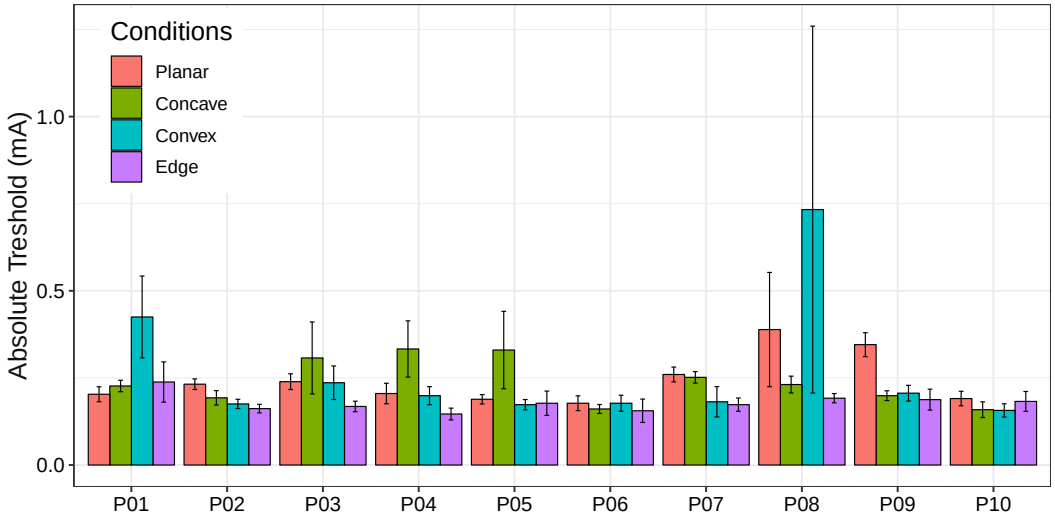

Figure 5.12: Study results: Absolute threshold of the stimulation intensity (mA) for each curvature condition for each subject.

5.4.2 Application case 1: Phone case

Inspired by Haptic Edge Displays [88], we aimed to prototype and explore a similar tactile interface on the edge of a smartphone, while leveraging the benefits of our approach: a slimmer form factor, compatibility with curved geometries, and rapid design iterations.

We downloaded a 3D model of a phone case[3] for a Pixel 3 smartphone and printed it on an Objet Connex3 260 printer. We imported the model into our design tool.

We started our design by exploring a slider on the side of the case, similar to the one presented in [88]. However, we placed it on the curved edge on the back to use this geometry as a tactile guide for eyes-free interaction (see Fig. 5.13a). We implemented a simple application for scrolling through the pages of a PDF displayed on the smartphone and used it to iteratively test various configurations of the slider: A simple input slider allows scrolling through the PDF, while a slider with distinct tick marks indicates different sections in the opened document.

We wondered whether the same interaction would be possible on a shorter slider placed on the strongly curved surface around the top left corner of the case. We designed and fabricated the slider (see Fig. 5.13b and d) and tested the same application. We found the geometry to provide good tactile orientation; however, scrolling the document was more difficult and tick marks were limited to two due to the smaller size. The real-time design mode of the design tool allowed us to quickly test the use of this slider for a different, eyes-free, scenario. We placed the phone in a pocket and manually set different progress values; this confirmed this slider's potential for in-pocket feedback, e.g. a "silent" countdown timer.

3 `https://www.thingiverse.com/thing:3207361`

Figure 5.13: Application case 1: Through several iterations different slider Tactlets are quickly prototyped on a smart phone case. (a) Three tactlets are digitally designed in the design tool. (b) A long slider on a curved edge on the back of the case, (c) a short slider wrapped around the top left curvature, and (d & e) a curved concave slider on the back of smart phone case as (d) inkjet-printed and (e) 3D-printed prototype.

As an additional promising location we tested the smartphone's back. We imagined that a circular slider around the centrally placed fingerprint reader would allow for back-of-device interaction while looking at the screen or while eyes-free. Using Rhino's CAD features, we quickly made a circular indent in the back of the case model to offer tactile guidance for interaction. We then 3D printed the modified model and designed a circular slider matching the indent's shape (Fig. 5.13c). By testing the finished prototype we found it to be suitable for both cases, looking at the screen and eyes-free interaction.

5.4.3 Application case 2: Presenter with tactile feedback

In our second application case, we aimed to explore the design of a new tangible presenter device with tactile feedback (Fig. 5.3). This served as inspiration for the example we have presented earlier in this paper (Fig. 5.3-5.5). We designed a simple 3D model of a presenter shape in Rhino3D. We then 3D printed the model (on an Objet Connex3 260 printer). In our design tool, we designed two buttons and one slider on the front of the device and tested the tactile feedback (Fig. 5.5a).

During exploration, we found that scanning the progress slider with a finger is difficult without looking at it. In a second iteration, we thus moved the slider to the back edge of the model as additional tactile guidance and tried different slider sizes, as illustrated in Fig. 5.5b & c. We then 3D printed the final design with embedded electrodes on an Ultimaker S5 printer (Fig. 5.1c) and implemented an application that interfaces the presenter prototype with Microsoft PowerPoint.

5.4.4 Lessons learned

For iteratively designing and fabricating the application cases, the Tactlet design tool and printing approach have been extensively used over the course of 8 weeks for a total of 15 design iterations. Here we summarize practical insights and limitations learned:

Rapid iterations

We found a key benefit of the approach for practical use is its rapidity. Being able to physically move a printed interface on the object, instead of re-printing a new design, was an important factor for saving time in day-to-day work, as it turned out that many design iterations relate to iteratively finding the best location for a tactile element on the object. To further speed up early explorations of electro-tactile feedback in initial design phases, we frequently simply placed a printed interface on the table rather than attaching it to an object. The Real-time Design Mode helped to rapidly test different behavior or stimulation parameters of a Tactlet without having to implement an interactive application. However, it is not possible yet in the design tool to directly link events to more extensive application logic. Future versions of the tool could create code stubs and connect to an IDE for implementing application logic. A future version should also include auto routing to facilitate the design process.

Our work allows initial insights into the usage of the design tool and the interaction with Tactlet controls. However, to gain a better understanding, a thorough study should investigate the extended usage of the tool, e.g. with novice makers, and the usage of the controls, e.g. for eyes-free discrimination.

Geometry

Inkjet-printed designs, despite printed on paper and attached onto the object, supported a surprisingly large set of geometries, including surfaces of slight double curvature, e.g. a whiteboard marker and a planter with ridges. Four examples are illustrated in Fig. 5.7 and 5.9. For our most challenging case, the indent on the smartphone with pronounced double curvature, we had to cut out the individual electrodes. This made the printed interface compatible with the geometry but introduced a less smooth surface, which affects the tactile feedback during sliding. In contrast, 3D printing allowed realizing a smoother result on this challenging geometry.

Scalability

We successfully inkjet-printed controls as small as a single taxel button (3mm radius, Fig. 5.7a) and as large as a 15-taxel slider spanning an A4 sheet (28cm length). While inkjet printing can realize electrodes with a separation of <0.5mm, for 3D printing realizing high taxel resolution can be difficult. This is related to printing parameters, where one has to ensure that clean boundaries are printed between conductive and non-conductive material (e.g. prevent stringing of the conductive filament). We were able to achieve a minimum separation of 2 mm.

Real-time refinement is limited within the scope of the printed electrode layout. Future work could address this through additional taxels to activate on demand. This would require a solution to facilitate the connection of more electrodes.

Electro-tactile feedback

From our experience it is important to calibrate a comfortable level of intensity. Too weak or too strong intensity can result in barely noticeable or uncomfortable sensation. We therefore opted against using variations of intensity to create different sensations. Instead, we experienced that variations in frequency offer a wide range of sensations (e.g. poking at 1 Hz vs. vibration at 50Hz). In contrast to mechanical feedback, such as vibrotactile actuators, electro-tactile feedback supports very localized stimuli. However, it requires the user to touch two electrodes simultaneously. This poses limits to the spatial design of taxels and controls; e.g. a button that is only partially touched may not be able to provide feedback. Printing mechanical actuators, e.g. electro-active polymers actuators, is actively investigated in material science. In future work, the Tactlets concept, digital design process, and templates could be transferred to such alternative actuation technologies.

Touch sensing

Our resistive sensing scheme works with the same electrodes used for electro-tactile stimulation, does not require additional components in the controller, and offers the SNR required for touch sensing. As commonly used in touch interfaces that offer no hover state, it relies on timing to distinguish between touch input and touch exploration. Confirming a selection during sliding is thus possible via tapping or double tapping. Additional sensing capabilities, e.g. to sense pressure or hovering, may offer a better scheme for distinction. For instance, capacitive touch sensing has been shown to sense pressure [193, 194] and hover states [51] and to work with inkjet-printed electrodes [51, 147] and conductive 3D printing [193, 194]. Our system can be extended to include a multi-stage multiplexing circuit to incorporate capacitive sensing.

5.5 Conclusion

This chapter presented a novel digital design and fabrication approach for tactile input and output on interactive objects. Tactlets enable rapid prototyping of electro-tactile output and touch sensing in a conformal form factor on various 3D-object geometries. The concept builds on a high-level digital design tool and parametric templates of tactile controls, paired with automatic generation of printable layouts. Interactive objects can be rapidly fabricated through conductive inkjet printing or conductive 3D printing. A novel real-time design mode supports hands-on testing and design refinement using the physical prototype. Results from an empirical study with users confirm the technical functionality of sensing and tactile output on various object geometries. In practical application cases, this chapter has demonstrated how this new process enables rapid design iterations and quick exploration of various tactile controls for interactive objects.

This chapter advances the field of rapid prototyping of interactive objects with rich materials. To this end, it addressed the three challenges introduced in the introduction as follows.

To address the challenges of abstracting from complex low-level design, this chapter contributed a high-level design tool and an inventory of parametric Tactlet templates. The templates encapsulate low-level parameters and expose high-level properties. Based on the templates, the tool allows the designer to place Tactlets on a 3D-object model and to customize their properties. The design tool then automatically parameterizes the Tactlet controls accordingly and generates files for fabrication.

In addition, this chapter addresses the challenges of extending the fabrication capabilities for custom interactive objects. To this end, this chapter presents the first digital design and fabrication approach for tactile interfaces on 3D objects. To realize this approach, this chapter demonstrates fabricating electro-tactile interfaces using two accessible approaches based on conductive inkjet printing and conductive 3D printing.

Last, this chapter presented a novel approach addressing the challenges of feedback and manipulation during designing interactive objects with rich materials. It focused on designing tactile input and output for which providing feedback is especially challenging since tactile properties cannot be perceived using traditional visual media. To this end, this chapter demonstrated how to leverage the interactivity of the fabricated object for real-time physical feedback by immediately reflecting changes of the designed tactile output. In addition, the presented approach leverages the object's touch sensing capabilities to allow refining the design in a hands-on fashion directly on the fabricated object.

Together the contributions of this chapter advance the field of rapid prototyping towards enabling use of tactile input and output controls for novel interactive objects, tangible interfaces, and ubiquitous computing devices. This chapter adds tactile input and output as an important modality to the contributions of the previous chapter of stretchable circuits and touch input and display output on 3D objects. However, while chapter 3 investigated prototyping soft and stretchable interfaces as a promising direction for interactive objects with rich materials, the 3D objects in this and the previous chapter have so far been limited to rigid and flexible objects. Thus, the next chapter investigates prototyping custom interactive 3D objects capable of shape and compliance change.

6 Fabricating Objects with Customizability of Shape and Compliance

The previous chapters have contributed solutions for prototyping interactive objects while focusing on different aspects of interactivity and rich materials. Chapter 3 focused on stretchable interfaces, chapter 4 on touch input and display output on complex 3D geometries and diverse materials, and chapter 5 on tactile input and output on 3D objects. These solutions have addressed challenges of the design and fabrication process. They have contributed approaches to enable high-level design abstracting from low-level parameters, to extend the fabrication capabilities for interactive objects, and to enhance the rapid prototyping process.

This chapter[1] presents the final contributions of this thesis that further advance the field of rapid prototyping interactive objects. It focuses on computer-controlled change of physical shape and material properties on 3D objects. Thus, this chapter moves beyond computer-controlled visual and haptic output elements, e.g. as in *ObjectSkin* and *Tactlets*, and towards softness and deformable objects, as explored for two-dimensional interfaces in chapter 3.

As a main contribution, this chapter presents *Hotflex*, a novel approach enabling end-users to customize, personalize, or re-model a 3D object *after* it is printed by using physical interaction. The approach is based on embedding computer-controlled elements inside the object. These are printed in custom geometries and can locally change their material properties, to transition from a solid into a deformable state and back. This enables precisely localized parts of a 3D object to become deformable upon user demand.

To support the high-level design of such objects, this chapter contributes a set of structural primitives and functional patterns (Challenge 1). Four structural primitives describe basic principles of possible customization enabled by the approach. Based on these primitives, this chapter presents a set of ten functional patterns, which represent a parameterized description of concrete customization and serve as building blocks for HotFlex objects. They allow end-users to physically customize an object in a variety of ways, upon demand and at precisely defined locations. This includes deforming the object's shape, altering the object's stiffness, translating or rotating parts of an object, and permanently connecting or disconnecting multiple pieces of an object.

1 This chapter is based on [55]. As the first author, I led the conceptual design, development of the composite structure and fabrication process, design and implementation of the structural primitives and functional patterns, technical evaluation, and development of application prototypes. The research intern Elena Chong Loo helped with fabrication, conducting the technical evaluation, implementing the application prototypes, and creating figures. My supervisor Jürgen Steimle advised me on the conceptual design, primitives and patterns, evaluation, and applications. He further contributed to the structure and writing of the publication.

Figure 6.1: a) 3D-printed object with embedded state-changing elements. The end-user can physically customize the object on-demand after it is fabricated. This enables user-tailored wearables, b) ergonomically personalized devices, and c) new kinds of interactive objects.

As a second contribution, this chapter presents how the approach can be technically realized. *Hotflex* is implemented as a computer-controlled composite structure that is embedded into the 3D object. The composite essentially consists of printed heating elements and surrounding structures which are printed with a material that has a low melting point. When the element is warming up, the surrounding material becomes viscous: the user can deform it. These structures are all printed in custom geometries and work in concert to enable a specific type of shape or compliance change. As this chapter will demonstrate below, this approach can be used to achieve an expansive range of post-print customizations, including very localized on-demand modifications and creation of shapes of high mechanical stability. In addition, it can be easily implemented using conventional printers and off-the-shelf hardware components.

With the *HotFlex* approach, this chapter offers a different perspective on the design and fabrication process (Challenge 3). It advances the idea of Tactlets to leverage the fabricated object's interactivity instead of fabricating new objects to implement design changes. However, instead of coupling the physical object with the digital model, this chapter explores incorporating a certain degree of customizability in the object. This enables a direct physical way of finalizing the object's design and fabrication using the object itself. For example, a designed and fabricated bracelet may incorporate shape customizability to be adapted to fit the user's body (cf. Figure 6.1).

Last, this chapter presents results from technical experiments and application examples that validate the approach. The experiments' results demonstrate the shape-change capabilities of the HotFlex primitives and validate the computer-controlled change of important physical properties, including softness, elasticity, and tensile strength. The results also demonstrate that heating can be used safely and realized even in mobile battery-driven implementations. To validate the practical feasibility of the approach, this chapter presents a variety of application examples that have been realized using Hotflex, including a shape-changing wearable device, interactive packaging, and a mouse that can be ergonomically adjusted to the user's hand shape.

The remainder of this chapter is structured as follows: Section 6.1 presents the HotFlex principle, design and fabrication, and user interaction with HotFlex objects. Section 6.2 then presents the structural primitives and functional patterns. Section 6.3 presents the validation of the HotFlex aproach including results from

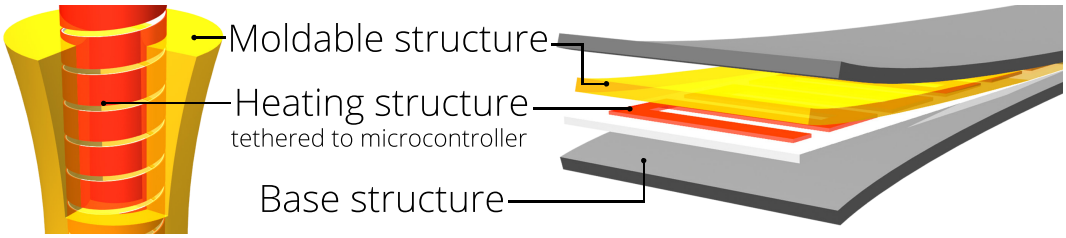

Figure 6.2: The HotFlex printed material composite consists of three structures. They can be realized as volumes (left) or thin layers (right).

technical experiments and example applications. Section 6.4 discusses the approach and its limitations. Last, Section 6.5 provides conclusions based on this chapter's contributions.

6.1 Design and fabrication process

This section introduces the basic principle of HotFlex and presents how it is implemented.

6.1.1 Basic Principle

HotFlex proposes the use of a printed material composite, which consists of three structures (see Fig. 6.2):

1. The *moldable structure* is used in parts that are to be modified after printing. It is made of a material with a low melting point.
2. The *heating structure* is embedded within the 3D-printed object and enables localized, computer controlled heating of the moldable structure. A thermistor is integrated for temperature sensing.
3. The *base structure* is used to realize non-modifiable parts of the 3D-printed object and to optionally encapsulate the moldable and heating structures. It is made of a solid or flexible material that can withstand high temperatures.

When the heating structure applies heat, the moldable material becomes increasingly soft. In this state, the structure can be deformed by applying an external force. This force can be generated by the user deforming the object, by gravity, or by releasing internal strain, for instance using an embedded spring. Once the moldable structure has cooled down, it returns to its solid state and permanently retains its altered shape, without consuming any further energy.

Robust functioning requires precise control of the melting process. To this end, we use a microcontroller for controlling the heating structures, while one or multiple integrated thermistors continuously monitor the temperature of the moldable structure. Heating structures can have a custom size and shape, and multiple structures can be embedded within an object and independently controlled. This

enables precise control of the location that is to be customizable, including its size and shape.

6.1.2 Design

The three structures are combined in functional patterns. Each functional pattern enables a specific type of post-print customization from a broad range of options, such as allowing the object to bend or to change its stiffness. A pattern is defined by the geometry of the material composite, the locations of heating elements, and the temperature to generate. We will present a variety of patterns below.

During design of the 3D object, the designer integrates one or more of these functional patterns into the digital model of the object. For our prototypes, we manually designed the geometry of the base and moldable structures using the CAD software Rhinoceros3D. Heating structures were designed in Adobe Illustrator. Future implementations could support the designer by automatically generating these structures to fit a given 3D model and desired modification possibilities, comparable to [17, 34, 148]. To this end, we have already started to partially abstract from the complexity by creating the patterns as reusable parameterized components in Grasshopper3D.

Of note is that designs that integrate HotFlex functional patterns can be made available in online repositories. This enables end-users who have no skills in digital modeling to simply download a model, print it, and then physically customize it to meet their personal demands.

6.1.3 Fabrication

In order to make the approach accessible to a wide audience, we chose to implement the principle using commonly available consumer-grade tools. We used a standard FDM 3D printer, a low-cost conductive ink-jet printer, and open-source Arduino microcontrollers.

Base and moldable structures

The base structure is made of commonly used 3D printing filaments. In our experiments, we have successfully used ABS, PLA, and TPE (thermoplastic elastomer, e.g., sold as *NinjaFlex*). For the moldable structure, we used PCL (polycaprolactone, e.g. sold as ESUN PCL Filament). PCL has the desirable property of a low melting point of 60 °C. In contrast, the base structure materials have a much higher melting point (PLA: 210 °C; ABS: 150 °C; TPE: 230 °C). We used a Makerbot Replicator 2 and Leapfrog Creatr HS printer to print the base structure and moldable structure and manually assembled the individual parts. We used both printers in parallel to speed up the fabrication of assembled parts. At 60 °C, PCL becomes increasingly soft as it transitions into a viscous liquid. While cooling down, the moldable structure stays deformable until its temperature drops below 45 °C.

Printed heating structure

HotFlex patterns apply heat through embedded printed heating elements. A heating element is a printed resistor, laid out in a serpentine pattern. It makes use of Joule heating, i.e., the resistor releases heat when an electric current passes through it. Heating elements are printed with conductive silver nanoparticle ink (Mitsubishi NBSIJ-FD02) on thin-film sheets (Mitsubishi NB-WF-3GF100) using a Canon Pixma iP100 printer [104, 105]. To allow for precise control of the temperature, a thermistor (TTF3A502F34D3AY) is attached onto the printed substrate next to the heating element with double-sided conductive adhesive tape (3M #9703).

The ink-jet printed heating structures are manually inserted into the 3D object during or after the 3D printing process. During the print process, the print can be paused and the heating structure placed in the object. Once the print continues the structure will be embedded in the object. For integration after printing, the structure can be slid into a cavity left open during printing. Alternatively, it can be attached on the outside of the object or placed between two parts during assembly. In the near future, 3D printers that are capable of printing conductive traces [225] are likely to render manual insertion of heating elements obsolete. The entire object can then be printed in one fully automatic printing pass.

For programmatic control of the heating process, we use an external Arduino microcontroller, which is tethered with the heating elements. It controls each heating element separately in a temperature feedback loop, by measuring the current temperature using the integrated thermistor and heating to the target temperature using a simple hysteresis cycle. The microcontroller measures the thermistor's resistance using a simple voltage divider circuit and calculates the temperature using the Steinhart-Hart equation [203].

The amount of heat released depends on the conductor's mass, its specific heat constant, and the power applied. We determined that a printed trace of 200 mm length and 0.7 mm width (covering a 20 x 10 mm^2 area) requires a current of 145 mA for reaching a temperature of 60 °C within 11 seconds at 9 V DC. A 1 mm thick piece of moldable structure completely melts in less than one minute at 60 °C and in 39 seconds at 80 °C.

For a mobile implementation, the microcontroller and battery can be embedded in or attached directly to the printed object. Since energy is only required while the object is being modified, even a regular battery can last a long time. Our experiments showed that a 9 V battery (5 Wh) contains enough energy for completely melting a moldable structure of 10 x 10 x 2 mm^3 more than 150 consecutive times (at ambient room temperature). Using more powerful mobile energy sources, such as cell phone batteries (up to 12 Wh, e.g. Samsung Galaxy Note 4), the longevity can be extended further.

6.1.4 User Interaction

Once fabricated, the default state of the object is a passive state, in which it is not heated and no energy is required. Upon demand by the user or triggered by the

Figure 6.3: Embedded input and output modalities: a) capacitive touch sensing, b) thermochromic display, and c) thin-film display.

system (the desired behavior is implemented by programming the microcontroller), the object turns into a customizable state: one or more heating elements are activated, allowing the user to physically customize the object.

Despite the relatively high temperature of 60 °C, the end-user can safely touch the moldable material. The same material is commercially used as clay material that allows for free hands-on modeling when it is heated [66]. This is possible because it has a high heat capacity and low thermal conductivity. It thereby differs from other materials, such as water or metal. The temperature on the outside of the object can be further reduced by adding an outer base structure that encapsulates the moldable structure.

To allow the user to control the customization functionality right on the object and to be aware of the element's current state, one or more input and output modalities can be embedded within the composite structure of a HotFlex element:

Embedded touch sensing (Fig. 6.3a) allows the user to manually activate and deactivate a HotFlex element. We implemented capacitive touch sensing by leveraging the element's heating structure itself. Inspired by [51], we use temporal multiplexing: the same printed resistor acts as a capacitive touch electrode for a short sensing interval (80 ms) between longer intervals that are used for heating (300 ms). We implemented capacitive touch sensing using the Capacitive Sensing Library [8]. We observed that heating has an insignificant effect on the accuracy of capacitive

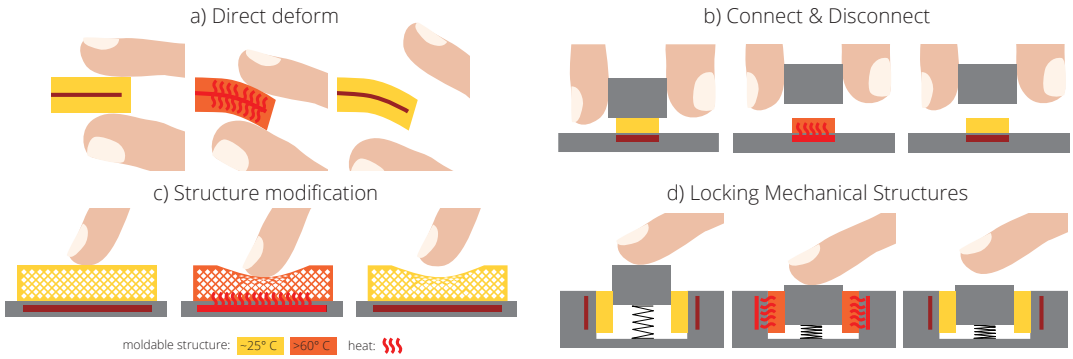

Figure 6.4: Deformation primitives enable four main types of object customization.

sensing, as it decreases the resistance by less than 5%. Once an element is activated, it transitions into the heating phase.

To inform the user about whether a HotFlex element is activated or ready to be deformed, we realized two types of embedded displays:

Embedded thermochromic display (Fig. 6.3b): A simple thermochromic display can be easily realized by leveraging a specific property of the moldable material: as the material gets warmer, it becomes more translucent. To increase the visibility of this effect, we have placed a colored sheet underneath the moldable structure. When cold, the moldable material is opaque and appears white (Fig. 6.3b left). At around 65 °C, it becomes fully transparent; the underlying sheet is clearly visible (right) and informs the user that the element is ready to be deformed. Optionally, a secondary display element can be integrated which provides visual feedback as soon as the element is slightly heated (outer ring in Fig. 6.3b center). We realized this with a thermochromic filament which becomes more transparent even at low temperatures of around 30 °C (Formfutura MagicFil™ Thermo PLA).

Embedded thin-film display (Fig. 6.3c): To realize a display that can be computer-controlled, we have integrated a PrintScreen thin-film display, which actively emits light through the slightly translucent object. The display was screen printed onto the flexible substrate that contains the heating elements, following the method introduced in [149]. The implementation can use blinking patterns, a change in brightness, or dedicated icons to inform the user about the element's current state.

6.2 Primitives and functional patterns

The HotFlex approach enables precisely controlled melting of moldable structures and can be used to implement a broad range of post-print customization. Through analysis of existing forms of object customization (on thingiverse.com) and through structured exploration of the HotFlex design space, we developed four deformation primitives: direct deform, connect/disconnect, structure modification, and locking (Fig. 6.4). These main principles enable a variety of functional patterns, which act as building blocks for customizable 3D objects. Each functional pattern realizes one

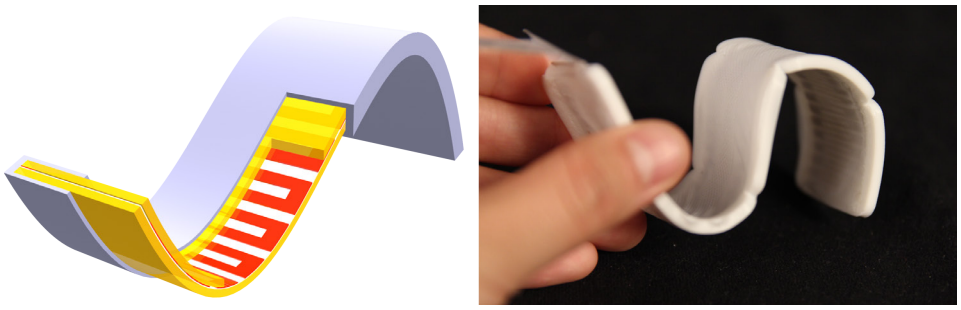

Figure 6.5: Bending: Heating element and moldable structure encapsulated by a thin base structure of flexible material (blue-gray).

specific type of object customization and leverages specific object geometries and heating structures.

6.2.1 Direct Deform

When warmed up, a piece of moldable material becomes like clay. It can be directly deformed by the user using physical interactions (Fig. 6.4a). In contrast to conventional clay, however, HotFlex enables users to make the object only partially deformable, at precisely defined locations, and to do so on-demand. We demonstrate the following functional patterns for free-form bending and folding of objects:

Free-form bending

To create a bendable structure, two structures of moldable material are placed on both sides of a thin film which contains the heating element (Fig. 6.5). The moldable material is stiff at room temperature and bendable when heated. Splitting the moldable structure into two layers has the benefit of faster heating and moreover protects the user from direct contact with the heating element. While it is not necessary to encapsulate the sandwich with an elastic base structure, we recommend doing so, as this presents two advantages: first, the structure is more robust to repeated bending, since the moldable material is kept in shape; and second, it allows for a higher heating temperature, as the user is not directly touching the moldable material.

It is possible to print multiple heating elements into the same structure, each having the same or different dimensions. This allows software to control, during use time, what parts of the structure should be deformable. For instance, we have realized a bracelet (see Fig. 6.15) that contains four separate heating elements. Each element can be warmed up on its own, allowing the bracelet to be deformed at this specific location. If all elements are heated at the same time, the entire band can be bent.

By changing the ratio between the moldable and base structures' thickness, one can achieve different bending effects. For thick moldable (2 mm) and thin base (0.3 mm) layers, the overall structure deforms very easily and retains its deformed shape within seconds. For thinner moldable (1 mm) and thicker base (1 mm) layers,

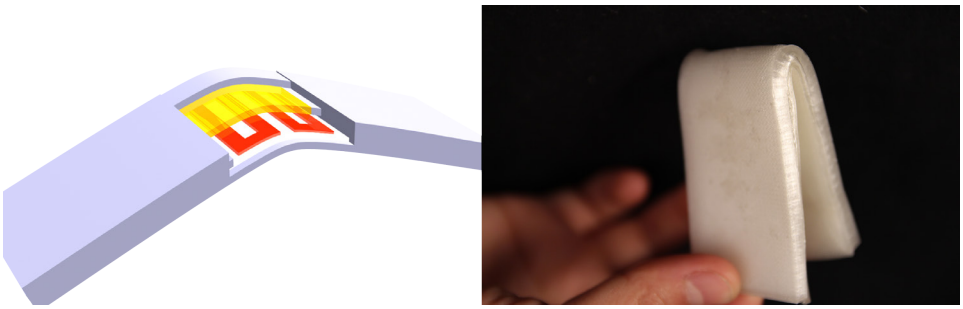

Figure 6.6: Folding.

in contrast, the structure becomes elastic; while heated, it snaps back into its non-deformed shape, unless the user holds or maintains the deformed shape until the moldable material has cooled down. This produces strain in the base structure that can then be released upon reheating the moldable structure, producing a form of actuation.

The ease of deformation can be further controlled in software, by setting a slightly lower or higher temperature, since this directly influences the deformability of the moldable material. We have found the range of 55–70 °C to be most effective.

Placing the heating structure inside the moldable structure limits the set of possible deformations to the deformability of the heating structure. The heating elements are printed onto a sheet of coated paper. Hence, the overall structure is highly bendable, but cannot be stretched or compressed.

Folding

Folding is a specific case of generic bending: folding an object at a precisely predefined location, while the surrounding areas are left undeformed. This behavior is achieved by localizing a heating element precisely along the line where the object is to be foldable (Fig. 6.6).

We have realized a foldable prototype that uses a heating element of 8 mm length across the fold. The overall structure is 5.6 mm thick and can be folded around a radius of 2.5 mm, as illustrated in Figure 6.6.

Free-form 3D deformation

Detailed free-form deformation of an object's surface can be realized by printing the outer surface with moldable material. For thin moldable layers, the underlying heating element is sealed from the moldable structure with a thin layer of base structure. When heated, the surface becomes soft and can be remodeled. We have realized a 3D-printed cat where the facial area can be customized by the end-user (Fig. 6.7).

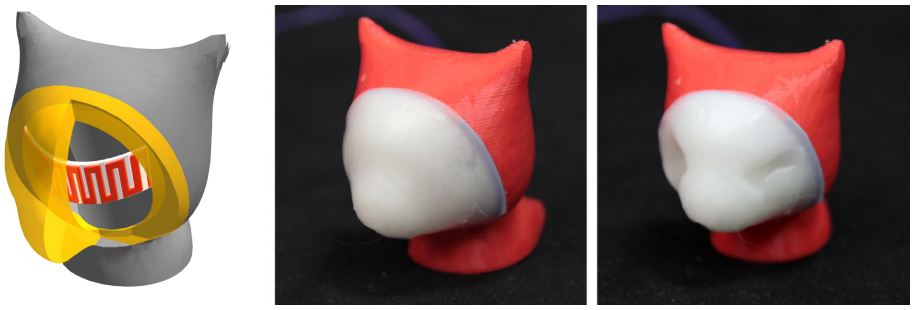

Figure 6.7: Free-form 3D deformation: 3D model, before hands-on modeling, after hands-on modeling.

6.2.2 Connect and Disconnect

HotFlex elements can be laid out so as to realize a firm physical connection between two objects, which can be split on demand. The basic principle consists of using moldable material as sort of glue between two objects. When heat is applied, this connection can be released or reconnected (see Fig. 6.4b). This offers a new way to customize objects through assembly of multiple parts.

Connect

A connector element consists of a heating element that is covered with a moldable structure, which is exposed on the object's surface (Fig. 6.8). When the element is heated, another object can adhere to the moldable structure. It creates a firm connection when the material has cooled down, without requiring further energy. The other object can either be a connector element (in heated or passive state), or a conventional 3D-printed surface made of non-moldable filament.

The connect pattern is especially useful for objects that require a strong mechanical connection. In the validation section below we demonstrate that even a very small connect element can hold a mass of several kilograms. It also offers unique benefits for objects that require a thin connector, as no mechanical interlocking is required.

The strength of the connection depends on the connecting area and the thickness of the moldable structure. In our experiments, we could print the moldable structure as thin as 0.2 mm and still firmly connect two parts. Thicker moldable structures, how-

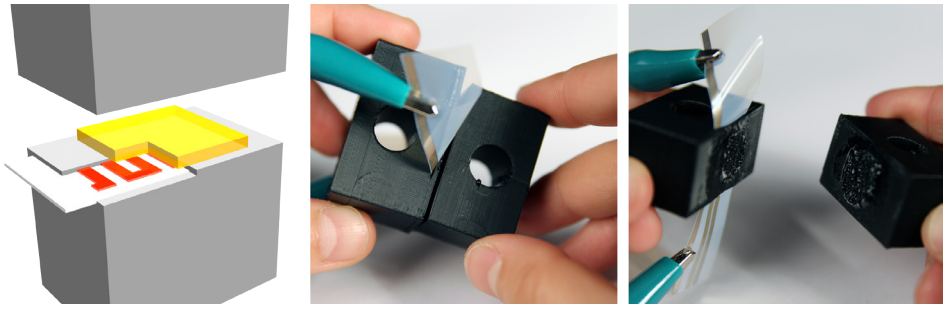

Figure 6.8: Connect and disconnect.

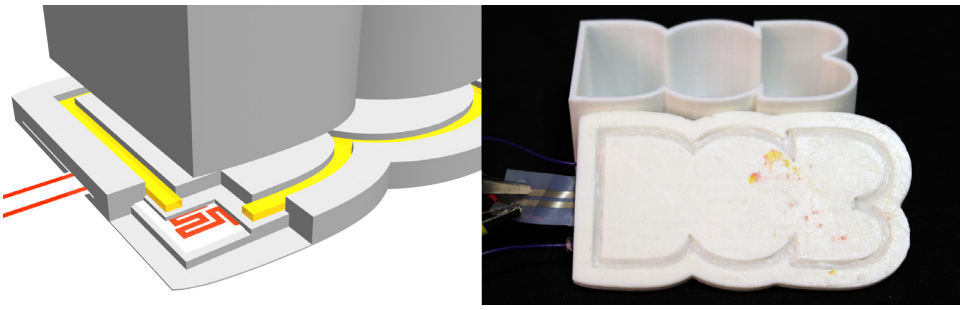

Figure 6.9: Sealing a complex contour: close-up cutaway model and realized prototype.

ever, can compensate for uneven surfaces or non-matching shapes. The maximum thickness of the moldable structure is limited by the heating element's temperature and desired activation time. Thin layers below 2 mm will melt within seconds at 80 °C, while thicker layers and lower temperatures increase the activation time to minutes.

Disconnect

Two connected pieces can be disconnected when heat is applied on the connector element. The two parts can then be separated by the user, by gravity, or by releasing stored strain. Gravity or released strain can be used to realize a form of computer-controlled actuation, for example to provide tangible feedback or notifications.

We recommend using temperatures of not more than 70 °C for disconnecting. At higher temperatures, the moldable structure may form strings between the objects while disconnecting. At lower temperatures we did not experience this issue.

Seal

A variation of the connect pattern can be used for sealing an object. For instance, sealing can prevent an object's lid from being opened; it can also be used to make an object watertight. We have realized a 3D-printed box which features a lid that can be sealed (see Fig. 6.15b). To allow for watertight sealing, we laid out a continuous sealing element, which is a serpentine pattern (1 mm trace width) that follows the lid all around along its contour (see Fig. 6.9). The trace consists of a heating element covered with moldable material. Since the entire composite structure is digitally designed and fully printed, highly customized shapes can be sealed, for example a curved outline as illustrated in our box application.

6.2.3 Structure Modification

HotFlex can also be used for permanently altering the physical properties of the 3D-printed object, by changing its internal structure. To this end, the moldable structure is not laid out as a solid layer of material, but in a detailed 3D geometry. When heat is applied, this moldable structure can deform in a specific way that is defined by the geometry (see Fig. 6.4c).

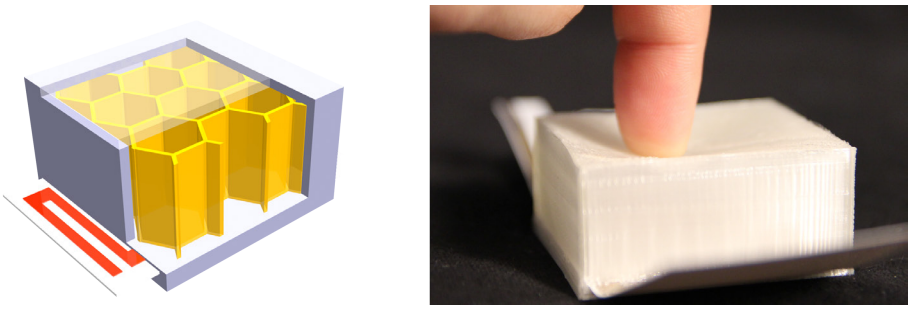

Figure 6.10: Increasing material softness: Cutaway model of initial state and image after heating.

Fine geometric structures are widely used in 3D printing, for instance to realize different surface textures.

Increasing material softness

As an example of structure modification, we have realized a functional pattern that can change an object's stiffness. It transforms an initially stiff object, upon demand, into a softer one. This adds to prior work which has contributed specific 3D-printed geometries to realize (non-changeable) haptic properties [211, 196].

The pattern consists of a heating element that underlies a moldable 3D geometry, all tightly encapsulated in an elastic base structure. The moldable geometry is made of a repetitive structural pattern (e.g., a honeycomb or diagonal pattern) that has an infill percentage of less than 100% (see Fig. 6.10). In its initial state, the overall structure is stiff because the moldable geometry cannot be deformed. When heat is applied from the bottom, the moldable structure starts to melt, causing it to sink towards the bottom. This creates empty space between the moldable structure and the elastic top layer. The elastic top layer can be pushed further into the structure, causing it to be softer.

The desired stiffness change can be fine-tuned by varying the infill percentage of the moldable structure. Conceptually, there exists a one-to-one mapping between the infill percentage and the fraction of empty space that will be generated in the upper part of the moldable structure, e.g., a 40% infill allows the structure to reduce its height by 40%. In practice there may remain some small enclosures of air within the melted structure; therefore, we recommend to use a slightly lower infill percentage.

This functional pattern can be applied not only to soften planar surfaces. The moldable structure and outer base structure can be realized in pretty much any geometry, provided that a heating structure can be integrated so as to heat the desired area. We demonstrate this by integrating stiffness change into a non-developable surface of a 3D object, the mouse application presented below (see Fig. 6.15c).

The temperature of the heating element should be at least 65 °C. At lower temperatures, the moldable structure may become soft but not liquid enough to sink.

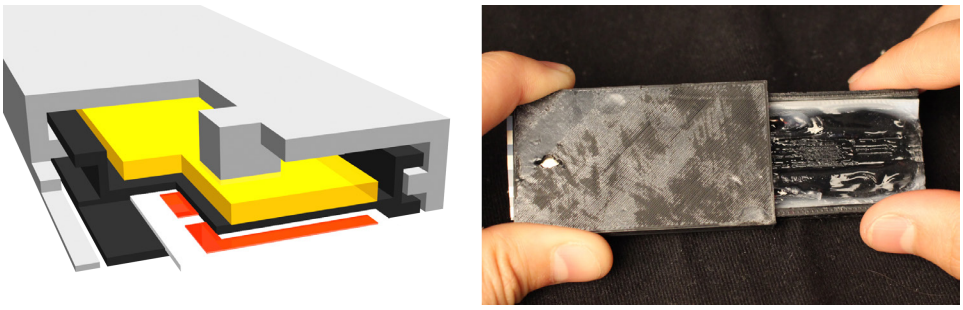

Figure 6.11: Translation: The pin on the top part (gray) locks to the moldable layer on the bottom part (black).

Once the moldable structure has deformed, it cannot transform back to its initial 3D structure. Hence, the softening process is not reversible. However, the pattern can be activated multiple times for further softening.

6.2.4 Locking Mechanical Structures

Combining the HotFlex principle with commonly used mechanical structures, such as sliding mechanisms, joints, and hinges, allows their function to be locked and unlocked on demand. Figure 6.4d illustrates this primitive: the button (light gray) is locked in place by the moldable structure (orange). Once the heating element warms up the moldable structure, the connection is loosened and the button can be depressed. Once the moldable structure cools down, the button is held in place again.

One-dimensional translation

Translation is implemented using the locking primitive on a mechanical sliding mechanism (see Fig. 6.11). Two rails, left and right, enable the top part to slide on the bottom part. A layer of moldable material is laid out on the bottom part, with a heating element placed underneath. When cold, this moldable structure holds the top part in place through a contact pin that is affixed on the top part and extends into the moldable structure. Once the moldable structure warms up, the upper part can be translated along the rails.

This pattern generalizes to all sliding mechanisms that can incorporate a moldable locking structure and heating structure. This includes curved trajectories and non-developable geometries, as long as the heating structure can follow a corresponding developable approximation (i.e. it can be flattened onto a plane without distortion). It therefore enables a broad range of customization, including changing an object in size.

Similar to the connect pattern, the locking strength depends on the contact surface between contact pin, moldable structure, and bottom part. In our technical experiments, detailed below, we have found that the pattern generates high locking strength (>100 N force), while the object can be easily translated in the activated state.

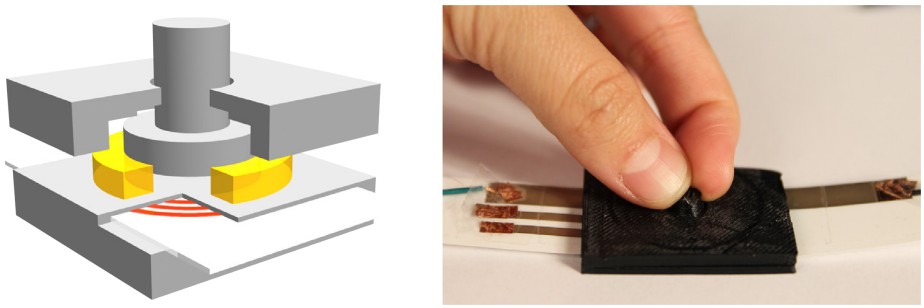

Figure 6.12: Rotation around one axis.

Rotation around one axis

A similar locking pattern can be applied to other mechanical structures. We have realized a pattern for rotating an object part around one axis using a 3D-printed joint, e.g. to pose the limbs of a figurine. It is made of a simple rotating disk, which can be locked and unlocked on demand by surrounding moldable material and an embedded heating structure, as illustrated in Figure 6.12.

Rotation around more than one axis

Rotation around multiple axes can be implemented using a ball joint structure (see Fig. 6.13). Placing moldable substrate between the bearing stud and the socket can lock the ball joint. For both rotation mechanisms the surface area of moldable material in-between both moving parts determines the physical strength of the connection. We realized a ball joint of 16 mm radius with 5 mm radius handles and a locking moldable structure of 20 x 10 x 1 mm^3.

6.3 Validation

To validate the HotFlex approach and to assess its practical feasibility, we conducted six technical experiments and realized three application examples.

6.3.1 Technical experiments

We empirically investigated the core mechanical properties of each of the four HotFlex primitives. Moreover, we investigated effects of repeatability and timing.

Direct deform

To characterize direct deformation behavior, we tested the change in elasticity produced by the bending pattern. We tested prototype samples of the same dimensions as our bracelet prototype: 2.7 mm thick strip, with 1.6 mm moldable layer and 0.9 mm elastic Ninjaflex enclosing structure. We measured Young's modulus at room temperature and when the moldable structure was heated to 80 °C. To this end we affixed the strip on both ends, applied a mass of 2.5 kg at the center, and measured the resulting displacement in both conditions.

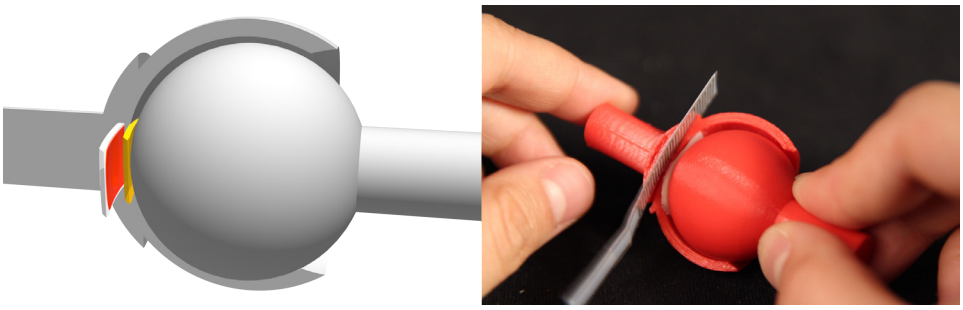

Figure 6.13: Rotation around three axis: implemented using a ball joint.

We identified a modulus of 0.21 GPa at room temperature and 0.12 GPa when heated, resulting in a considerable change of factor 1.7.

Structure modification

To test the stiffness change generated by the soften pattern, we measured the change of the force that is required for pressing into an object. We used a sample consisting of a 20 mm thick moldable structure (with a diagonal infill of 20%) and a Ninjaflex enclosure of 2 mm thickness. Our mechanical apparatus pushed a flat tip of 10 mm radius vertically into the sample and used a pressure sensor to measure the normal force required for the displacement. We measured the required force for a constant 2 mm displacement in the sample's initial state and after heating (2 mm was the maximum displacement possible in the initial state).

Initially, 67.6 N were required to press 2 mm into the structure. This was reduced to 41.1 N after heating the sample for 120 seconds at 80 °C – a reduction by 39%. The required force can even be significantly further reduced, but this requires heating for an extended period: after heating an additional 10 minutes, the force decreased to 23.3 N.

Locking

To determine the strength of mechanical locking, we tested an implementation of a sliding element (translation pattern). The sample measured 60 x 30 x 7.5 mm; the locking contact surface between both movable parts of the object was 60 mm².

We affixed the bottom part, which holds the heating element, and moved the upper part to its maximally extended position. We measured the force that is required for moving the element, both in the locked (room temperature) state and when heated to 80 °C for 45 seconds.

In the locked state, we measured it to withstand more than 100 N without moving even slightly (at which point we did not increase the force further). In the unlocked state, a force of 2.5 N, i.e. 40 times smaller, was sufficient to move the upper part.

Connect & Disconnect

We determined the mechanical characteristics of connect/disconnect with a sample consisting of two parts: one part implemented the connect pattern on a 10 x 10 mm²

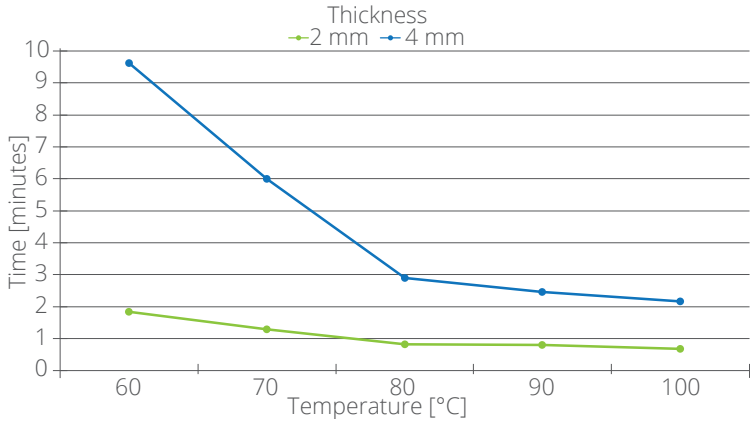

Figure 6.14: Heating time until the entire sample is fully deformable.

area with a 1 mm thick moldable structure. The other part featured a passive surface of the same size. We affixed the active part to the ceiling, with the connect surface facing down, and connected the passive part to its underside. We then successively added weight to the lower part.

The connection was capable of holding 8 kg (78 N) and broke when we applied a mass of 8.5 kg. When heated to 80 °C for 60 seconds, a force of 1 N was sufficient to separate the two parts, 1.25% of the required force in the non-heated state.

Repeatability

Repeatability of HotFlex interactions essentially depends on the ability of the moldable structure to retain its initial structure after repeated heating/cooling cycles and after being subject to external mechanical forces. For many patterns, repeatability is fostered by encapsulating the moldable material. The most critical case is the connect/disconnect pattern because it does not contain any encapsulation. This puts the highest demands on the moldable structure. We tested this pattern to identify a conservative estimate of repeatability of the functional patterns.

We heated up the connection between two pieces, successively disconnected and connected them 10 times, and let the connection cool down. To ensure the pieces were correctly connected, we applied a mass of 5 kg for 20 s. We repeated this process 5 times, resulting in a total of 50 reconnections. Since we could not notice any degradation of performance in the sample, we stopped after these iterations. As a final test, we applied 5 kg of mass over a period of 24 hours, still resulting in a stable mechanical connection.

Melting time

We explored how temperature and geometry influence the required time for heating a piece of PCL, which is a property related to all primitives. To this end, we heated samples of 10 x 10 mm, 100% infill, and 2 mm and 4 mm thickness to the point where they were fully transparent, which indicates full deformability. We repeated the experiment for temperatures of 60, 70, 80, 90, and 100 °C. While full deformability is

generally not required to enable modification, the onset of deformability is difficult to measure and full transparency therefore serves as a conservative estimate.

Figure 6.14 shows that the required time depends on the heating temperature and on the thickness of the structure. While a thin structure can be fully melted in less than one minute, time increases with thickness of the sample and reduced heating temperature. The results further show that the highest reduction in heating time can be achieved when increasing the temperature from 70 to 80 °C. This indicates that 80 °C is a good trade-off between low temperature and fast heating. Note that the temperatures here apply to the temperature of the heating element – the temperature at the outside of the object is much lower.

In practice, typical activation times of a HotFlex element are considerably shorter than the times reported here. We have tested here for full deformability of the entire moldable structure. However, in typical cases this full deformability is not required for shape change. Our rough estimate is that in most cases the element is deformable after only 20–30% of the times identified here.

6.3.2 Application 1: Shape-changeable interactive bracelet

As our first application case, we have designed and printed a shape-changeable bracelet. It provides the user with ambient notifications through an embedded LED (Fig. 6.15a). This prototype demonstrates how easily a user can physically customize HotFlex objects, e.g. adapt the shape to fit the user's wrist or transform it into other useful shapes upon demand, illustrated by the phone holder with ambient output (Fig. 6.15b). To this end, the bracelet contains two heating elements, which can be heated independently, implementing the bending pattern. It further shows how HotFlex can be implemented in a thin (2.7 mm) form factor including output elements and embedded touch sensing, allowing the user to control the customization functionality and accept notifications.

6.3.3 Application 2: Interactive sealable treasure box

A custom treasure box was printed in the shape of the user's name (Fig. 6.15b). The lid has the sealing pattern embedded, allowing it to be sealed to the box (watertight). The box can be unlocked using a secret tapping pattern. This application illustrates how HotFlex expands the possibilities of makers to create highly customized interactive objects. To this end, a custom-shaped sealing element follows the box's outline with moldable material integrated in the lid's groove. An embedded capacitive touch sensor is used for capturing the tapping pattern and triggering the heating elements on correct entry. Printed on the same substrate, a TFEL display provides feedback on tapping and when the box is unlocking.

6.3.4 Application 3: Ergonomically customizable mouse

A 3D-printed mouse case (Fig. 6.1b) implements the soften pattern. It features a thumb rest, which can be ergonomically adapted by the end-user to fit her hand,

Figure 6.15: Application examples. a) An interactive shape-changeable bracelet. b) Interactive sealable treasure box with embedded TFEL display. c) Ergonomically customizable mouse: cutaway rendering and prototype after customization (cover removed to reveal deformation).

allowing for a better grip and more comfortable use. The mouse case is realized in PLA with a thumb supporting structure of moldable material covered by a thin layer of elastic Ninjaflex. The moldable structure allows the user to freely personalize the softness at any location on the thumb rest. The cutaway rendering in Figure 6.15c illustrates the embedded heating structures underneath the moldable structure. The image on the right shows the deformed moldable structure (flexible cover removed) after customization. The case is designed to fit on an existing electronics board of an optical mouse (Speedlink Fiori).

6.4 Discussion and limitations

Scalability

The HotFlex approach, its primitives, and patterns scale for fabrication of small and medium-sized objects. Objects can be as thin as 1.25 mm (2 x 0.5 mm moldable; 0.25 mm heating and thermistor) and very small (trace width of heating element is 0.5 mm). Scalability to large sizes is limited by two factors: the maximum thickness of a moldable structure and maximum size of the heating structure. We have realized 20 mm thick moldable structures; these became slightly deformable after 2 minutes but needed more than 20 minutes to become fully deformable. The maximum size of a heating structure depends mainly on the energy source. A 9 V battery can power a 30 cm long and 0.5 mm wide heating trace at 0.15 A. Considering a maximum safe voltage of 60 V [243], a more performant energy supply can power traces up to 160 cm length. Using multiple elements in parallel reduces the voltage and increases the required current.

The maximum number of separately controllable heating elements is limited by the microcontroller. Our implementation using an Arduino uno can control 6 individual elements without multiplexing.

Energy consumption

Energy consumption scales with the heating element's size. We showed that elements up to 20 x 15 mm can be powered using a 9 V battery for more than 3 hours. Larger elements can be powered for shorter durations or using higher capacity batteries. There seems to be room for future implementations to significantly reduce energy consumption. First, other resistive materials, such as nichrome, are more efficient in heating. Second, the geometries of the moldable and heating structures of our prototypes have not been optimized with respect to energy consumption. Future implementations can optimize these geometries using physical simulation of heat localization and spreading.

Responsiveness

We showed that the time needed for heating is reasonable for small to medium-sized applications; for instance, the bracelet fully heats up in less than one minute. To improve responsiveness for larger applications, simulation and optimization of the heating process should be employed. The time may also be reduced by incorporating 3D-printed heating structures directly within the moldable structure.

Safety

Electric shock is prevented by implementing safety extra-low voltage (SELV) circuits with a maximum of 60 V DC [243]. These circuits are usually powered by batteries or power supplies that ensure user safety. Besides these precautions, the heating element should always be isolated (e.g. using a spray or tape isolator).

The moldable structure and base structure, insulating the heating element, are designed to ensure a safe surface temperature below 65 °C. For example in our bracelet, two thin layers of 0.9 mm moldable and 0.4 mm flexible material, reduce a 60 °C warm heating element to a maximum surface temperature of 48 °C. Higher temperatures are used in some of our prototypes to speed up the melting process. In this case, the surface temperature is reduced by increasing the layers' thickness or by reducing the heating time. For the bracelet example, the 0.9 mm moldable structure melts in 39 seconds at 80 °C, while the surface temperature does not reach 65 °C within 2 minutes.

Materials & Printing

The HotFlex approach generalizes to other combinations of materials, which may have higher or lower melting points. This opens up the possibility to explore other temperature ranges, melting behaviors, and material properties. In our implementation, the combination of PCL with ABS, PLA, and TPE worked well. Notably, PLA has a low softening temperature of around 60 °C, which might cause parts to deform while heating. We prevented this issue by avoiding placement of thin and fragile parts made of PLA close to the heating structure. Another possibility is to use formulations of PLA that can withstand higher temperatures, such as HTPLA [163].

The different melting points cause printing problems on current 3D multi-material printers. Since PCL has a very low melting point, it melts when the printer prints other materials onto it. For this reason, we used single-material printing and manually assembled the parts. It is very likely that future multi-material printers can solve this issue by employing better cooling techniques or by adapting the print path to avoid heating of already printed PCL parts.

6.5 Conclusion

This chapter contributed a new approach to post-print customization of 3D-printed objects. It comprises embedding localized and computer-controlled structures that can change their deformation characteristics when heat is applied through embedded heating elements. This chapter introduced the approach and presented a set of functional patterns that act as building blocks for realizing desired customization options in a 3D object. Results from technical experiments and from practical application examples demonstrated the practical feasibility and showed that the approach can be implemented using commodity hardware and supplies.

This chapter advances the field of rapid prototyping of interactive objects with rich materials regarding three aspects:

First, The approach supports designers in creating designs with embedded customizability by abstracting from low-level properties of the composite structure. To this end, HotFlex provides structural primitives and functional patterns as guidance

for creating HotFlex objects. These primitives and patterns enable designers to embed a range of customizability of shape and compliance in interactive objects.

Second, this chapter extends the possible capabilities of fabricated interactive objects. It enables fabricating objects with the embedded ability of shape or compliance change. This chapter demonstrates how to leverage these capabilities for post-print customization of 3D printed objects. However, the generic ability of embedded shape or compliance change offers a general potential to be explored for interactive objects with rich materials.

Last, HotFlex enables interactive objects that can be adapted on-demand by the user in a computer-controlled way. This enables the user to customize the object to their needs using direct physical manipulation and real-time hands-on feedback. This chapter thus demonstrates a possible direction to improve the rapid prototyping process. Designers can incorporate a certain degree of customizability in the object design. The design thus needs to be less precise and can leave finalizing the design to the end user, who can adapt the object with little skills.

Together these contributions advance the field of prototyping interactive objects with rich materials beyond the contributions of the previous chapters. They add embedded shape change and compliance change to the possible capabilities of digitally fabricated interactive objects and demonstrate their use for a new digital fabrication approach for interactive objects with rich materials.

7 Conclusions

The goal of this thesis was to advance the fields of digital fabrication, rapid prototyping, and ubiquitous computing towards leveraging rich materials for interactive objects. To this end, this thesis presented novel design and fabrication approaches for interactive objects with rich materials.

The presented contributions address important challenges to enable easy, accessible, and versatile design and fabrication of custom interactive objects with extended support for custom geometries and materials and advanced input and output capabilities. They enable the high-level digital design of interactive objects with rich materials through computational models and parametric patterns. In addition, the contributions of this thesis propose novel approaches to enhance the rapid prototyping process through increasing the fabrication speed and leveraging the interactivity of the fabricated object. Together, the four major contributions address three major challenges while each contribution focuses on different aspects of interactivity and rich object properties, covering key points in a design space.

This last chapter concludes this thesis by summarizing the main contributions, revisiting the three challenges introduced in the introduction, and providing an outlook on directions and challenges for future work.

7.1 Summary

With *LASEC*, this thesis presented a novel approach enabling high-level digital design and rapid fabrication of interfaces with custom circuitry and custom stretchability (Chapter 3). To realize LASEC, this thesis contributed a novel approach for interfaces with multiple areas of custom stretchability, a digital design tool for high-level design, and a novel approach for instant fabrication of stretchable circuits. Together, these contributions facilitate and speed-up the design and fabrication of interfaces with custom circuitry and custom stretchability. This enhances the design and fabrication process compared to prior work that relied on manual fabrication steps. It also extends the capabilities of the process compared to traditional fabrication of custom 3D objects. In addition to rapid fabrication of custom geometry, it enables designers to rapidly design and fabricate stretchable prototypes. This allows for quick access to hands-on feedback on the designed material properties throughout the iterative design process.

Beyond 2D surfaces, *ObjectSkin* enables digitally fabricating interactive 3D objects of strongly double-curved geometries and diverse materials (Chapter 4). To this end, this thesis contributed a versatile approach to augment existing 3D objects with interactivity through fabricating conformal thin-film overlays. These thin overlays

add touch input and display output to strongly curved geometries of an object while largely preserving its visuo-haptic properties. This enables a designer to leverage the geometry and surface properties of everyday objects for interaction. It further allows the designer to explore an object's geometry and properties before augmenting it with interaction, knowing that they will remain largely unchanged.

In addition to visual output as an interaction modality for 3D objects, this thesis contributed a novel approach for conformal haptic interfaces. Chapter 5 presented a novel digital design and fabrication approach for tactile input and output on interactive objects. *Tactlets* enable rapid prototyping of electro-tactile output and touch sensing in a conformal form factor on various 3D-object geometries. The concept builds on a high-level digital design tool and parametric templates of tactile controls, paired with automatic generation of printable layouts. This thesis presented the concept, details on the tool and templates, and how the generated haptic interfaces can be rapidly fabricated through conductive inkjet printing or conductive 3D printing. In addition, this thesis presented the benefits of a novel real-time design mode offered by the *Tactlets* design tool. Instead of fabricating a new prototype to implement design changes, this mode enables real-time exploration and hands-on refinement of the design using the fabricated interactive prototype.

Beyond computer-controlled visual and haptic output elements, *HotFlex* enables interactive objects capable of changing their physical shape and material properties (Chapter 6). To realize *HotFlex*, this thesis contributed a new approach for post-print customization of 3D-printed objects. It consists of embedding localized and computer-controlled structures that can change their deformation characteristics when heat is applied through embedded heating elements. This thesis introduced the approach and presented a set of high-level primitives and concrete functional patterns that act as building blocks for realizing desired customization options in a 3D object. The *HotFlex* approach enables interactive objects that are customizable after their initial design and fabrication. This enables users without special skills, prior knowledge, or access to fabrication equipment, to adapt an object to their needs within a pre-defined degree of customizability. Instead of designing the final object in an iterative cycle of design and fabrication, the design process thus incorporates a novel element of embedding parts of the design and fabrication process in the interactive object itself.

Together, the contributions of this thesis address three major challenges for the design and fabrication of interactive objects with rich materials, as introduced in the introduction (illustrated in Figure 7.1).

High-level Design

The contributions of this thesis add novel solutions for high-level design of interactive objects with rich materials. They abstract from low-level design parameters by offering parameterized components and by automatically generating low-level details. *LASEC* (Chapter 3) offers parameterized patterns for stretchability and a high-level control to adapt stretchability of multiple seamlessly connected regions. It further allows to specify a circuit at a high level and generates the corresponding

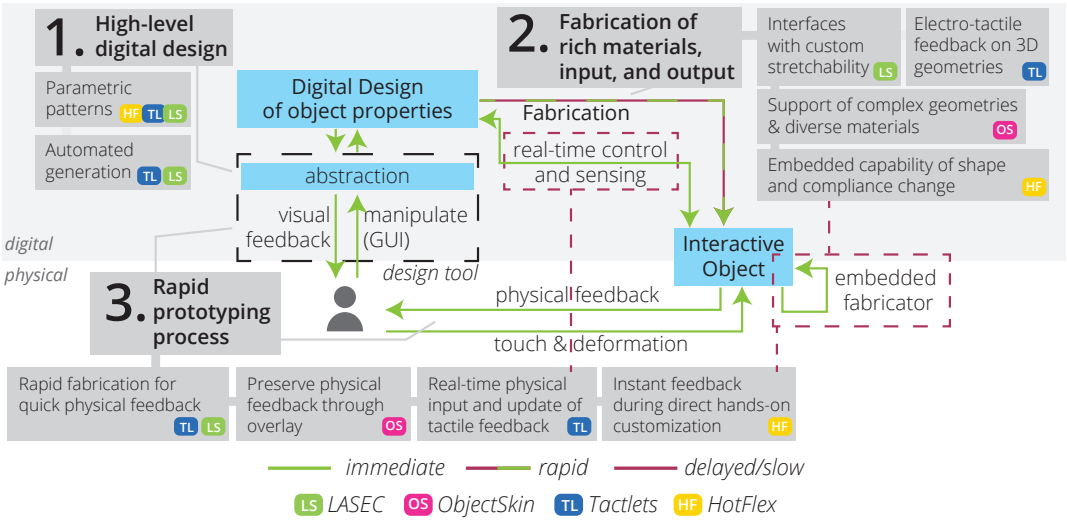

Figure 7.1: A summary of the contributions of this thesis in respect to the three major challenges of the design and fabrication process for interactive objects with rich materials.

low-level details, including necessary circuit traces and cut and ablation patterns. *Tactlets* (Chapter 5) contributes a library of parameterized controls for tactile input and output. The presented digital design tool automatically generates a concrete control based on a parameterized template and a selected geometry. It also abstracts from low-level input and output behavior to provide high-level properties for controls. *HotFlex* (Chapter 6) provides high-level primitives and a set of parametric functional patterns. Each primitive captures an abstract description of one possible shape or compliance change in a 3D object. The parametric functional patterns implement one specific shape or compliance change serving as building blocks for *HotFlex* objects.

These approaches demonstrate high-level design of objects at the intersection of custom geometry, custom interactivity and custom rich materials. As a result they enable design of prior unsupported interactive elements, e.g. high-resolution tactile feedback (Chapter 5), or support for extended custom rich material properties, e.g. multiple areas of custom stretchability (Chapter 3). By combining abstraction for interactivity and rich materials in one solution (Chapter 3), this thesis points towards a promising direction of holistic high-level design approaches for interactive objects with rich materials.

Fabrication Support of Rich Materials and Interactivity

The contributions of this thesis further address the fabrication challenge of extending fabrication capabilities towards supporting interactive object with rich materials. Chapter 3 presents *LASEC*, the first technique for instant do-it-yourself fabrication of circuits with custom stretchability on a conventional laser cutter and in a single pass. It enables instant fabrication of stretchable interfaces with multiple seamless areas of custom stretchability. *ObjectSkin* (Chapter 4) contributes a novel approach

using conformal thin-film overlays for touch input and display output on objects of complex geometries and diverse materials. *Tactlets* (Chapter 5) enables conformal tactile interfaces on 3D geometries through two fabrication techniques. *HotFlex* (Chapter 6) contributes a novel approach to digitally fabricate 3D objects with embedded computer-controlled capabilities of on-demand shape and compliance change.

Together, these contributions push the boundaries of accessible fabrication approaches towards realizing interactive objects with rich materials. To this end, this thesis provides insight into two aspects: First, it demonstrates how novel fabrication approaches can leverage common equipment to extend the range of fabrication capabilities. In particular, this thesis demonstrates the use of subtractive fabrication, using a common laser cutter, for custom circuitry and custom material properties in a single process step (Chapter 3). It further demonstrates how to extend established printing methods to new supported geometries, e.g. using water transfer printing of functional inks (Chapter 4). As a second aspect, this thesis demonstrates the versatility of existing fabrication techniques by extending their use to novel principles and applications. For instance, Chapters 5 and 6 leverage conductive inkjet printing to realize novel approaches: tactile interfaces on 3D geometries and custom-shaped heating elements embedded in 3D-printed materials to enable on-demand phase change. Chapter 5 further extends the use of an existing technology by presenting the first approach to realize electro-tactile interfaces on 3D geometries via conductive multi-material 3D-printing. Last, this thesis demonstrates the advantages and disadvantages of two contrasting approaches: fabricating interactivity and materials from scratch (Chapter 3, 5, & 6) or augmenting existing objects of rich materials with fabricated interactive elements (Chapter 4).

Rapid Prototyping Process for Interactive Objects with Rich Materials

The contributions of this thesis enable new approaches to enhance the design and fabrication process of interactive objects with rich materials. As one major aspect, they leverage physical elements for feedback and manipulation during the digital design process. *LASEC* (Chapter 3) enables instant fabrication of stretchable circuits for rapid physical feedback on the designed stretchability. *ObjectSkin* (Chapter 4) allows to explore the surface properties and geometry of an existing object in a hands-on fashion before augmenting it. *Tactlets* (Chapter 5) offers a real-time design mode that leverages the fabricated object's interactivity through live updates of the designed tactile output and touch sensing. *HotFlex* (Chapter 6) incorporates parts of the design and fabrication process in the object itself, enabling hands-on manipulation and immediate feedback on shape and compliance changes.

These approaches show promising directions towards enhancing the design and fabrication process of interactive objects with rich materials. First, they demonstrate the potential of leveraging the interactive capabilities of fabricated prototypes to incorporate physical elements in the digital design process of interactive objects. This thesis demonstrated two approaches for this concept. One approach is to sync the designed property of the digital design with the physical interactive object in real time. The second approach is to create a coarse initial design and to embed

capabilities of customization in the interactive object. Design details and fabrication can then be finalized in a direct hands-on fashion using the object itself. Second, the approaches demonstrates that novel fabrication techniques allow exploring the transfer of existing approaches to the design of interactive objects with rich materials, e.g. speeding up fabrication to produce physical objects for hands-on feedback.

In summary, the contributions of this advance the fields of digital fabrication, rapid prototyping, and ubiquitous computing. They present novel approaches and extend the capabilities of digital design and fabrication of interactive objects with rich materials.

7.2 Directions for Future Work

During the work of this thesis, we focused on addressing three major challenges of the digital design and fabrication of interactive objects with rich materials. At the same time, we identified unaddressed problems and directions for future research. This last section of this thesis gives an overview of these problems and directions for future research.

New materials and capabilities

The approaches in this thesis focused on accessible fabrication techniques. This includes using materials that are available off-the-shelf and equipment that is accessible to a wide audience. We see great potential in novel materials and fabrication approaches that are currently being researched in other disciplines, e.g. material science. However, these need to be made accessible to non-experts outside of material labs to leverage their potential benefits for rapid prototyping.

Creating novel materials optimized for rapid fabrication may offer improved material properties. For example, a compound material optimized for cutting and ablation could allow for increased stretchability or conductivity of stretchable circuits using the *LASEC* approach. Developing stretchable conductive materials for 3D-printing could allow leveraging the *HotFlex* approach for embedding customization capabilities into stretchable objects.

Novel fabrication approaches could speed-up the fabrication process and make it more accessible. Ink-jet printing, for example, has been used in material science to print a wide range of functional materials, realizing super capacitors [29], e-textiles [100], or microelectronic devices [107]. Ink-jet printing is fast, e.g. compared to screen-printing, and has been widely adopted by consumers. It thus may speed up and facilitate additive fabrication approaches relying on other printing techniques, e.g. creating displays on 3D objects via screen-printing (Chapter 4). In addition, it bares the potential to easily integrate additive fabrication into other processes. For example, additive printing of conductive and dielectric material could be combined with subtractive laser cutting to extend the *LASEC* approach to stretchable multi-layer circuits. To this end, an inkjet head could be integrated inside a laser cutter to

apply additional layers if necessary. First steps towards making inkjet-printing with extended capabilities based on material science accessible to the HCI community have been presented in recent work [108]. Khan *et al.* [108] demonstrated how to print a variety of inks, including conductors and dielectric inks, on a range of substrates using a consumer ink-jet printer, e.g. to print soft circuits.

From rapid prototyping towards custom consumer products

This thesis focused on novel approaches to enable rapid prototyping of interactive objects with rich materials. The goal is primarily to enable researchers to explore the use of interactivity and rich materials on objects for novel interaction. Enabling consumers to create and customize interactive ubiquitous objects, however, presents further challenges.

In contrast to research prototypes, consumer products require increased robustness and reliability. This includes aspects such as safety and robustness to wear but also fault tolerance regarding interaction. While a research prototype may be usable despite minor errors or inaccuracies in input sensing or output, the same behavior may lead to a frustrating user experience of a consumer product. Similarly, a lack of robustness of the design and fabrication process may cause issues, for example, waste of time and material due to failed fabrication. To transition from rapid prototyping to consumer grade solutions, future research thus needs to address the challenges of robustness of the design and fabrication process and the resulting interactive objects.

A second aspect for future research towards custom consumer products is the accessibility of materials and devices. The approaches in this thesis focus on prototyping using off-the-shelf materials and accessible equipment. However, for consumers a better integration into an end-to-end process may be required. For example, most functional materials, e.g. conductors, used in this thesis come in a form factor designed for industry or lab use. The ink is sold in bulk and shipped in larger containers. This means that acquiring small amounts is difficult and that the ink needs to be handled in a lab setting, e.g. refilled into cartridges or prepared for screen-printing. This stands in contrast to typical materials for consumer devices, e.g. cartridges for ink-jet printers or spools of filament for FDM 3D printers. Addressing these challenges requires engineering effort to offer end-to-end solutions but also research to optimize processes for consumers based on user-centered design.

Integration of approaches

The approaches presented in this thesis have focused on individual rich material properties and interaction modalities. Creating approaches that integrate different properties and modalities presents additional challenges and opportunities for future work.

Extending rapid fabrication of stretchable interactive objects from 2D to 3D is a remaining challenge for future work. Integrating LASEC with other approaches

presents opportunities towards addressing this challenge. Leveraging stretchable 2D interfaces as object overlays, for example, could enable stretchable 3D objects with touch input, visual output, or tactile output. Prior work has already demonstrated how to optimize cut patterns for 2D sheets to approximate a target 3D geometry [113]. Also, integrating the *LASEC* and *HotFlex* approaches, could enable stretchable 3D objects with capabilities of shape and compliance change through embedded stretchable heating elements.

This thesis has presented tactile feedback controls with integrated touch sensing as promising modality to interact with 3D objects. Integrating this approach with conformal *ObjectSkin* overlays, offers the opportunity to include visual output as an additional modality and to leverage the underlying surface structure of existing objects in conjunction with tactile feedback. Integrating the *Tactlets* approach with *HotFlex* objects, on the other hand, enables exploration of tactile feedback to enhance hands-on customization of shape and compliance.

Generalization of high-level design

This thesis presented several approaches for high-level design. These abstract from low-level design parameters and expert knowledge to facilitate the design for novice users.

One challenge for future work is to provide solutions that provide benefits for a broad range of users. This includes novice users but also expert users. In this context, future work may investigate how novice and expert designers use and appropriate the proposed technology and tools. One question, for example, is how the degree of abstraction affects designers of different skill level. A second question is how abstraction and generating low-level parts of the design affects the designers' process and capabilities. This is especially important considering that expert designers may rely on fine tuning parameters, debugging problems, or artistic freedom.

Sustainability

This thesis has presented different approaches for rapid prototyping. One general challenge of rapid iterative prototyping is sustainability. New iterations typically produce new prototypes, often rendering the old prototypes obsolete. The contributions of this thesis have pointed towards directions to improve sustainability. Using existing objects, as supported by *ObjectSkin* and *Tactlets*, may help to reduce the amount of wasted material. Leveraging the fabricated object's interactivity, as in *Tactlets* and *HotFlex*, may allow to reduce the number of required fabricated prototypes, as design changes can be reflected in the existing prototype. Approaches like *LASEC*, on the other hand, rely on rapid iterative fabrication and thus require additional solutions to improve sustainability. One direction could be to modify previous prototypes if possible, e.g. by further cutting or ablation, or to investigate materials that can be recycled or are biodegradable.

Self-contained objects

Interactive objects are largely self-contained. Yet, integrating all required parts into an object is a remaining open challenge. This thesis has presented different fabrication approaches, e.g. embedding functional elements in the object (Chapter 3, 5, & 6) or attaching overlays on an object's surface (Chapter 4, & 5). For embedding components inside objects, achieving stretchability and softness are major challenges. Current rigid components require parts of the object to be rigid, e.g. as rigid islands (cf. Chapter 3). For overlays, rigid objects also present challenges when using rigid components. This is partially due to the bulky form-factor of current electronic components that do not integrate with the object surface. For non-developable geometries, it is also due to stretchability issues. As the overlay need to conform to the geometry, it needs to stretch, which causes problems with rigid components. Thus, realizing fully self-contained interactive objects with rich materials requires novel solutions for soft and stretchable components, e.g. batteries based on research in material science [47, 116], to be incorporated into the design and fabrication process.

This thesis has presented several contributions towards the digital design and fabrication of interactive objects with rich materials. We envisions that these contributions will enable HCI researchers, interaction designers, and makers to explore rich materials for rapid prototyping of novel interactive objects, tangible interfaces, and ubiquitous computing devices.

Creating novel interactive objects that leverage rich materials may allow to change the way people interact with digital information. It promises to make better use of the human rich sensory feedback and manipulation capabilities for interaction while further merging the digital world of computing with the physical world of things. We envision that this will have a profound impact on society by making interaction more efficient, more intuitive, and more enjoyable.

List of Figures

List of Tables

Bibliography

[1] 3D Matter. *FDM 3D Printing materials compared*. URL: https://www.3dhubs.com/knowledge-base/fdm-3d-printing-materials-compared (visited on 09/04/2019).

[2] Jacob J. Adams, Eric B. Duoss, Thomas F. Malkowski, Michael J. Motala, Bok Yeop Ahn, Ralph G. Nuzzo, Jennifer T. Bernhard, and Jennifer A. Lewis. "Conformal Printing of Electrically Small Antennas on Three-Dimensional Surfaces." In: *Advanced Materials* 23.11 (2011), pp. 1335–1340. ISSN: 1521-4095. DOI: 10.1002/adma.201003734. URL: http://dx.doi.org/10.1002/adma.201003734.

[3] Lea Albaugh, Scott Hudson, and Lining Yao. "Digital Fabrication of Soft Actuated Objects by Machine Knitting." In: *Proceedings of the 2019 CHI Conference on Human Factors in Computing Systems*. CHI '19. Glasgow, Scotland Uk: ACM, 2019, 184:1–184:13. ISBN: 978-1-4503-5970-2. DOI: 10.1145/3290605.3300414. URL: http://doi.acm.org/10.1145/3290605.3300414.

[4] Byoungkwon An et al. "Thermorph: Democratizing 4D Printing of Self-Folding Materials and Interfaces." In: *Proceedings of the 2018 CHI Conference on Human Factors in Computing Systems*. CHI '18. Montreal QC, Canada: ACM, 2018, 260:1–260:12. ISBN: 978-1-4503-5620-6. DOI: 10.1145/3173574.3173834. URL: http://doi.acm.org/10.1145/3173574.3173834.

[5] Apple Inc. *SwiftUI | Apple Developer Documentation*. URL: https://developer.apple.com/documentation/swiftui (visited on 09/10/2019).

[6] Autodesk Inc. *Inventor | Mechanical Design And 3D CAD Software | Autodesk*. URL: https://www.autodesk.com/products/inventor/overview (visited on 08/03/2019).

[7] Moritz Bächer, Benjamin Hepp, Fabrizio Pece, Paul G. Kry, Bernd Bickel, Bernhard Thomaszewski, and Otmar Hilliges. "DefSense: Computational Design of Customized Deformable Input Devices." In: *Proceedings of the 2016 CHI Conference on Human Factors in Computing Systems*. CHI '16. Santa Clara, California, USA: ACM, 2016, pp. 3806–3816. ISBN: 978-1-4503-3362-7. DOI: 10.1145/2858036.2858354. URL: http://doi.acm.org/10.1145/2858036.2858354.

[8] Paul Badger. *Capacitive Sensing Library*. URL: http://playground.arduino.cc/Main/CapacitiveSensor (visited on 09/20/2015).

[9] D. A. Bahamon, Zenan Qi, Harold S. Park, Vitor M. Pereira, and David K. Campbell. "Graphene kirigami as a platform for stretchable and tunable quantum dot arrays." In: *Phys. Rev. B* 93 (23 June 2016), p. 235408. DOI: 10.1103/PhysRevB.93.235408. URL: https://link.aps.org/doi/10.1103/PhysRevB.93.235408.

[10] Rafael Ballagas, Sarthak Ghosh, and James Landay. "The Design Space of 3D Printable Interactivity." In: *Proc. ACM Interact. Mob. Wearable Ubiquitous Technol.* 2.2 (July 2018), 61:1–61:21. ISSN: 2474-9567. DOI: 10.1145/3214264. URL: http://doi.acm.org/10.1145/3214264.

[11] D. Bandyopadhyay, R. Raskar, and H. Fuchs. "Dynamic shader lamps : painting on movable objects." In: *Proceedings IEEE and ACM International Symposium on Augmented Reality*. Oct. 2001, pp. 207–216. DOI: 10.1109/ISAR.2001.970539.

[12] Olivier Bau and Ivan Poupyrev. "REVEL: Tactile Feedback Technology for Augmented Reality." In: *ACM Trans. Graph.* 31.4 (July 2012), 89:1–89:11. ISSN: 0730-0301. DOI: 10.1145/2185520.2185585. URL: http://doi.acm.org/10.1145/2185520.2185585.

[13] Patrick Baudisch, Arthur Silber, Yannis Kommana, Milan Gruner, Ludwig Wall, Kevin Reuss, Lukas Heilman, Robert Kovacs, Daniel Rechlitz, and Thijs Roumen. "Kyub: A 3D Editor for Modeling Sturdy Laser-Cut Objects." In: *Proceedings of the 2019 CHI Conference on Human Factors in Computing Systems*. CHI '19. Glasgow, Scotland Uk: ACM, 2019, 566:1–566:12. ISBN: 978-1-4503-5970-2. DOI: 10.1145/3290605.3300796. URL: http://doi.acm.org/10.1145/3290605.3300796.

[14] Frederik Bedrich. *2019 Best Desktop CNC Routers & DIY CNC Router Kits*. June 2019. URL: https://all3dp.com/1/best-diy-cnc-router-kit/ (visited on 09/03/2019).

[15] J. M. Bern, G. Kumagai, and S. Coros. "Fabrication, modeling, and control of plush robots." In: *2017 IEEE/RSJ International Conference on Intelligent Robots and Systems (IROS)*. Sept. 2017, pp. 3739–3746. DOI: 10.1109/IROS.2017.8206223.

[16] Dustin Beyer, Serafima Gurevich, Stefanie Mueller, Hsiang-Ting Chen, and Patrick Baudisch. "Platener: Low-Fidelity Fabrication of 3D Objects by Substituting 3D Print with Laser-Cut Plates." In: *Proceedings of the 33rd Annual ACM Conference on Human Factors in Computing Systems*. CHI '15. Seoul, Republic of Korea: ACM, 2015, pp. 1799–1806. ISBN: 978-1-4503-3145-6. DOI: 10.1145/2702123.2702225. URL: http://doi.acm.org/10.1145/2702123.2702225.

[17] Bernd Bickel, Moritz Bächer, Miguel A. Otaduy, Hyunho Richard Lee, Hanspeter Pfister, Markus Gross, and Wojciech Matusik. "Design and Fabrication of Materials with Desired Deformation Behavior." In: *ACM SIGGRAPH 2010 Papers*. SIGGRAPH '10. Los Angeles, California: ACM, 2010, 63:1–63:10. ISBN: 978-1-4503-0210-4. DOI: 10.1145/1833349.1778800. URL: http://doi.acm.org/10.1145/1833349.1778800.

[18] Stephen Brewster and Lorna M. Brown. "Tactons: Structured Tactile Messages for Non-visual Information Display." In: *Proceedings of the Fifth Conference on Australasian User Interface - Volume 28*. AUIC '04. Dunedin, New Zealand: Australian Computer Society, Inc., 2004, pp. 15–23. URL: http://dl.acm.org/citation.cfm?id=976310.976313.

[19] Eric Brockmeyer, Ivan Poupyrev, and Scott Hudson. "PAPILLON: Designing Curved Display Surfaces with Printed Optics." In: *Proceedings of the 26th Annual ACM Symposium on User Interface Software and Technology*. UIST '13. St. Andrews, Scotland, United Kingdom: ACM, 2013, pp. 457–462. ISBN: 978-1-4503-2268-3. DOI: 10.1145/2501988.2502027. URL: http://doi.acm.org/10.1145/2501988.2502027.

[20] Paul Bucci, Xi Laura Cang, Anasazi Valair, David Marino, Lucia Tseng, Merel Jung, Jussi Rantala, Oliver S. Schneider, and Karon E. MacLean. "Sketching CuddleBits: Coupled Prototyping of Body and Behaviour for an Affective Robot Pet." In: *Proceedings of the 2017 CHI Conference on Human Factors in Computing Systems*. CHI '17. Denver, Colorado, USA: ACM, 2017, pp. 3681–3692. ISBN: 978-1-4503-4655-9. DOI: 10.1145/3025453.3025774. URL: http://doi.acm.org/10.1145/3025453.3025774.

[21] Jesse Burstyn, Nicholas Fellion, Paul Strohmeier, and Roel Vertegaal. "PrintPut: Resistive and Capacitive Input Widgets for Interactive 3D Prints." English. In: *Human-Computer Interaction – INTERACT 2015*. Ed. by Julio Abascal, Simone Barbosa, Mirko Fetter, Tom Gross, Philippe Palanque, and Marco Winckler. Vol. 9296. Lecture Notes in Computer Science. Springer International Publishing, 2015, pp. 332–339. ISBN: 978-3-319-22700-9. DOI: 10.1007/978-3-319-22701-6_25. URL: http://dx.doi.org/10.1007/978-3-319-22701-6_25.

[22] Terry C Shyu, Pablo Damasceno, Paul M Dodd, Aaron Lamoureux, Lizhi Xu, Matthew Shlian, Max Shtein, Sharon C Glotzer, and Nicholas Kotov. "A kirigami approach to engineering elasticity in nanocomposites through patterned defects." In: *Nature materials* 14 (June 2015).

[23] Varun Perumal C and Daniel Wigdor. "Printem: Instant Printed Circuit Boards with Standard Office Printers & Inks." In: *Proceedings of the 28th Annual ACM Symposium on User Interface Software & Technology*. UIST '15. Charlotte, NC, USA: ACM, 2015, pp. 243–251. ISBN: 978-1-4503-3779-3. DOI: 10.1145/2807442.2807511. URL: http://doi.acm.org/10.1145/2807442.2807511.

[24] Varun Perumal C and Daniel Wigdor. "Foldem: Heterogeneous Object Fabrication via Selective Ablation of Multi-Material Sheets." In: *Proceedings of the 2016 CHI Conference on Human Factors in Computing Systems*. CHI '16. San Jose, California, USA: ACM, 2016, pp. 5765–5775. ISBN: 978-1-4503-3362-7. DOI: 10.1145/2858036.2858135. URL: http://doi.acm.org/10.1145/2858036.2858135.

[25] Carbon, Inc. *Silicone (SIL) 3D Printer Material - Carbon*. URL: https://www.carbon3d.com/materials/silicone/ (visited on 09/04/2019).

[26] D. Cebon and M.F. Ashby. "Engineering Materials Informatics." In: *MRS Bulletin* 31.12 (2006), pp. 1004–1012. DOI: 10.1557/mrs2006.229.

[27] Xiang "Anthony" Chen, Stelian Coros, Jennifer Mankoff, and Scott E. Hudson. "Encore: 3D Printed Augmentation of Everyday Objects with Printed-Over, Affixed and Interlocked Attachments." In: *Proceedings of the 28th Annual ACM Symposium on User Interface Software & Technology*. UIST '15. Daegu,

Kyungpook, Republic of Korea: ACM, 2015, pp. 73–82. ISBN: 978-1-4503-3779-3. DOI: 10.1145/2807442.2807498. URL: http://doi.acm.org/10.1145/2807442.2807498.

[28] Xiang "Anthony" Chen, Ye Tao, Guanyun Wang, Runchang Kang, Tovi Grossman, Stelian Coros, and Scott E. Hudson. "Forte: User-Driven Generative Design." In: *Proceedings of the 2018 CHI Conference on Human Factors in Computing Systems*. CHI '18. Montreal QC, Canada: ACM, 2018, 496:1–496:12. ISBN: 978-1-4503-5620-6. DOI: 10.1145/3173574.3174070. URL: http://doi.acm.org/10.1145/3173574.3174070.

[29] Keun-Ho Choi, JongTae Yoo, Chang Kee Lee, and Sang-Young Lee. "All-inkjet-printed, solid-state flexible supercapacitors on paper." In: *Energy Environ. Sci.* 9 (9 2016), pp. 2812–2821. DOI: 10.1039/C6EE00966B. URL: http://dx.doi.org/10.1039/C6EE00966B.

[30] C.K. Chua, K.F. Leong, and C.S. Lim. *Rapid Prototyping: Principles and Applications*. Rapid Prototyping: Principles and Applications v. 1. World Scientific, 2003. ISBN: 9789812381170. URL: https://books.google.de/books?id=hpNT01xw4EEC.

[31] Marcelo Coelho and Pattie Maes. "Shutters: A Permeable Surface for Environmental Control and Communication." In: *Proceedings of the 3rd International Conference on Tangible and Embedded Interaction*. TEI '09. Cambridge, United Kingdom: ACM, 2009, pp. 13–18. ISBN: 978-1-60558-493-5. DOI: 10.1145/1517664.1517671. URL: http://doi.acm.org/10.1145/1517664.1517671.

[32] Barrett Comiskey, J. D. Albert, Hidekazu Yoshizawa, and Joseph Jacobson. "An electrophoretic ink for all-printed reflective electronic displays." In: *Nature* 394.6690 (July 1998), pp. 253–255. ISSN: 1476-4687. URL: https://doi.org/10.1038/28349.

[33] Tom N. Cornsweet. "The Staircase-Method in Psychophysics." In: *The American Journal of Psychology* 75.3 (Sept. 1962), p. 485. ISSN: 00029556. DOI: 10.2307/1419876. URL: http://www.jstor.org/stable/1419876?origin=crossref%20https://www.jstor.org/stable/1419876?origin=crossref.

[34] Stelian Coros, Bernhard Thomaszewski, Gioacchino Noris, Shinjiro Sueda, Moira Forberg, Robert W. Sumner, Wojciech Matusik, and Bernd Bickel. "Computational Design of Mechanical Characters." In: *ACM Trans. Graph.* 32.4 (July 2013), 83:1–83:12. ISSN: 0730-0301. DOI: 10.1145/2461912.2461953. URL: http://doi.acm.org/10.1145/2461912.2461953.

[35] Christian Corsten, Ignacio Avellino, Max Möllers, and Jan Borchers. "Instant User Interfaces: Repurposing Everyday Objects As Input Devices." In: *Proceedings of the 2013 ACM International Conference on Interactive Tabletops and Surfaces*. ITS '13. St. Andrews, Scotland, United Kingdom: ACM, 2013, pp. 71–80. ISBN: 978-1-4503-2271-3. DOI: 10.1145/2512349.2512799. URL: http://doi.acm.org/10.1145/2512349.2512799.

[36] Andries van Dam. "Post-WIMP User Interfaces." In: *Commun. ACM* 40.2 (Feb. 1997), pp. 63–67. ISSN: 0001-0782. DOI: 10.1145/253671.253708. URL: http://doi.acm.org/10.1145/253671.253708.

[37] Burke Davison. "Techniques for robust touch sensing design." In: *AN1334 Microchip Technology Inc* (2010), p. 53.

[38] Artem Dementyev, Hsin-Liu (Cindy) Kao, and Joseph A. Paradiso. "SensorTape: Modular and Programmable 3D-Aware Dense Sensor Network on a Tape." In: *Proceedings of the 28th Annual ACM Symposium on User Interface Software & Technology*. UIST '15. Charlotte, NC, USA: ACM, 2015, pp. 649–658. ISBN: 978-1-4503-3779-3. DOI: 10.1145/2807442.2807507. URL: http://doi.acm.org/10.1145/2807442.2807507.

[39] Artem Dementyev and Joseph A. Paradiso. "WristFlex: Low-power Gesture Input with Wrist-worn Pressure Sensors." In: *Proceedings of the 27th Annual ACM Symposium on User Interface Software and Technology*. UIST '14. Honolulu, Hawaii, USA: ACM, 2014, pp. 161–166. ISBN: 978-1-4503-3069-5. DOI: 10.1145/2642918.2647396. URL: http://doi.acm.org/10.1145/2642918.2647396.

[40] Ruta Desai, James McCann, and Stelian Coros. "Assembly-aware Design of Printable Electromechanical Devices." In: *Proceedings of the 31st Annual ACM Symposium on User Interface Software and Technology*. UIST '18. Berlin, Germany: ACM, 2018, pp. 457–472. ISBN: 978-1-4503-5948-1. DOI: 10.1145/3242587.3242655. URL: http://doi.acm.org/10.1145/3242587.3242655.

[41] Christine Dierk, Molly Jane Pearce Nicholas, and Eric Paulos. "AlterWear: Battery-Free Wearable Displays for Opportunistic Interactions." In: *Proceedings of the 2018 CHI Conference on Human Factors in Computing Systems*. CHI '18. Montreal QC, Canada: ACM, 2018, 220:1–220:11. ISBN: 978-1-4503-5620-6. DOI: 10.1145/3173574.3173794. URL: http://doi.acm.org/10.1145/3173574.3173794.

[42] Paul Dietz and Darren Leigh. "DiamondTouch: A Multi-user Touch Technology." In: *Proceedings of the 14th Annual ACM Symposium on User Interface Software and Technology*. UIST '01. Orlando, Florida: ACM, 2001, pp. 219–226. ISBN: 1-58113-438-X. DOI: 10.1145/502348.502389. URL: http://doi.acm.org/10.1145/502348.502389.

[43] Doug Englebart. "The Augmented Knowledge Workshop." In: *Proceedings of the ACM Conference on The History of Personal Workstations*. HPW '86. Palo Alto, California, USA: ACM, 1986, pp. 73–83. ISBN: 0-89791-176-8. DOI: 10.1145/12178.12184. URL: http://doi.acm.org/10.1145/12178.12184.

[44] Fenner Inc. *NinjaTek | NinjaFlex*. URL: https://ninjatek.com/ninjaflex/ (visited on 09/09/2019).

[45] Sean Follmer, Daniel Leithinger, Alex Olwal, Nadia Cheng, and Hiroshi Ishii. "Jamming User Interfaces: Programmable Particle Stiffness and Sensing for Malleable and Shape-changing Devices." In: *Proceedings of the 25th Annual ACM Symposium on User Interface Software and Technology*. UIST '12. Cambridge, Massachusetts, USA: ACM, 2012, pp. 519–528. ISBN: 978-1-4503-1580-7. DOI: 10.1145/2380116.2380181. URL: http://doi.acm.org/10.1145/2380116.2380181.

[46] Sean Follmer, Daniel Leithinger, Alex Olwal, Akimitsu Hogge, and Hiroshi Ishii. "inFORM: Dynamic Physical Affordances and Constraints Through Shape and Object Actuation." In: *Proceedings of the 26th Annual ACM Symposium on User Interface Software and Technology*. UIST '13. St. Andrews, Scotland, United Kingdom: ACM, 2013, pp. 417–426. ISBN: 978-1-4503-2268-3. DOI: 10.1145/2501988.2502032. URL: http://doi.acm.org/10.1145/2501988.2502032.

[47] Abhinav M. Gaikwad, Alla M. Zamarayeva, Jamesley Rousseau, Howie Chu, Irving Derin, and Daniel A Steingart. "Highly Stretchable Alkaline Batteries Based on an Embedded Conductive Fabric." In: *Advanced Materials* 24.37 (2012), pp. 5071–5076. DOI: 10.1002/adma.201201329. eprint: https://onlinelibrary.wiley.com/doi/pdf/10.1002/adma.201201329. URL: https://onlinelibrary.wiley.com/doi/abs/10.1002/adma.201201329.

[48] Neil Gershenfeld. "How to make almost anything: The digital fabrication revolution." In: *Foreign Aff.* 91 (2012), p. 43.

[49] George A Gescheider. *Psychophysics: The Fundamentals*. Vol. 435. 1997, p. 435. ISBN: 080582281X. URL: http://www.google.dk/books?hl=da%7B%5C&%7Dlr=%7B%5C&%7Did=gATPDTj8QoYC%7B%5C&%7Doi=fnd%7B%5C&%7Dpg=PP1%7B%5C&%7Ddq=Psychophysics:+the+fundamentals+(3rd+ed.).+Lawrence+Erlbaum+Associates.%7B%5C&%7Dots=ytvqCsmsnr%7B%5C&%7Dsig=8ifysR3qkGCsIxtYBRzzk7Zne10%7B%5C&%7Dredir%7B%5C_%7Desc=y%7B%5C#%7Dv=onepage%7B%5C&%7Dq=Psychophysics:%20the%20fundamentals%20(3rd%20ed.)..

[50] Gluon. *JavaFX*. URL: https://openjfx.io/ (visited on 09/10/2019).

[51] Nan-Wei Gong, Jürgen Steimle, Simon Olberding, Steve Hodges, Nicholas Edward Gillian, Yoshihiro Kawahara, and Joseph A. Paradiso. "PrintSense: A Versatile Sensing Technique to Support Multimodal Flexible Surface Interaction." In: *Proceedings of the SIGCHI Conference on Human Factors in Computing Systems*. CHI '14. Toronto, Ontario, Canada: ACM, 2014, pp. 1407–1410. ISBN: 978-1-4503-2473-1. DOI: 10.1145/2556288.2557173. URL: http://doi.acm.org/10.1145/2556288.2557173.

[52] Saul Greenberg and Chester Fitchett. "Phidgets: Easy Development of Physical Interfaces Through Physical Widgets." In: *Proceedings of the 14th Annual ACM Symposium on User Interface Software and Technology*. UIST '01. Orlando, Florida: ACM, 2001, pp. 209–218. ISBN: 1-58113-438-X. DOI: 10.1145/502348.502388. URL: http://doi.acm.org/10.1145/502348.502388.

[53] Joseph N. Grima, Ruben Gatt, Brian Ellul, and Elaine Chetcuti. "Auxetic behaviour in non-crystalline materials having star or triangular shaped perforations." In: *Journal of Non-Crystalline Solids* 356.37 (2010). Joint Conferences on Advanced Materials: Functional and Nanonstructured Materials - FNMA'09; Intermolecular and Magnetic Interactions in Matter - IMIM'09, pp. 1980–1987. ISSN: 0022-3093. DOI: https://doi.org/10.1016/j.jnoncrysol.2010.05.074. URL: http://www.sciencedirect.com/science/article/pii/S0022309310003224.

[54] Joseph N Grima, Ruben Gatt, Andrew Alderson, and KE Evans. "On the potential of connected stars as auxetic systems." In: *Molecular Simulation* 31.13 (2005), pp. 925–935.

[55] Daniel Groeger, Elena Chong Loo, and Jürgen Steimle. "HotFlex: Post-print Customization of 3D Prints Using Embedded State Change." In: *Proceedings of the 2016 CHI Conference on Human Factors in Computing Systems*. CHI '16. Santa Clara, California, USA: ACM, 2016, pp. 420–432. ISBN: 978-1-4503-3362-7. DOI: 10.1145/2858036.2858191. URL: http://doi.acm.org/10.1145/2858036.2858191.

[56] Daniel Groeger, Martin Feick, Anusha Withana, and Jürgen Steimle. "Tactlets: Adding Tactile Feedback to 3D Objects Using Custom Printed Controls." In: *Proceedings of the 32nd Annual ACM Symposium on User Interface Software and Technology*. UIST '19. New Orleans, LA, USA: ACM, 2019. ISBN: 978-1-4503-6816-2/19/10. DOI: 10.475/3332165.3347937. URL: http://doi.acm.org/10.475/3332165.3347937.

[57] Daniel Groeger and Jürgen Steimle. "ObjectSkin: Augmenting Everyday Objects with Hydroprinted Touch Sensors and Displays." In: *Proc. ACM Interact. Mob. Wearable Ubiquitous Technol.* 1.4 (Jan. 2018), 134:1–134:23. ISSN: 2474-9567. DOI: 10.1145/3161165. URL: http://doi.acm.org/10.1145/3161165.

[58] Daniel Groeger and Jürgen Steimle. "LASEC: Instant Fabrication of Stretchable Circuits Using a Laser Cutter." In: *Proceedings of the 2019 CHI Conference on Human Factors in Computing Systems*. CHI '19. Glasgow, Scotland Uk: ACM, 2019, 699:1–699:14. ISBN: 978-1-4503-5970-2. DOI: 10.1145/3290605.3300929. URL: http://doi.acm.org/10.1145/3290605.3300929.

[59] Jianzhe Gu, David E. Breen, Jenny Hu, Lifeng Zhu, Ye Tao, Tyson Van de Zande, Guanyun Wang, Yongjie Jessica Zhang, and Lining Yao. "Geodesy: Self-rising 2.5D Tiles by Printing Along 2D Geodesic Closed Path." In: *Proceedings of the 2019 CHI Conference on Human Factors in Computing Systems*. CHI '19. Glasgow, Scotland Uk: ACM, 2019, 37:1–37:10. ISBN: 978-1-4503-5970-2. DOI: 10.1145/3290605.3300267. URL: http://doi.acm.org/10.1145/3290605.3300267.

[60] Ying-Shi Guan, Zhuolei Zhang, Yichao Tang, Jie Yin, and Shenqiang Ren. "Kirigami-Inspired Nanoconfined Polymer Conducting Nanosheets with 2000% Stretchability." In: *Advanced Materials* 30.20 (2018), p. 1706390. DOI: 10.1002/adma.201706390.

[61] Hengyu Guo, Min-Hsin Yeh, Ying-Chih Lai, Yunlong Zi, Changsheng Wu, Zhen Wen, Chenguo Hu, and Zhong Lin Wang. "All-in-One Shape-Adaptive Self-Charging Power Package for Wearable Electronics." In: *ACS Nano* 10.11 (2016). PMID: 27934070, pp. 10580–10588. DOI: 10.1021/acsnano.6b06621.

[62] Ruslan Guseinov, Eder Miguel, and Bernd Bickel. "CurveUps: Shaping Objects from Flat Plates with Tension-actuated Curvature." In: *ACM Trans. Graph.* 36.4 (July 2017), 64:1–64:12. ISSN: 0730-0301. DOI: 10.1145/3072959.3073709. URL: http://doi.acm.org/10.1145/3072959.3073709.

[63] Gwent Electronic Materials Ltd. *Product Information Sheet C210423D2 Silver Paste*. Issue 2. Oct. 2018. URL: http://gwent.org/gem_data_sheets/polymer_systems_products/electroluminescent_display_materials/C2180423D2%20Silver%20Paste%20issue%202.pdf (visited on 09/13/2019).

[64] Malcolm Hall, Eve Hoggan, and Stephen Brewster. "T-Bars: Towards Tactile User Interfaces for Mobile Touchscreens." In: *Proceedings of the 10th international conference on Human computer interaction with mobile devices and services - MobileHCI '08*. New York, New York, USA: ACM Press, 2008, p. 411. ISBN: 9781595939524. DOI: 10.1145/1409240.1409301. URL: http://portal.acm.org/citation.cfm?doid=1409240.1409301.

[65] Nur Al-huda Hamdan, Simon Voelker, and Jan Borchers. "Sketch&Stitch: Interactive Embroidery for E-textiles." In: *Proceedings of the 2018 CHI Conference on Human Factors in Computing Systems*. CHI '18. Montreal QC, Canada: ACM, 2018, 82:1–82:13. ISBN: 978-1-4503-5620-6. DOI: 10.1145/3173574.3173656. URL: http://doi.acm.org/10.1145/3173574.3173656.

[66] Happy Wire Dog, LLC. *Instamorph - Moldable Plasitc*. URL: https://www.instamorph.com/ (visited on 09/23/2015).

[67] Chris Harrison, Hrvoje Benko, and Andrew D. Wilson. "OmniTouch: Wearable Multitouch Interaction Everywhere." In: *Proceedings of the 24th Annual ACM Symposium on User Interface Software and Technology*. UIST '11. Santa Barbara, California, USA: ACM, 2011, pp. 441–450. ISBN: 978-1-4503-0716-1. DOI: 10.1145/2047196.2047255. URL: http://doi.acm.org/10.1145/2047196.2047255.

[68] P. E. Hart, N. J. Nilsson, and B. Raphael. "A Formal Basis for the Heuristic Determination of Minimum Cost Paths." In: *IEEE Transactions on Systems Science and Cybernetics* 4.2 (July 1968), pp. 100–107. ISSN: 0536-1567. DOI: 10.1109/TSSC.1968.300136.

[69] Liang He, Gierad Laput, Eric Brockmeyer, and Jon E. Froehlich. "SqueezaPulse: Adding Interactive Input to Fabricated Objects Using Corrugated Tubes and Air Pulses." In: *Proceedings of the Eleventh International Conference on Tangible, Embedded, and Embodied Interaction*. TEI '17. Yokohama, Japan: ACM, 2017, pp. 341–350. ISBN: 978-1-4503-4676-4. DOI: 10.1145/3024969.3024976. URL: http://doi.acm.org/10.1145/3024969.3024976.

[70] Liang He, Huaishu Peng, Michelle Lin, Ravikanth Konjeti, François Guimbretière, and Jon E. Froehlich. "Ondulé: Designing and Controlling 3D Printable Springs." In: *Proceedings of the 32Nd Annual ACM Symposium on User Interface Software and Technology*. UIST '19. New Orleans, LA, USA: ACM, 2019, pp. 739–750. ISBN: 978-1-4503-6816-2. DOI: 10.1145/3332165.3347951. URL: http://doi.acm.org/10.1145/3332165.3347951.

[71] Felix Heibeck, Basheer Tome, Clark Della Silva, and Hiroshi Ishii. "uniMorph: Fabricating Thin Film Composites for Shape-Changing Interfaces." In: *Proceedings of the 28th Annual ACM Symposium on User Interface Software & Technology*. UIST '15. Daegu, Kyungpook, Republic of Korea: ACM, 2015, pp. 233–242. ISBN: 978-1-4503-3779-3. DOI: 10.1145/2807442.2807472. URL: http://doi.acm.org/10.1145/2807442.2807472.

[72] Steve Hodges, Nicolas Villar, Nicholas Chen, Tushar Chugh, Jie Qi, Diana Nowacka, and Yoshihiro Kawahara. "Circuit Stickers: Peel-and-stick Construction of Interactive Electronic Prototypes." In: *Proceedings of the 32Nd Annual ACM Conference on Human Factors in Computing Systems*. CHI '14. Toronto, Ontario, Canada: ACM, 2014, pp. 1743–1746. ISBN: 978-1-4503-2473-1. DOI: 10.1145/2556288.2557150. URL: http://doi.acm.org/10.1145/2556288.2557150.

[73] David Holman, Nicholas Fellion, and Roel Vertegaal. "Sensing Touch Using Resistive Graphs." In: *Proceedings of the 2014 Conference on Designing Interactive Systems*. DIS '14. Vancouver, BC, Canada: ACM, 2014, pp. 195–198. ISBN: 978-1-4503-2902-6. DOI: 10.1145/2598510.2598552. URL: http://doi.acm.org/10.1145/2598510.2598552.

[74] David Holman and Roel Vertegaal. "Organic User Interfaces: Designing Computers in Any Way, Shape, or Form." In: *Commun. ACM* 51.6 (June 2008), pp. 48–55. ISSN: 0001-0782. DOI: 10.1145/1349026.1349037. URL: http://doi.acm.org/10.1145/1349026.1349037.

[75] Jonathan Hook, Thomas Nappey, Steve Hodges, Peter Wright, and Patrick Olivier. "Making 3D Printed Objects Interactive Using Wireless Accelerometers." In: *Proceedings of the Extended Abstracts of the 32Nd Annual ACM Conference on Human Factors in Computing Systems*. CHI EA '14. Toronto, Ontario, Canada: ACM, 2014, pp. 1435–1440. ISBN: 978-1-4503-2474-8. DOI: 10.1145/2559206.2581137. URL: http://doi.acm.org/10.1145/2559206.2581137.

[76] Zhenlong Huang et al. "Three-dimensional integrated stretchable electronics." In: *Nature Electronics* 1.8 (Aug. 2018), pp. 473–480. ISSN: 2520-1131. URL: https://doi.org/10.1038/s41928-018-0116-y.

[77] Charles Hudin, Sabrina Panëels, and Steven Strachan. "INTACT: Instant Interaction for 3D Printed Objects." In: *Proceedings of the 2016 CHI Conference Extended Abstracts on Human Factors in Computing Systems*. CHI EA '16. San Jose, California, USA: ACM, 2016, pp. 3687–3690. ISBN: 978-1-4503-4082-3. DOI: 10.1145/2851581.2890251. URL: http://doi.acm.org/10.1145/2851581.2890251.

[78] Scott E. Hudson. "Printing Teddy Bears: A Technique for 3D Printing of Soft Interactive Objects." In: *Proceedings of the SIGCHI Conference on Human Factors in Computing Systems*. CHI '14. Toronto, Ontario, Canada: ACM, 2014, pp. 459–468. ISBN: 978-1-4503-2473-1. DOI: 10.1145/2556288.2557338. URL: http://doi.acm.org/10.1145/2556288.2557338.

[79] Charles W Hull. *Apparatus for production of three-dimensional objects by stereolithography*. US Patent 4,575,330. Mar. 1986.

[80] Alexandra Ion, Johannes Frohnhofen, Ludwig Wall, Robert Kovacs, Mirela Alistar, Jack Lindsay, Pedro Lopes, Hsiang-Ting Chen, and Patrick Baudisch. "Metamaterial Mechanisms." In: *Proceedings of the 29th Annual Symposium on User Interface Software and Technology*. UIST '16. Tokyo, Japan: ACM, 2016, pp. 529–539. ISBN: 978-1-4503-4189-9. DOI: 10.1145/2984511.2984540. URL: http://doi.acm.org/10.1145/2984511.2984540.

[81] Alexandra Ion, David Lindlbauer, Philipp Herholz, Marc Alexa, and Patrick Baudisch. "Understanding Metamaterial Mechanisms." In: *Proceedings of the 2019 CHI Conference on Human Factors in Computing Systems*. CHI '19. Glasgow, Scotland Uk: ACM, 2019, 647:1–647:14. ISBN: 978-1-4503-5970-2. DOI: 10.1145/3290605.3300877. URL: http://doi.acm.org/10.1145/3290605.3300877.

[82] Yoshio Ishiguro and Ivan Poupyrev. "3D Printed Interactive Speakers." In: *Proceedings of the 32Nd Annual ACM Conference on Human Factors in Computing Systems*. CHI '14. Toronto, Ontario, Canada: ACM, 2014, pp. 1733–1742. ISBN: 978-1-4503-2473-1. DOI: 10.1145/2556288.2557046. URL: http://doi.acm.org/10.1145/2556288.2557046.

[83] Hiroshi Ishii. "Tangible Bits: Beyond Pixels." In: *Proceedings of the 2Nd International Conference on Tangible and Embedded Interaction*. TEI '08. Bonn, Germany: ACM, 2008, pp. xv–xxv. ISBN: 978-1-60558-004-3. DOI: 10.1145/1347390.1347392. URL: http://doi.acm.org/10.1145/1347390.1347392.

[84] Hiroshi Ishii and Brygg Ullmer. "Tangible Bits: Towards Seamless Interfaces Between People, Bits and Atoms." In: *Proceedings of the ACM SIGCHI Conference on Human Factors in Computing Systems*. CHI '97. Atlanta, Georgia, USA: ACM, 1997, pp. 234–241. ISBN: 0-89791-802-9. DOI: 10.1145/258549.258715. URL: http://doi.acm.org/10.1145/258549.258715.

[85] *Ergonomic requirements for office work with visual display terminals (VDTs), part 4: keyboard requirements*. Standard. Geneva, CH: International Organization for Standardization (ISO), 1998.

[86] Ali Israr and Ivan Poupyrev. "Tactile Brush: Drawing on Skin with a Tactile Grid Display." In: *Proceedings of the SIGCHI Conference on Human Factors in Computing Systems*. CHI '11. Vancouver, BC, Canada: ACM, 2011, pp. 2019–2028. ISBN: 978-1-4503-0228-9. DOI: 10.1145/1978942.1979235. URL: http://doi.acm.org/10.1145/1978942.1979235.

[87] Konami Izumi, Yasunori Yoshida, and Shizuo Tokito. "Soft Blanket Gravure (SBG) Printing Technology for Fine Electronic Interconnect Layers for Three-Dimensional Curved Surfaces." In: *Convertech & e-print* 6.1 (Jan. 2016), pp. 70–74. ISSN: 2185-6931. URL: http://ci.nii.ac.jp/naid/40020715041/en/.

[88] Sungjune Jang, Lawrence H. Kim, Kesler Tanner, Hiroshi Ishii, and Sean Follmer. "Haptic Edge Display for Mobile Tactile Interaction." In: *Proceedings of the 2016 CHI Conference on Human Factors in Computing Systems*. CHI '16. San Jose, California, USA: ACM, 2016, pp. 3706–3716. ISBN: 978-1-4503-3362-7. DOI: 10.1145/2858036.2858264. URL: http://doi.acm.org/10.1145/2858036.2858264.

[89] Bernard J. Jansen. "The Graphical User Interface." In: *SIGCHI Bull.* 30.2 (Apr. 1998), pp. 22–26. ISSN: 0736-6906. DOI: 10.1145/279044.279051. URL: http://doi.acm.org/10.1145/279044.279051.

[90] Yvonne Jansen, Thorsten Karrer, and Jan Borchers. "MudPad: Tactile Feedback and Haptic Texture Overlay for Touch Surfaces." In: *ACM International Conference on Interactive Tabletops and Surfaces*. ITS '10. Saarbrücken, Germany: ACM, 2010, pp. 11–14. ISBN: 978-1-4503-0399-6. DOI: 10.1145/1936652.1936655. URL: http://doi.acm.org/10.1145/1936652.1936655.

[91] Yuhua Jin, Isabel Qamar, Michael Wessely, Aradhana Adhikari, Katarina Bulovic, Parinya Punpongsanon, and Stefanie Mueller. "Photo-Chromeleon: Re-Programmable Multi-Color Textures Using Photochromic Dyes." In: *Proceedings of the 32Nd Annual ACM Symposium on User Interface Software and Technology*. UIST '19. New Orleans, LA, USA: ACM, 2019, pp. 701–712. ISBN: 978-1-4503-6816-2. DOI: 10.1145/3332165.3347905. URL: http://doi.acm.org/10.1145/3332165.3347905.

[92] Lynette A. Jones and Hong Z. Tan. "Application of psychophysical techniques to haptic research." In: *IEEE Transactions on Haptics* 6.3 (2013), pp. 268–284. ISSN: 19391412. DOI: 10.1109/TOH.2012.74.

[93] Michael D. Jones, Zann Anderson, Casey Walker, and Kevin Seppi. "PHUIkit: Interface Layout and Fabrication on Curved 3D Printed Objects." In: *Proceedings of the 2018 CHI Conference on Human Factors in Computing Systems*. CHI '18. Montreal QC, Canada: ACM, 2018, 110:1–110:11. ISBN: 978-1-4503-5620-6. DOI: 10.1145/3173574.3173684. URL: http://doi.acm.org/10.1145/3173574.3173684.

[94] Michael D. Jones, Kevin Seppi, and Dan R. Olsen. "What You Sculpt is What You Get: Modeling Physical Interactive Devices with Clay and 3D Printed Widgets." In: *Proceedings of the 2016 CHI Conference on Human Factors in Computing Systems*. CHI '16. San Jose, California, USA: ACM, 2016, pp. 876–886. ISBN: 978-1-4503-3362-7. DOI: 10.1145/2858036.2858493. URL: http://doi.acm.org/10.1145/2858036.2858493.

[95] K. A. Kaczmarek, J. G. Webster, P. Bach-y-Rita, and W. J. Tompkins. "Electrotactile and vibrotactile displays for sensory substitution systems." In: *IEEE Transactions on Biomedical Engineering* 38.1 (Jan. 1991), pp. 1–16. ISSN: 0018-9294. DOI: 10.1109/10.68204.

[96] H. Kajimoto, N. Kawakami, S. Tachi, and M. Inami. "SmartTouch: electric skin to touch the untouchable." In: *IEEE Computer Graphics and Applications* 24.1 (Jan. 2004), pp. 36–43. ISSN: 0272-1716. DOI: 10.1109/MCG.2004.1255807.

[97] Hiroyuki Kajimoto. "Electro-tactile Display: Principle and Hardware." In: *Pervasive Haptics*. Ed. by Hiroyuki Kajimoto, Satoshi Saga, and Masashi Konyo. Tokyo: Springer Japan, 2016, pp. 79–96. ISBN: 978-4-431-55771-5. DOI: 10.1007/978-4-431-55772-2_5. URL: http://link.springer.com/10.1007/978-4-431-55772-2%20http://link.springer.com/10.1007/978-4-431-55772-2%7B%5C_%7D5.

[98] Hsin-Liu (Cindy) Kao, Christian Holz, Asta Roseway, Andres Calvo, and Chris Schmandt. "DuoSkin: Rapidly Prototyping On-skin User Interfaces Using Skin-friendly Materials." In: *Proceedings of the 2016 ACM International Symposium on Wearable Computers*. ISWC '16. Heidelberg, Germany: ACM,

2016, pp. 16–23. ISBN: 978-1-4503-4460-9. DOI: 10.1145/2971763.2971777. URL: http://doi.acm.org/10.1145/2971763.2971777.

[99] Hsin-Liu (Cindy) Kao, Manisha Mohan, Chris Schmandt, Joseph A. Paradiso, and Katia Vega. "ChromoSkin: Towards Interactive Cosmetics Using Thermochromic Pigments." In: *Proceedings of the 2016 CHI Conference Extended Abstracts on Human Factors in Computing Systems*. CHI EA '16. San Jose, California, USA: ACM, 2016, pp. 3703–3706. ISBN: 978-1-4503-4082-3. DOI: 10.1145/2851581.2890270. URL: http://doi.acm.org/10.1145/2851581.2890270.

[100] Julia Kastner et al. "Silver-based reactive ink for inkjet-printing of conductive lines on textiles." In: *Microelectronic Engineering* 176 (2017). Micro- and Nano-Fabrication, pp. 84–88. ISSN: 0167-9317. DOI: https://doi.org/10.1016/j.mee.2017.02.004. URL: http://www.sciencedirect.com/science/article/pii/S0167931717300527.

[101] Shohei Katakura and Keita Watanabe. "ProtoHole: Prototyping Interactive 3D Printed Objects Using Holes and Acoustic Sensing." In: *Extended Abstracts of the 2018 CHI Conference on Human Factors in Computing Systems*. CHI EA '18. Montreal QC, Canada: ACM, 2018, LBW112:1–LBW112:6. ISBN: 978-1-4503-5621-3. DOI: 10.1145/3170427.3188471. URL: http://doi.acm.org/10.1145/3170427.3188471.

[102] Kunihiro Kato, Hiroki Ishizuka, Hiroyuki Kajimoto, and Homei Miyashita. "Double-sided Printed Tactile Display with Electro Stimuli and Electrostatic Forces and Its Assessment." In: *Proceedings of the 2018 CHI Conference on Human Factors in Computing Systems*. CHI '18. Montreal QC, Canada: ACM, 2018, 450:1–450:12. ISBN: 978-1-4503-5620-6. DOI: 10.1145/3173574.3174024. URL: http://doi.acm.org/10.1145/3173574.3174024.

[103] Kunihiro Kato and Homei Miyashita. "Extension Sticker: A Method for Transferring External Touch Input Using a Striped Pattern Sticker." In: *Proceedings of the Adjunct Publication of the 27th Annual ACM Symposium on User Interface Software and Technology*. UIST'14 Adjunct. Honolulu, Hawaii, USA: ACM, 2014, pp. 59–60. ISBN: 978-1-4503-3068-8. DOI: 10.1145/2658779.2668032. URL: http://doi.acm.org/10.1145/2658779.2668032.

[104] Yoshihiro Kawahara, Steve Hodges, Benjamin S. Cook, Cheng Zhang, and Gregory D. Abowd. "Instant Inkjet Circuits: Lab-based Inkjet Printing to Support Rapid Prototyping of UbiComp Devices." In: *Proceedings of the 2013 ACM International Joint Conference on Pervasive and Ubiquitous Computing*. UbiComp '13. Zurich, Switzerland: ACM, 2013, pp. 363–372. ISBN: 978-1-4503-1770-2. DOI: 10.1145/2493432.2493486. URL: http://doi.acm.org/10.1145/2493432.2493486.

[105] Yoshihiro Kawahara, Steve Hodges, Nan-Wei Gong, Simon Olberding, and Jürgen Steimle. "Building Functional Prototypes Using Conductive Inkjet Printing." In: *Pervasive Computing, IEEE* 13.3 (July 2014), pp. 30–38. ISSN: 1536-1268. DOI: 10.1109/MPRV.2014.41.

[106] Yukihiko Kawaharada, Akihiro Sawaguchi, Mitsutaka Nanbo, Hiroyuki Tabe, Shinji Kato, and Shuzo Mizuno. "Hydraulic transfer method." U.S. pat. US6902642B2. June 2005.

[107] Arshad Khan, Khalid Rahman, Myung-Taek Hyun, Dong-Soo Kim, and Kyung-Hyun Choi. "Multi-nozzle electrohydrodynamic inkjet printing of silver colloidal solution for the fabrication of electrically functional microstructures." In: *Applied Physics A* 104.4 (Apr. 2011), p. 1113. ISSN: 1432-0630. DOI: 10.1007/s00339-011-6386-0. URL: https://doi.org/10.1007/s00339-011-6386-0.

[108] Arshad Khan, Joan Sol Roo, Tobias Kraus, and Jürgen Steimle. "Soft Inkjet Circuits: Rapid Multi-Material Fabrication of Soft Circuits Using a Commodity Inkjet Printer." In: *Proceedings of the 32Nd Annual ACM Symposium on User Interface Software and Technology*. UIST '19. New Orleans, LA, USA: ACM, 2019, pp. 341–354. ISBN: 978-1-4503-6816-2. DOI: 10.1145/3332165.3347892. URL: http://doi.acm.org/10.1145/3332165.3347892.

[109] Sugarragchaa Khurelbaatar, Yuriko Nakai, Ryuta Okazaki, Vibol Yem, and Hiroyuki Kajimoto. "Tactile Presentation to the Back of a Smartphone with Simultaneous Screen Operation." In: *Proceedings of the 2016 CHI Conference on Human Factors in Computing Systems*. CHI '16. San Jose, California, USA: ACM, 2016, pp. 3717–3721. ISBN: 978-1-4503-3362-7. DOI: 10.1145/2858036.2858099. URL: http://doi.acm.org/10.1145/2858036.2858099.

[110] Dae-Hyeong Kim et al. "Epidermal Electronics." In: *Science* 333.6044 (2011), pp. 838–843. ISSN: 0036-8075. DOI: 10.1126/science.1206157. eprint: http://science.sciencemag.org/content/333/6044/838.full.pdf. URL: http://science.sciencemag.org/content/333/6044/838.

[111] Seung-Chan Kim, Ali Israr, and Ivan Poupyrev. "Tactile Rendering of 3D Features on Touch Surfaces." In: *Proceedings of the 26th Annual ACM Symposium on User Interface Software and Technology*. UIST '13. St. Andrews, Scotland, United Kingdom: ACM, 2013, pp. 531–538. ISBN: 978-1-4503-2268-3. DOI: 10.1145/2501988.2502020. URL: http://doi.acm.org/10.1145/2501988.2502020.

[112] Petherbridge Kirstie, Evans Peter, and Harrison David. "The origins and evolution of the PCB: a review." In: *Circuit World* 31.1 (Sept. 2005), pp. 41–45. ISSN: 0305-6120. URL: https://doi.org/10.1108/03056120510553211.

[113] Mina Konaković, Keenan Crane, Bailin Deng, Sofien Bouaziz, Daniel Piker, and Mark Pauly. "Beyond Developable: Computational Design and Fabrication with Auxetic Materials." In: *ACM Trans. Graph.* 35.4 (July 2016), 89:1–89:11. ISSN: 0730-0301. DOI: 10.1145/2897824.2925944. URL: http://doi.acm.org/10.1145/2897824.2925944.

[114] Tyler Koslow. *2019 Best Resin (LCD/DLP/SLA) 3D Printers (Summer Update)*. June 2019. URL: https://all3dp.com/1/best-resin-dlp-sla-3d-printer-kit-stereolithography/ (visited on 09/03/2019).

[115] Robert Kovacs et al. "TrussFab: Fabricating Sturdy Large-Scale Structures on Desktop 3D Printers." In: *Proceedings of the 2017 CHI Conference on Human Factors in Computing Systems*. CHI '17. Denver, Colorado, USA: ACM, 2017, pp. 2606–2616. ISBN: 978-1-4503-4655-9. DOI: 10.1145/3025453.3026016. URL: http://doi.acm.org/10.1145/3025453.3026016.

[116] Rajan Kumar, Jaewook Shin, Lu Yin, Jung-Min You, Ying Shirley Meng, and Joseph Wang. "All-Printed, Stretchable Zn-Ag2O Rechargeable Battery via Hyperelastic Binder for Self-Powering Wearable Electronics." In: *Advanced Energy Materials* 7.8 (2017), p. 1602096. DOI: 10.1002/aenm.201602096. eprint: https://onlinelibrary.wiley.com/doi/pdf/10.1002/aenm.201602096. URL: https://onlinelibrary.wiley.com/doi/abs/10.1002/aenm.201602096.

[117] Valentin Kunin, Shu Yang, Yigil Cho, Pierre Deymier, and David J. Srolovitz. "Static and dynamic elastic properties of fractal-cut materials." In: *Extreme Mechanics Letters* 6 (2016), pp. 103–114. ISSN: 2352-4316. DOI: https://doi.org/10.1016/j.eml.2015.12.003. URL: http://www.sciencedirect.com/science/article/pii/S2352431615300043.

[118] Haresh Lalvani. "Multi-directional and variably expanded sheet material surfaces." US8084117B2. 2011.

[119] Gierad Laput, Eric Brockmeyer, Scott E. Hudson, and Chris Harrison. "Acoustruments: Passive, Acoustically-Driven, Interactive Controls for Handheld Devices." In: *Proceedings of the 33rd Annual ACM Conference on Human Factors in Computing Systems*. CHI '15. Seoul, Republic of Korea: ACM, 2015, pp. 2161–2170. ISBN: 978-1-4503-3145-6. DOI: 10.1145/2702123.2702414. URL: http://doi.acm.org/10.1145/2702123.2702414.

[120] Gierad Laput, Xiang "Anthony" Chen, and Chris Harrison. "3D Printed Hair: Fused Deposition Modeling of Soft Strands, Fibers, and Bristles." In: *Proceedings of the 28th Annual ACM Symposium on User Interface Software & Technology*. UIST '15. Daegu, Kyungpook, Republic of Korea: ACM, 2015, pp. 593–597. ISBN: 978-1-4503-3779-3. DOI: 10.1145/2807442.2807484. URL: http://doi.acm.org/10.1145/2807442.2807484.

[121] Mathieu Le Goc, Lawrence H. Kim, Ali Parsaei, Jean-Daniel Fekete, Pierre Dragicevic, and Sean Follmer. "Zooids: Building Blocks for Swarm User Interfaces." In: *Proceedings of the 29th Annual Symposium on User Interface Software and Technology*. UIST '16. Tokyo, Japan: ACM, 2016, pp. 97–109. ISBN: 978-1-4503-4189-9. DOI: 10.1145/2984511.2984547. URL: http://doi.acm.org/10.1145/2984511.2984547.

[122] David Ledo, Fraser Anderson, Ryan Schmidt, Lora Oehlberg, Saul Greenberg, and Tovi Grossman. "Pineal: Bringing Passive Objects to Life with Embedded Mobile Devices." In: *Proceedings of the 2017 CHI Conference on Human Factors in Computing Systems*. CHI '17. Denver, Colorado, USA: ACM, 2017, pp. 2583–2593. ISBN: 978-1-4503-4655-9. DOI: 10.1145/3025453.3025652. URL: http://doi.acm.org/10.1145/3025453.3025652.

[123] C. Y. Lee. "An Algorithm for Path Connections and Its Applications." In: *IRE Transactions on Electronic Computers* EC-10.3 (Sept. 1961), pp. 346–365. ISSN: 0367-9950. DOI: 10.1109/TEC.1961.5219222.

[124] Jaemyon Lee, Seungjun Chung, Hyunsoo Song, Sangwoo Kim, and Yongtaek Hong. "Lateral-crack-free, buckled, inkjet-printed silver electrodes on highly pre-stretched elastomeric substrates." In: *Journal of Physics D: Applied Physics* 46.10 (Feb. 2013), p. 105305. DOI: 10.1088/0022-3727/46/10/105305. URL: https://doi.org/10.1088%2F0022-3727%2F46%2F10%2F105305.

[125] Johnny C. Lee, Daniel Avrahami, Scott E. Hudson, Jodi Forlizzi, Paul H. Dietz, and Darren Leigh. "The Calder Toolkit: Wired and Wireless Components for Rapidly Prototyping Interactive Devices." In: *Proceedings of the 5th Conference on Designing Interactive Systems: Processes, Practices, Methods, and Techniques*. DIS '04. Cambridge, MA, USA: ACM, 2004, pp. 167–175. ISBN: 1-58113-787-7. DOI: 10.1145/1013115.1013139.

[126] Joanne Lo, Doris Jung Lin Lee, Nathan Wong, David Bui, and Eric Paulos. "Skintillates: Designing and Creating Epidermal Interactions." In: *Proceedings of the 2016 ACM Conference on Designing Interactive Systems*. DIS '16. Brisbane, QLD, Australia: ACM, 2016, pp. 853–864. ISBN: 978-1-4503-4031-1. DOI: 10.1145/2901790.2901885. URL: http://doi.acm.org/10.1145/2901790.2901885.

[127] Anatol Locker. *2019 Best Cheap 3D Printers Priced Under $200/300/500/1000*. June 2019. URL: https://all3dp.com/1/best-cheap-budget-3d-printer-affordable-under-500-1000/ (visited on 09/03/2019).

[128] Tong Lu, Lauren Finkenauer, James Wissman, and Carmel Majidi. "Rapid Prototyping for Soft-Matter Electronics." In: *Advanced Functional Materials* 24.22 (2014), pp. 3351–3356. DOI: 10.1002/adfm.201303732.

[129] Linjie Luo, Ilya Baran, Szymon Rusinkiewicz, and Wojciech Matusik. "Chopper: Partitioning Models into 3D-printable Parts." In: *ACM Trans. Graph.* 31.6 (Nov. 2012), 129:1–129:9. ISSN: 0730-0301. DOI: 10.1145/2366145.2366148. URL: http://doi.acm.org/10.1145/2366145.2366148.

[130] R. MacCurdy, R. Katzschmann, Youbin Kim, and D. Rus. "Printable hydraulics: A method for fabricating robots by 3D co-printing solids and liquids." In: *2016 IEEE International Conference on Robotics and Automation (ICRA)*. May 2016, pp. 3878–3885. DOI: 10.1109/ICRA.2016.7487576.

[131] Karon E. MacLean. "Designing with haptic feedback." In: *Proceedings 2000 ICRA. Millennium Conference. IEEE International Conference on Robotics and Automation. Symposia Proceedings (Cat. No.00CH37065)*. Vol. 1. Apr. 2000, 783–788 vol.1. DOI: 10.1109/ROBOT.2000.844146.

[132] Karon MacLean and Mario Enriquez. "Perceptual design of haptic icons." In: *In Proceedings of Eurohaptics*. 2003, pp. 351–363.

[133] MakerBot Industries, LLC. *Thingiverse - Digital Designs for Physical Objects*. URL: https://www.thingiverse.com/about/ (visited on 09/06/2019).

[134] Viktor Miruchna, Robert Walter, David Lindlbauer, Maren Lehmann, Regine von Klitzing, and Jörg Müller. "GelTouch: Localized Tactile Feedback Through Thin, Programmable Gel." In: *Proceedings of the 28th Annual ACM Symposium on User Interface Software & Technology*. UIST '15. Daegu, Kyungpook, Republic of Korea: ACM, 2015, pp. 3–10. ISBN: 978-1-4503-3779-3. DOI: 10.1145/2807442.2807487. URL: http://doi.acm.org/10.1145/2807442.2807487.

[135] Ella Moore, Michael Porter, Ioannis Karamouzas, and Victor Zordan. "Precision Control of Tensile Properties in Fabric for Computational Fabrication." In: *Proceedings of the 2Nd ACM Symposium on Computational Fabrication*. SCF '18. Cambridge, Massachusetts: ACM, 2018, 3:1–3:7. ISBN: 978-1-4503-5854-5. DOI: 10.1145/3213512.3213514. URL: http://doi.acm.org/10.1145/3213512.3213514.

[136] Stefanie Mueller, Sangha Im, Serafima Gurevich, Alexander Teibrich, Lisa Pfisterer, François Guimbretière, and Patrick Baudisch. "WirePrint: 3D Printed Previews for Fast Prototyping." In: *Proceedings of the 27th Annual ACM Symposium on User Interface Software and Technology*. UIST '14. Honolulu, Hawaii, USA: ACM, 2014, pp. 273–280. ISBN: 978-1-4503-3069-5. DOI: 10.1145/2642918.2647359. URL: http://doi.acm.org/10.1145/2642918.2647359.

[137] Stefanie Mueller, Bastian Kruck, and Patrick Baudisch. "LaserOrigami: Laser-cutting 3D Objects." In: *Proceedings of the SIGCHI Conference on Human Factors in Computing Systems*. CHI '13. Paris, France: ACM, 2013, pp. 2585–2592. ISBN: 978-1-4503-1899-0. DOI: 10.1145/2470654.2481358. URL: http://doi.acm.org/10.1145/2470654.2481358.

[138] Stefanie Mueller, Pedro Lopes, and Patrick Baudisch. "Interactive Construction: Interactive Fabrication of Functional Mechanical Devices." In: *Proceedings of the 25th Annual ACM Symposium on User Interface Software and Technology*. UIST '12. Cambridge, Massachusetts, USA: ACM, 2012, pp. 599–606. ISBN: 978-1-4503-1580-7. DOI: 10.1145/2380116.2380191. URL: http://doi.acm.org/10.1145/2380116.2380191.

[139] Stefanie Mueller, Tobias Mohr, Kerstin Guenther, Johannes Frohnhofen, and Patrick Baudisch. "faBrickation: Fast 3D Printing of Functional Objects by Integrating Construction Kit Building Blocks." In: *Proceedings of the 32Nd Annual ACM Conference on Human Factors in Computing Systems*. CHI '14. Toronto, Ontario, Canada: ACM, 2014, pp. 3827–3834. ISBN: 978-1-4503-2473-1. DOI: 10.1145/2556288.2557005. URL: http://doi.acm.org/10.1145/2556288.2557005.

[140] Stefanie Mueller, Anna Seufert, Huaishu Peng, Robert Kovacs, Kevin Reuss, François Guimbretière, and Patrick Baudisch. "FormFab: Continuous Interactive Fabrication." In: *Proceedings of the Thirteenth International Conference on Tangible, Embedded, and Embodied Interaction*. TEI '19. Tempe, Arizona, USA: ACM, 2019, pp. 315–323. ISBN: 978-1-4503-6196-5. DOI: 10.1145/3294109.3295620. URL: http://doi.acm.org/10.1145/3294109.3295620.

[141] Tamotsu Murakami and Naomasa Nakajima. "Direct and Intuitive Input Device for 3-D Shape Deformation." In: *Proceedings of the SIGCHI Conference on Human Factors in Computing Systems*. CHI '94. Boston, Massachusetts, USA: ACM, 1994, pp. 465–470. ISBN: 0-89791-650-6. DOI: 10.1145/191666.191823. URL: http://doi.acm.org/10.1145/191666.191823.

[142] Steven Nagels, Raf Ramakers, Kris Luyten, and Wim Deferme. "Silicone Devices: A Scalable DIY Approach for Fabricating Self-Contained Multi-Layered Soft Circuits Using Microfluidics." In: *Proceedings of the 2018 CHI Conference on Human Factors in Computing Systems*. CHI '18. Montreal QC, Canada: ACM, 2018, 188:1–188:13. ISBN: 978-1-4503-5620-6. DOI: 10.1145/3173574.3173762. URL: http://doi.acm.org/10.1145/3173574.3173762.

[143] Andrew Nashel and Sharif Razzaque. "Tactile virtual buttons for mobile devices." In: *CHI '03 extended abstracts on Human factors in computer systems - CHI '03*. New York, New York, USA: ACM Press, 2003, p. 854. ISBN: 1581136374. DOI: 10.1145/766028.766032. URL: http://portal.acm.org/citation.cfm?doid=765891.766032.

[144] Aditya Shekhar Nittala, Anusha Withana, Narjes Pourjafarian, and Jürgen Steimle. "Multi-Touch Skin: A Thin and Flexible Multi-Touch Sensor for On-Skin Input." In: *Proceedings of the 2018 CHI Conference on Human Factors in Computing Systems*. CHI '18. Montreal QC, Canada: ACM, 2018, 33:1–33:12. ISBN: 978-1-4503-5620-6. DOI: 10.1145/3173574.3173607. URL: http://doi.acm.org/10.1145/3173574.3173607.

[145] Ian Oakley, DoYoung Lee, MD. Rasel Islam, and Augusto Esteves. "Beats: Tapping Gestures for Smart Watches." In: *Proceedings of the 33rd Annual ACM Conference on Human Factors in Computing Systems*. CHI '15. Seoul, Republic of Korea: ACM, 2015, pp. 1237–1246. ISBN: 978-1-4503-3145-6. DOI: 10.1145/2702123.2702226. URL: http://doi.acm.org/10.1145/2702123.2702226.

[146] Hyunjoo Oh, Tung D. Ta, Ryo Suzuki, Mark D. Gross, Yoshihiro Kawahara, and Lining Yao. "PEP (3D Printed Electronic Papercrafts): An Integrated Approach for 3D Sculpting Paper-Based Electronic Devices." In: *Proceedings of the 2018 CHI Conference on Human Factors in Computing Systems*. CHI '18. Montreal QC, Canada: ACM, 2018, 441:1–441:12. ISBN: 978-1-4503-5620-6. DOI: 10.1145/3173574.3174015. URL: http://doi.acm.org/10.1145/3173574.3174015.

[147] Simon Olberding, Nan-Wei Gong, John Tiab, Joseph A. Paradiso, and Jürgen Steimle. "A Cuttable Multi-touch Sensor." In: *Proceedings of the 26th Annual ACM Symposium on User Interface Software and Technology*. UIST '13. St. Andrews, Scotland, United Kingdom: ACM, 2013, pp. 245–254. ISBN: 978-1-4503-2268-3. DOI: 10.1145/2501988.2502048. URL: http://doi.acm.org/10.1145/2501988.2502048.

[148] Simon Olberding, Sergio Soto Ortega, Klaus Hildebrandt, and Jürgen Steimle. "Foldio: Digital Fabrication of Interactive and Shape-Changing Objects With Foldable Printed Electronics." In: *Proceedings of the 28th Annual ACM Symposium on User Interface Software & Technology*. UIST '15. Daegu, Kyungpook, Republic of Korea: ACM, 2015, pp. 223–232. ISBN: 978-1-4503-3779-3. DOI:

10.1145/2807442.2807494. URL: http://doi.acm.org/10.1145/2807442.2807494.

[149] Simon Olberding, Michael Wessely, and Jürgen Steimle. "PrintScreen: Fabricating Highly Customizable Thin-film Touch-displays." In: *Proceedings of the 27th Annual ACM Symposium on User Interface Software and Technology*. UIST '14. Honolulu, Hawaii, USA: ACM, 2014, pp. 281–290. ISBN: 978-1-4503-3069-5. DOI: 10.1145/2642918.2647413. URL: http://doi.acm.org/10.1145/2642918.2647413.

[150] Makoto Ono, Buntarou Shizuki, and Jiro Tanaka. "Touch & Activate: Adding Interactivity to Existing Objects Using Active Acoustic Sensing." In: *Proceedings of the 26th Annual ACM Symposium on User Interface Software and Technology*. UIST '13. St. Andrews, Scotland, United Kingdom: ACM, 2013, pp. 31–40. ISBN: 978-1-4503-2268-3. DOI: 10.1145/2501988.2501989. URL: http://doi.acm.org/10.1145/2501988.2501989.

[151] Jifei Ou, Gershon Dublon, Chin-Yi Cheng, Felix Heibeck, Karl Willis, and Hiroshi Ishii. "Cilllia: 3D Printed Micro-Pillar Structures for Surface Texture, Actuation and Sensing." In: *Proceedings of the 2016 CHI Conference on Human Factors in Computing Systems*. CHI '16. Santa Clara, California, USA: ACM, 2016, pp. 5753–5764. ISBN: 978-1-4503-3362-7. DOI: 10.1145/2858036.2858257. URL: http://doi.acm.org/10.1145/2858036.2858257.

[152] Jifei Ou, Zhao Ma, Jannik Peters, Sen Dai, Nikolaos Vlavianos, and Hiroshi Ishii. "KinetiX - designing auxetic-inspired deformable material structures." In: *Computers & Graphics* (2018). ISSN: 0097-8493. DOI: https://doi.org/10.1016/j.cag.2018.06.003. URL: http://www.sciencedirect.com/science/article/pii/S0097849318301006.

[153] Jifei Ou, Lining Yao, Daniel Tauber, Jürgen Steimle, Ryuma Niiyama, and Hiroshi Ishii. "jamSheets: Thin Interfaces with Tunable Stiffness Enabled by Layer Jamming." In: *Proceedings of the 8th International Conference on Tangible, Embedded and Embodied Interaction*. TEI '14. Munich, Germany: ACM, 2013, pp. 65–72. ISBN: 978-1-4503-2635-3. DOI: 10.1145/2540930.2540971. URL: http://doi.acm.org/10.1145/2540930.2540971.

[154] Patrick Parzer, Kathrin Probst, Teo Babic, Christian Rendl, Anita Vogl, Alex Olwal, and Michael Haller. "FlexTiles: A Flexible, Stretchable, Formable, Pressure-Sensitive, Tactile Input Sensor." In: *Proceedings of the 2016 CHI Conference Extended Abstracts on Human Factors in Computing Systems*. CHI EA '16. Santa Clara, California, USA: ACM, 2016, pp. 3754–3757. ISBN: 978-1-4503-4082-3. DOI: 10.1145/2851581.2890253. URL: http://doi.acm.org/10.1145/2851581.2890253.

[155] Fabrizio Pece, Juan Jose Zarate, Velko Vechev, Nadine Besse, Olexandr Gudozhnik, Herbert Shea, and Otmar Hilliges. "MagTics: Flexible and Thin Form Factor Magnetic Actuators for Dynamic and Wearable Haptic Feedback." In: *Proceedings of the 30th Annual ACM Symposium on User Interface Software and Technology - UIST '17*. New York, New York, USA: ACM Press, 2017, pp. 143–154. ISBN: 9781450349819. DOI: 10.1145/3126594.3126609. URL: http://dl.acm.org/citation.cfm?doid=3126594.3126609.

[156] Huaishu Peng, Jimmy Briggs, Cheng-Yao Wang, Kevin Guo, Joseph Kider, Stefanie Mueller, Patrick Baudisch, and François Guimbretière. "RoMA: Interactive Fabrication with Augmented Reality and a Robotic 3D Printer." In: *Proceedings of the 2018 CHI Conference on Human Factors in Computing Systems*. CHI '18. Montreal QC, Canada: ACM, 2018, 579:1–579:12. ISBN: 978-1-4503-5620-6. DOI: 10.1145/3173574.3174153. URL: http://doi.acm.org/10.1145/3173574.3174153.

[157] Huaishu Peng, François Guimbretière, James McCann, and Scott Hudson. "A 3D Printer for Interactive Electromagnetic Devices." In: *Proceedings of the 29th Annual Symposium on User Interface Software and Technology*. UIST '16. Tokyo, Japan: ACM, 2016, pp. 553–562. ISBN: 978-1-4503-4189-9. DOI: 10.1145/2984511.2984523. URL: http://doi.acm.org/10.1145/2984511.2984523.

[158] Huaishu Peng, Jennifer Mankoff, Scott E. Hudson, and James McCann. "A Layered Fabric 3D Printer for Soft Interactive Objects." In: *Proceedings of the 33rd Annual ACM Conference on Human Factors in Computing Systems*. CHI '15. Seoul, Republic of Korea: ACM, 2015, pp. 1789–1798. ISBN: 978-1-4503-3145-6. DOI: 10.1145/2702123.2702327. URL: http://doi.acm.org/10.1145/2702123.2702327.

[159] Huaishu Peng, Rundong Wu, Steve Marschner, and François Guimbretière. "On-The-Fly Print: Incremental Printing While Modelling." In: *Proceedings of the 2016 CHI Conference on Human Factors in Computing Systems*. CHI '16. San Jose, California, USA: ACM, 2016, pp. 887–896. ISBN: 978-1-4503-3362-7. DOI: 10.1145/2858036.2858106. URL: http://doi.acm.org/10.1145/2858036.2858106.

[160] Martin Pielot, Anastasia Kazakova, Tobias Hesselmann, Wilko Heuten, and Susanne Boll. "PocketMenu: Non-visual Menus for Touch Screen Devices." In: *Proceedings of the 14th International Conference on Human-computer Interaction with Mobile Devices and Services*. MobileHCI '12. San Francisco, California, USA: ACM, 2012, pp. 327–330. ISBN: 978-1-4503-1105-2. DOI: 10.1145/2371574.2371624. URL: http://doi.acm.org/10.1145/2371574.2371624.

[161] Ben Piper, Carlo Ratti, and Hiroshi Ishii. "Illuminating Clay: A 3-D Tangible Interface for Landscape Analysis." In: *Proceedings of the SIGCHI Conference on Human Factors in Computing Systems*. CHI '02. Minneapolis, Minnesota, USA: ACM, 2002, pp. 355–362. ISBN: 1-58113-453-3. DOI: 10.1145/503376.503439. URL: http://doi.acm.org/10.1145/503376.503439.

[162] Narjes Pourjafarian, Anusha Withana, Joseph A. Paradiso, and Jürgen Steimle. "Multi-Touch Kit: A Do-It-Yourself Technique for Capacitive Multi-Touch Sensing Using a Commodity Microcontroller." In: *Proceedings of the 32Nd Annual ACM Symposium on User Interface Software and Technology*. UIST '19. New Orleans, LA, USA: ACM, 2019, pp. 1071–1083. ISBN: 978-1-4503-6816-2. DOI: 10.1145/3332165.3347895. URL: http://doi.acm.org/10.1145/3332165.3347895.

[163] ProtoPlant. *High Temp PLA v2.0 — ProtoPlant, Makers of Proto-pasta*. URL: http://www.proto-pasta.com/collections/retail/products/high-temp-pla-v2-0 (visited on 09/23/2015).

[164] ProtoPlant, Inc. *Conductive PLA – ProtoPlant, makers of Proto-pasta*. URL: https://www.proto-pasta.com/pages/conductive-pla (visited on 09/04/2019).

[165] Parinya Punpongsanon, Xin Wen, David S. Kim, and Stefanie Mueller. "ColorMod: Recoloring 3D Printed Objects Using Photochromic Inks." In: *Proceedings of the 2018 CHI Conference on Human Factors in Computing Systems*. CHI '18. Montreal QC, Canada: ACM, 2018, 213:1–213:12. ISBN: 978-1-4503-5620-6. DOI: 10.1145/3173574.3173787. URL: http://doi.acm.org/10.1145/3173574.3173787.

[166] Hayes Solos Raffle, Amanda J. Parkes, and Hiroshi Ishii. "Topobo: A Constructive Assembly System with Kinetic Memory." In: *Proceedings of the SIGCHI Conference on Human Factors in Computing Systems*. CHI '04. Vienna, Austria: ACM, 2004, pp. 647–654. ISBN: 1-58113-702-8. DOI: 10.1145/985692.985774. URL: http://doi.acm.org/10.1145/985692.985774.

[167] Raf Ramakers, Fraser Anderson, Tovi Grossman, and George Fitzmaurice. "RetroFab: A Design Tool for Retrofitting Physical Interfaces Using Actuators, Sensors and 3D Printing." In: *Proceedings of the 2016 CHI Conference on Human Factors in Computing Systems*. CHI '16. San Jose, California, USA: ACM, 2016, pp. 409–419. ISBN: 978-1-4503-3362-7. DOI: 10.1145/2858036.2858485. URL: http://doi.acm.org/10.1145/2858036.2858485.

[168] Raf Ramakers, Kashyap Todi, and Kris Luyten. "PaperPulse: An Integrated Approach for Embedding Electronics in Paper Designs." In: *Proceedings of the 33rd Annual ACM Conference on Human Factors in Computing Systems*. CHI '15. Seoul, Republic of Korea: ACM, 2015, pp. 2457–2466. ISBN: 978-1-4503-3145-6. DOI: 10.1145/2702123.2702487. URL: http://doi.acm.org/10.1145/2702123.2702487.

[169] Ramesh Raskar, Greg Welch, and Henry Fuchs. "Spatially augmented reality." In: *First IEEE Workshop on Augmented Reality (IWAR'98)*. 1998, pp. 11–20.

[170] Ramesh Raskar, Greg Welch, Kok-Lim Low, and Deepak Bandyopadhyay. "Shader Lamps: Animating Real Objects With Image-Based Illumination." In: *Rendering Techniques 2001*. Ed. by Steven J. Gortler and Karol Myszkowski. Vienna: Springer Vienna, 2001, pp. 89–102. ISBN: 978-3-7091-6242-2.

[171] Majken K. Rasmussen, Esben W. Pedersen, Marianne G. Petersen, and Kasper Hornbæk. "Shape-changing Interfaces: A Review of the Design Space and Open Research Questions." In: *Proceedings of the SIGCHI Conference on Human Factors in Computing Systems*. CHI '12. Austin, Texas, USA: ACM, 2012, pp. 735–744. ISBN: 978-1-4503-1015-4. DOI: 10.1145/2207676.2207781. URL: http://doi.acm.org/10.1145/2207676.2207781.

[172] Jacqueline Rausch, Larisa Salun, Stefan Griesheimer, Mesut Ibis, and Roland Werthschützky. "Printed piezoresistive strain sensors for monitoring of light-weight structures." In: *SENSOR & TEST Conference*. June 2011. URL: http://tubiblio.ulb.tu-darmstadt.de/53881/.

[173] Yosra Rekik, Eric Vezzoli, Laurent Grisoni, and Frédéric Giraud. "Localized Haptic Texture : A Rendering Technique Based on Taxels for High Density Tactile Feedback." In: *Proceedings of the 2017 CHI Conference on Human Factors in Computing Systems - CHI '17*. New York, New York, USA: ACM Press, 2017, pp. 5006–5015. ISBN: 9781450346559. DOI: 10.1145/3025453.3026010. URL: http://dl.acm.org/citation.cfm?doid=3025453.3026010.

[174] Christian Rendl et al. "FlexSense: A Transparent Self-sensing Deformable Surface." In: *Proceedings of the 27th Annual ACM Symposium on User Interface Software and Technology*. UIST '14. Honolulu, Hawaii, USA: ACM, 2014, pp. 129–138. ISBN: 978-1-4503-3069-5. DOI: 10.1145/2642918.2647405. URL: http://doi.acm.org/10.1145/2642918.2647405.

[175] Michael L. Rivera and Scott E. Hudson. "Desktop Electrospinning: A Single Extruder 3D Printer for Producing Rigid Plastic and Electrospun Textiles." In: *Proceedings of the 2019 CHI Conference on Human Factors in Computing Systems*. CHI '19. Glasgow, Scotland Uk: ACM, 2019, 204:1–204:12. ISBN: 978-1-4503-5970-2. DOI: 10.1145/3290605.3300434. URL: http://doi.acm.org/10.1145/3290605.3300434.

[176] Michael L. Rivera, Melissa Moukperian, Daniel Ashbrook, Jennifer Mankoff, and Scott E. Hudson. "Stretching the Bounds of 3D Printing with Embedded Textiles." In: *Proceedings of the 2017 CHI Conference on Human Factors in Computing Systems*. CHI '17. Denver, Colorado, USA: ACM, 2017, pp. 497–508. ISBN: 978-1-4503-4655-9. DOI: 10.1145/3025453.3025460. URL: http://doi.acm.org/10.1145/3025453.3025460.

[177] Robert McNeel & Associates. *Rhino 6 for Windows and Mac*. URL: https://www.rhino3d.com/ (visited on 08/03/2019).

[178] Douglas T. Ross. "Origins of the APT Language for Automatically Programmed Tools." In: *SIGPLAN Not.* 13.8 (Aug. 1978), pp. 61–99. ISSN: 0362-1340. DOI: 10.1145/960118.808374. URL: http://doi.acm.org/10.1145/960118.808374.

[179] Anne Roudaut, Henning Pohl, and Patrick Baudisch. "Touch Input on Curved Surfaces." In: *Proceedings of the SIGCHI Conference on Human Factors in Computing Systems*. CHI '11. Vancouver, BC, Canada: ACM, 2011, pp. 1011–1020. ISBN: 978-1-4503-0228-9. DOI: 10.1145/1978942.1979094. URL: http://doi.acm.org/10.1145/1978942.1979094.

[180] Gabriel Saada, Michael Layani, Avi Chernevousky, and Shlomo Magdassi. "Hydroprinting Conductive Patterns onto 3D Structures." In: *Advanced Materials Technologies* 2.5 (2017). 1600289, 1600289–n/a. ISSN: 2365-709X. DOI: 10.1002/admt.201600289. URL: http://dx.doi.org/10.1002/admt.201600289.

[181] Giovanni Saggio, Francesco Riillo, Laura Sbernini, and Lucia Rita Quitadamo. "Resistive flex sensors: a survey." In: *Smart Materials and Structures* 25.1 (2015), p. 013001.

[182] Neralagatta M. Sangeetha, Nicolas Decorde, Benoit Viallet, Guillaume Viau, and Laurence Ressier. "Nanoparticle-Based Strain Gauges Fabricated by Convective Self Assembly: Strain Sensitivity and Hysteresis with Respect to Nanoparticle Sizes." In: *The Journal of Physical Chemistry C* 117.4 (2013), pp. 1935–1940. DOI: 10.1021/jp310077r. eprint: http://dx.doi.org/10.1021/jp310077r. URL: http://dx.doi.org/10.1021/jp310077r.

[183] Harpreet Sareen, Udayan Umapathi, Patrick Shin, Yasuaki Kakehi, Jifei Ou, Hiroshi Ishii, and Pattie Maes. "Printflatables: Printing Human-Scale, Functional and Dynamic Inflatable Objects." In: *Proceedings of the 2017 CHI Conference on Human Factors in Computing Systems*. CHI '17. Denver, Colorado, USA: ACM, 2017, pp. 3669–3680. ISBN: 978-1-4503-4655-9. DOI: 10.1145/3025453.3025898. URL: http://doi.acm.org/10.1145/3025453.3025898.

[184] Munehiko Sato, Ivan Poupyrev, and Chris Harrison. "Touché: Enhancing Touch Interaction on Humans, Screens, Liquids, and Everyday Objects." In: *Proceedings of the SIGCHI Conference on Human Factors in Computing Systems*. CHI '12. Austin, Texas, USA: ACM, 2012, pp. 483–492. ISBN: 978-1-4503-1015-4. DOI: 10.1145/2207676.2207743. URL: http://doi.acm.org/10.1145/2207676.2207743.

[185] Greg Saul, Manfred Lau, Jun Mitani, and Takeo Igarashi. "SketchChair: An All-in-one Chair Design System for End Users." In: *Proceedings of the Fifth International Conference on Tangible, Embedded, and Embodied Interaction*. TEI '11. Funchal, Portugal: ACM, 2011, pp. 73–80. ISBN: 978-1-4503-0478-8. DOI: 10.1145/1935701.1935717. URL: http://doi.acm.org/10.1145/1935701.1935717.

[186] Valkyrie Savage, Colin Chang, and Björn Hartmann. "Sauron: Embedded Single-camera Sensing of Printed Physical User Interfaces." In: *Proceedings of the 26th Annual ACM Symposium on User Interface Software and Technology*. UIST '13. St. Andrews, Scotland, United Kingdom: ACM, 2013, pp. 447–456. ISBN: 978-1-4503-2268-3. DOI: 10.1145/2501988.2501992. URL: http://doi.acm.org/10.1145/2501988.2501992.

[187] Valkyrie Savage, Sean Follmer, Jingyi Li, and Björn Hartmann. "Makers' Marks: Physical Markup for Designing and Fabricating Functional Objects." In: *Proceedings of the 28th Annual ACM Symposium on User Interface Software & Technology*. UIST '15. Daegu, Kyungpook, Republic of Korea: ACM, 2015, pp. 103–108. ISBN: 978-1-4503-3779-3. DOI: 10.1145/2807442.2807508. URL: http://doi.acm.org/10.1145/2807442.2807508.

[188] Valkyrie Savage, Andrew Head, Björn Hartmann, Dan B. Goldman, Gautham Mysore, and Wilmot Li. "Lamello: Passive Acoustic Sensing for Tangible Input Components." In: *Proceedings of the 33rd Annual ACM Conference on Human Factors in Computing Systems*. CHI '15. Seoul, Republic of Korea: ACM, 2015, pp. 1277–1280. ISBN: 978-1-4503-3145-6. DOI: 10.1145/2702123.2702207. URL: http://doi.acm.org/10.1145/2702123.2702207.

[189] Valkyrie Savage, Ryan Schmidt, Tovi Grossman, George Fitzmaurice, and Björn Hartmann. "A Series of Tubes: Adding Interactivity to 3D Prints Using Internal Pipes." In: *Proceedings of the 27th Annual ACM Symposium on User*

Interface Software and Technology. UIST '14. Honolulu, Hawaii, USA: ACM, 2014, pp. 3–12. ISBN: 978-1-4503-3069-5. DOI: 10.1145/2642918.2647374. URL: http://doi.acm.org/10.1145/2642918.2647374.

[190] Valkyrie Savage, Xiaohan Zhang, and Björn Hartmann. "Midas: Fabricating Custom Capacitive Touch Sensors to Prototype Interactive Objects." In: *Proceedings of the 25th Annual ACM Symposium on User Interface Software and Technology*. UIST '12. Cambridge, Massachusetts, USA: ACM, 2012, pp. 579–588. ISBN: 978-1-4503-1580-7. DOI: 10.1145/2380116.2380189. URL: http://doi.acm.org/10.1145/2380116.2380189.

[191] F Scarpa, P Panayiotou, and G Tomlinson. "Numerical and experimental uniaxial loading on in-plane auxetic honeycombs." In: *The Journal of Strain Analysis for Engineering Design* 35.5 (2000), pp. 383–388. DOI: 10.1243/0309324001514152.

[192] Martin Schmitz, Mohammadreza Khalilbeigi, Matthias Balwierz, Roman Lissermann, Max Mühlhäuser, and Jürgen Steimle. "Capricate: A Fabrication Pipeline to Design and 3D Print Capacitive Touch Sensors for Interactive Objects." In: *Proceedings of the 28th Annual ACM Symposium on User Interface Software & Technology*. UIST '15. Daegu, Kyungpook, Republic of Korea: ACM, 2015, pp. 253–258. ISBN: 978-1-4503-3779-3. DOI: 10.1145/2807442.2807503. URL: http://doi.acm.org/10.1145/2807442.2807503.

[193] Martin Schmitz, Jürgen Steimle, Jochen Huber, Niloofar Dezfuli, and Max Mühlhäuser. "Flexibles: Deformation-Aware 3D-Printed Tangibles for Capacitive Touchscreens." In: *Proceedings of the 2017 CHI Conference on Human Factors in Computing Systems*. CHI '17. Denver, Colorado, USA: ACM, 2017, pp. 1001–1014. ISBN: 978-1-4503-4655-9. DOI: 10.1145/3025453.3025663. URL: http://doi.acm.org/10.1145/3025453.3025663.

[194] Martin Schmitz, Martin Stitz, Florian Müller, Markus Funk, and Max Mühlhäuser. "./trilaterate: A Fabrication Pipeline to Design and 3D Print Hover-, Touch-, and Force-Sensitive Objects." In: *Proceedings of the 2019 CHI Conference on Human Factors in Computing Systems*. CHI '19. Glasgow, Scotland Uk: ACM, 2019, 454:1–454:13. ISBN: 978-1-4503-5970-2. DOI: 10.1145/3290605.3300684. URL: http://doi.acm.org/10.1145/3290605.3300684.

[195] Adriana Schulz, Ariel Shamir, David I. W. Levin, Pitchaya Sitthi-amorn, and Wojciech Matusik. "Design and Fabrication by Example." In: *ACM Trans. Graph.* 33.4 (July 2014), 62:1–62:11. ISSN: 0730-0301. DOI: 10.1145/2601097.2601127. URL: http://doi.acm.org/10.1145/2601097.2601127.

[196] Christian Schumacher, Bernd Bickel, Jan Rys, Steve Marschner, Chiara Daraio, and Markus Gross. "Microstructures to Control Elasticity in 3D Printing." In: *ACM Trans. Graph.* 34.4 (July 2015), 136:1–136:13. ISSN: 0730-0301. DOI: 10.1145/2766926. URL: http://doi.acm.org/10.1145/2766926.

[197] R. Slyper and J. Hodgins. "Prototyping robot appearance, movement, and interactions using flexible 3D printing and air pressure sensors." In: *2012 IEEE RO-MAN: The 21st IEEE International Symposium on Robot and Human Interactive Communication*. Sept. 2012, pp. 6–11. DOI: 10.1109/ROMAN.2012.6343723.

[198] Ronit Slyper, Ivan Poupyrev, and Jessica Hodgins. "Sensing Through Structure: Designing Soft Silicone Sensors." In: *Proceedings of the Fifth International Conference on Tangible, Embedded, and Embodied Interaction*. TEI '11. Funchal, Portugal: ACM, 2011, pp. 213–220. ISBN: 978-1-4503-0478-8. DOI: 10.1145/1935701.1935744. URL: http://doi.acm.org/10.1145/1935701.1935744.

[199] Hyunyoung Song, François Guimbretière, Chang Hu, and Hod Lipson. "ModelCraft: Capturing Freehand Annotations and Edits on Physical 3D Models." In: *Proceedings of the 19th Annual ACM Symposium on User Interface Software and Technology*. UIST '06. Montreux, Switzerland: ACM, 2006, pp. 13–22. ISBN: 1-59593-313-1. DOI: 10.1145/1166253.1166258. URL: http://doi.acm.org/10.1145/1166253.1166258.

[200] Spectra Symbol Corp. *Flex Sensor FS*. v.2014 Rev A. 2014. URL: https://www.spectrasymbol.com/wp-content/uploads/2019/07/flexsensordatasheetv2019revA.pdf (visited on 09/13/2019).

[201] C. Srichan, T. Saikrajang, T. Lomas, A. Jomphoak, T. Maturos, D. Phokaratkul, T. Kerdcharoen, and A. Tuantranont. "Inkjet printing PEDOT:PSS using desktop inkjet printer." In: *2009 6th International Conference on Electrical Engineering/Electronics, Computer, Telecommunications and Information Technology*. Vol. 01. May 2009, pp. 465–468. DOI: 10.1109/ECTICON.2009.5137049.

[202] Jürgen Steimle, Andreas Jordt, and Pattie Maes. "Flexpad: Highly Flexible Bending Interactions for Projected Handheld Displays." In: *Proceedings of the SIGCHI Conference on Human Factors in Computing Systems*. CHI '13. Paris, France: ACM, 2013, pp. 237–246. ISBN: 978-1-4503-1899-0. DOI: 10.1145/2470654.2470688. URL: http://doi.acm.org/10.1145/2470654.2470688.

[203] John S. Steinhart and Stanley R. Hart. "Calibration Curves for Thermistors." In: *Deep Sea Research and Oceanographic Abstracts* 15.4 (1968), pp. 497–503. ISSN: 0011-7471. DOI: http://dx.doi.org/10.1016/0011-7471(68)90057-0. URL: http://www.sciencedirect.com/science/article/pii/0011747168900570.

[204] Stratasys Ltd. *What is PolyJet Technology for 3D Printing? | Stratasys*. URL: https://www.stratasys.com/polyjet-technology (visited on 09/09/2019).

[205] Katsuaki Suganuma. *Introduction to Printed Electronics*. SpringerBriefs in Electrical and Computer Engineering. Springer New York, 2014. ISBN: 978-1-4614-9625-0.

[206] Yuta Sugiura, Gota Kakehi, Anusha Withana, Calista Lee, Daisuke Sakamoto, Maki Sugimoto, Masahiko Inami, and Takeo Igarashi. "Detecting Shape Deformation of Soft Objects Using Directional Photoreflectivity Measurement." In: *Proceedings of the 24th Annual ACM Symposium on User Interface Software and Technology*. UIST '11. Santa Barbara, California, USA: ACM, 2011, pp. 509–516. ISBN: 978-1-4503-0716-1. DOI: 10.1145/2047196.2047263. URL: http://doi.acm.org/10.1145/2047196.2047263.

[207] Subramanian Sundaram, Ziwen Jiang, Pitchaya Sitthi-Amorn, David S. Kim, Marc A. Baldo, and Wojciech Matusik. "3D-Printed Autonomous Sensory Composites." In: *Advanced Materials Technologies* 2.3 (2017), p. 1600257. DOI: 10.1002/admt.201600257. eprint: https://onlinelibrary.wiley.com/doi/pdf/10.1002/admt.201600257. URL: https://onlinelibrary.wiley.com/doi/abs/10.1002/admt.201600257.

[208] Ivan E. Sutherland. "Sketchpad: A Man-machine Graphical Communication System." In: *Proceedings of the May 21-23, 1963, Spring Joint Computer Conference*. AFIPS '63 (Spring). Detroit, Michigan: ACM, 1963, pp. 329–346. DOI: 10.1145/1461551.1461591. URL: http://doi.acm.org/10.1145/1461551.1461591.

[209] Haruki Takahashi and Homei Miyashita. "Expressive Fused Deposition Modeling by Controlling Extruder Height and Extrusion Amount." In: *Proceedings of the 2017 CHI Conference on Human Factors in Computing Systems*. CHI '17. Denver, Colorado, USA: ACM, 2017, pp. 5065–5074. ISBN: 978-1-4503-4655-9. DOI: 10.1145/3025453.3025933. URL: http://doi.acm.org/10.1145/3025453.3025933.

[210] The GTK Team. *The GTK Project*. URL: https://www.gtk.org/ (visited on 09/10/2019).

[211] Cesar Torres, Tim Campbell, Neil Kumar, and Eric Paulos. "HapticPrint: Designing Feel Aesthetics for Digital Fabrication." In: *Proceedings of the 28th Annual ACM Symposium on User Interface Software & Technology*. UIST '15. Daegu, Kyungpook, Republic of Korea: ACM, 2015, pp. 583–591. ISBN: 978-1-4503-3779-3. DOI: 10.1145/2807442.2807492. URL: http://doi.acm.org/10.1145/2807442.2807492.

[212] Cesar Torres, Jessica Chang, Advaita Patel, and Eric Paulos. "Phosphenes: Crafting Resistive Heaters Within Thermoreactive Composites." In: *Proceedings of the 2019 on Designing Interactive Systems Conference*. DIS '19. San Diego, CA, USA: ACM, 2019, pp. 907–919. ISBN: 978-1-4503-5850-7. DOI: 10.1145/3322276.3322375. URL: http://doi.acm.org/10.1145/3322276.3322375.

[213] Trimble Inc. *3D Design Software | 3D Modeling on the Web | SketchUp*. URL: https://www.sketchup.com/ (visited on 08/03/2019).

[214] Giovanni Maria Troiano, Esben Warming Pedersen, and Kasper Hornbæk. "Deformable Interfaces for Performing Music." In: *Proceedings of the 33rd Annual ACM Conference on Human Factors in Computing Systems*. CHI '15. Seoul, Republic of Korea: ACM, 2015, pp. 377–386. ISBN: 978-1-4503-3145-6. DOI: 10.1145/2702123.2702492. URL: http://doi.acm.org/10.1145/2702123.2702492.

[215] Brygg Ullmer and Hiroshi Ishii. "The metaDESK: Models and Prototypes for Tangible User Interfaces." In: *Proceedings of the 10th Annual ACM Symposium on User Interface Software and Technology*. UIST '97. Banff, Alberta, Canada: ACM, 1997, pp. 223–232. ISBN: 0-89791-881-9. DOI: 10.1145/263407.263551. URL: http://doi.acm.org/10.1145/263407.263551.

[216] Udayan Umapathi, Hsiang-Ting Chen, Stefanie Mueller, Ludwig Wall, Anna Seufert, and Patrick Baudisch. "LaserStacker: Fabricating 3D Objects by Laser Cutting and Welding." In: *Proceedings of the 28th Annual ACM Symposium on User Interface Software & Technology*. UIST '15. Charlotte, NC, USA: ACM, 2015, pp. 575–582. ISBN: 978-1-4503-3779-3. DOI: 10.1145/2807442.2807512. URL: http://doi.acm.org/10.1145/2807442.2807512.

[217] Nobuyuki Umetani and Ryan Schmidt. "SurfCuit: Surface-Mounted Circuits on 3D Prints." In: *IEEE Computer Graphics and Applications* 37.3 (May 2017), pp. 52–60. ISSN: 0272-1716. DOI: 10.1109/MCG.2017.40.

[218] Nicolas Vachicouras, Christina M. Tringides, Philippe B. Campiche, and Stéphanie P. Lacour. "Engineering reversible elasticity in ductile and brittle thin films supported by a plastic foil." In: *Extreme Mechanics Letters* 15 (2017), pp. 63–69. ISSN: 2352-4316. DOI: 10.1016/j.eml.2017.05.005. URL: http://www.sciencedirect.com/science/article/pii/S2352431617300512.

[219] Nirzaree Vadgama and Jürgen Steimle. "Flexy: Shape-Customizable, Single-Layer, Inkjet Printable Patterns for 1D and 2D Flex Sensing." In: *Proceedings of the Eleventh International Conference on Tangible, Embedded, and Embodied Interaction*. TEI '17. Yokohama, Japan: ACM, 2017, pp. 153–162. ISBN: 978-1-4503-4676-4. DOI: 10.1145/3024969.3024989. URL: http://doi.acm.org/10.1145/3024969.3024989.

[220] Karen Vanderloock, Vero Vanden Abeele, Johan A.K. Suykens, and Luc Geurts. "The Skweezee System: Enabling the Design and the Programming of Squeeze Interactions." In: *Proceedings of the 26th Annual ACM Symposium on User Interface Software and Technology*. UIST '13. St. Andrews, Scotland, United Kingdom: ACM, 2013, pp. 521–530. ISBN: 978-1-4503-2268-3. DOI: 10.1145/2501988.2502033. URL: http://doi.acm.org/10.1145/2501988.2502033.

[221] Tatyana Vasilevitsky and Amit Zoran. "Steel-Sense: Integrating Machine Elements with Sensors by Additive Manufacturing." In: *Proceedings of the 2016 CHI Conference on Human Factors in Computing Systems*. CHI '16. Santa Clara, California, USA: ACM, 2016, pp. 5731–5742. ISBN: 978-1-4503-3362-7. DOI: 10.1145/2858036.2858309. URL: http://doi.acm.org/10.1145/2858036.2858309.

[222] Marynel Vázquez, Eric Brockmeyer, Ruta Desai, Chris Harrison, and Scott E. Hudson. "3D Printing Pneumatic Device Controls with Variable Activation Force Capabilities." In: *Proceedings of the 33rd Annual ACM Conference on Human Factors in Computing Systems*. CHI '15. Seoul, Republic of Korea: ACM, 2015, pp. 1295–1304. ISBN: 978-1-4503-3145-6. DOI: 10.1145/2702123.2702569. URL: http://doi.acm.org/10.1145/2702123.2702569.

[223] Nicolas Villar, James Scott, Steve Hodges, Kerry Hammil, and Colin Miller. ".NET Gadgeteer: A Platform for Custom Devices." In: *Pervasive Computing*. Ed. by Judy Kay, Paul Lukowicz, Hideyuki Tokuda, Patrick Olivier, and Antonio Krüger. Berlin, Heidelberg: Springer Berlin Heidelberg, 2012, pp. 216–233. ISBN: 978-3-642-31205-2.

[224] Anita Vogl, Patrick Parzer, Teo Babic, Joanne Leong, Alex Olwal, and Michael Haller. "StretchEBand: Enabling Fabric-based Interactions Through Rapid Fabrication of Textile Stretch Sensors." In: *Proceedings of the 2017 CHI Conference on Human Factors in Computing Systems*. CHI '17. Denver, Colorado, USA: ACM, 2017, pp. 2617–2627. ISBN: 978-1-4503-4655-9. DOI: 10.1145/3025453.3025938. URL: http://doi.acm.org/10.1145/3025453.3025938.

[225] Voxel8. *Voxel8 - 3D Printed Electronics*. URL: http://www.voxel8.co/ (visited on 09/11/2015).

[226] Geoff Walker. "A review of technologies for sensing contact location on the surface of a display." In: *Journal of the Society for Information Display* 20.8 (2012), pp. 413–440. DOI: 10.1002/jsid.100. URL: https://onlinelibrary.wiley.com/doi/abs/10.1002/jsid.100.

[227] Guanyun Wang, Ye Tao, Ozguc Bertug Capunaman, Humphrey Yang, and Lining Yao. "A-line: 4D Printing Morphing Linear Composite Structures." In: *Proceedings of the 2019 CHI Conference on Human Factors in Computing Systems*. CHI '19. Glasgow, Scotland Uk: ACM, 2019, 426:1–426:12. ISBN: 978-1-4503-5970-2. DOI: 10.1145/3290605.3300656. URL: http://doi.acm.org/10.1145/3290605.3300656.

[228] Guanyun Wang, Humphrey Yang, Zeyu Yan, Nurcan Gecer Ulu, Ye Tao, Jianzhe Gu, Levent Burak Kara, and Lining Yao. "4DMesh: 4D Printing Morphing Non-Developable Mesh Surfaces." In: *Proceedings of the 31st Annual ACM Symposium on User Interface Software and Technology*. UIST '18. Berlin, Germany: ACM, 2018, pp. 623–635. ISBN: 978-1-4503-5948-1. DOI: 10.1145/3242587.3242625. URL: http://doi.acm.org/10.1145/3242587.3242625.

[229] Tianyi Wang, Ke Huo, Pratik Chawla, Guiming Chen, Siddharth Banerjee, and Karthik Ramani. "Plain2Fun: Augmenting Ordinary Objects with Interactive Functions by Auto-Fabricating Surface Painted Circuits." In: *Proceedings of the 2018 Designing Interactive Systems Conference*. DIS '18. Hong Kong, China: ACM, 2018, pp. 1095–1106. ISBN: 978-1-4503-5198-0. DOI: 10.1145/3196709.3196791. URL: http://doi.acm.org/10.1145/3196709.3196791.

[230] Yanan Wang, Shijian Luo, Yujia Lu, Hebo Gong, Yexing Zhou, Shuai Liu, and Preben Hansen. "AnimSkin: Fabricating Epidermis with Interactive, Functional and Aesthetic Color Animation." In: *Proceedings of the 2017 Conference on Designing Interactive Systems*. DIS '17. Edinburgh, United Kingdom: ACM, 2017, pp. 397–401. ISBN: 978-1-4503-4922-2. DOI: 10.1145/3064663.3064687. URL: http://doi.acm.org/10.1145/3064663.3064687.

[231] Zhihui Wang, Ling Zhang, Shasha Duan, Hao Jiang, Jianhua Shen, and Chunzhong Li. "Kirigami-patterned highly stretchable conductors from flexible carbon nanotube-embedded polymer films." In: *J. Mater. Chem. C* 5 (34 2017), pp. 8714–8722. DOI: 10.1039/C7TC01727H. URL: http://dx.doi.org/10.1039/C7TC01727H.

[232] Michael Wehner, Ryan L. Truby, Daniel J. Fitzgerald, Bobak Mosadegh, George M. Whitesides, Jennifer A. Lewis, and Robert J. Wood. "An integrated design and fabrication strategy for entirely soft, autonomous robots." In: *Nature* 536 (Aug. 2016), p. 451. URL: https://doi.org/10.1038/nature19100.

[233] Christian Weichel, Jason Alexander, Abhijit Karnik, and Hans Gellersen. "SPATA: Spatio-Tangible Tools for Fabrication-Aware Design." In: *Proceedings of the Ninth International Conference on Tangible, Embedded, and Embodied Interaction*. TEI '15. Stanford, California, USA: ACM, 2015, pp. 189–196. ISBN: 978-1-4503-3305-4. DOI: 10.1145/2677199.2680576. URL: http://doi.acm.org/10.1145/2677199.2680576.

[234] Christian Weichel, John Hardy, Jason Alexander, and Hans Gellersen. "ReForm: Integrating Physical and Digital Design Through Bidirectional Fabrication." In: *Proceedings of the 28th Annual ACM Symposium on User Interface Software & Technology*. UIST '15. Daegu, Kyungpook, Republic of Korea: ACM, 2015, pp. 93–102. ISBN: 978-1-4503-3779-3. DOI: 10.1145/2807442.2807451. URL: http://doi.acm.org/10.1145/2807442.2807451.

[235] Christian Weichel, Manfred Lau, David Kim, Nicolas Villar, and Hans W. Gellersen. "MixFab: A Mixed-reality Environment for Personal Fabrication." In: *Proceedings of the 32nd Annual ACM Conference on Human Factors in Computing Systems*. CHI '14. Toronto, Ontario, Canada: ACM, 2014, pp. 3855–3864. ISBN: 978-1-4503-2473-1. DOI: 10.1145/2556288.2557090. URL: http://doi.acm.org/10.1145/2556288.2557090.

[236] Martin Weigel, Tong Lu, Gilles Bailly, Antti Oulasvirta, Carmel Majidi, and Jürgen Steimle. "iSkin: Flexible, Stretchable and Visually Customizable On-Body Touch Sensors for Mobile Computing." In: *Proceedings of the 33rd Annual ACM Conference on Human Factors in Computing Systems*. CHI '15. Seoul, Republic of Korea: ACM, 2015, pp. 2991–3000. ISBN: 978-1-4503-3145-6. DOI: 10.1145/2702123.2702391. URL: http://doi.acm.org/10.1145/2702123.2702391.

[237] Martin Weigel, Aditya Shekhar Nittala, Alex Olwal, and Jürgen Steimle. "SkinMarks: Enabling Interactions on Body Landmarks Using Conformal Skin Electronics." In: *Proceedings of the 2017 CHI Conference on Human Factors in Computing Systems*. CHI '17. Denver, Colorado, USA: ACM, 2017, pp. 3095–3105. ISBN: 978-1-4503-4655-9. DOI: 10.1145/3025453.3025704. URL: http://doi.acm.org/10.1145/3025453.3025704.

[238] Mark Weiser. "The Computer for the 21st Century." In: *SIGMOBILE Mob. Comput. Commun. Rev.* 3.3 (July 1999), pp. 3–11. ISSN: 1559-1662. DOI: 10.1145/329124.329126. URL: http://doi.acm.org/10.1145/329124.329126.

[239] Malte Weiss, Chat Wacharamanotham, Simon Voelker, and Jan Borchers. "FingerFlux: Near-surface Haptic Feedback on Tabletops." In: *Proceedings of the 24th Annual ACM Symposium on User Interface Software and Technology*. UIST '11. Santa Barbara, California, USA: ACM, 2011, pp. 615–620. ISBN: 978-1-4503-0716-1. DOI: 10.1145/2047196.2047277. URL: http://doi.acm.org/10.1145/2047196.2047277.

[240] Malte Weiss, Julie Wagner, Yvonne Jansen, Roger Jennings, Ramsin Khoshabeh, James D. Hollan, and Jan Borchers. "SLAP Widgets: Bridging the Gap Between Virtual and Physical Controls on Tabletops." In: *Proceedings of the SIGCHI Conference on Human Factors in Computing Systems*. CHI '09. Boston,

MA, USA: ACM, 2009, pp. 481–490. ISBN: 978-1-60558-246-7. DOI: 10.1145/1518701.1518779. URL: http://doi.acm.org/10.1145/1518701.1518779.

[241] Pierre Wellner. "Interacting with Paper on the DigitalDesk." In: *Commun. ACM* 36.7 (July 1993), pp. 87–96. ISSN: 0001-0782. DOI: 10.1145/159544.159630. URL: http://doi.acm.org/10.1145/159544.159630.

[242] Michael Wessely, Theophanis Tsandilas, and Wendy E. Mackay. "Stretchis: Fabricating Highly Stretchable User Interfaces." In: *Proceedings of the 29th Annual Symposium on User Interface Software and Technology*. UIST '16. Tokyo, Japan: ACM, 2016, pp. 697–704. ISBN: 978-1-4503-4189-9. DOI: 10.1145/2984511.2984521. URL: http://doi.acm.org/10.1145/2984511.2984521.

[243] John F. Whitfield. *The Electrician's Guide to the 17th Edition of the IEE Wiring Regulations BS 7671:2011 and Part P of the Building Regulations*. Environmental Protection Agency, 2012. ISBN: 9780953788576.

[244] Karl Willis, Eric Brockmeyer, Scott Hudson, and Ivan Poupyrev. "Printed Optics: 3D Printing of Embedded Optical Elements for Interactive Devices." In: *Proceedings of the 25th Annual ACM Symposium on User Interface Software and Technology*. UIST '12. Cambridge, Massachusetts, USA: ACM, 2012, pp. 589–598. ISBN: 978-1-4503-1580-7. DOI: 10.1145/2380116.2380190. URL: http://doi.acm.org/10.1145/2380116.2380190.

[245] Anusha Withana, Daniel Groeger, and Jürgen Steimle. "Tacttoo: A Thin and Feel-Through Tattoo for On-Skin Tactile Output." In: *Proceedings of the 31st Annual ACM Symposium on User Interface Software and Technology*. UIST '18. Berlin, Germany: ACM, 2018, pp. 365–378. ISBN: 978-1-4503-5948-1. DOI: 10.1145/3242587.3242645. URL: http://doi.acm.org/10.1145/3242587.3242645.

[246] Terry T. Wohlers, Tim Caffrey, and R. I. Campbell. *Wohlers report 2016 : 3D printing and additive manufacturing state of the industry*. 2016. ISBN: 978-0-9913332-2-6.

[247] Terry T. Wohlers, Ian Campbell, Olaf Diegel, Ray Huff, and Joseph Kowen. *Wohlers report 2019: 3D printing and additive manufacturing state of the industry*. 2019. ISBN: 978-0-9913332-5-7.

[248] Robert Xiao, Chris Harrison, and Scott E. Hudson. "WorldKit: Rapid and Easy Creation of Ad-hoc Interactive Applications on Everyday Surfaces." In: *Proceedings of the SIGCHI Conference on Human Factors in Computing Systems*. CHI '13. Paris, France: ACM, 2013, pp. 879–888. ISBN: 978-1-4503-1899-0. DOI: 10.1145/2470654.2466113. URL: http://doi.acm.org/10.1145/2470654.2466113.

[249] Junichi Yamaoka, Mustafa Doga Dogan, Katarina Bulovic, Kazuya Saito, Yoshihiro Kawahara, Yasuaki Kakehi, and Stefanie Mueller. "FoldTronics: Creating 3D Objects with Integrated Electronics Using Foldable Honeycomb Structures." In: *Proceedings of the 2019 CHI Conference on Human Factors in Computing Systems*. CHI '19. Glasgow, Scotland Uk: ACM, 2019, 628:1–628:14. ISBN: 978-1-4503-5970-2. DOI: 10.1145/3290605.3300858. URL: http://doi.acm.org/10.1145/3290605.3300858.

[250] Lining Yao, Ryuma Niiyama, Jifei Ou, Sean Follmer, Clark Della Silva, and Hiroshi Ishii. "PneUI: Pneumatically Actuated Soft Composite Materials for Shape Changing Interfaces." In: *Proceedings of the 26th Annual ACM Symposium on User Interface Software and Technology*. UIST '13. St. Andrews, Scotland, United Kingdom: ACM, 2013, pp. 13–22. ISBN: 978-1-4503-2268-3. DOI: 10.1145/2501988.2502037. URL: http://doi.acm.org/10.1145/2501988.2502037.

[251] Lining Yao, Jifei Ou, Chin-Yi Cheng, Helene Steiner, Wen Wang, Guanyun Wang, and Hiroshi Ishii. "bioLogic: Natto Cells as Nanoactuators for Shape Changing." In: *Proceedings of the 33rd Annual ACM Conference on Human Factors in Computing Systems - CHI '15*. Ed. by David Schlossberg. New York, New York, USA: ACM Press, 2015, pp. 1–10. ISBN: 9781450331456. DOI: 10.1145/2702123.2702611. URL: https://www.cambridge.org/core/product/identifier/CBO9781139855952A104/type/book%7B%5C_%7Dpart%20http://dl.acm.org/citation.cfm?doid=2702123.2702611.

[252] Kentaro Yasu. "Magnetact: Magnetic-sheet-based Haptic Interfaces for Touch Devices." In: *Proceedings of the 2019 CHI Conference on Human Factors in Computing Systems*. CHI '19. Glasgow, Scotland Uk: ACM, 2019, 240:1–240:8. ISBN: 978-1-4503-5970-2. DOI: 10.1145/3290605.3300470. URL: http://doi.acm.org/10.1145/3290605.3300470.

[253] Koji Yatani and Khai Nhut Truong. "SemFeel: A User Interface with Semantic Tactile Feedback for Mobile Touch-screen Devices." In: *Proceedings of the 22Nd Annual ACM Symposium on User Interface Software and Technology*. UIST '09. Victoria, BC, Canada: ACM, 2009, pp. 111–120. ISBN: 978-1-60558-745-5. DOI: 10.1145/1622176.1622198. URL: http://doi.acm.org/10.1145/1622176.1622198.

[254] Mika Yeap. *2019 Best Laser Cutters/Engravers & AIO Machines – Top 10*. June 2019. URL: https://all3dp.com/1/best-home-desktop-laser-cutter-engraver-aio-machine/ (visited on 09/03/2019).

[255] Vibol Yem and Hiroyuki Kajimoto. "Wearable tactile device using mechanical and electrical stimulation for fingertip interaction with virtual world." In: *2017 IEEE Virtual Reality (VR)*. Mar. 2017, pp. 99–104. DOI: 10.1109/VR.2017.7892236.

[256] Sang Ho Yoon, Ke Huo, Yunbo Zhang, Guiming Chen, Luis Paredes, Subramanian Chidambaram, and Karthik Ramani. "iSoft: A Customizable Soft Sensor with Real-time Continuous Contact and Stretching Sensing." In: *Proceedings of the 30th Annual ACM Symposium on User Interface Software and Technology*. UIST '17. Québec City, QC, Canada: ACM, 2017, pp. 665–678. ISBN: 978-1-4503-4981-9. DOI: 10.1145/3126594.3126654. URL: http://doi.acm.org/10.1145/3126594.3126654.

[257] Yasunori Yoshida, Konami Izumi, and Shizuo Tokito. "Development of Omnidirectional Inkjet (OIJ) Printing Technology Using a Vertically Articulated Robot." In: *Convertech & e-print* 6.1 (Jan. 2016), pp. 75–79. ISSN: 2185-6931. URL: http://ci.nii.ac.jp/naid/40020715046/en/.

[258] Jonas Zehnder, Espen Knoop, Moritz Bächer, and Bernhard Thomaszewski. "Metasilicone: Design and Fabrication of Composite Silicone with Desired Mechanical Properties." In: *ACM Trans. Graph.* 36.6 (Nov. 2017), 240:1–240:13. ISSN: 0730-0301. DOI: 10.1145/3130800.3130881. URL: http://doi.acm.org/10.1145/3130800.3130881.

[259] Yang Zhang and Chris Harrison. "Tomo: Wearable, Low-Cost Electrical Impedance Tomography for Hand Gesture Recognition." In: *Proceedings of the 28th Annual ACM Symposium on User Interface Software & Technology*. UIST '15. Daegu, Kyungpook, Republic of Korea: ACM, 2015, pp. 167–173. ISBN: 978-1-4503-3779-3. DOI: 10.1145/2807442.2807480. URL: http://doi.acm.org/10.1145/2807442.2807480.

[260] Yang Zhang, Gierad Laput, and Chris Harrison. "Electrick: Low-Cost Touch Sensing Using Electric Field Tomography." In: *Proceedings of the 2017 CHI Conference on Human Factors in Computing Systems*. CHI '17. Denver, Colorado, USA: ACM, 2017, pp. 1–14. ISBN: 978-1-4503-4655-9. DOI: 10.1145/3025453.3025842. URL: http://doi.acm.org/10.1145/3025453.3025842.

[261] Yizhong Zhang, Chunji Yin, Changxi Zheng, and Kun Zhou. "Computational Hydrographic Printing." In: *ACM Trans. Graph.* 34.4 (July 2015), 131:1–131:11. ISSN: 0730-0301. DOI: 10.1145/2766932. URL: http://doi.acm.org/10.1145/2766932.

[262] Ruike Zhao, Shaoting Lin, Hyunwoo Yuk, and Xuanhe Zhao. "Kirigami enhances film adhesion." In: *Soft Matter* 14 (13 2018), pp. 2515–2525. DOI: 10.1039/C7SM02338C. URL: http://dx.doi.org/10.1039/C7SM02338C.

[263] Simone Zimmermann, Sonja Rümelin, and Andreas Butz. "I Feel It in My Fingers: Haptic Guidance on Touch Surfaces." In: *Proceedings of the 8th International Conference on Tangible, Embedded and Embodied Interaction*. TEI '14. Munich, Germany: ACM, 2013, pp. 9–12. ISBN: 978-1-4503-2635-3. DOI: 10.1145/2540930.2540938. URL: http://doi.acm.org/10.1145/2540930.2540938.